

ÉCOLE DOCTORALE DES SCIENCES CHIMIQUES

INSTITUT DE CHIMIE, UMR 7177 CNRS

THÈSE

PRESENTEE PAR

THIERRY CHAVAGNAN

SOUTENUE LE : **26 SEPTEMBRE 2016**

POUR OBTENIR LE GRADE DE : **DOCTEUR DE L'UNIVERSITE DE STRASBOURG**

DISCIPLINE/ SPECIALITE : CHIMIE

**PHOSPHINES ET IMINOPHOSPHORANES
RESORCINARENIQUES POUR LA CATALYSE.
FORMATION DE COMPLEXES CAPSULAIRES**

Thèse dirigée par :

Dr SEMERIL David
Dr MATT Dominique

Chargé de recherche CNRS, Université de Strasbourg
Directeur de recherche CNRS, Université de Strasbourg

Rapporteurs :

Pr SAUTHIER Mathieu
Dr MANOURY Eric

Professeur, Université de Sciences et Technologies de Lille
Directeur de recherche CNRS, Université Paul Sabatier,
Toulouse

Autres membres du jury :

Dr MATT Dominique
Dr SEMERIL David

Directeur de recherche CNRS, Université de Strasbourg
Chargé de recherche CNRS, Université de Strasbourg

ÉCOLE DOCTORALE DES SCIENCES CHIMIQUES

INSTITUT DE CHIMIE, UMR 7177 CNRS

THÈSE

PRESENTEE PAR

THIERRY CHAVAGNAN

SOUTENUE LE : **26 SEPTEMBRE 2016**

POUR OBTENIR LE GRADE DE : **DOCTEUR DE L'UNIVERSITE DE STRASBOURG**

DISCIPLINE/ SPECIALITE : CHIMIE

**PHOSPHINES ET IMINOPHOSPHORANES
RESORCINARENIQUES POUR LA CATALYSE.
FORMATION DE COMPLEXES CAPSULAIRES**

Thèse dirigée par :

Dr SEMERIL David
Dr MATT Dominique

Chargé de recherche CNRS, Université de Strasbourg
Directeur de recherche CNRS, Université de Strasbourg

Rapporteurs :

Pr SAUTHIER Mathieu
Dr MANOURY Eric

Professeur, Université de Sciences et Technologies de Lille
Directeur de recherche CNRS, Université Paul Sabatier,
Toulouse

Autres membres du jury :

Dr MATT Dominique
Dr SEMERIL David

Directeur de recherche CNRS, Université de Strasbourg
Chargé de recherche CNRS, Université de Strasbourg

If a problem can be solved, there is no use worrying about it. If it can't be solved, worrying will do no good.

Dalai Lama

Table of contents

List of abbreviations	7
-----------------------------	---

Chapter I

Introduction générale et objectifs

Introduction générale et objectifs	9
Ligands résorcinaréniques en catalyse homogène	11
1. Phosphites résorcinarénique pour l'alkylation allylique régiosélective	11
2. Complexes 'introvertis' d'or pour l'hydratation ou cyclisation d'alcyne	13
3. Utilisation de phosphines en couplage croisé	15
4. Sels d'imidazolium greffés sur des plateformes résorcinaréniques	17
Annexe du chapitre I	27
Références	31

Chapter II

Cracking cavitands: Metal-directed scission of phosphinyl-substituted resorcinarenes

Abstract	33
Introduction	34
Results and discussion	34
Conclusion	38
Experimental Section	39
References	59

Chapter III

Cavitand scission by transition metal centres: Cleaved cavitand chirality and its consequences

Abstract	61
Introduction	62

Results and discussion.....	63
Conclusion.....	70
Experimental Section	71
References	84

Chapter IV

Substrate-selective olefin hydrogenation with a cavitand-based bis-*N*-anisyl- iminophosphorane

Abstract.....	86
Introduction.....	87
Results and discussion.....	88
Conclusion.....	94
Experimental Section.....	94
References.....	120

Chapitre V

Cavitand chemistry: towards metallo-capsular catalysts

Abstract.....	121
Introduction.....	122
Results and discussion.....	122
Conclusion.....	130
Experimental Section.....	131
References.....	166
Conclusion générale et perspectives.....	168

List of abbreviations

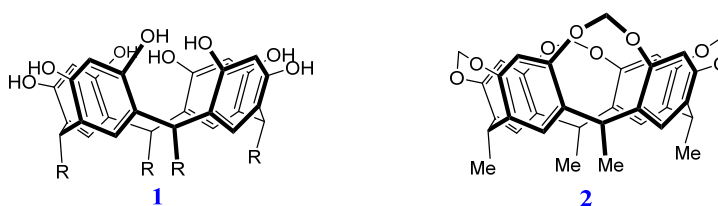
[α] _D	specific rotation
δ	chemical shift
1D	one-dimensional
2D	two-dimensional
Å	Ångström
Anal. Calcd.	Analysis calculated
Ac	acetate
AcOEt	ethyl acetate
Ar	aryl
arom.	aromatic
<i>n</i> -Bu	<i>n</i> -butyl
<i>n</i> BuLi	<i>n</i> butyl lithium
<i>t</i> -Bu	tert-butyl
br	broad
bn	benzyl
CCDC	Cambridge Crystallographic Data Centre
CIF	crystallographic information file
COD	1,5-cyclooctadiene
Cp	cyclopentadienyl
d	doublet
dt	doublet of triplets
dd	doublet of doublets
ddd	doublet of doublet of doublets
dba	dibenzylideneacetone
DEPT	Distortionless enhancement by polarization transfer
DOSY	Diffusion-Ordered Spectroscopy
DMF	Dimethylformamide
DMSO	Dimethylsulfoxide
eq.	Equivalent
ESI-TOF	Electron Spray Ionisation - Time-of-flight mass analyzer
Fig.	Figure
GC	Gas chromatography

h	hour
hept.	heptuplet
HMBC	Heteronuclear Multiple Bond Correlation
HMQC	Heteronuclear Multiple Quantum Correlation
HSQC	Heteronuclear
Hz	Hertz
ⁱ Pr	iso-propyl
IR	Infrared
<i>J</i>	coupling constant
m	multiplet
Me	methyl
Mes	2,4,6-trimethylphenyl
min	minutes
MALDI	Matrix-Assisted Laser Desorption/Ionisation
<i>M_r</i>	relative molecular mass
MS	Mass spectrometry
<i>m/z</i>	Mass to charge ratio
NHC	<i>N</i> -heterocyclic carbene
NMR	Nuclear Magnetic resonance
PEPPSI	Pyridine Enhanced precatalyst preparation, stabilisation, initiation
Ph	phenyl
ppm	parts per million
<i>R_f</i>	retardation factor
ROESY	Rotating frame nuclear Overhauser effect spectroscopy
r.t	room temperature
s	singulet
t	triplet
Tf	Triflate
THF	Tetrahydrofuran
THT	Tetrahydrothiophene
TOF	Turnover Frequency
TON	Turnover Number
UV	Ultra-Violet

Chapitre 1

Introduction générale et objectifs

Les résorcine[4]arènes sont des molécules macrocycliques constituées de quatre entités *résorcinol* reliées deux à deux par un pont "CHR". L'histoire de cette classe de composés débuta en 1872, lorsque Adolf Baeyer découvrit que l'addition d'acide sulfurique concentré à un mélange de benzaldéhyde et de résorcinol conduisait à un produit de couleur rouge virant au violet en solution alcaline. N'étant pas à même d'identifier la nature exacte des produits formés, il se contenta de conclure qu'il s'agissait de produits de condensation de stoechiométrie 1:1.^[1] Plus tard, en 1883, en reprenant les travaux de Baeyer, Michael réussit à isoler des composés cristallins et suggéra une structure dimérique pour l'un des produits isolés de la condensation benzaldéhyde/résorcinol.^[2] En 1940, après avoir effectué des mesures de masse moléculaire, Niederl et Vogel attribuèrent, pour la première fois, une structure de tétramère cyclique à l'un des produits formés au cours d'une telle réaction.^[3] La première structure à l'état solide d'un composé résorcinarénique de type **1** (R= *p*-Br-C₆H₄) ne fut publiée qu'en 1968, par Erdtman et Högberg.^[4]



Aspects conformationnels des résorcine[4]arènes

Les résorcinarènes sont des composés dotés d'une grande flexibilité due à la rotation des unités résorcinoliques autour des ponts CHR. Ainsi, ces composés peuvent exister dans différentes conformations, respectivement appelées *cône* (C_{4v}), *bateau* (C_{2v}), *chaise* (C_{2h}), *1,3-alternée* (D_{2d}) et *1,2-alternée* (C_s). Une variante de la conformation *cône* est la conformation dite *cône aplati* (Schéma 1).

Les résorcinarènes génériques peuvent être rigidifiés par l'introduction d'un élément de liaison entre chacune des paires de groupements hydroxyles voisins. Après rigidification, ces macrocycles adoptent la conformation *cône*. Les résorcinarènes ainsi formés sont parfois qualifiés de "cavitands", un terme qui signifie qu'il s'agit de cavités moléculaires à structure renforcée. Le premier cavitand résorcinarénique a été synthétisé par Cram en 1982; celui-ci a été obtenu en reliant les paires d'atomes d'oxygène résorcinoliques adjacents par des ponts –CH₂– (composé **2**).^[5] La rigidification des macrocycles peut également être réalisée au moyen d'hétéroatomes.^[6]

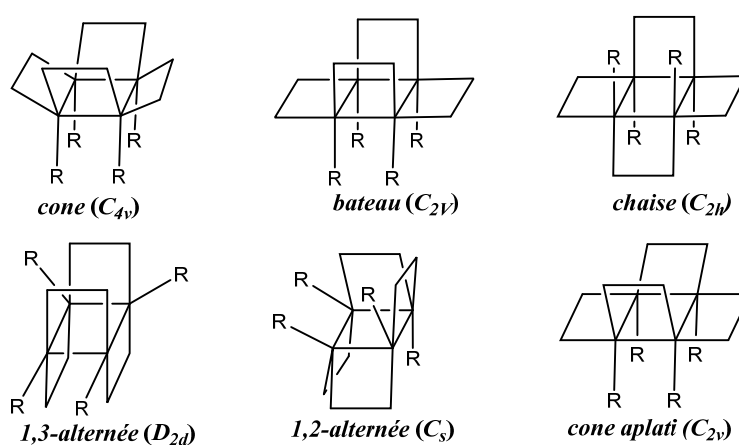


Schéma 1. Conformations des résorcinarènes

Les résorcinarènes ont donné lieu à de nombreuses applications. On pourra notamment citer leur emploi pour la confection de phases stationnaires HPLC permettant la séparation de bases pyrimidiques et de composés racémiques.^[7] Les résorcinarènes ont également été employés dans l'extraction sélective de lanthanides et d'actinides,^[8] comme récepteurs moléculaires,^[9] ou encore comme ligands en chimie de coordination^[10] et catalyse.^[11]

Ce sont de nouvelles applications en catalyse homogène qui ont été explorées dans cette thèse consacrée à trois familles de ligands ayant pour caractéristique commune la présence d'un ou de deux atomes de phosphore trivalents connectés au bord supérieur d'un cavitand résorcinarénique. La mise au point bibliographique qui suit, qui n'est pas exhaustive, décrit quelques exemples marquants de publications ayant trait à ce sujet.

Ligands résorcinaréniques en catalyse homogène

1. Phosphites résorcinaréniques pour l'alkylation allylique régiosélective

La première utilisation d'un ligand résorcinarénique en catalyse homogène a été publiée par Gibson et Rebek en 2002. Elle a trait à des réactions d'alkylation allylique utilisant le phosphito-résorcinarène **6**.^[12] L'obtention de ce ligand (Schéma 2) impliquait la synthèse du chlorophosphite **4** synthétisable par réaction du diol **3** avec PCl_3 en présence de pyridine. L'addition *in situ* de l'oxaxoline-alcool **5** au phosphite **4** préformé conduit à un mélange 7:3 des complexes *exo-6* et *endo-6* qui ont été séparés par chromatographie sur colonne de silice.

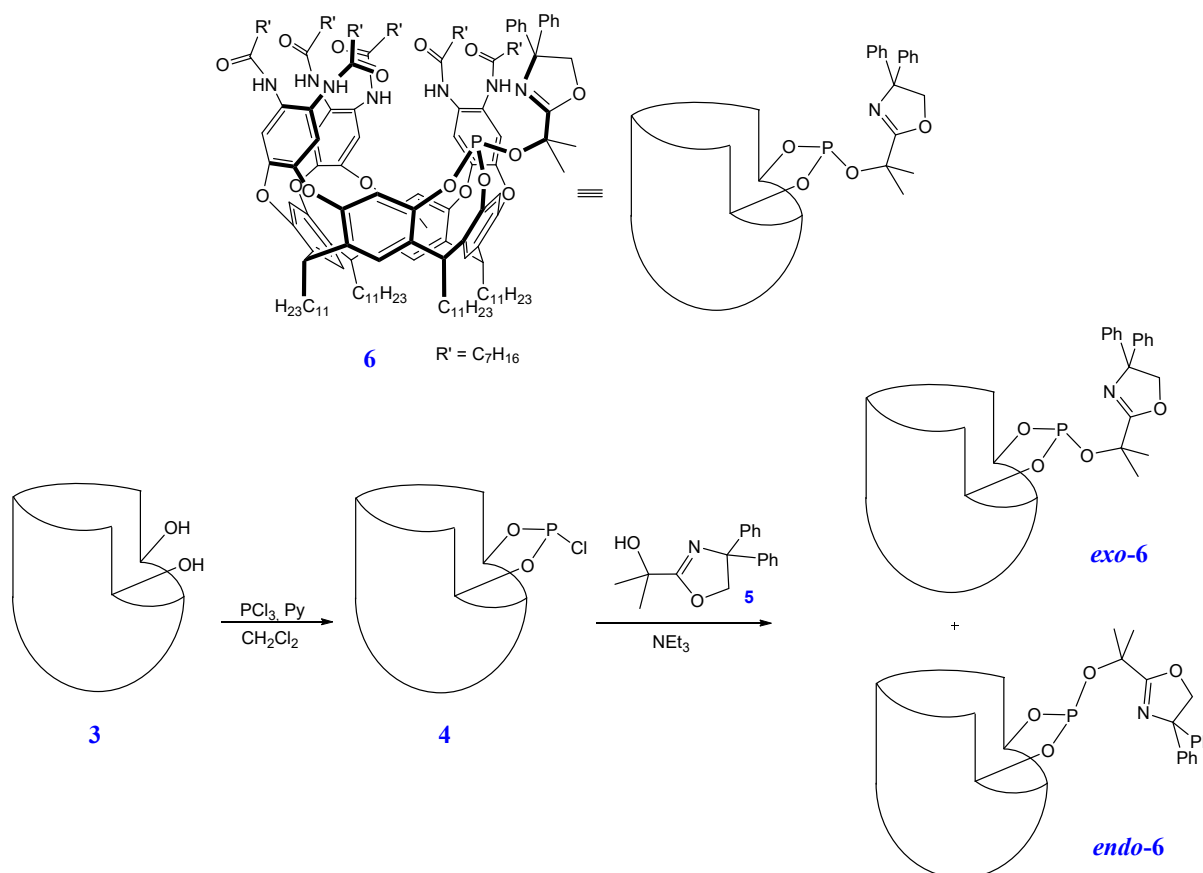


Schéma 2. Synthèse du phosphito-résorcinarène **6**

En présence de palladium et d'acétate d'allyle, le ligand **6** conduit à un complexe η^3 -allyle palladium dans lequel le groupement allyle est orienté vers l'axe de la cavité. Deux

façons de coordonner le groupement allyle ($\text{H}_2\text{C}^1\text{-C}^2\text{H}=\text{C}^3\text{HR}'$) sont envisageables, selon que le carbone en *trans* du phosphore est l'atome de carbone C^1 ou l'atome C^3 du coordinat allyle (complexes **8** et **9** ; Schéma 3). Pour des raisons d'accessibilité, l'attaque d'un nucléophile, par exemple un malonate, se fait préférentiellement sur l'atome C^1 , ce qui conduit à la formation majoritaire du produit linéaire. Les auteurs ont étudié des réactions d'alkylation avec divers substrats et ont constaté que, contrairement au ligand de référence **7** (un ligand décrit par Pfaltz; Schéma 3), la vitesse de réaction dépend de la nature du substrat. En combinant des expériences d'alkylation compétitives (effectuées avec un mélange de deux substrats allyliques) et des mesures de spectrométrie de masse, les auteurs ont montré que les réactions d'alkylation avec le cavitand **6** dépendent à la fois de la facilité à former le complexe allylique et de la réactivité de ce dernier vis-à-vis du nucléophile entrant, les deux étapes n'étant pas nécessairement corrélées. Ainsi, un substrat allylique donné peut former un complexe allylique plus rapidement qu'un autre, mais le complexe résultant peut-être inactif, contrairement à d'autres complexes allyliques. Dans l'ensemble, cette étude démontre que l'activité catalytique du cavitand **6** repose sur les propriétés de reconnaissance moléculaire ainsi que les propriétés stériques de la cavité.

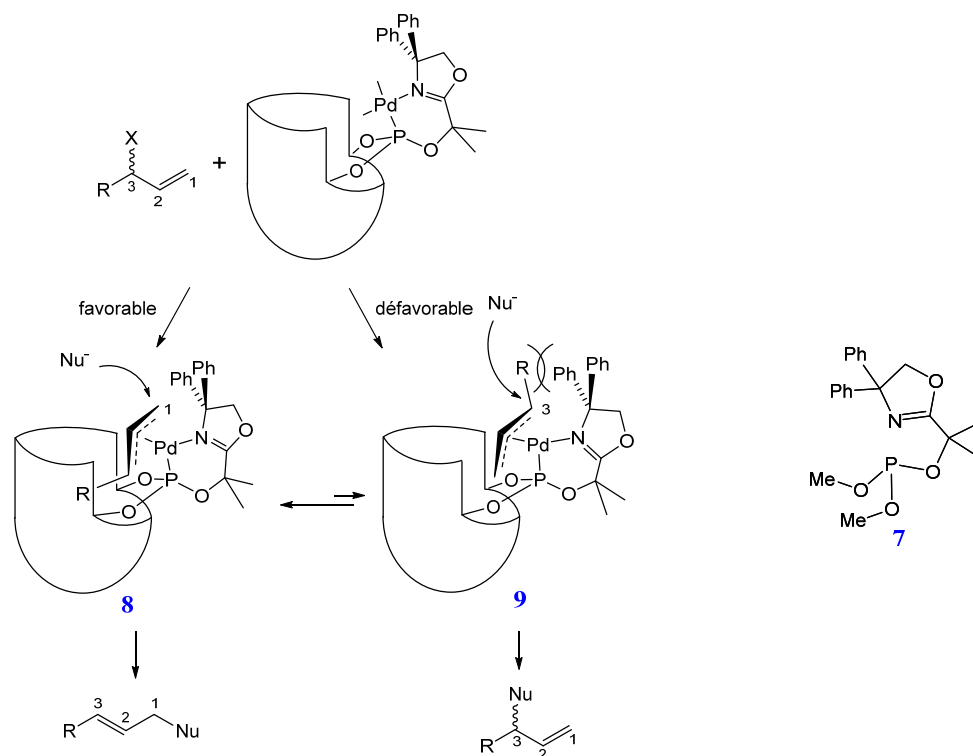


Schéma 3. Alkylation allylique régiosélective à partir du complexe $[\text{Pd}(\text{R-allyl})(\mathbf{6})]^+$ et le ligand de Pfaltz **7**

2. Complexes "introvertis" d'or pour l'hydratation ou la cyclisation d'alcynes

Récemment, Schramm *et coll.* ont décrit la synthèse de trois complexes résorcinaréniques d'or ayant leur centre métallique positionné à l'intérieur de la cavité formée par trois substituants quinoxaline (Schéma 4).^[13] Ces complexes ont été obtenus en deux étapes à partir du cavitand tris-quinoxaline **10**. La première étape a consisté en une phosphorylation des groupements hydroxy de **10**, suivie d'une réaction avec le précurseur d'or $[\text{AuCl}\cdot\text{S}(\text{CH}_3)_2]$ en donnant le complexe phosphoramidite **12**. Le même protocole a été appliqué pour la synthèse des complexes **13** et **14**, dont l'atome d'or est coordonné, respectivement, à un substituant phosphonite et phosphite (Schéma 4).

L'étude cristallographique du complexe **12** a permis d'établir que l'atome d'or est positionné à l'intérieur du macrocycle. Pour les complexes **13** et **14**, le confinement *endo* de l'atome d'or a été déduit des spectres RMN du proton.

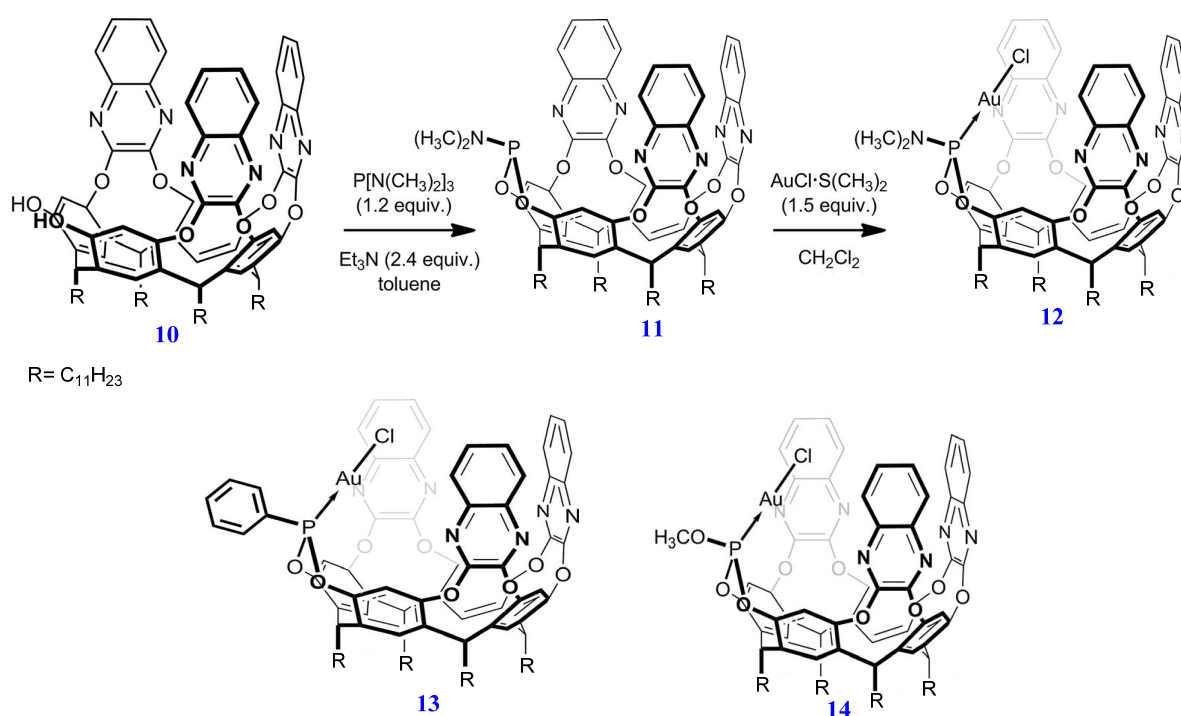


Schéma 4. Synthèses de complexes "introvertis" d'or **12-14**

Les auteurs ont testé les propriétés catalytiques du complexe **12** en hydratation d'alcynes terminaux (**Schéma 5**). Dans ces réactions, les alcynes terminaux aromatiques (R = Ph ou 1-naphthyle) sont convertis avec des rendements modestes, inférieurs à 50 %, à l'exception du 9-éthynylantracène dont la conversion est totale après 19 h. Des activités plus importantes ont été observées pour les alcynes aliphatiques, par exemple le 1-hexyne, qui est converti en 2-hexanone en moins d'une heure. De bonnes conversions ont également été observées pour des alcynes plus encombrés (R = CH₂CH₂Ph et ^tBu: 79 %); R = C(CH₃)₃: 89 %). Il est intéressant de noter que les réactions avec ces substrats encombrés ont une cinétique particulière, conduisant à 50 % de conversion dès la première heure, mais nécessitant 16 heures pour atteindre des conversions quasi complètes. Un des objectifs fixés par les auteurs pour la suite est de pouvoir utiliser le complexe **12** dans des catalyses sélectives en substrat, dans lesquelles la sélectivité résulterait de l'adéquation entre la taille du réactif et celle de l'espace cavitaire.

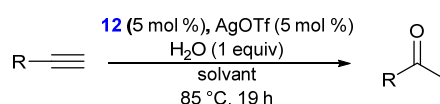


Schéma 5. Hydratation catalytique d'alcynes terminaux

Les complexes **12-14** ont été utilisés pour la conversion de l'alcyne montré dans le **Schéma 6** en composé **15**. Au cours de cette réaction, un produit secondaire peut se former, le composé **16**, produit résultant de l'hydratation directe de la triple liaison. La meilleure conversion en **15** a été obtenue avec le complexe **12** (62 %), les analogues **13** et **14** donnant de des rendements sensiblement plus faibles (~ 25 %)

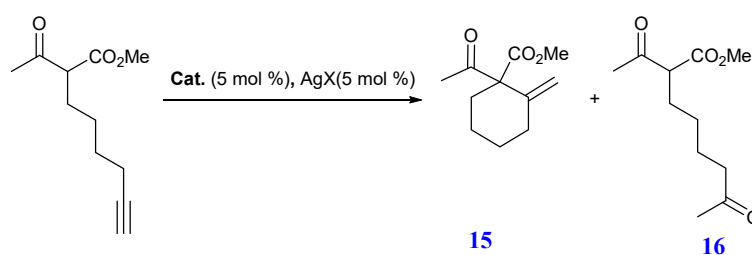


Schéma 6. Cyclisation d'un alcyne

3. Utilisation de phosphines en couplage croisé

Avant mon arrivée au laboratoire, une série de cavitands résorcinaréniques portant un^[14] (**17**), deux^[14] (**18** et **19**) ou quatre^[15] (**20**) substituants méthyldiphénylphosphines avaient déjà été synthétisés. Dans tous ces composés, les groupes $-\text{CH}_2\text{PPh}_2$ ont été greffés sur des positions C2 (c'est-à-dire l'atome de carbone OCCO) d'une unité résorcinoïde (**Figure 1**). Ces phosphines ont été obtenues à partir de précurseurs mono-, di- ou tétra-bromés, respectivement. Par exemple, la diphosphine **18** a été synthétisée en 5 étapes à partir du cavitand dibromé du **Schéma 18** ; elle a été obtenue avec un rendement global d'environ 50 %. Dans cette synthèse, l'entité diphénylphosphino a été introduite par réaction d'Arbuzov. La réduction de l'oxyde de phosphine résultant a été réalisée dans du phénylsilane au reflux (**Schéma 7**).

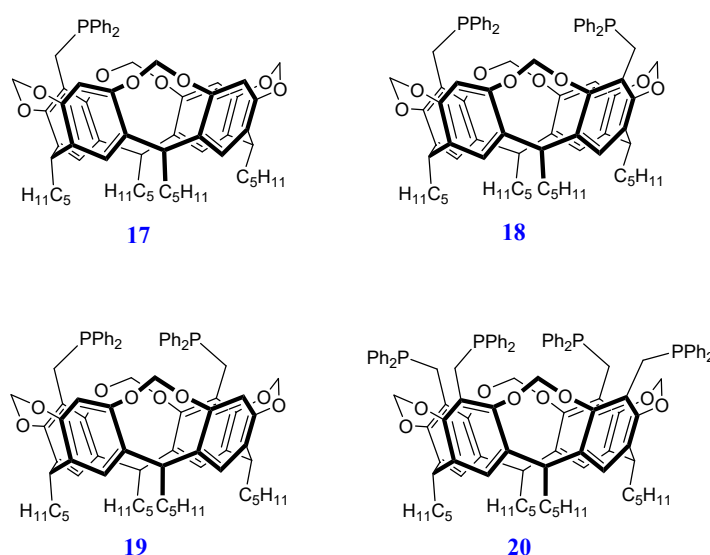


Figure 1. Phosphines **17-20** bâties sur une plateforme résorcinarénique

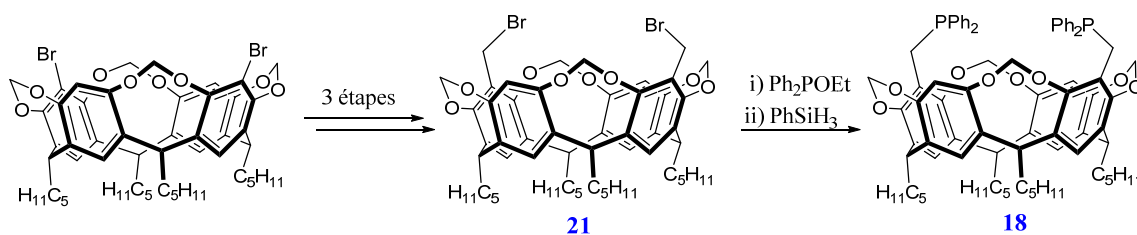


Schéma 7. Synthèse de la phosphine résorcinarénique **18**

La tétraphosphine **20** a été testée en couplage de Mizoroki-Heck entre bromures d'aryles et le styrène (Schéma 8). Le système catalytique a été généré *in situ*. Les meilleurs résultats ont été obtenus avec $[\text{Pd}(\text{OAc})_2]$ en présence de carbonate de césium comme base dans le DMF à 130°C , en employant un rapport de tétraphosphine/Pd de 1:1. L'activité maximale du catalyseur a été observée pour le couplage du 4-bromoanisole ($\text{TOF} = 2000 \text{ mol}(\text{ArBr})\cdot\text{mol}(\text{Pd})^{-1}\cdot\text{h}^{-1}$).

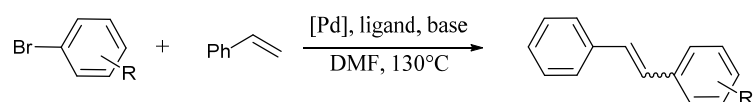


Schéma 8. Réaction de Mizoroki-Heck

Les ligands monophosphine **17** et diphosphines **18** et **19** ont été testés en couplage croisé de Suzuki-Miyaura entre des bromures d'aryles et l'acide phénylboronique^[16] (Schéma 9). Le système catalytique a été généré *in situ* et les meilleurs résultats ont été obtenus en utilisant $[\text{Pd}(\text{OAc})_2]$ en présence d'hydruure de sodium comme base, et en opérant dans le dioxane à 100°C . Le ligand le plus efficace, à savoir le cavitand proximale disubstitué **19**, a donné lieu à des activités catalytiques remarquables atteignant $34570 \text{ mol}(4\text{-bromoanisole})\cdot\text{mol}(\text{Pd})^{-1}\cdot\text{h}^{-1}$.

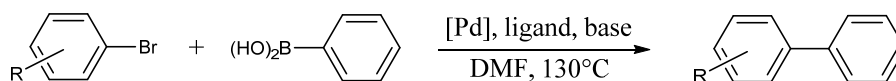


Schéma 9. Réaction de Suzuki-Miyaura

Les auteurs ont attribué les bonnes performances de ces coordinats en couplage de Suzuki-Miyaura à deux causes :

- i) la possibilité de former transitoirement, dans le cas de la monophosphine **17**, des complexes chélate-*P,O* impliquant les atomes d'oxygène de l'unité résorcinolique portant l'atome de phosphore. Cette coordination a pour effet de favoriser des espèces mono-

ligandées, connues pour faciliter l'étape élémentaire d'addition oxydante du bromure d'aryle.

- ii) la propension des ligands **18** et **19** à générer des espèces intermédiaires possédant un grand angle phosphore-métal-phosphore (ceci se produisant dans des oligomères cycliques avec le ligand **18** et dans un complexe chélate fortement tendu dans le cas de **19**). De telles espèces favorisent l'élimination réductrice par suite d'un repli des substituants du phosphore vers le centre de coordination lorsque l'angle PMP augmente.

4. Sels d'imidazolium greffés sur des plateformes résorcinaréniques

Les résorcinarènes mono- ou poly-bromométhylé(s) du type de **21** (*vide supra* Schéma 7) ont également été utilisés pour la confection de trois familles de cavitants substitués au niveau du bord supérieur par un, deux ou quatre groupements imidazolium (Schéma 10). Ces sels d'imidazolium ont été employés en couplage de Suzuki-Miyaura de bromures d'aryle avec l'acide phénylboronique.^[17] Le système catalytique, généré *in-situ*, a été obtenu en mélangeant sel d'imidazolium, $[Pd(OAc)_2]$ et une base. L'activité la plus élevée (TOF = 41600 mol(ArBr).mol(Pd)⁻¹.h⁻¹) a été observée dans le cas de l'arylation du 1-bromonaphtalène avec le cavitant disubstitué représenté dans le schéma 10 (R = Mes).

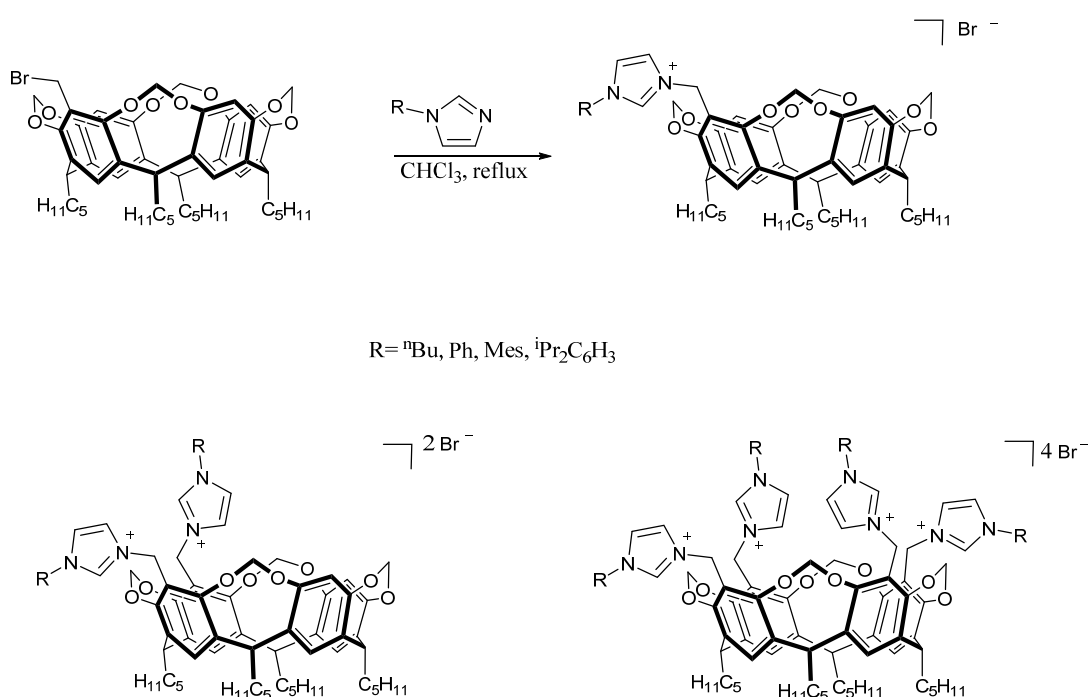


Schéma 10. Synthèse de sels d'imidazolium résorcinaréniques

Les sels d'imidazolium **22-27** (Schéma 11) sont les premiers exemples de cavitands dans lesquels l'un des atomes d'azote de l'hétérocycle est directement greffé à un cycle résorcinolique, l'autre étant substitué par un groupement alkyle ou aryle.^[18] Ces ligands monodentates pro-carbéniques ont été utilisés comme précurseurs catalytiques dans des réactions de couplage croisé de Suzuki-Miyaura catalysées au palladium,^[18a, 19] de Kumada-Tamao-Corriu catalysées au nickel^[20] et de réactions Cu-catalysées d'arylation allylique entre le bromure de cinnamyle et des arylmagnésiens.^[21]

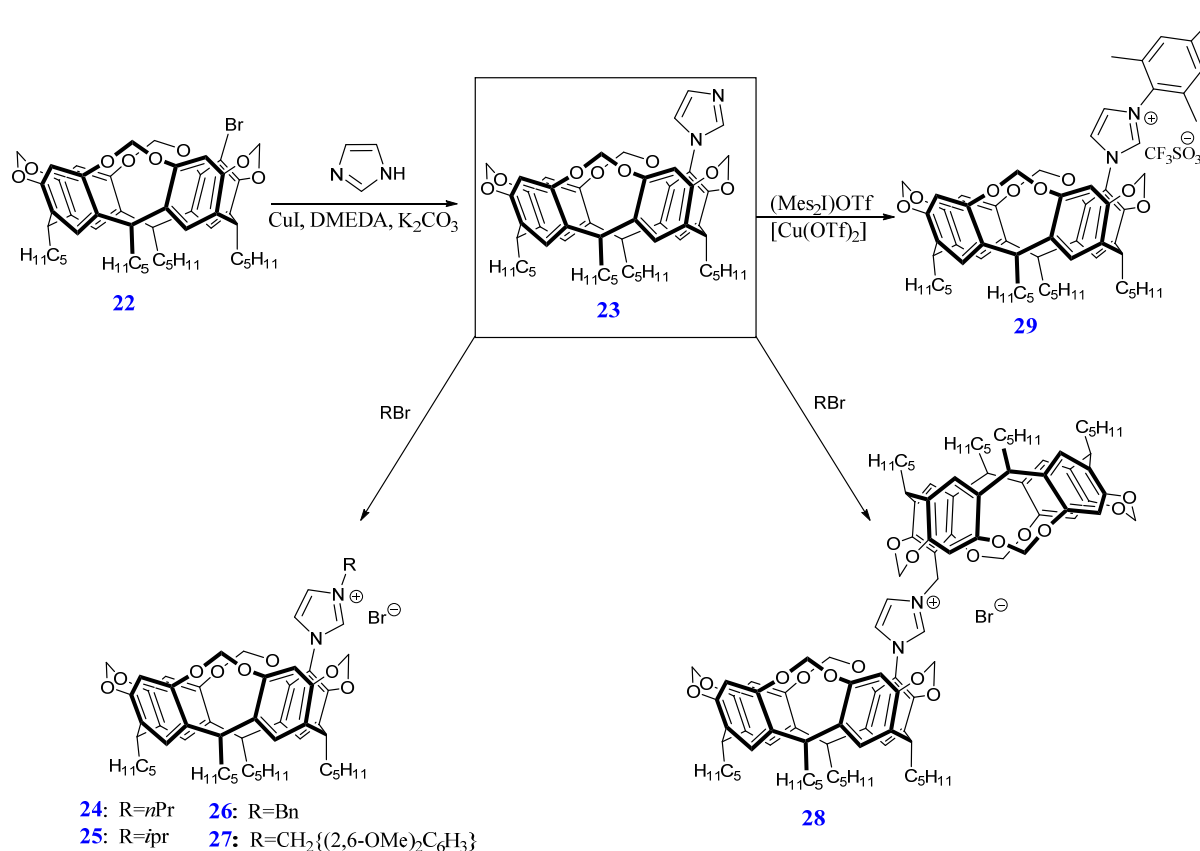


Schéma 11. Synthèse de sels d'imidazoliums **24-29**

Les sels d'imidazolium **24-29** ont été synthétisés selon le schéma 11. La première étape consiste en un couplage d'Ullmann entre le cavitant monobromé **22** et l'imidazole en présence de CuI/DMEDA (DMEDA = *N,N*-diméthyléthylènediamine) dans le DMF avec K₂CO₃ comme base. Le cavitant **23** ainsi obtenu a été alkylé avec divers bromures d'allyle (RBr : R = *n*-propyle, *iso*-propyle, benzyle, 2,6-diméthoxybenzyle et bromométhyl-

résorcinarène), conduisant aux sels d'imidazolium **24-28**. Le sel **29** est, quant à lui, obtenu en faisant réagir le cavitant **23** avec (Mes₂I)OTf dans DMF à 100°C en présence de cuivre.

Ces imidazoliums permettent d'accéder facilement à des complexes de type PEPPSI (PEPPSI = *pyridine enhanced precatalyst, preparation, stabilisation and initiation*) avec des précurseurs de palladium. Par exemple, la réaction de **26** et de **29** avec [PdCl₂] dans la pyridine en présence de KBr et de K₂CO₃ conduit, respectivement, aux complexes **30** et **31** (Schéma 12). Une étude par diffraction des rayons X a permis d'établir la configuration *trans* des atomes de brome du complexe **30** (Figure 2). Fait intéressant, une des chaînes pentyle du macrocycle se rapproche fortement du substituant pyridine, la distance H•••H la plus courte étant de 2.3 Å. Des expériences RMN ROESY ¹H-¹H montrent que cette proximité persiste en solution.

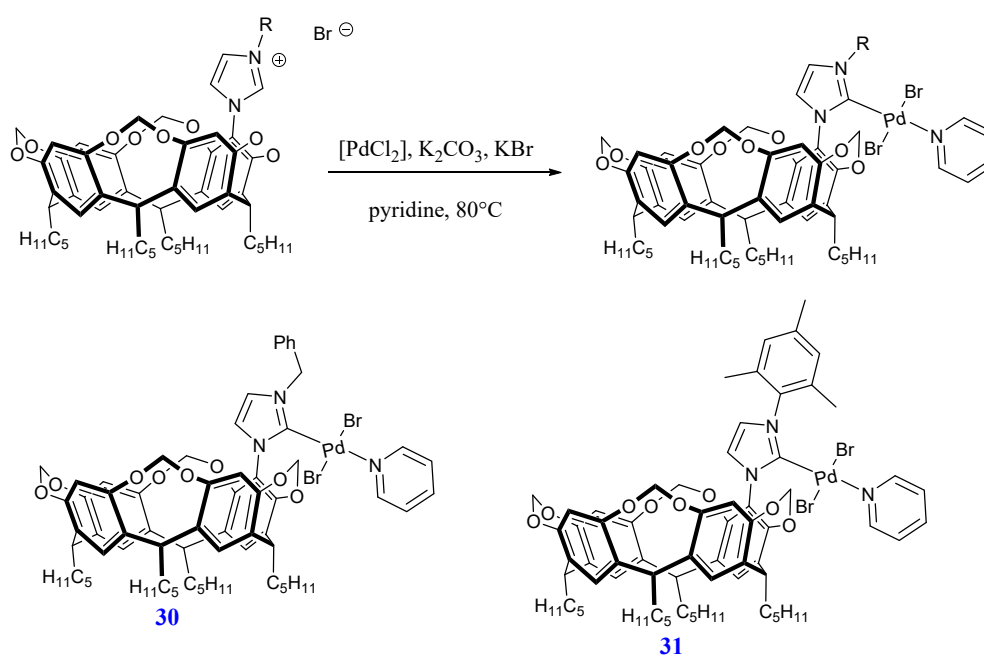


Schéma 12. Synthèse des complexes de type PEPPSI **30** et **31**

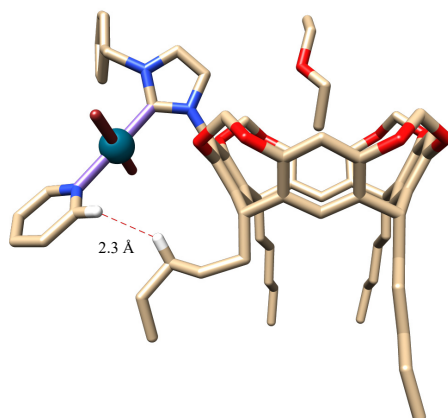


Figure 4. Structure du complexe de type PEPPSI **30**

Les précurseurs carbéniques **24-26** ont été testés en couplage croisé de Suzuki-Miyaura. Le système catalytique correspondant a été généré *in-situ* à partir des sels d'imidazolium et un précurseur de palladium. Les trois sels ont donné lieu à des systèmes catalytiques très efficaces pour le couplage de bromures d'aryles non encombrés avec l'acide phénylboronique (TOF jusqu'à 30100 mol(PhBr).mol(Pd)⁻¹h⁻¹ pour **26**), une nette augmentation de l'activité étant observée lorsque la taille du ligand augmente (**24** < **25** < **26**). Le complexe **31** s'est, lui, montré particulièrement efficace pour les chlorures d'aryles encombrés.^[19] Afin d'évaluer l'influence du groupement résorcinarénique au cours de la catalyse, trois analogues dépourvus de cavité (**32-34**) ont été testés (Figure 3).

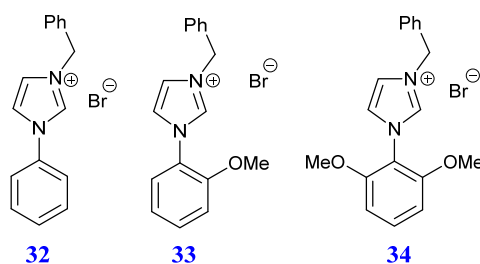


Figure 3. Analogues de sels d'imidazolium dépourvus de cavité

L'étude a montré que la vitesse du couplage augmente avec le nombre de substituants méthoxy (**32** < **33** < **34**). Il est raisonnable d'admettre que la formation, au cours de la

catalyse, de chélates hémilabiles impliquant les fonctions méthoxy en ortho des ligands **33** et **34** augmente par intermittence la densité électronique du centre métallique et favorise ainsi l'étape d'addition oxydante. De plus, l'accroissement d'encombrement stérique créé par la présence des deux groupements méthoxy dans **34**, est de nature à faciliter l'étape d'élimination réductrice. Ces effets combinés conduisent donc à une augmentation de l'activité catalytique en allant de **32** à **34**. Cependant, il faut préciser que les conversions correspondantes restent nettement inférieures à celles obtenues avec le sel d'imidazolium **26**.

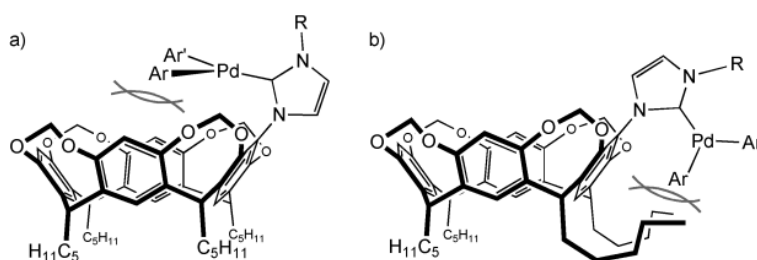


Figure 4. Interactions stériques possibles dans les intermédiaires catalytiques

L'efficacité catalytique élevée du système **26**/Pd résulte probablement d'effets stériques marqués, et ce, quelle que soit l'orientation, *endo* ou *exo*, du vecteur $C_{\text{carbène}}\text{-Pd}$ dans les intermédiaires $\text{PdArAr}'\text{L}$ (Figure 4). Dans le premier cas, c'est le bord supérieur de la cavité qui va globalement exercer une forte pression stérique sur les deux groupements aryles de l'entité PdArAr' tournés vers la cavité (Figure 4a). Par contre, si le vecteur $C_{\text{carbène}}\text{-Pd}$ est orienté vers l'extérieur, la pression stérique provient des deux groupes pentyle les plus proches de l'unité carbénique (Figure 4b). Pour confirmer l'influence possible de ces deux chaînes pentyle sur le résultat catalytique, l'analogue **35**, porteur sur le bord inférieur de groupements phényle au lieu de pentyle, a été synthétisé. Les modèles moléculaires montrent que, dans ce cas aucune interaction n'est possible entre le centre catalytique et les substituants (Ph) du bord inférieur (Figure 7). Les expériences de couplage croisé réalisées avec **35** conduisent à des résultats identiques à ceux obtenus avec l'analogue **34**, dépourvu de cavité. Ces résultats démontrent clairement l'importance des chaînes pentyle lors de la catalyse, substituants opérant probablement lors de l'étape d'élimination réductrice. Par contre, l'utilisation du sel d'imidazolium **28**, doublement substitué par des cavitands, ne conduit qu'à une augmentation de 15 % de l'activité catalytique en couplage de Suzuki-Miyaura comparée à celle du cavitand

26. Son impact modéré sur l'activité catalytique est probablement lié à la libre rotation du groupe "méthylrésorcinarényle", qui limite l'augmentation de l'effet stérique sur le centre métallique.^[19]

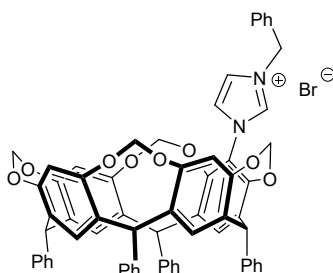


Figure 5. Sel d'imidazolium **35** portant des groupements phényles

Les proligands **24-26** ont également été testés en couplage croisé de Kumada-Tamao-Corriu catalysé au nickel (schéma 13), le système catalytique correspondant étant généré *in situ* à partir des sels d'imidazolium et de $[\text{Ni}(\text{cod})_2]$.^[20] Chacun des trois sels produit un système catalytique très efficace en couplage d'halogénures d'aryle avec deux Grignards, PhMgBr et *o*-TolMgCl (TOF jusqu'à $60400 \text{ mol}(\text{PhBr})\text{mol}(\text{Pd})^{-1}\text{h}^{-1}$ pour **25**), une augmentation de l'activité étant observée avec un accroissement de la taille du substituant R de l'azote N-2 ($24 < 25 < 26$). Des études comparatives avec le cavitand **35** et des analogues dépourvus de cavité (**32-34**) ont montré que, à l'instar de ce qui avait déjà été observé en couplage de Suzuki-Miyaura, l'efficacité de ces systèmes est corrélée aux interactions stériques entre les chaînes pentyle et le centre catalytique. Cet effet sera probablement accentué si, au cours du cycle catalytique, l'un des deux atomes d'oxygène qui flanque le cycle résorcinolique porteur du centre carbénique, vient se coordiner au centre métallique.

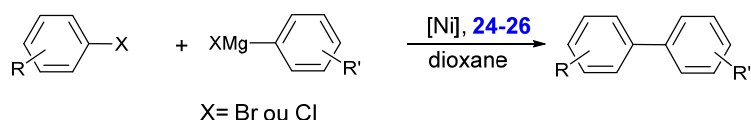


Schéma 13. Réaction de couplage croisé de Kumada-Tamao-Corriu

Finalement, les sels d'imidazolium résorcinaréniques **24-27**, associés à un précurseur de cuivre, ont été testés dans la réaction d'arylation allylique entre le bromure de cinnamyle et des aryles magnésiens (Schéma 14).^[21]

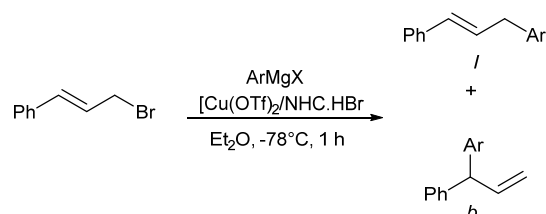


Schéma 14. Substitution allylique du bromure de cinnamyle avec des aryles magnésiens

Les NHC dérivés de ces sels possèdent des propriétés électroniques similaires, mais diffèrent par leur encombrement stérique (ordre : **26** < **28** < **27** < **29**) (Schéma 11). Les systèmes catalytiques ont là encore été générés *in situ*, à partir des sels d'imidazolium et de [Cu(OTf)₂]. On constate que la proportion de produit branché augmente avec la taille du substituant de l'azote N-2 du ligand (**26** < **28** < **27** < **29**). Le ratio b/l passe de 22 :78 pour **24** à 78 :22 pour **25** (Tableau 1). Il y a donc une corrélation sensible entre l'encombrement stérique des ligands pré-carbéniques et le ratio b/l des produits d'allylation. Cet effet est également observé avec les sels stériquement moins encombrés **36** et **37** (Figure 6).

Tableau 1. Alkylation allylique catalysée au cuivre du bromure de cinnamyle avec du bromure de phénylmagnésium. Influence des sels d'imidazolium **26-29**, **36** et **37**.

Entrée	NHC.HCl	Conversion (%)	Branché (%)	Linéaire (%)
1	26	100	22	78
2	28	100	31	69
3	27	100	47	53
4	29	100	78	22
5	36	100	16	84
6	37	100	20	80

Conditions: [Cu(OTf)₂] (1 mol %), sel d'imidazolium (1 mol %), PhCH=CHCH₂Br (0,32 mmol), PhMgBr (0,39 mmol), Et₂O (3 mL), -78 °C, 1 h.

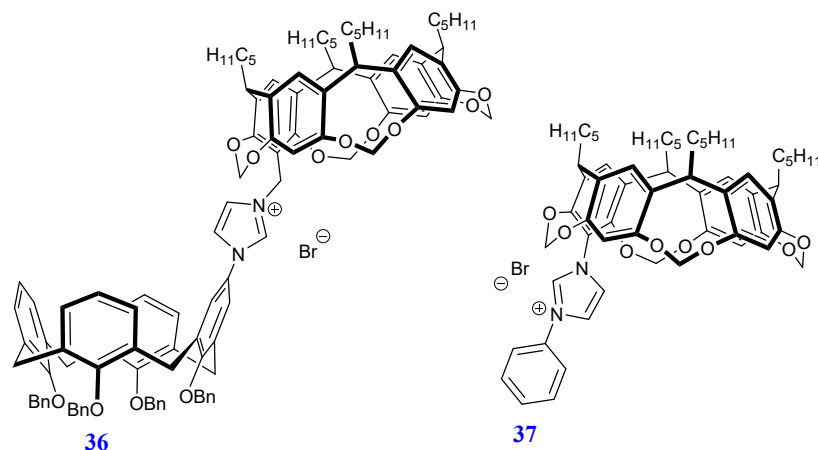


Figure 6. Sels d'imidazolium **36** et **37**

Les auteurs ont ensuite étudié l'influence de la substitution du noyau aromatique des Grignard sur la régiosélectivité de la réaction. Cette étude a été réalisée avec le système catalytique $[\text{Cu}(\text{OTf})_2]/\mathbf{29}$ (Tableau 2).

Les vitesses des réactions observées pour les deux Grignard "para substitués" sont comparables à celle obtenue avec PhMgBr , mais la proportion de produit branché est plus faible (Tableau 2, entrées 1-3). Le substrat $o\text{-Me-(C}_6\text{H}_4\text{)MgCl}$, stériquement plus encombré, conduit à une conversion beaucoup plus faible, alors que le produit branché est formé exclusivement (Tableau 2, entrée 4).

Tableau 2. Alkylation allylique catalysée au cuivre du bromure de cinnamyle avec des halogénures d'arylmagnésien.

Entrée	ArMgX	Conversion (%)	Branché (%)	Linéaire (%)
1	PhMgBr	100	78	22
2	$p\text{-Cl-(C}_6\text{H}_4\text{)MgBr}$	94	52	48
3	$p\text{-F-(C}_6\text{H}_4\text{)MgBr}$	100	62	38
4	$o\text{-Me-(C}_6\text{H}_4\text{)MgCl}$	2	100	0

Conditions: $[\text{Cu}(\text{OTf})_2]$ (1 mol %), sels d'imidazolium **29** (1 mol %), $\text{PhCH=CHCH}_2\text{Br}$ (0,32 mmol), ArMgX (0,39 mmol), Et_2O (3 mL), $-78\text{ }^\circ\text{C}$, 1 h.

Concernant le mécanisme de cette réaction (Schéma 15), on admet que l'aryle-cuprate **A** formé initialement réagit avec le bromure allylique pour former le complexe **B**. Ce dernier conduit, après élimination réductrice, au produit branché alors que son isomérisation en complexe **C** donne le complexe allylique **D**, précurseur du produit linéaire. Ainsi, la régiosélectivité dépend des vitesses relatives de l'élimination réductrice de **B**, et de l'isomérisation de **B** en **D** couplée à l'élimination réductrice subséquente. Pour chacune de ces deux voies, un ligand stériquement très encombré sera de nature à accélérer l'étape d'élimination réductrice, qui conduit au produit branché. Par ailleurs, l'utilisation de substrats stériquement encombrés doit, logiquement, accélérer l'étape d'élimination réductrice et donc favoriser le produit branché. Ce phénomène a pu être observé avec *o*-Me-C₆H₄MgCl (Tableau 2, entrée 4).

Cependant, les résultats expérimentaux montrent que les sélectivités observées avec les sels d'imidazolium ci-dessus restent en-deçà de celles obtenues avec le complexe de Tomioka^[22] (Figure 7). Par exemple, avec le dérivé *p*-Cl-(C₆H₄)MgBr, le ratio branché/linéaire atteint une valeur de b/l de 93/7 avec le sel de Tomioka, contre 52/48 pour le précurseur résorcinarénique **29**.

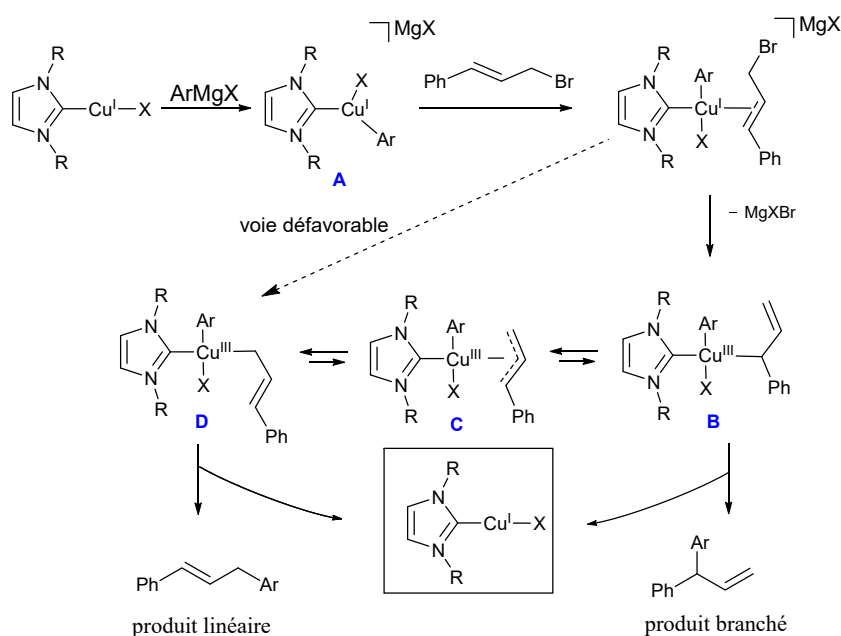


Schéma 15. Mécanisme de la réaction de substitution allylique catalysée par un complexe de cuivre

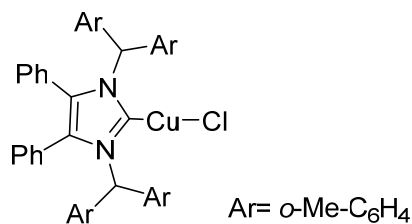


Figure 7. Complexe de Tomioka

Conclusion et objectifs

Comme montré plus haut, l'utilisation en catalyse homogène de coordinats dérivés de cavitands résorcinaréniques a permis d'exploiter efficacement trois propriétés intrinsèques de ces macrocycles : a) leur fort encombrement stérique résultant de la présence d'une cavité rigide ; b) leur capacité à confiner un centre catalytique dans un espace restreint ; c) leur caractère de plateforme multifonctionnalisable. Ces trois propriétés ont, dans certains cas, pu être combinées, donnant alors accès à des catalyseurs dotés de caractéristiques remarquables.

Cette thèse avait pour objectif de synthétiser de nouveaux cavitands résorcinaréniques phosphorés et d'en étudier leurs applications en catalyse homogène. Les objectifs étaient de deux types : a) étudier la possibilité d'utiliser de tels ligands comme chélateurs hétéro-ditopiques bâtis sur un fragment macrocyclique ; b) exploiter la partie cavitaire des ligands synthétisés pour la confection de métallo-capsules autorisant le déroulement d'une réaction catalytique intra-cavité. Ce dernier objectif n'a pour l'instant été réalisé par aucun groupe de recherche.

Annexe du Chapitre 1

Les chapitres 2 et 3 de cette thèse ont trait à la chimie de la phosphine-cavitand **L**, précédemment préparée au laboratoire.^[23] Nous décrivons brièvement, ci-après, les principales propriétés de ce coordinat telles qu'elles étaient connues avant l'étude présentée dans les deux chapitres suivants.

La phosphine **L** peut être obtenue par une synthèse *one-pot* à partir du précurseur monobromé **1** : après échange halogène/lithium, le lithien formé est piégé avec Ph_2PCL , conduisant à la phosphine avec 70 % de rendement (Schéma 1). Le coordinat **L** forme facilement des complexes de palladium(II) comportant un (**2**) ou deux (**3**) ligands (Schéma 1).

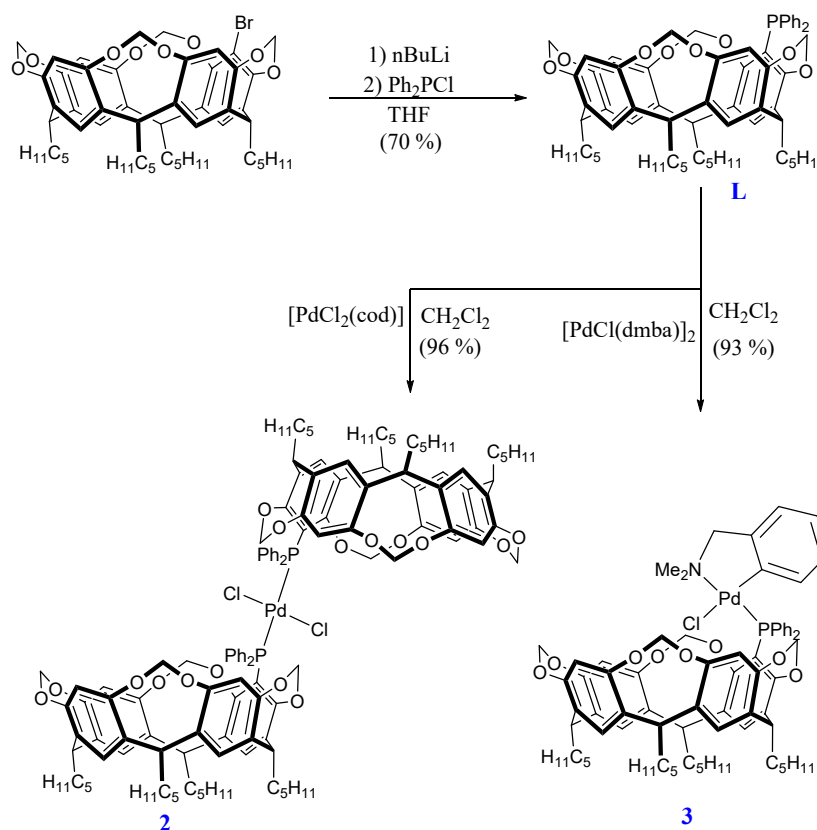


Schéma 1. Synthèse des complexes de palladium **2** et **3**

La caractéristique principale de **L** est d'avoir un encombrement stérique dépendant de la position du groupe PPh₂ par rapport à la cavité. Une étude cristallographique réalisée pour l'oxyde correspondant (Figure 1), combinée à des calculs de modélisation moléculaire montrent que l'angle de Tolman de la version *endo* de la phosphine est d'environ 45° plus grand que celui du composé *exo*.

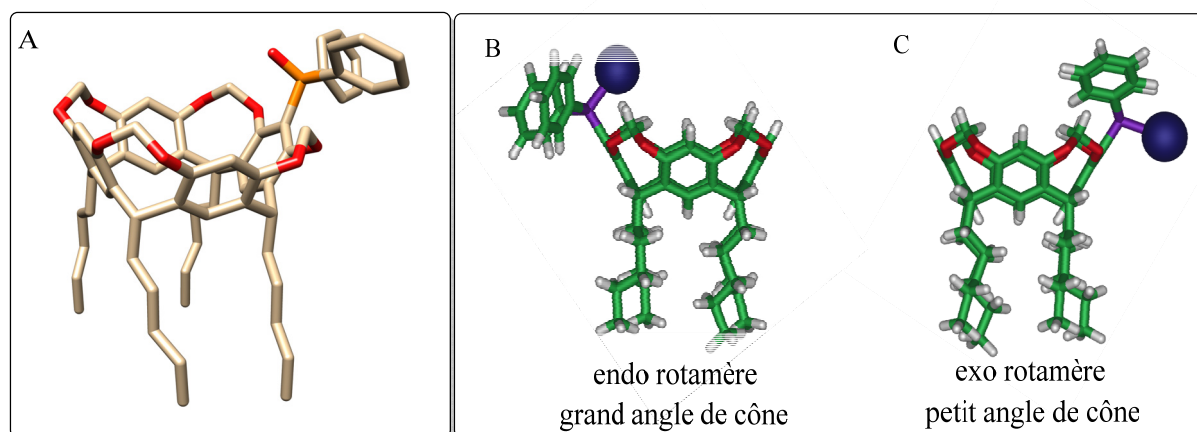


Figure 1. Structure à l'état solide de l'oxyde de phosphine **L=O** (A) et complexes *endo* (B) et *exo* (C) calculés ayant servi à déterminer la variation de l'angle de cône en fonction de l'orientation du doublet du phosphore

La phosphine **L** a été testée dans la réaction de couplage de Suzuki-Miyaura entre halogénures d'aryles et des acides boroniques (Schéma 2). Elle s'est avérée être très efficace, la meilleure activité, 266000 mol(ArBr)mol(Pd)⁻¹h⁻¹ ayant été observée pour le couplage du 4-bromotoluène avec l'acide phénylboronique. Les bonnes performances de ce ligand ont été attribuées à son encombrement stérique important qui favorise la formation d'intermédiaires mono-ligandés [Pd(ArX)L] au cours du cycle catalytique (Schéma ---3). Ces intermédiaires sont réputés favoriser l'étape élémentaire d'addition oxydante de l'halogénure d'aryle, étape généralement cinétiquement déterminante.

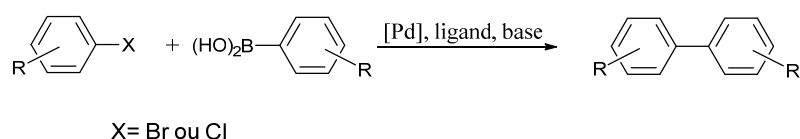


Schéma 2. Réaction de couplage de Suzuki-Miyaura

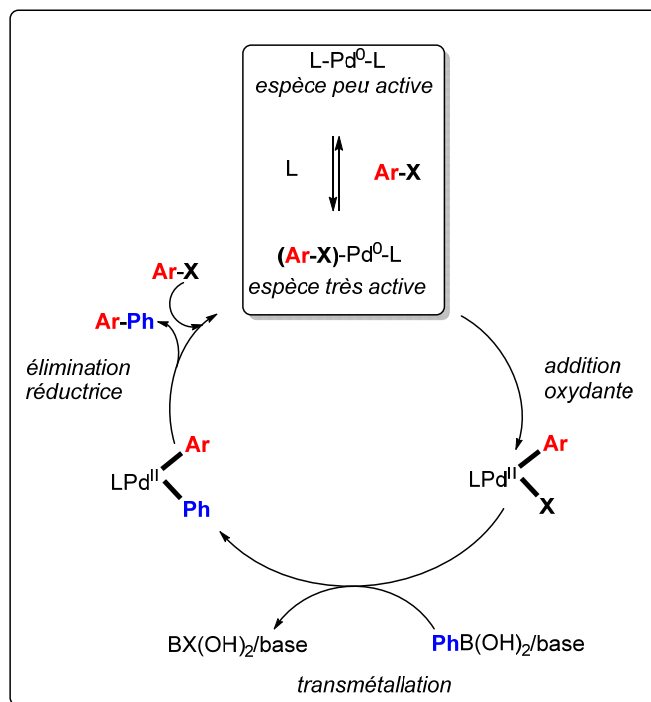


Schéma 3. Mécanisme de couplage de Suzuki-Miyaura pour des phosphines stériquement encombrées favorisant la formation d'espèces mono-ligandés $[Pd^0(\eta^6-ArX)L]$

Une autre phosphine résorcinarénique, **4** (Figure 2), coordinat plus basique et stériquement plus encombré, s'est révélée particulièrement performante dans la réaction de couplage de Suzuki-Miyaura entre chlorures d'aryles et acides boroniques. Il a été ainsi possible d'obtenir des biphényles ortho-disubstitués avec de bonnes conversions.

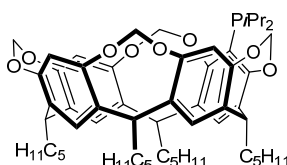


Figure 2. Phosphine-cavitand **4**

Enfin, l'activité de la phosphine **L** a été comparée aux trois triarylphosphines **5-7**, toutes dépourvues d'unités cavitaires. Les conversions observées, qui augmentent dans l'ordre $5 < 6 < 7 < L$ (Schéma 4), montrent clairement le rôle bénéfique joué par les fonctions éther

du cavitant ainsi que celui de l'entité macrocyclique elle-même. La présence de substituants méthoxy ou OCH_2 augmente à la fois l'encombrement stérique et la basicité de la phosphine, deux paramètres qui facilitent chacun l'étape élémentaire d'addition oxydante. En outre, la présence d'atomes d'oxygène dans **6**, **7** et **1** est susceptible de conduire à la formation de chélates P,O hémilabiles au cours du cycle catalytique. Dans les intermédiaires correspondants, le centre métallique sera enrichi en électron et l'encombrement stérique autour de ce dernier augmenté. Ces deux phénomènes auront pour effet de faciliter les étapes élémentaires d'addition oxydante et d'élimination réductrice du cycle catalytique.

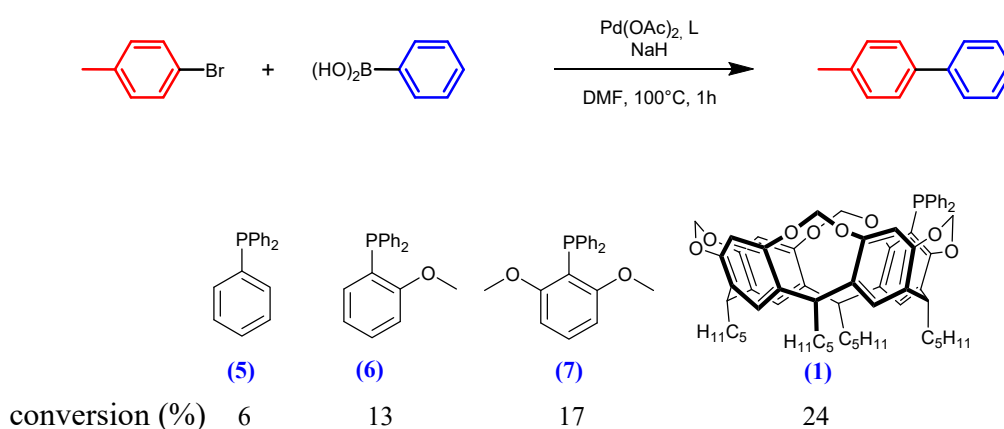


Schéma 4. Comparaison de l'activité des différentes triarylphosphines

Une des questions que nous nous sommes posées était de savoir si la phosphine résorcinarénique **1** pouvait effectivement former des complexes chélates hémilabiles phosphore-oxygène (P,O) à 4 électrons (Figure 2).

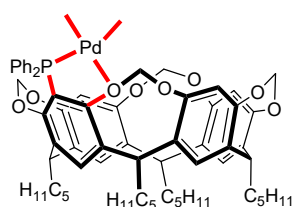


Figure 2. Complexe chélate P,O hypothétique

C'est cette dernière interrogation qui a été à l'origine des études développées dans les chapitres 2 et 3.

Références

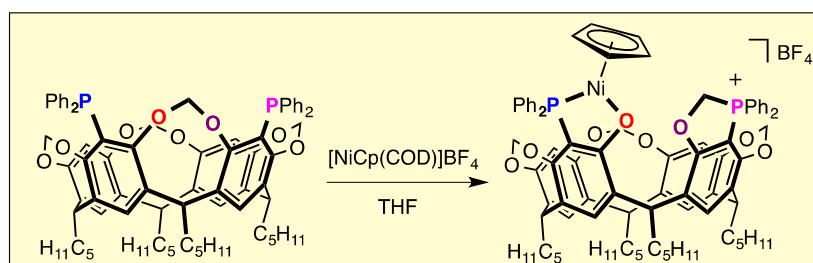
- [1] a) A. Baeyer, *Ber. Dtsch. Chem. Ges.* **1872**, *5*, 25-26; b) A. Baeyer, *Ber. Dtsch. Chem. Ges.* **1872**, *5*, 280-282.
- [2] A. Michael, *Am. Chem. J.* **1883**, *5*, 338-339.
- [3] J. B. Niederl and H. J. Vogel, *J. Am. Chem. Soc.* **1940**, *62*, 2512-2514.
- [4] H. Erdtman, S. Högberg, S. Abrahamsson and B. Nilsson, *Tetrahedron Lett.* **1968**, *9*, 1679-1682.
- [5] J. R. Moran, S. Karbach and D. J. Cram, *J. Am. Chem. Soc.* **1982**, *104*, 5826-5828.
- [6] a) J. R. Moran, J. L. Ericson, E. Dalcanale, J. A. Bryant, C. B. Knobler and D. J. Cram, *J. Am. Chem. Soc.* **1991**, *113*, 5707-5714; b) V. A. Azov, A. Beeby, M. Cacciarini, A. G. Cheetham, F. Diederich, M. Frei, J. K. Gimzewski, V. Gramlich, B. Hecht, B. Jaun, T. Latychevskaia, A. Lieb, Y. Lill, F. Marotti, A. Schlegel, R. R. Schlittler, P. J. Skinner, P. Seiler and Y. Yamakoshi, *Adv. Funct. Mater.* **2006**, *16*, 147-156.
- [7] a) T. Sokolies, A. Opolka, U. Menyes, U. Roth and T. Jira, *Die Pharmazie* **2002**, *57*, 589-590; b) O. Pietraszkiewicz and M. Pietraszkiewicz, *J. Inclusion Phenom. Macrocyclic Chem.* **1999**, *35*, 261-270.
- [8] a) H. Boerrigter, W. Verboom and D. N. Reinhoudt, *J. Org. Chem.* **1997**, *62*, 7148-7155; b) P. Amrhein, A. Shivanyuk, D. W. Johnson and J. Rebek, *J. Am. Chem. Soc.* **2002**, *124*, 10349-10358.
- [9] a) I. Higler, P. Timmerman, W. Verboom and D. N. Reinhoudt, *J. Org. Chem.* **1996**, *61*, 5920-5931; b) B. Botta, F. Caporuscio, I. D'Acquarica, G. Delle Monache, D. Subissati, A. Tafi, M. Botta, A. Filippi and M. Speranza, *Chem. Eur. J.* **2006**, *12*, 8096-8105.
- [10] a) F. S. McQuillan, T. E. Berridge, H. Chen, T. A. Hamor and C. J. Jones, *Inorg. Chem.* **1998**, *37*, 4959-4970; b) L. Pirondini, D. Bonifazi, E. Menozzi, E. Wegelius, K. Rissanen, C. Massera and E. Dalcanale, *Eur. J. Org. Chem.* **2001**, *2001*, 2311-2320.
- [11] D. Sémeril and D. Matt, *Coord. Chem. Rev.* **2014**, *279*, 58-95.
- [12] C. Gibson and J. Rebek, *Org. Lett.* **2002**, *4*, 1887-1890.
- [13] M. P. Schramm, M. Kanaura, K. Ito, M. Ide and T. Iwasawa, *Eur. J. Org. Chem.* **2016**, *2016*, 813-820.
- [14] H. El Moll, D. Sémeril, D. Matt and L. Toupet, *Eur. J. Org. Chem.* **2010**, *2010*, 1158-1168.
- [15] H. E. Moll, D. Sémeril, D. Matt, M.-T. Youinou and L. Toupet, *Org. Biomol. Chem.* **2009**, *7*, 495-501.
- [16] H. El Moll, D. Sémeril, D. Matt and L. Toupet, *Adv. Synth. Catal.* **2010**, *352*, 901-908.
- [17] H. El Moll, D. Sémeril, D. Matt, L. Toupet and J.-J. Harrowfield, *Org. Biomol. Chem.* **2012**, *10*, 372-382.
- [18] a) N. Şahin, D. Sémeril, E. Brenner, D. Matt, İ. Özdemir, C. Kaya and L. Toupet, *ChemCatChem* **2013**, *5*, 1116-1125; b) M. Kaloğlu, D. Sémeril, E. Brenner, D. Matt, İ. Özdemir and L. Toupet, *Eur. J. Inorg. Chem.* **2016**, *2016*, 1115-1120.
- [19] N. Şahin, D. Sémeril, E. Brenner, D. Matt, C. Kaya and L. Toupet, *Turk. J. Chem.* **2015**, *39*, 1171-1179.
- [20] N. Şahin, D. Sémeril, E. Brenner, D. Matt, İ. Özdemir, C. Kaya and L. Toupet, *Eur. J. Org. Chem.* **2013**, *2013*, 4443-4449.
- [21] M. Kaloğlu, N. Şahin, D. Sémeril, E. Brenner, D. Matt, İ. Özdemir, C. Kaya and L. Toupet, *Eur. J. Org. Chem.* **2015**, *2015*, 7310-7316.

- [22] a) K. B. Selim, Y. Matsumoto, K.-i. Yamada and K. Tomioka, *Angew. Chem. Int. Ed* **2009**, *48*, 8733-8735; b) K. B. Selim, H. Nakanishi, Y. Matsumoto, Y. Yamamoto, K.-i. Yamada and K. Tomioka, *Eur. J. Org. Chem.* **2011**, *76*, 1398-1408.
- [23] L. Monnereau, H. El Moll, D. Sémeril, D. Matt, and L. Toupet, *Eur. J. Inorg. Chem.* **2014**, 1364-1372.

Chapter II

Cracking cavitands: Metal-directed scission of phosphinyl-substituted resorcinarenes

Abstract: Resorcinarene-derived tetramethylene cavitands bearing a diphenylphosphino group grafted to their wider rim undergo facile, directed C–O bond breaking upon reaction with transition metal ions in the presence of nucleophiles. One possible reaction mechanism involves formation of a *P,O* chelate complex which weakens the adjacent O–CH₂ bond, leading to the formation of an oxocarbenium intermediate.



Introduction

Resorcinarenes which have been made conformationally rigid by placing methylene linkers between all pairs of neighbouring hydroxy oxygen atoms constitute an important class of bowl-shaped molecules (cavitands) widely used as building blocks for applications in host-guest chemistry, coordination chemistry, homogeneous catalysis and materials science.^[1] The scaffold of such cavitands is regarded as extremely robust, a wide variety of reactions aimed at the introduction of functional groups at the periphery leaving the container structure unaffected.^[2] Thus, while partially bridged cavitands have been prepared in one-step procedures from generic resorcinarene skeletons, core modification/breaking of a tetramethylene cavitand scaffold has not been reported.^[3]

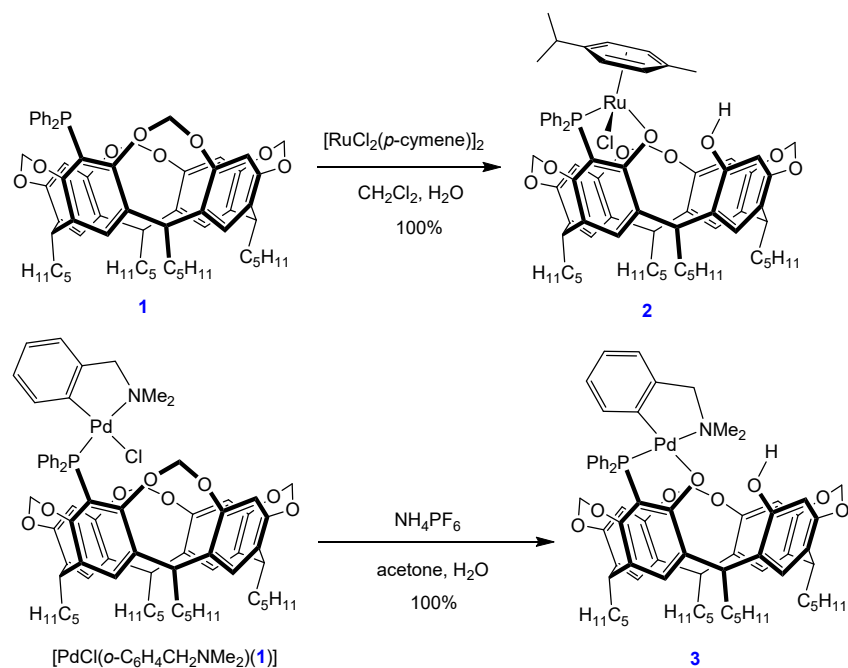
We have recently reported the synthesis of cavitand **1**, having a diphenylphosphino group grafted to its wider rim.^[4] The capacity of **1** to behave as a bulky, P-monodentate ligand was demonstrated in the synthesis of several Pd^{II} complexes. As the phosphino-aryl moiety of **1** is flanked by two ether oxygen atoms which could enable the formation of highly crowded *P,O*-chelate complexes, we considered that this might influence the strain within the cavity core and possibly modify the cavitand structure. In the present report, we show that under conditions that lead to the formation of *P,O*-chelate complexes, cavitand **1** readily undergoes selective breaking of a specific C–O bond of the resorcinarene skeleton.

Results and discussion

Reaction at room temperature of **1** with [Ru(*p*-cymene)Cl₂]₂ in *wet* CH₂Cl₂ resulted after cleavage of a C–O bond and loss of a methylene group nearly quantitatively in chelate complex **2** (Scheme 1, top). Consistent with a "cracked cavitand" structure, the corresponding ¹H NMR spectrum showed only three distinct AB patterns arising from OCH₂ groups as well as a singlet at 9.34 ppm typical of a phenolic OH proton.

The structure of **2** was confirmed by an X-ray diffraction study (Figure 1), which also revealed that the Ru-(*p*-cymene) bond is turned away from the cavity wall, thus minimising the steric interactions of the "Ru(arene)Cl" unit with the cavitand core. Consistent with the expected strain release induced by the crack, the separation between the *O*(Ru) and *O*(H) atoms is 0.25 Å longer than that between methylene-bridged O atoms (mean 2.36 Å). The

related palladium complex **3** was obtained by chloride abstraction from $[\text{Pd}(o\text{-C}_6\text{H}_4\text{CH}_2\text{NMe}_2)\text{Cl}\cdot\mathbf{1}]^{[4]}$ with $\text{NH}_4\text{PF}_6/\text{H}_2\text{O}$ (Scheme 1, bottom and Figure 1).



Scheme 1. Complexation induced, selective C–O bond breaking of phosphino-cavitand **1**. Top: starting from free **1**; bottom: starting from the phosphine complex $[\text{Pd}(o\text{-C}_6\text{H}_4\text{CH}_2\text{NMe}_2)\text{Cl}]$

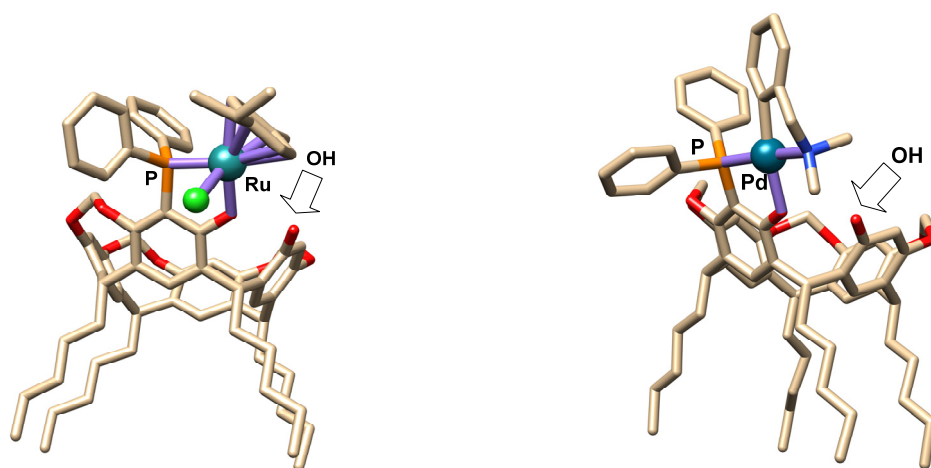
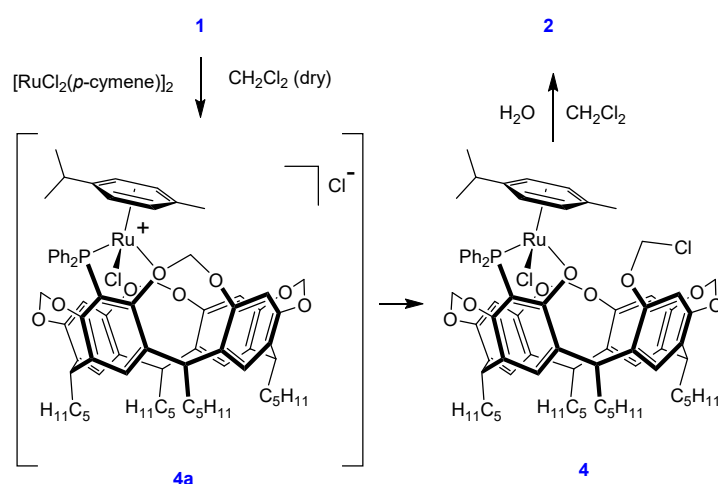


Figure 1. Molecular structure of complexes **2** (left) and **3** (right). Cavitand **2** contains an entrapped CH_2Cl_2 molecule which has been omitted for clarity. The unit cells contain also the mirror images of the molecules shown

Repeating the reaction leading to **2** under rigorously dry conditions produced **4**, which unlike **2**, contains *four* (distinct) OCH₂ groups and no hydroxyl group (Scheme 2). The presence of a pendent OCH₂Cl group was inferred from the ¹³C NMR spectrum of **4** which showed the corresponding methylene signal at 87.1 ppm (*cf.* 84.8 ppm for ClCH₂OMe^[5]), the three bridging methylene groups being, as usual for tetramethylene cavitands, found near 99 ppm. It is worth mentioning that monitoring this reaction by NMR spectroscopy did not enable the observation of the probable intermediate **4a**. Note that **4** is extremely water sensitive, addition of traces of water to a solution of **4** producing instantaneously complex **2**.



Scheme 2. Reaction of phosphino-cavitand **1** with [Ru(*p*-cymene)Cl₂]₂ in CH₂Cl₂

One plausible mechanism for the formation of **4** involves cleavage of the RuO–CH₂O bond of **4a** with subsequent formation of an oxacarbenium unit (Ar–O⁺=CH₂), this latter step being a consequence of the complexation-induced strain increase within the 8-membered ring containing the coordinated –OCH₂O– fragment. Once formed, such an oxacarbenium moiety would be highly susceptible to nucleophilic attack by an external nucleophile, if available. To evaluate this possibility, ligand **5**, which contains two remote P(III) atoms, was reacted in dry CH₂Cl₂ with one equivalent of the chloride-free complex [Ni(η⁵-C₅H₅)(COD)]BF₄ (COD = 1,5-cyclooctadiene), a potential precursor of cationic *P,O*-chelate complexes (Scheme 3).

Monitoring the reaction by NMR spectroscopy revealed the presence of several transient species, but after 5 days' reaction time only the phosphonium-nickel complex **6** was formed, in quantitative yield. Reaction of **6** with water in air slowly resulted in loss of nickel with production of the mixed phosphonium-phosphine oxide **7**, the structure of which was confirmed by an X-ray diffraction study (Figure 2). This structure determination constitutes also an unambiguous proof for the regioselectivity of the C–O bond cleavage. Clearly, only the formation of a pendent $[-O=CH_2]^+$ oxocarbenium moiety as in **6b** (Scheme 3) able to approach the pro-phosphonium atom P2 makes formation of a P–C bond possible, direct nucleophilic attack of the P2 atom on a coordinated, remote $-OCH_2O$ fragment as in **6a** being impeded by the conformational restrictions of the cavitand. The fact that complex **6** formed very slowly and that several transient species can be seen before formation of **6** is consistent with the reversible generation of an oxonium unit from any of the two OCH_2O bridges attached to the phosphino-aryl group undergoing nickel binding but with only one of them being able to react with P2.^[6]

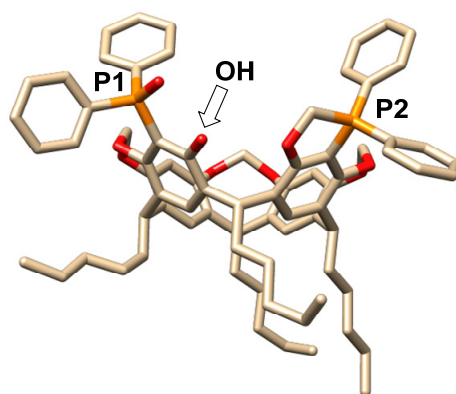
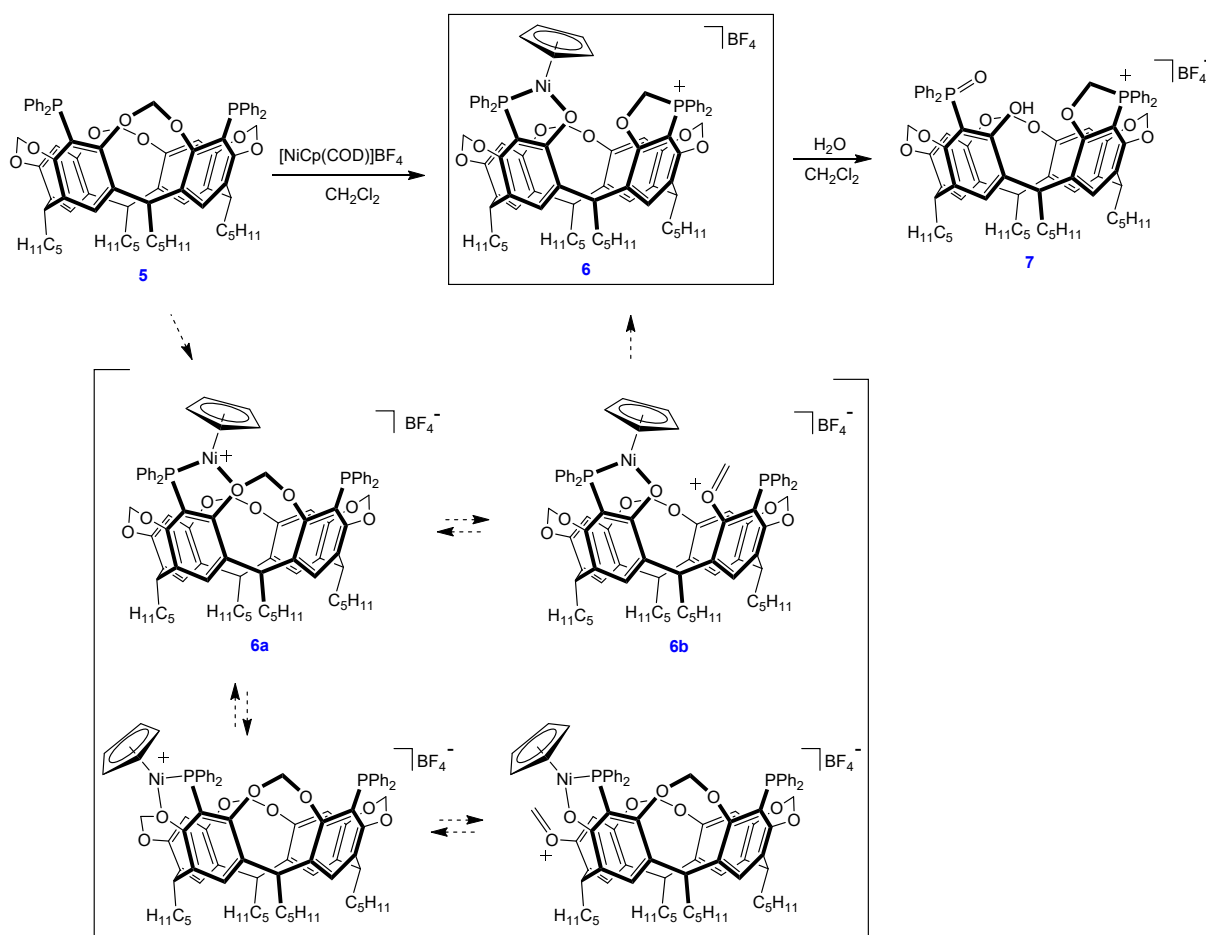


Figure 2. Molecular structure of the mixed phosphine oxide-phosphonium salt **7**. The $[BF_4]^-$ anion and all CH_2Cl_2 molecules have been omitted for clarity

Finally, we tested the reactivity of **6** towards ethylene. Thus, after activation of **6** with $NaBH_4$,^[7] and by operating in toluene at $90^\circ C$, ethylene was rapidly converted mainly into 1-butene and 1-hexene (TOF: $2520 \text{ mol}(C_2H_4) \cdot \text{mol}(Ni)^{-1} \cdot h^{-1}$; 1-butene: 72.4%; 1-hexene: 27.4%; 1-octene: 0.2%; only trace amounts of isomerisation products were seen).^[8] The catalytic outcome contrasts with that observed for classical phosphino-enolato nickel complexes that do not contain an additional phosphine ligand, which typically result in long

chain α -olefins under the above conditions.^[9] Similar results were obtained when replacing NaBH_4 with NBu_4BH_4 , this excluding a cation effect. We tentatively propose that after activation with tetraborohydride, the borane formed binds the enolato oxygen atom of **6** thereby rendering the latter a weaker donor. Such an electronic effect is known to favour β -elimination over chain growth in ethylene oligomerisation/polymerisation.



Scheme 3. Formation of **6** and **7** through the proposed “oxocarbenium mechanism”

Conclusion

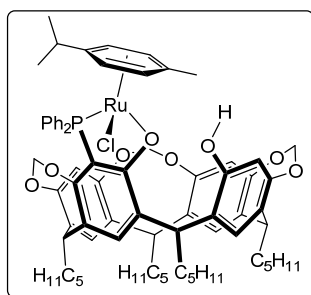
Thus, we have shown, for the first time, that properly functionalised tetramethylene cavitaands can be cleaved regioselectively in the presence of a metal centre, thereby resulting in slightly more flexible and enlarged, hydroxylated cavities suitable for further functionalisation. Incidentally, this study provides also a new entry to the valuable family of industrially-relevant nickel P,O chelate complexes. As, in principle, X,O -analogues of the 3-electron P,O -chelates obtained in the above reactions may form with resorcinarenes substituted by functional groups containing other donor atoms (X), we anticipate that our findings will give

access to a variety of new partly open, functionalised cavitands. The associated C–O bond cleavage may, of course, not necessarily involve metal ions of the transition series.

Experimental Section

General Methods: All manipulations involving phosphorus derivatives were performed in Schlenk-type flasks under dry nitrogen. Solvents were dried by conventional methods and distilled immediately prior to use. CDCl₃ was passed down a 5 cm thick alumina column and stored under nitrogen over molecular sieves (4 Å). Routine ¹H, ¹³C{¹H} and ³¹P{¹H} NMR spectra were recorded with Bruker FT spectrometers (AVANCE 400 and 500). ¹H chemical shifts are referenced to residual protonated solvents ($\delta = 7.26$ ppm for CDCl₃), ¹³C chemical shifts are reported relative to deuteriated solvents ($\delta = 77.16$ ppm for CDCl₃) and the ³¹P NMR spectroscopic data are given relative to external H₃PO₄. Chemical shifts and coupling constants are reported in ppm and Hz, respectively. Elemental analyses were performed by the Service de Microanalyse, Institut de Chimie, Université de Strasbourg. Gas chromatographic analyses were performed on a VARIAN 3900 gas chromatograph using a WCOT fused silica column (25 m, 0.32 mm inside diameter, 0.25 mm film thickness). 5-Diphenylphosphanyl-4(24),6(10),12(16),18(22)-tetramethylenedioxy-2,8,14,20-tetra-pentylresorcin[4]arene (**1**),^[10] chlorido(*o*-dimethylaminomethylphenyl-*C,N*)[5-diphenylphosphanyl-4(24),6(10),12(16),18(22)-tetramethylenedioxy-2,8,14,20-tetrapentylresorcin[4]arene]palladium(II),^[10] 5,11-dibromo-4(24),6(10),12(16),18(22)-tetramethylenedioxy-2,8,14,20-tetrapentylresorcin[4]arene,^[11] [NiCp(cod)]BF₄^[12] (cod = 1,5-cyclooctadiene), [RuCl₂(*p*-cymene)]₂^[13] and [PdCl(dmba)]₂^[14] (dmbaH = *o*-C₆H₅CH₂NMe₂) were prepared according to literature procedures.

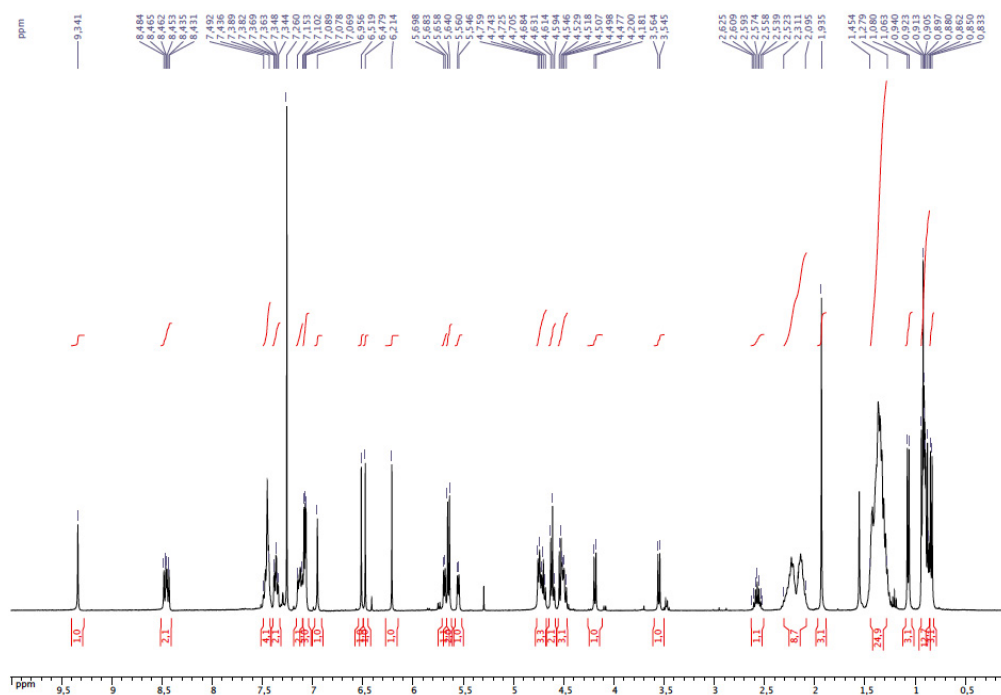
Synthesis of complex **2**



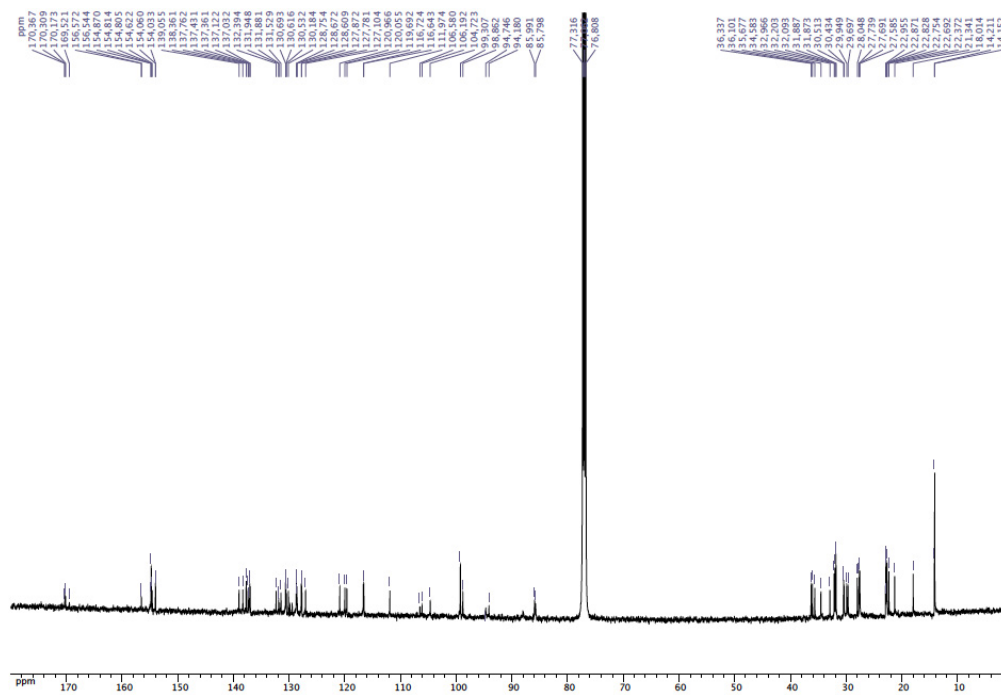
A solution of $[\text{RuCl}_2(p\text{-cymene})]_2$ (0.031 g, 0.05 mmol) in *wet* CH_2Cl_2 (5 mL) was added to a stirred solution of phosphine **1** (0.100 g, 0.10 mmol) in *wet* CH_2Cl_2 (5 mL). After stirring at r.t. for 16 h, the reaction mixture was concentrated to ca. 2 mL, then *n*-hexane (20 mL) was added. The orange precipitate formed was separated by filtration and dried under vacuum, yield 0.122 g, 93 %. ^1H NMR (400 MHz, CDCl_3): δ = 9.34 (s, 1H, OH), 8.48-8.43 (m, 2H, arom. CH, PPh_2), 7.49-7.44 (m, 4H, arom. CH, PPh_2), 7.36 (dt, 2H, arom. CH, PPh_2 , $^3J = 8.0$ Hz, $^4J = 2.8$ Hz), 7.15-7.10 (m, 2H, arom. CH, PPh_2), 7.09 (s, 1H, arom. CH, resorcinarene), 7.08 (s, 1H, arom. CH, resorcinarene), 7.07 (s, 1H, arom. CH, resorcinarene), 6.96 (s, 1H, arom. CH, resorcinarene), 6.52 (s, 1H, arom. CH, resorcinarene), 6.48 (s, 1H, arom. CH, resorcinarene), 6.21 (s, 1H, arom. CH, resorcinarene), 5.69 and 4.75 (AA' of an AA'BB' spin system, 2H, arom. CH, *p*-cymene, $^3J = 6.0$ Hz), 5.65 and 4.62 (AB spin system, 2H, OCH_2O , $^2J = 7.2$ Hz), 5.65 and 4.54 (AB spin system, 2H, OCH_2O , $^2J = 7.2$ Hz), 5.55 and 4.51 (BB' of an AA'BB' spin system, 2H, arom. CH, *p*-cymene, $^3J = 5.6$ Hz), 4.70 (t, 2H, CHCH_2 , $^3J = 8.2$ Hz), 4.61 (t, 1H, CHCH_2 , $^3J = 8.0$ Hz), 4.50 (t, 1H, CHCH_2 , $^3J = 8.0$ Hz), 4.19 and 3.55 (AB spin system, 2H, OCH_2O , $^2J = 7.6$ Hz), 2.57 (hept, 1H, $\text{CH}(\text{CH}_3)_2$, $^3J = 7.0$ Hz), 2.31-2.22 (m, 4H, CHCH_2), 2.22-2.09 (m, 4H, CHCH_2), 1.93 (s, 3H, CH_3 of *p*-cymene), 1.45-1.28 (m, 24H, $\text{CH}_2\text{CH}_2\text{CH}_2\text{CH}_3$), 1.07 (d, 3H, $\text{CH}(\text{CH}_3)_2$, $^3J = 7.0$ Hz), 0.92 (t, 6H, CH_2CH_3 , $^3J = 6.8$ Hz), 0.91 (t, 3H, CH_2CH_3 , $^3J = 6.4$ Hz), 0.88 (t, 3H, CH_2CH_3 , $^3J = 7.2$ Hz), 0.84 (d, 3H, $\text{CH}(\text{CH}_3)_2$, $^3J = 7.0$ Hz); $^{13}\text{C}\{^1\text{H}\}$ NMR (125 MHz, CDCl_3): δ = 170.37-104.72 (arom. C's), 99.31 (s, OCH_2O), 98.86 (s, OCH_2O), 94.75 (s, arom. CH, *p*-cymene), 94.18 (s, arom. Cquat, *p*-cymene), 88.00 (s, arom. CH, *p*-cymene), 85.99 (s, arom. CH, *p*-cymene), 85.80 (s, arom. CH, *p*-cymene), 36.34 (s, CHCH_2), 36.10 (s, CHCH_2), 35.68 (s, CHCH_2), 34.58 (s, CHCH_2), 32.97 (s, CHCH_2), 32.20 (s, $\text{CH}_2\text{CH}_2\text{CH}_3$), 32.09 (s, $\text{CH}_2\text{CH}_2\text{CH}_3$), 31.89 (s, $\text{CH}_2\text{CH}_2\text{CH}_3$), 31.87 (s, $\text{CH}_2\text{CH}_2\text{CH}_3$), 30.51 (s, $\text{CH}(\text{CH}_3)_2$), 30.43 (s, CHCH_2), 29.95 (s, CHCH_2), 29.70 (s,

CHCH₂), 28.04 (s, CHCH₂CH₂), 27.74 (s, CHCH₂CH₂), 27.69 (s, CHCH₂CH₂), 27.58 (s, CHCH₂CH₂), 22.95 (s, CH₂CH₃), 22.87 (s, CH₂CH₃), 22.83 (s, CH₂CH₃), 22.69 (s, CH₂CH₃), 22.37 (s, CH(CH₃)₂), 21.34 (s, CH(CH₃)₂), 18.01 (s, CH₃ of *p*-cymene), 14.21 (s, CH₂CH₃), 14.15 (s, CH₂CH₃); ³¹P{¹H} NMR (162 MHz, CDCl₃): δ = 43.6 (s, PPh₂); MS (ESI-TOF): *m/z* = 1258.49 [M⁺] expected isotopic profile; elemental analysis calcd (%) for C₇₃H₈₆ClO₈PRu (1258.48): C 69.64, H 6.88; found (%): C 69.95, H 6.75.

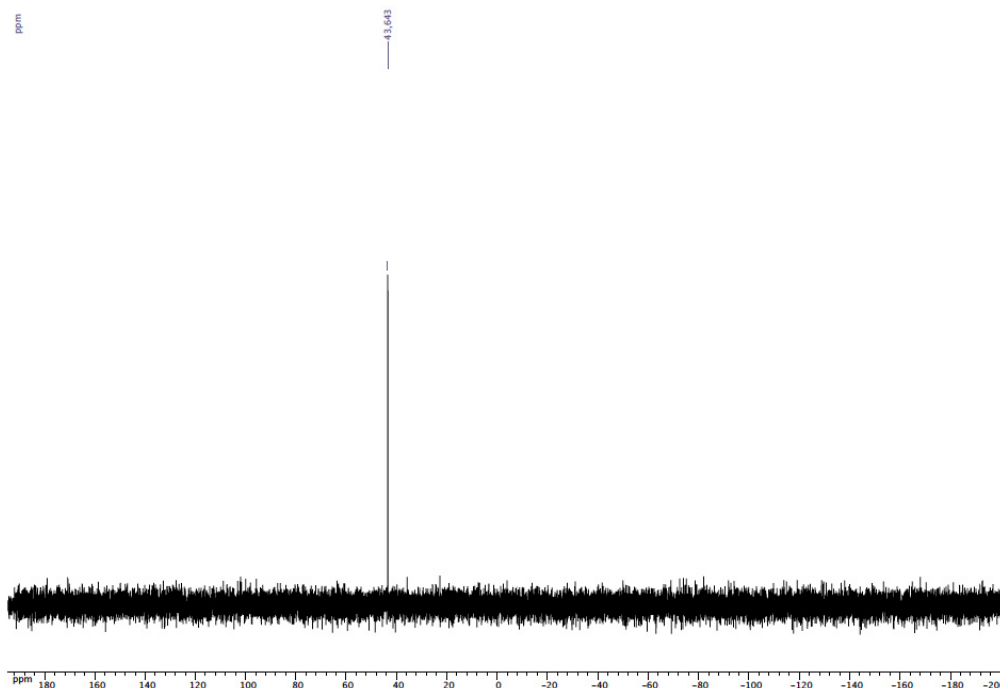
X-ray Crystallographic Data: Orange single crystals of **2** suitable for X-ray diffraction were obtained by slow diffusion of methanol into a CH₂Cl₂ solution of **2** at room temperature. The sample (0.201 X 0.077 X 0.075 mm) was mounted on an Oxford Diffraction Xcalibur Saphir 3 diffractometer with graphite-monochromatised Mo-*K*_α radiation. Formula of the crystals: C₇₃H₈₆ClO₈PRu·CH₄O, *M*_r = 1291.00, monoclinic, space group *P*2₁/*c*, *a* = 10.4928(3), *b* = 36.6719(10), *c* = 17.2895(5) Å, β = 92.530(3)°, *V* = 646.4(3) Å³, *Z* = 4, *D*_x = 1.290 mg·m⁻³, λ(Mo-*K*_α) = 0.71073 Å, μ = 0.357 mm⁻¹, *F*(000) = 2728, *T* = 130(2) K. Data collection (2θ_{max} = 27.5°, ω scan frames via 0.7° ω rotation and 30 s per frame, range *hkl*: *h* -12 to 13, *k* -46 to 44, *l* -21 to 22) gave 55643 reflections. The data revealed 14493 independent reflections of which 8805 were observed with *I* > 2.0 σ(*I*). The structure was solved by using SIR-97,^[15] which revealed the non-hydrogen atoms of the molecule. After anisotropic refinement, all the hydrogen atoms were found by Fourier difference. The whole structure was refined with SHELXL97^[16] by using the full-matrix least squares technique {use of *F*²; *x*, *y*, *z*, β_{*ij*} for C, Cl, O, P and Ru atoms, *x*, *y*, *z* in the riding mode for H atoms; 777 variables and 8805 observations with *I* > 2.0 σ(*I*); calcd. *w* = 1/[σ²(*F*_o²) + (0.0503*P*)² + 4.3607*P*] in which *P* = (*F*_o² + 2 *F*_c²)/3 with the resulting *R* = 0.0621, *R*_w = 0.1182 and *S*_w = 1.02, Δρ < 1.000 eÅ⁻³}. CCDC-981375 contains the supplementary crystallographic data for **2** which can be obtained free of charge from The Cambridge Crystallographic Data Centre via www.ccdc.cam.ac.uk/data_request/cif.



^1H NMR spectrum of **2** (CDCl_3)

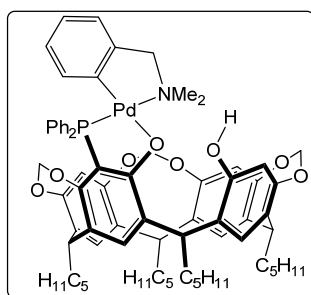


$^{13}\text{C}\{^1\text{H}\}$ NMR spectrum of **2** (CDCl_3)



$^{31}\text{P}\{^1\text{H}\}$ NMR spectrum of **2** (CDCl_3)

Synthesis of complex **3**

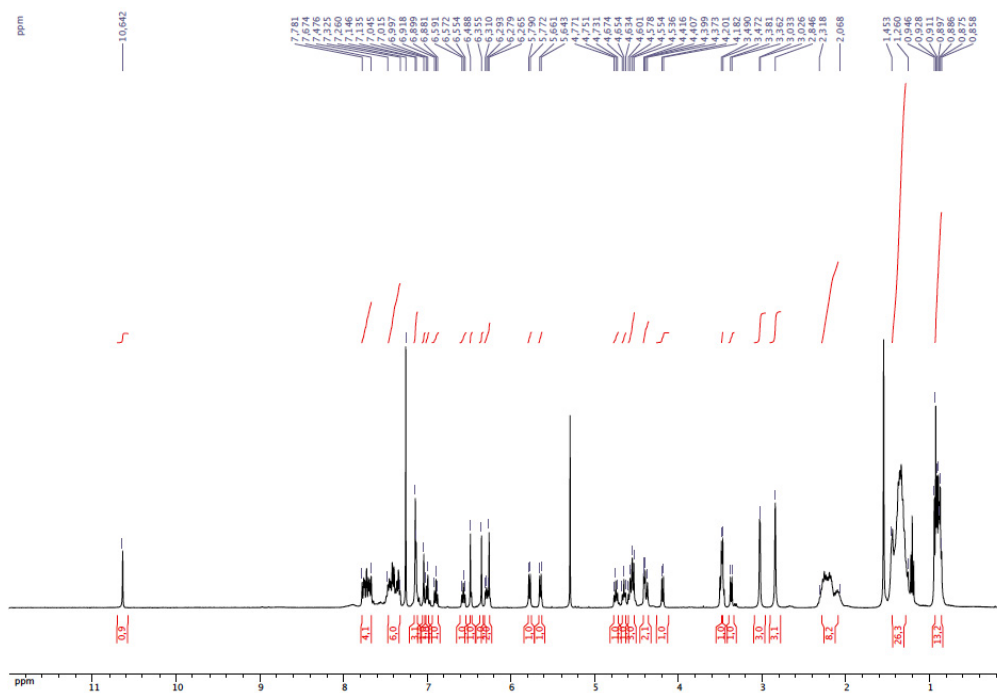


A solution of $[\text{PdCl}(\text{dmba})\mathbf{1}]$ (0.090 g, 0.07 mmol) in *wet* acetone (20 mL) was stirred in the presence of NH_4PF_6 (0.011g, 0.07 mmol) at room temperature for 5 d. The mixture was concentrated to ca. 2 mL and *n*-hexane (20 mL) was added. The yellow precipitate formed was separated by filtration and purified by column chromatography ($\text{CH}_2\text{Cl}_2/\text{MeOH}$, 9:1 v/v) to afford complex **3** as a yellow solid, yield 0.064 g, 75 %. ^1H NMR (400 MHz, CDCl_3): δ = 10.64 (s, 1H, OH), 7.78-7.67 (m, 4H, arom. CH, PPh_2), 7.47-7.32 (m, 6H, arom. CH, PPh_2), 7.15 (s, 2H, arom. CH, resorcinarene), 7.13 (s, 1H, arom. CH, resorcinarene), 7.04 (s, 1H,

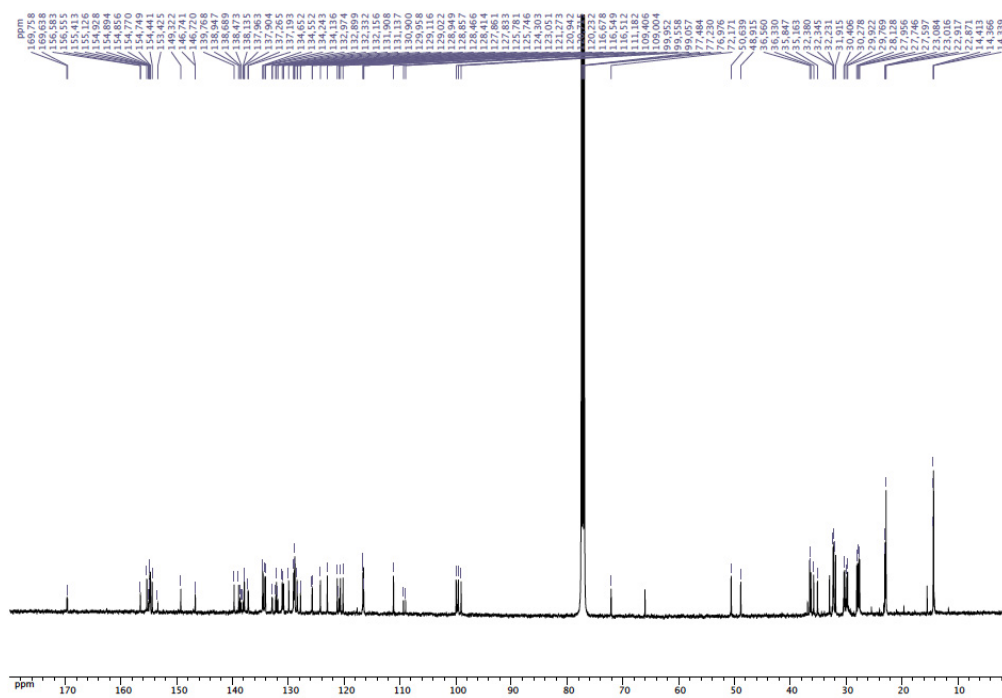
arom. CH, resorcinarene), 7.06 (d, 1H, arom. CH, dmbs, $^3J = 7.2$ Hz), 6.90 (t, 1H, arom. CH, dmbs, $^3J = 7.4$ Hz), 6.57 (t, 1H, arom. CH, dmbs, $^3J = 7.4$ Hz), 6.49 (s, 1H, arom. CH, resorcinarene), 6.35 (s, 1H, arom. CH, resorcinarene), 6.30 (d, 1H, arom. CH, dmbs, $^3J = 7.2$ Hz), 6.26 (s, 1H, arom. CH, resorcinarene), 5.78 and 4.54 (AB spin system, 2H, OCH₂O, $^2J = 7.2$ Hz), 5.65 and 4.41 (AB spin system, 2H, OCH₂O, $^2J = 7.2$ Hz), 4.75 (t, 1H, CHCH₂, $^3J = 8.0$ Hz), 4.65 (t, 1H, CHCH₂, $^3J = 8.0$ Hz), 4.58 (t, 1H, CHCH₂, $^3J = 8.0$ Hz), 4.55 (t, 1H, CHCH₂, $^3J = 8.0$ Hz), 4.41 and 3.48 (AB spin system, 2H, NCH₂, $^3J = 7.2$ Hz), 4.19 and 3.37 (AB spin system, 2H, OCH₂O, $^2J = 7.6$ Hz), 3.03 (d, 3H, N(CH₃)₂, $^4J_{\text{PH}} = 2.8$ Hz), 2.85 (s, 3H, N(CH₃)₂), 2.32-2.07 (m, 8H, CHCH₂), 1.45-1.26 (m, 24H, CH₂CH₂CH₂CH₃), 0.93 (t, 6H, CH₂CH₃, $^3J = 7.0$ Hz), 0.90 (t, 3H, CH₂CH₃, $^3J = 7.0$ Hz), 0.87 (t, 3H, CH₂CH₃, $^3J = 6.8$ Hz); ¹³C{¹H} NMR (125 MHz, CDCl₃): $\delta = 169.76$ - 109.00 (arom. C's), 99.95 (s, OCH₂O), 99.56 (s, OCH₂O), 99.06 (s, OCH₂O), 72.17 (s, NCH₂), 50.64 (s, N(CH₃)₂), 48.91 (s, N(CH₃)₂), 36.56 (s, CHCH₂), 36.33 (s, CHCH₂), 35.85 (s, CHCH₂), 35.16 (s, CHCH₂), 32.38 (s, CH₂CH₂CH₃), 32.34 (s, CH₂CH₂CH₃), 32.23 (s, CH₂CH₂CH₃), 31.91 (s, CH₂CH₂CH₃), 30.41 (s, CHCH₂), 30.28 (s, CHCH₂), 29.92 (s, CHCH₂), 29.77 (s, CHCH₂), 28.13 (s, CHCH₂CH₂), 27.96 (s, CHCH₂CH₂), 27.75 (s, CHCH₂CH₂), 27.60 (s, CHCH₂CH₂), 23.08 (s, CH₂CH₃), 23.02 (s, CH₂CH₃), 22.92 (s, CH₂CH₃), 22.87 (s, CH₂CH₃), 14.41 (s, CH₂CH₃), 14.37 (s, CH₂CH₃), 14.34 (s, CH₂CH₃); ³¹P{¹H} NMR (162 MHz, CDCl₃): $\delta = 36.2$ (s, PPh₂); MS (ESI-TOF): $m/z = 1228.51$ [M + H⁺] expected isotopic profile; elemental analysis calcd (%) for C₇₂H₈₄NO₈PPd (1228.83): C 70.37, H 6.89, N 1.14; found (%): C 70.41, H 6.98, N 1.02.

X-ray Crystallographic Data: Colourless single crystals of **3** suitable for X-ray diffraction were obtained by slow diffusion of methanol into a CH₂Cl₂ solution of **3** at room temperature. The sample (0.292 x 0.175 x 0.061 mm) was mounted on an Oxford Diffraction Xcalibur Saphir 3 diffractometer with graphite-monochromatised Mo-K α radiation. Formula of the crystals: C₇₂H₈₄NO₈PPd, $M_r = 1228.83$, orthorhombic, space group *Pbca*, $a = 14.5816(2)$, $b = 27.2736(4)$, $c = 33.6655(5)$ Å, $V = 13388.5(3)$ Å³, $Z = 8$, $D_x = 1.219$ mg.m⁻³, $\lambda(\text{Mo-K}\alpha) = 0.71073$ Å, $\mu = 0.354$ mm⁻¹, $F(000) = 5184$, $T = 120(2)$ K. Data collection ($2\theta_{\text{max}} = 27.5^\circ$, ω scan frames via 0.7° ω rotation and 30 s per frame, range hkl : h -18 to 18, k -34 to 34, l -43 to 42) gave 113636 reflections. The data revealed 14590 independent reflections of which 10587 were observed with $I > 2.0 \sigma(I)$. The structure was solved by using SIR-97,^[15] which revealed the non-hydrogen atoms of the molecule. After anisotropic refinement, all the hydrogen atoms were found by Fourier difference. The whole structure was refined with SHELXL97^[16] by using the full-matrix least squares technique {use of F^2 ; x , y , z , β_{ij} for C, N, O, P and Pd

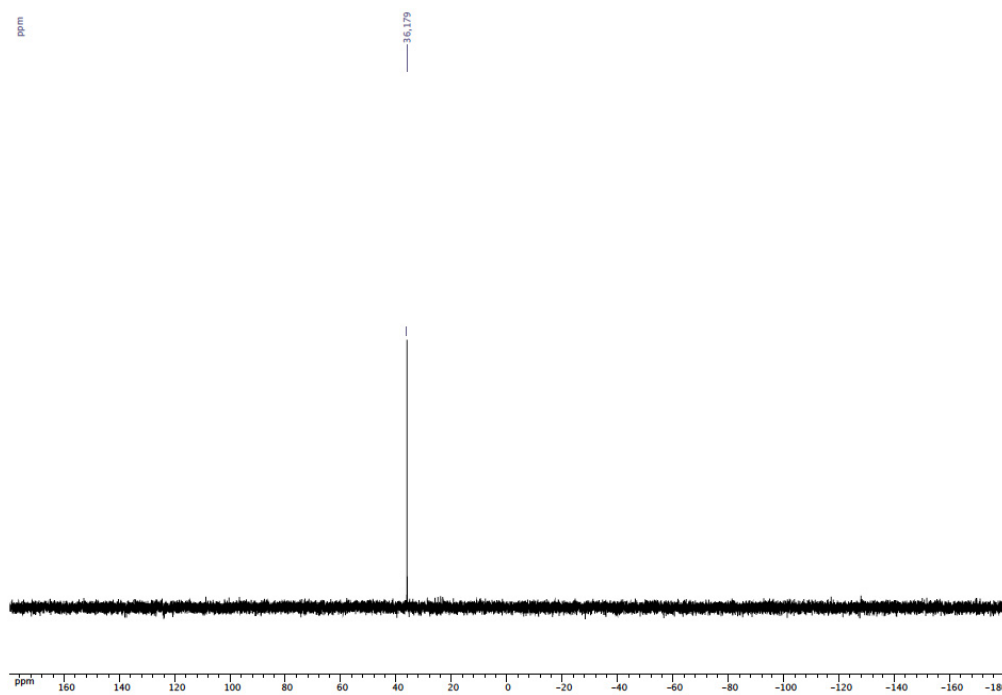
atoms, x , y , z in the riding mode for H atoms; 767 variables and 10587 observations with $I > 2.0 \sigma(I)$; calcd. $w = 1/[\sigma^2(F_o^2) + (0.0446P)^2 + 17.0362P]$ in which $P = (F_o^2 + 2 F_c^2)/3$ with the resulting $R = 0.0449$, $R_w = 0.1008$ and $S_w = 1.025$, $\Delta\rho < 1.108 \text{ e}\text{\AA}^{-3}$. The alerts level B are due to the disorder of the pentyl chain C37...C41AB. CCDC-1022893 contains the supplementary crystallographic data for **3** which can be obtained free of charge from The Cambridge Crystallographic Data Centre via www.ccdc.cam.ac.uk/data_request/cif.



^1H NMR spectrum of **3** (CDCl_3)

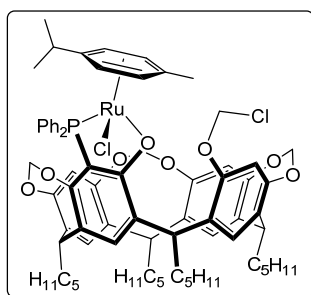


$^{13}\text{C}\{^1\text{H}\}$ NMR spectrum of **3** (CDCl_3)



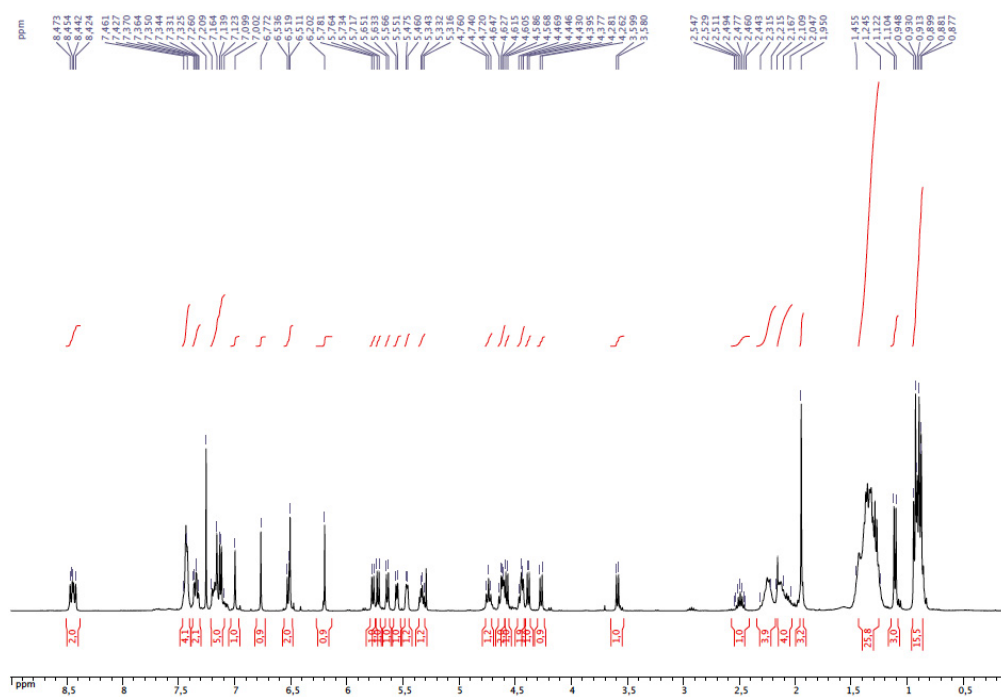
$^{31}\text{P}\{^1\text{H}\}$ NMR spectrum of **3** (CDCl_3)

Synthesis of complex **4**

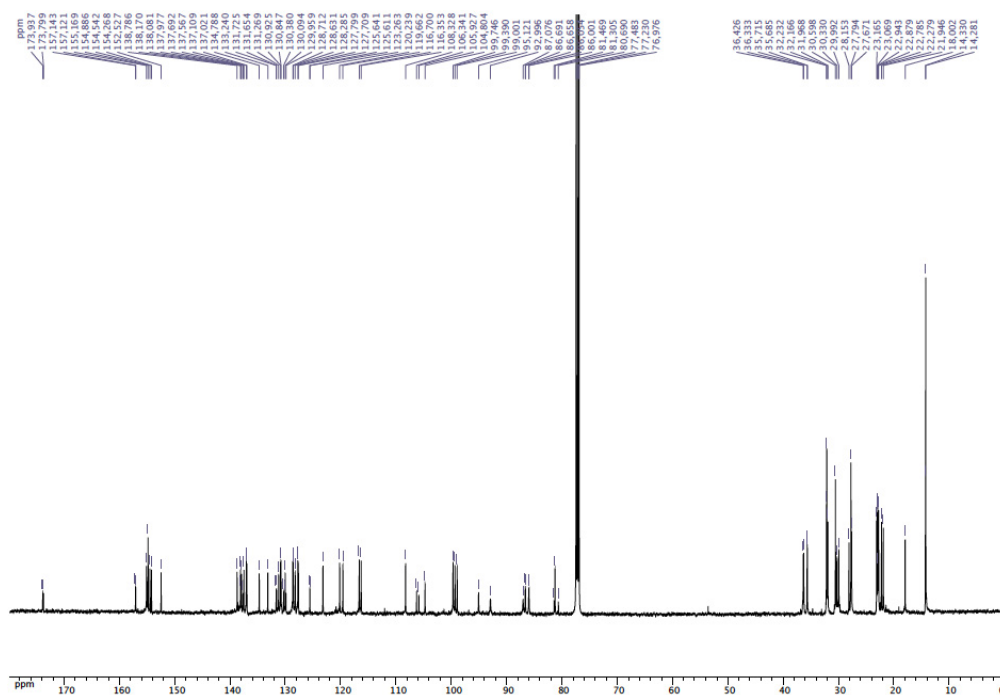


A solution of $[\text{RuCl}_2(p\text{-cymene})]_2$ (0.031 g, 0.05 mmol) in dry CH_2Cl_2 (5 mL) was added to a stirred solution of phosphine **1** (0.100 g, 0.10 mmol) in dry CH_2Cl_2 (5 mL). After stirring at r.t. for 5 min, the reaction mixture was concentrated to about 2 mL and then *n*-hexane (20 mL) was added. The orange precipitate was separated by filtration and dried under vacuum, yield 0.115 g, 88 %. ^1H NMR (400 MHz, CDCl_3): δ = 8.47-8.42 (m, 2H, arom. CH, PPh_2), 7.46-7.43 (m, 4H, arom. CH, PPh_2), 7.34 (dt, 2H, arom. CH, PPh_2 , $^3J = 8.0$ Hz, $^4J = 2.4$ Hz), 7.21-7.18 (m, 2H, arom. CH, PPh_2), 7.16 (s, 1H, arom. CH, resorcinarene), 7.14 (s, 1H, arom. CH, resorcinarene), 7.12 (s, 1H, arom. CH, resorcinarene), 7.00 (s, 1H, arom. CH, resorcinarene), 6.77 (s, 1H, arom. CH, resorcinarene), 6.53 and 5.77 (AB spin system, 2H, OCH_2Cl , $^2J = 6.8$ Hz), 6.55 (s, 1H, arom. CH, resorcinarene), 6.20 (s, 1H, arom. CH, resorcinarene), 5.73 and 4.58 (AB spin system, 2H, OCH_2O , $^2J = 7.2$ Hz), 5.64 and 4.39 (AB spin system, 2H, OCH_2O , $^2J = 7.2$ Hz), 5.56 and 4.61 (AA' of an AA'BB' spin system, 2H, arom. CH, *p*-cymene, $^3J = 6.0$ Hz), 5.47 and 4.44 (BB' of an AA'BB' spin system, 2H, arom. CH, *p*-cymene, $^3J = 6.4$ Hz), 5.36-5.32 (m, 1H, CHCH_2), 4.74 (t, 1H, CHCH_2 , $^3J = 8.0$ Hz), 4.63 (t, 1H, CHCH_2 , $^3J = 8.4$ Hz), 4.45 (t, 1H, CHCH_2 , $^3J = 6.8$ Hz), 4.27 and 3.59 (AB spin system, 2H, OCH_2O , $^2J = 7.6$ Hz), 2.49 (hept, 1H, $\text{CH}(\text{CH}_3)_2$, $^3J = 7.0$ Hz), 2.31-2.19 (m, 4H, CHCH_2), 2.16-2.05 (m, 4H, CHCH_2), 1.95 (s, 3H, CH_3 of *p*-cymene), 1.46-1.26 (m, 24H, $\text{CH}_2\text{CH}_2\text{CH}_2\text{CH}_3$), 1.11 (d, 3H, $\text{CH}(\text{CH}_3)_2$, $^3J = 7.0$ Hz), 0.93 (t, 6H, CH_2CH_3 , $^3J = 7.0$ Hz), 0.90 (t, 3H, CH_2CH_3 , $^3J = 7.2$ Hz), 0.89 (d, 3H, $\text{CH}(\text{CH}_3)_2$, $^3J = 7.0$ Hz), 0.88 (t, 3H, CH_2CH_3 , $^3J = 6.8$ Hz); $^{13}\text{C}\{^1\text{H}\}$ NMR (125 MHz, CDCl_3): δ = 173.94-104.80 (arom. C's), 99.74 (s, OCH_2O), 99.39 (s, OCH_2O), 99.00 (s, OCH_2O), 95.12 (s, arom. Cquat, *p*-cymene), 92.99 (s, arom. CH, *p*-cymene), 87.08 (s, arom. CH, *p*-cymene), 86.67 (d, arom. CH, *p*-cymene, $J_{\text{PC}} = 4.1$ Hz), 86.03 (d, arom. CH, *p*-cymene, $J_{\text{PC}} = 4.1$ Hz), 81.31 (s, OCH_2Cl), 36.43 (s, CHCH_2), 36.33 (s, CHCH_2), 35.71 (s, CHCH_2), 35.68 (s, CHCH_2), 32.23 (s, $\text{CH}_2\text{CH}_2\text{CH}_3$), 32.17 (s,

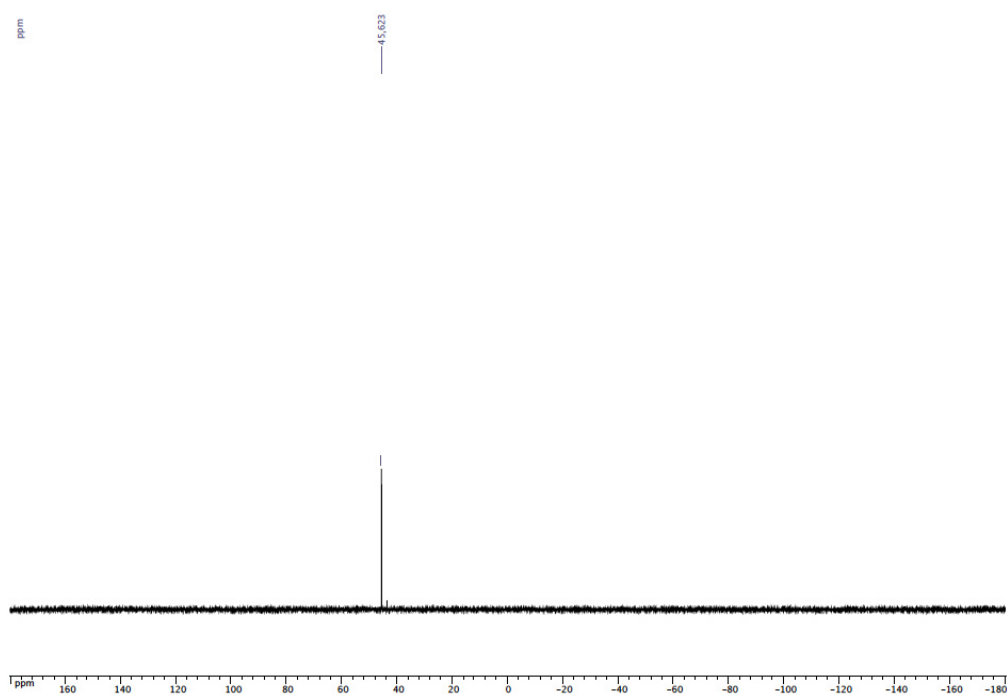
CH₂CH₂CH₃), 31.97 (s, CH₂CH₂CH₃), 30.60 (s, CHCH₂), 30.59 (s, CH(CH₃)₂), 30.33 (s, CHCH₂), 29.99 (s, CHCH₂), 28.15 (s, CHCH₂CH₂), 27.79 (s, CHCH₂CH₂), 27.67 (s, CHCH₂CH₂), 23.16 (s, CH₂CH₃), 23.07 (s, CH₂CH₃), 22.94 (s, CH₂CH₃), 22.78 (s, CH₂CH₃), 22.28 (s, CH(CH₃)₂), 21.95 (s, CH(CH₃)₂), 18.00 (s, CH₃ of *p*-cymene), 14.33 (s, CH₂CH₃), 14.28 (s, CH₂CH₃); ³¹P{¹H} NMR (162 MHz, CDCl₃): δ = 45.6 (s, PPh₂); MS (ESI-TOF): *m/z* = 1329.46 [4%, M + Na⁺] expected isotopic profile.



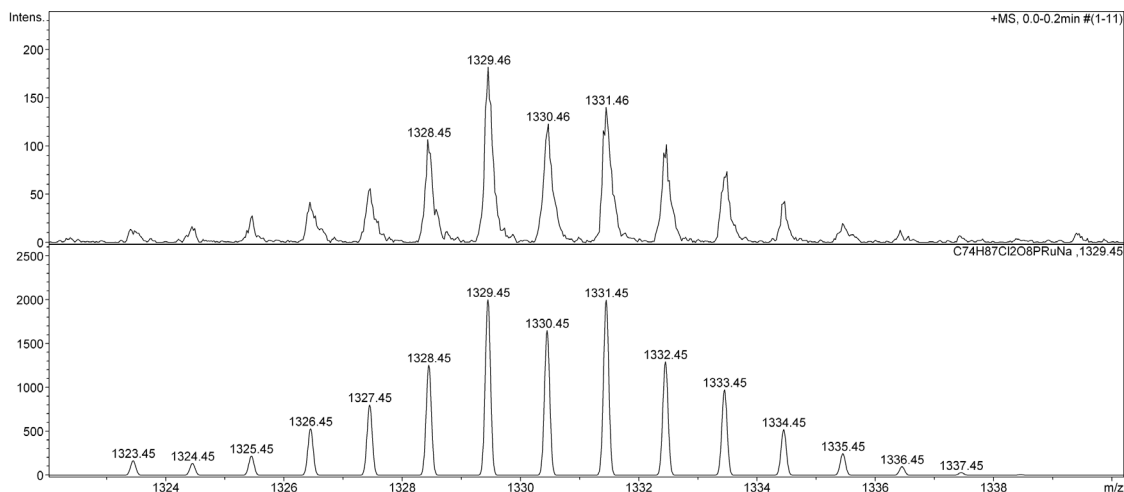
¹H NMR spectrum of **4** (CDCl₃)



$^{13}\text{C}\{^1\text{H}\}$ NMR spectrum of **4** (CDCl_3)

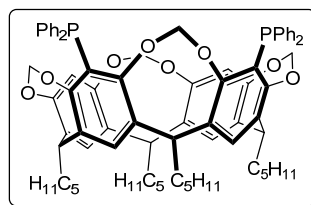


$^{31}\text{P}\{^1\text{H}\}$ NMR spectrum of **4** (CDCl_3)



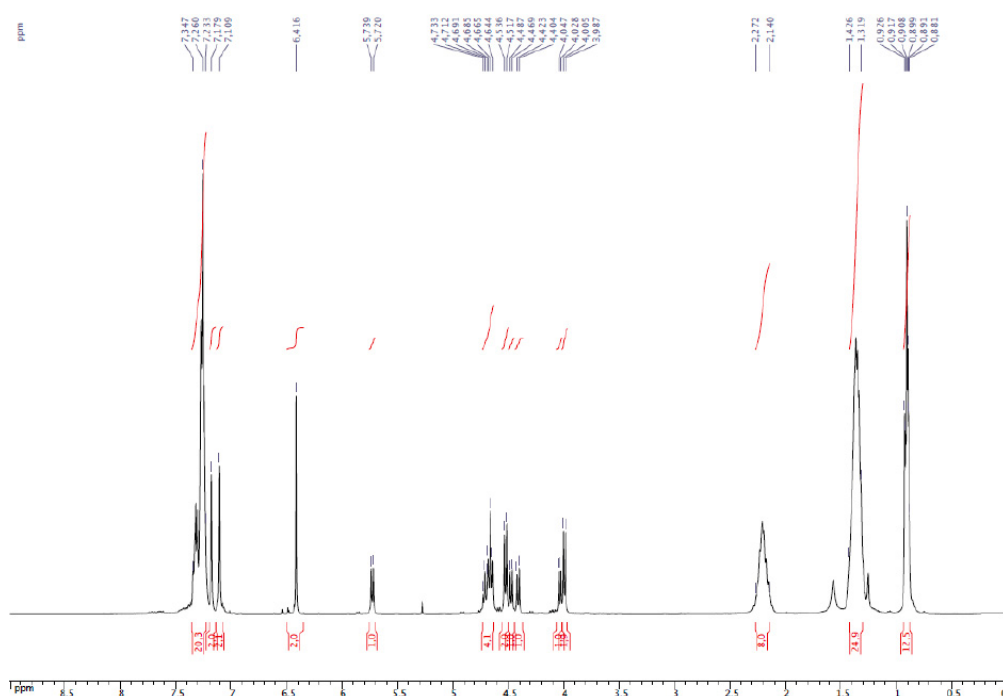
Mass spectrum (ESI-TOF) of **4** (exp. spectrum (top); calculated spectrum (bottom) for $C_{74}H_{87}Cl_2O_8PRu + Na$)

Synthesis of bis-phosphine **5**

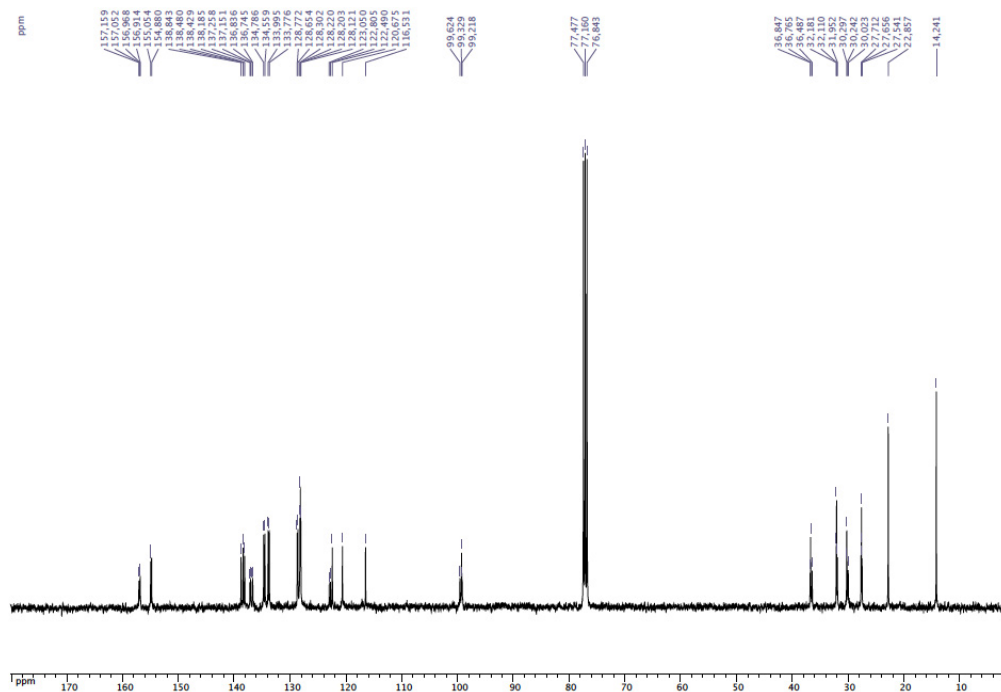


n-Butyllithium (1.6 M in hexane, 0.68 mL, 1.08 mmol) was slowly added to a solution of 5,11-dibromo-4(24),6(10),12(16),18(22)-tetramethylenedioxy-2,8,14,20-tetrapentylresorcin [4]arene (0.500 g, 0.51 mmol) in THF (50 mL) at $-78^{\circ}C$. After 0.5 h, the generated carbanion was quenched with chlorodiphenylphosphine (0.24 mL, 1.10 mmol) and the mixture stirred at $40^{\circ}C$ for 16 h. The solvent was then evaporated under reduced pressure and the crude product purified by column chromatography (Et₂O/petroleum ether, 2:8 v/v), yield 0.360 g, 60%. ¹H NMR (400 MHz, CDCl₃): δ = 7.37-7.33 (m, 4H, arom. CH, PPh₂), 7.30-7.27 (m, 16H, arom. CH, PPh₂), 7.20 (s, 2H, arom. CH, resorcinarene), 7.13 (s, 2H, arom. CH, resorcinarene), 6.44 (s, 2H, arom. CH, resorcinarene), 5.75 and 4.50 (AB spin system, 2H, OCH₂O, ²*J* = 7.0 Hz), 4.74 (t, 1H, CHCH₂, ³*J* = 8.4 Hz), 4.69 (t, 3H, CHCH₂, ³*J* = 8.2 Hz), 4.55 and 4.02 (AB spin system, 4H, OCH₂O, ²*J* = 7.4 Hz), 4.44 and 4.04 (AB spin system, 2H, OCH₂O, ²*J* = 7.4 Hz), 2.29-2.18 (m, 8H, CHCH₂), 1.43-1.34 (m, 24H CH₂CH₂CH₂CH₃) 0.93 (t, 12H, CH₂CH₃, ³*J* =

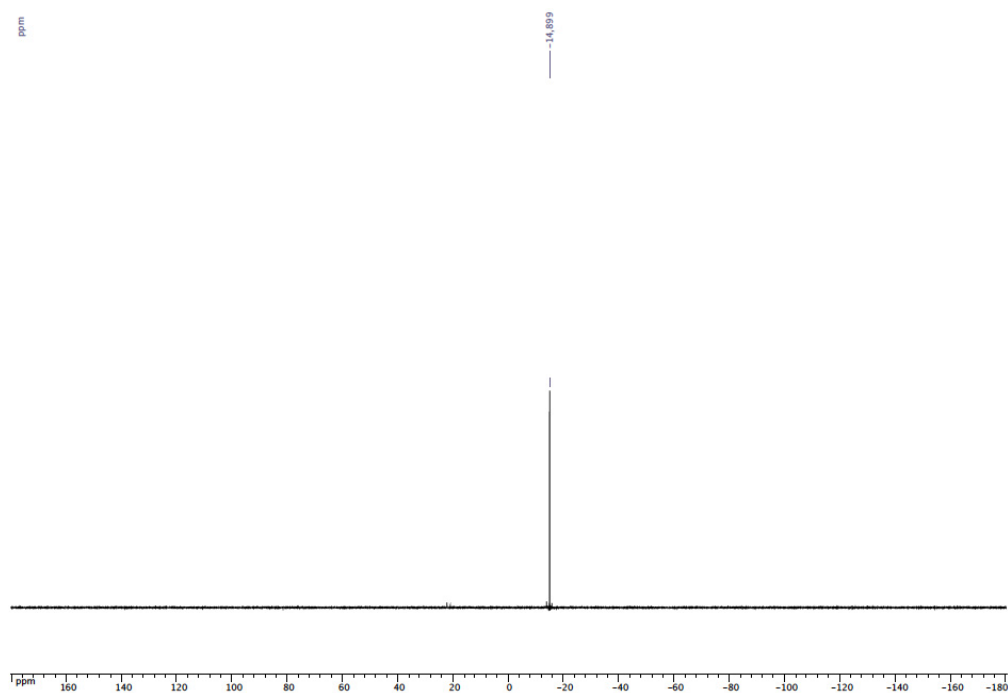
7.0 Hz); $^{13}\text{C}\{^1\text{H}\}$ NMR (125 MHz, CDCl_3): δ = 157.10-116.53 (arom. C's), 99.62 (s, OCH_2O), 99.33 (s, OCH_2O), 99.21 (s, OCH_2O), 36.85 (s, CHCH_2), 36.76 (s, CHCH_2), 36.49 (s, CHCH_2), 32.18 (s, $\text{CH}_2\text{CH}_2\text{CH}_3$), 32.11 (s, $\text{CH}_2\text{CH}_2\text{CH}_3$), 31.95 (s, $\text{CH}_2\text{CH}_2\text{CH}_3$), 30.30 (s, CHCH_2), 30.24 (s, CHCH_2), 30.02 (s, CHCH_2), 27.71 (s, CHCH_2CH_2), 27.66 (s, CHCH_2CH_2), 27.54 (s, CHCH_2CH_2), 22.86 (s, CH_2CH_3), 14.24 (s, CH_2CH_3); $^{31}\text{P}\{^1\text{H}\}$ NMR (162 MHz, CDCl_3): δ = -14.9 (s, PPh_2); MS (ESI-TOF): m/z = 1185.54 [$\text{M} + \text{H}^+$] expected isotopic profile; elemental analysis calcd (%) for $\text{C}_{76}\text{H}_{82}\text{O}_8\text{P}_2$ (1185.41): calcd. C 77.00, H 6.97; found (%): C 77.19, H 7.20.



^1H NMR spectrum of **5** (CDCl_3)

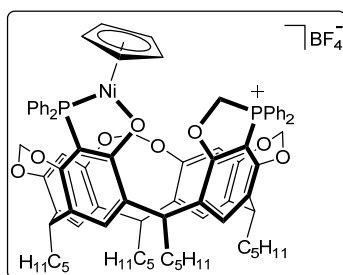


$^{13}\text{C}\{^1\text{H}\}$ NMR spectrum of **5** (CDCl_3)

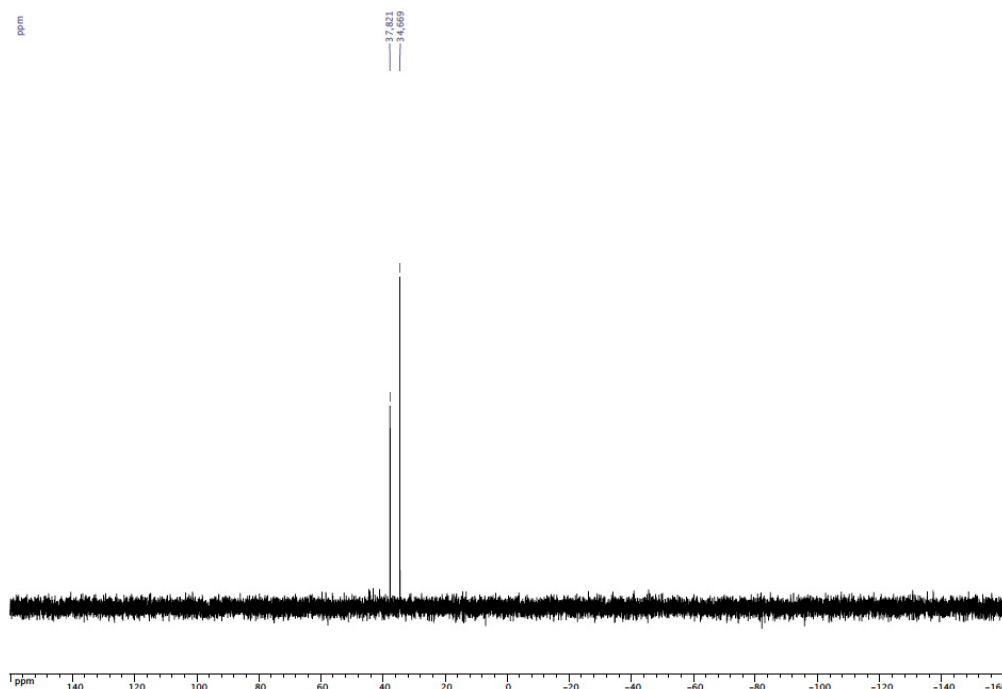


$^{31}\text{P}\{^1\text{H}\}$ NMR spectrum of **5** (CDCl_3)

Synthesis of complex **6**

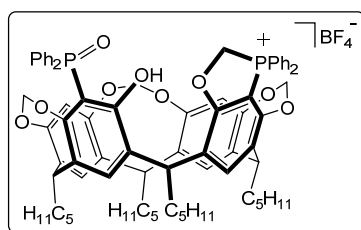


A solution of $[\text{NiCp}(\text{cod})]\text{BF}_4$ (0.026 g, 0.08 mmol) in dry CH_2Cl_2 (20 mL) was added dropwise to a stirred solution of **5** (0.100 g, 0.08 mmol) in dry CH_2Cl_2 (200 mL). After stirring at 30°C for 7 days, the reaction mixture was concentrated to ca. 2 mL, then *n*-hexane (20 mL) was added. The orange precipitate formed was separated by filtration and dried under vacuum, yield 0.093 g, 82 %. ^1H NMR (400 MHz, CDCl_3): δ = 8.04-7.91 (m, 4H, arom. CH, PPh_2), 7.88-7.79 (m, 4H, arom. CH, PPh_2), 7.74-7.67 (m, 4H, arom. CH, PPh_2), 7.51 (s, 1H, arom. CH, resorcinarene), 7.50-7.36 (m, 8H, arom. CH, PPh_2), 7.19 (s, 1H, arom. CH, resorcinarene), 7.17 (s, 1H, arom. CH, resorcinarene), 6.93 (s, 1H, arom. CH, resorcinarene), 6.38 (s, 1H, arom. CH, resorcinarene), 6.27 (s, 1H, arom. CH, resorcinarene), 5.82 (d, 2H, CH_2P , $^2J = 2.8$ Hz), 5.60 and 4.27 (AB spin system, 2H, OCH_2O , $^2J = 7.2$ Hz), 5.30 (s, 5H, C_5H_5), 4.98 and 3.80 (AB spin system, 2H, OCH_2O , $^2J = 7.2$ Hz), 4.86 (t, 1H, CHCH_2 , $^3J = 7.2$ Hz), 4.69 (t, 1H, CHCH_2 , $^3J = 8.2$ Hz), 4.68 and 3.38 (AB spin system, 2H, OCH_2O , $^2J = 7.6$ Hz), 4.66 (t, 1H, CHCH_2 , $^3J = 8.0$ Hz), 4.60 (t, 1H, CHCH_2 , $^3J = 8.0$ Hz), 2.37-2.08 (m, 8H, CHCH_2CH_2), 1.46-1.23 (m, 24 H $\text{CH}_2\text{CH}_2\text{CH}_2\text{CH}_3$), 0.94 (t, 3H, CH_2CH_3 , $^3J = 6.4$ Hz), 0.93 (t, 3H, CH_2CH_3 , $^3J = 6.6$ Hz), 0.87 (t, 3H, CH_2CH_3 , $^3J = 6.8$ Hz), 0.81 (t, 3H, CH_2CH_3 , $^3J = 6.6$ Hz); $^{13}\text{C}\{^1\text{H}\}$ NMR (125 MHz, CDCl_3): δ = 163.18-116.60 (arom. C's), 99.49 (s, OCH_2O), 99.37 (s, OCH_2O), 99.25 (s, OCH_2O), 92.70 (s, C_5H_5), 60.31 (s, CH_2P), 36.38 (s, CHCH_2), 36.13 (s, CHCH_2), 35.47 (s, CHCH_2), 34.51 (s, $\text{CH}_2\text{CH}_2\text{CH}_3$), 32.82 (s, CHCH_2), 32.07 (s, $\text{CH}_2\text{CH}_2\text{CH}_3$), 31.89 (s, $\text{CH}_2\text{CH}_2\text{CH}_3$), 31.79 (s, $\text{CH}_2\text{CH}_2\text{CH}_3$), 31.47 (s, CHCH_2), 30.46 (s, CHCH_2), 30.09 (s, CHCH_2), 29.83 (s, CHCH_2), 27.68 (s, CHCH_2CH_2), 27.54 (s, CHCH_2CH_2), 27.50 (s, CHCH_2CH_2), 23.06 (s, CH_2CH_3), 22.92 (s, CH_2CH_3), 22.75 (s, CH_2CH_3), 22.48 (s, CH_2CH_3), 14.26 (s, CH_2CH_3), 14.09 (s, CH_2CH_3), 13.93 (s, CH_2CH_3); $^{31}\text{P}\{^1\text{H}\}$ NMR (162 MHz, CDCl_3): δ = 37.8 (s, PPh_2), 34.7 (s, Ph_2PCH_2); MS (ESI-TOF): m/z = 1307.53 [$\text{M} - \text{BF}_4^-$] expected isotopic profile; elemental analysis calcd (%) for $\text{C}_{81}\text{H}_{87}\text{BF}_4\text{NiO}_8\text{P}_2$ (1396.00): C 69.69, H 6.28; found: C 69.81, H 6.14.



$^{31}\text{P}\{^1\text{H}\}$ NMR spectrum of **6** (CDCl_3)

Synthesis of phosphine oxide – phosphonium salt **7**

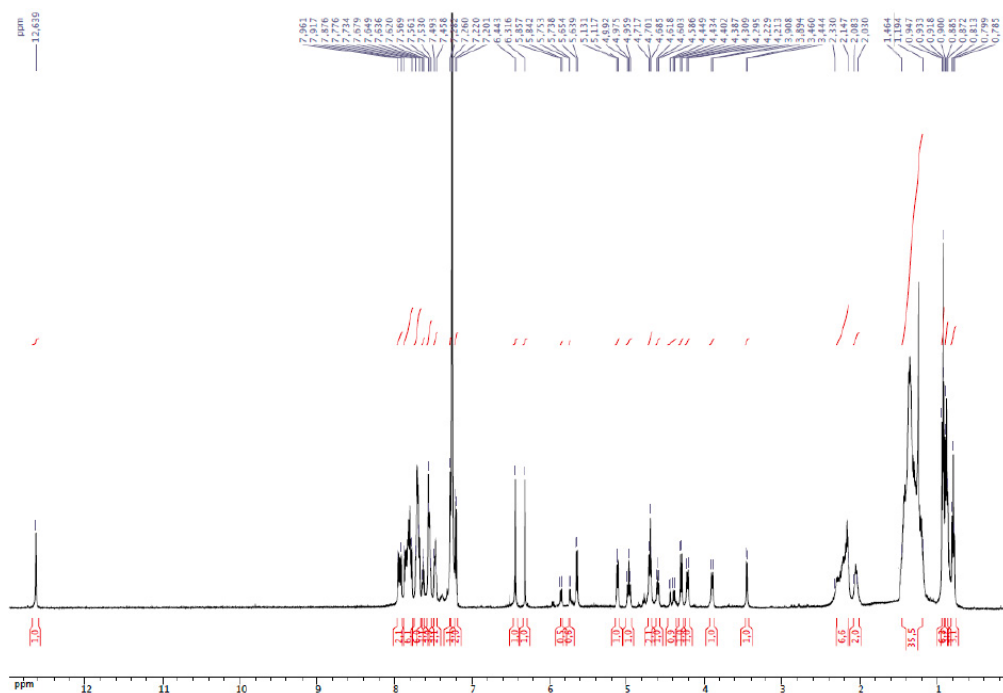


A solution of nickel complex **6** (0.090 g, 0.06 mmol) was stirred in *wet* CH_2Cl_2 (20 mL) under air atmosphere for 96 h. The reaction mixture was concentrated to ca. 2 mL and *n*-hexane (20 mL) was added. The white precipitate formed was separated by filtration, washed with *n*-hexane (3 x 20 mL) and dried under vacuum, yield 0.066 g, 75 %. ^1H NMR (400 MHz, CDCl_3): δ = 12.64 (s, 1H, OH), 7.96-7.92 (m, 2H, arom. CH, PPh_2), 7.88-7.78 (m, 6H, arom. CH, PPh_2), 7.73-7.68 (m, 6H, arom. CH, PPh_2), 7.64 (t, 1H, arom. CH, PPh_2 , $^3J = 7.2$ Hz), 7.60 (s, 1H, arom. CH, resorcinarene), 7.51-7.53 (m, 3H, arom. CH, PPh_2), 7.49-7.46 (m, 2H,

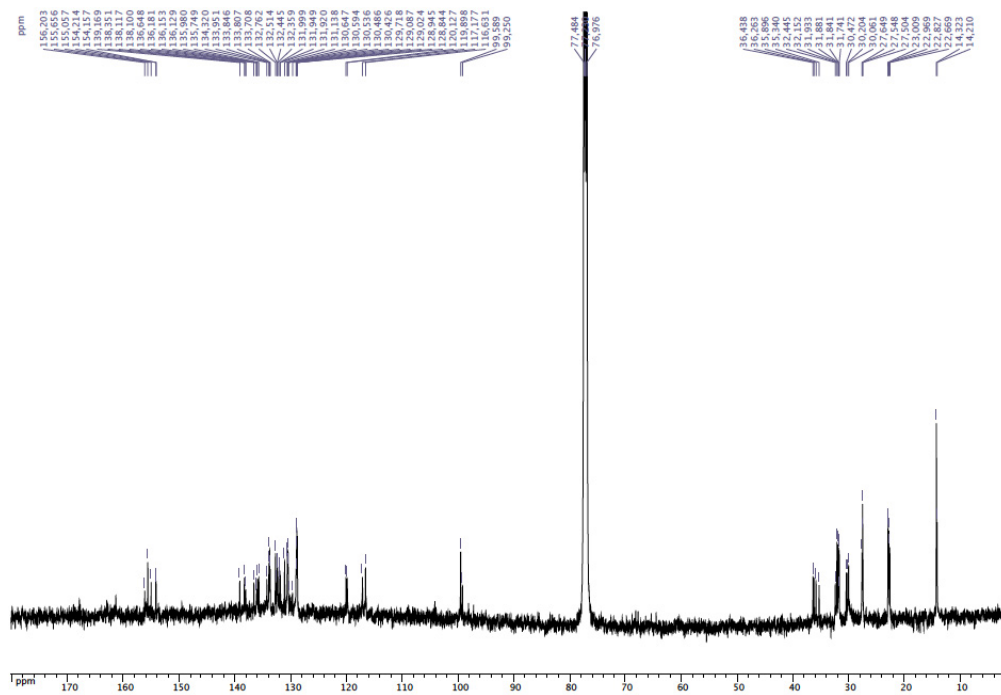
arom. CH, PPh₂), 7.28 (s, 1H, arom. CH, resorcinarene), 7.22 (s, 1H, arom. CH, resorcinarene), 7.20 (s, 1H, arom. CH, resorcinarene), 6.44 (s, 1H, arom. CH, resorcinarene), 6.32 (s, 1H, arom. CH, resorcinarene), 5.80 (dd, 1H, CH₂P, ²J_{PH} = 52.0 Hz, ²J = 7.0 Hz), 5.64 and 4.30 (AB spin system, 2H, OCH₂O, ²J = 7.2 Hz), 5.12 and 3.90 (AB spin system, 2H, OCH₂O, ²J = 7.0 Hz), 4.97 (t, 1H, CHCH₂, ³J = 8.2 Hz), 4.70 (t, 2H, CHCH₂, ³J = 8.0 Hz), 4.60 (t, 1H, CHCH₂, ³J = 8.0 Hz), 4.43 (dd, 1H, CH₂P, ²J_{PH} = 23.0 Hz, ²J = 7.0 Hz), 4.22 and 3.45 (AB spin system, 2H, OCH₂O, ²J = 8.0 Hz), 2.33-2.15 (m, 6H, CHCH₂CH₂), 2.08-2.03 (m, 2H, CHCH₂CH₂), 1.46-1.19 (m, 24 H CH₂CH₂CH₂CH₃), 0.99 (t, 6H, CH₂CH₃, ³J = 7.2 Hz), 0.88 (t, 3H, CH₂CH₃, ³J = 7.0 Hz), 0.80 (t, 3H, CH₂CH₃, ³J = 7.0 Hz); ¹³C{¹H} NMR (125 MHz, CDCl₃): δ = 156.20-116.63 (arom. C's), 99.59 (s, OCH₂O), 99.25 (s, OCH₂O), 68.00 (d, CH₂P, ¹J_{PC} = 52.1 Hz), 36.44 (s, CHCH₂), 36.26 (s, CHCH₂), 35.90 (s, CHCH₂), 35.34 (s, CHCH₂), 32.44 (s, CHCH₂), 32.15 (s, CH₂CH₂CH₃), 31.93 (s, CH₂CH₂CH₃), 31.84 (s, CH₂CH₂CH₃), 31.74 (s, CH₂CH₂CH₃), 30.47 (s, CHCH₂), 30.20 (s, CHCH₂), 30.06 (s, CHCH₂), 27.65 (s, CHCH₂CH₂), 27.55 (s, CHCH₂CH₂), 27.50 (s, CHCH₂CH₂), 23.01 (s, CH₂CH₃), 22.97 (s, CH₂CH₃), 22.83 (s, CH₂CH₃), 22.67 (s, CH₂CH₃), 14.32 (s, CH₂CH₃), 14.21 (s, CH₂CH₃); ³¹P{¹H} NMR (162 MHz, CDCl₃): δ = 40.3 (s, P(O)Ph₂), 34.6 (s, Ph₂PCH₂); MS (ESI-TOF): *m/z* = 1201.55 [M - BF₄⁻] expected isotopic profile; elemental analysis calcd (%) for C₇₆H₈₃BF₄O₉P₂ (1289.22): C 70.80, H 6.49; found: C 70.92, H 6.65.

X-ray Crystallographic Data: Yellow single crystals of **7** suitable for X-ray diffraction were obtained by slow diffusion of hexane into a CH₂Cl₂ solution of **7** at room temperature. The sample (0.376 x 0.243 x 0.198 mm) was mounted on an Oxford Diffraction Xcalibur Saphir 3 diffractometer with graphite-monochromatised Mo-K_α radiation. Formula of the crystals: C₇₆H₈₃BF₄O₉P₂·4CH₂Cl₂, *M_r* = 1628.95, monoclinic, space group *P2₁/c*, *a* = 13.8945(3), *b* = 32.6398(6), *c* = 18.4866(4) Å, β = 107.8130(2)°, *V* = 7982.0(3) Å³, *Z* = 4, *D_x* = 1.355 mg·m⁻³, λ(Mo-K_α) = 0.71073 Å, μ = 0.387 mm⁻¹, *F*(000) = 3400, *T* = 100(2) K. Data collection (2θ_{max} = 27.5°, ω scan frames via 0.7° ω rotation and 30 s per frame, range *hkl*: *h* - 17 to 17, *k* -41 to 40, *l* -23 to 23) gave 62479 reflections. The data revealed 17364 independent reflections of which 9035 were observed with *I* > 2.0 σ(*I*). The structure was solved by using SIR-97,^[15] which revealed the non-hydrogen atoms of the molecule. After anisotropic refinement, all the hydrogen atoms were found by Fourier difference. The whole structure was refined with SHELXL97^[16] by using the full-matrix least squares technique {use of *F*²; *x*, *y*, *z*, β_{*ij*} for C, B, Cl, F, O and P atoms, *x*, *y*, *z* in the riding mode for H atoms; 941 variables and 9035 observations with *I* > 2.0 σ(*I*); calcd. *w* = 1/[σ²(*F_o*²) + (0.1225*P*)²] in

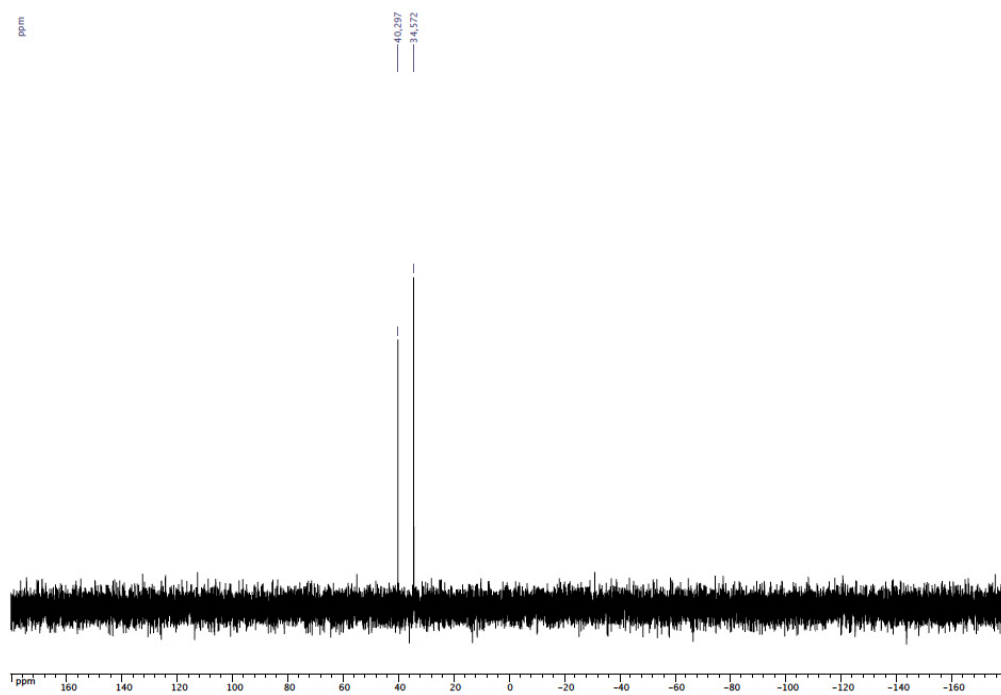
which $P = (F_o^2 + 2 F_c^2)/3$ with the resulting $R = 0.0734$, $R_w = 0.2001$ and $S_w = 0.968$, $\Delta\rho < 1.485 \text{ e}\text{\AA}^{-3}$. The alerts level A and B are due to the disorder of atoms C46A and C46B. CCDC-967903 contains the supplementary crystallographic data for **7** which can be obtained free of charge from The Cambridge Crystallographic Data Centre via www.ccdc.cam.ac.uk/data_request/cif.



^1H NMR spectrum of **7** (CDCl_3)



$^{13}\text{C}\{^1\text{H}\}$ NMR spectrum of **7** (CDCl_3)



$^{31}\text{P}\{^1\text{H}\}$ NMR spectrum of **7** (CDCl_3)

Catalytic run (oligomerisation of ethylene with complex **6**)

A solution of NaBH₄ (0.0003 g, 0.008 mmol) in toluene (3 mL) and heptane (internal reference; 0.1 mL) were introduced into a 100 mL autoclave containing a solution of **6** (0.0052 g, 0.004 mmol) in toluene (17 mL). The autoclave was pressurised with 20 bar of ethylene and heated up to 90°C. After 1 h, the autoclave was cooled down to 7°C and depressurised over 0.5 h. The flask containing the reaction mixture was weighed. This procedure was performed as quickly as possible to minimise the potential evolution of the oligomeric products. The products were analysed by GC. The reaction yield was determined from the final mass of reaction mixture vs. the mass of the control reaction solution. To determine the mass of the control reaction solution (reaction mixture without catalyst or co-catalyst), toluene (20 mL) and heptane (0.1 mL) were added to the autoclave and stirred under 20 bar of ethylene at 90°C for 1 h. The reactor was cooled down to 7°C and depressurised over 0.5 h. The flask containing the toluene solution was then weighed.

References

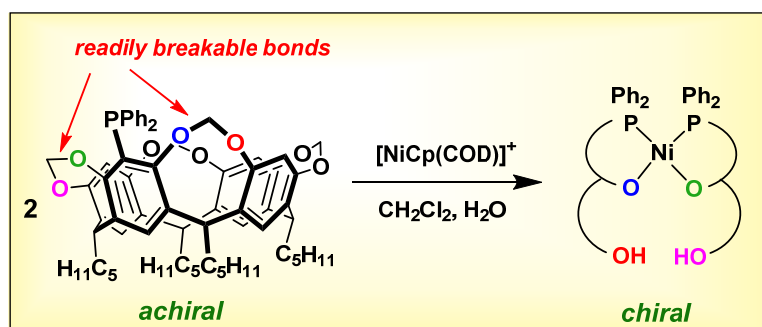
- [1] a) D. J. Cram, *Angew. Chem. Int. Ed.* **1988**, *27*, 1009-1020; b) W. Verboom, in *Calixarenes 2001*, Z. Asfari, V. Böhmer, J. Harrowfield, J. Vicens, Eds. Kluwer, Dordrecht, 2001, pp 181-198; c) F. Hof, S. L. Craig, C. Nuckolls and J. Rebek Jr., *Angew. Chem., Int. Ed.* **2002**, *41*, 1488-1508; d) S. S. Zhu, H. Staats, K. Brandhorst, J. Grunenberg, F. Gruppi, E. Dalcanale, A. Luetzen, K. Rissanen and C. A. Schalley, *Angew. Chem. Int. Ed.* **2008**, *47*, 788-792; e) W. Sliwa and C. Kozłowski, *Calixarenes and Resorcinarenes, Properties and Applications*, Wiley-VCH, 2009; f) V. K. Jain and P. H. Kanaiya, *Russ. Chem. Rev.* **2011**, *80*, 75-102; g) R. Gramage-Doria, D. Armspach and D. Matt, *Coord. Chem. Rev.* **2013**, *257*, 776-816; h) N. Montes-Garcia, J. Perez-Juste, I. Pastoriza-Santos and L. M. Liz-Marzan, *Chem. Eur. J.* **2014**, *20*, 10874-10883; i) D. Sémeril and D. Matt, *Coord. Chem. Rev.* **2014**, *279*, 58-95.
- [2] a) G. Arnott, H. Heaney, R. Hunter and P. C. B. Page, *Eur. J. Org. Chem.* **2004**, 5126-5134; b) O. Hass, A. Schierholt, M. Jordan and A. Lützen, *Synthesis* **2005**, 519-527.
- [3] a) D. J. Cram, S. Karbach, H. E. Kim, C. B. Knobler, E. F. Maverick, J. L. Ericson and R. C. Helgeson, *J. Am. Chem. Soc.* **1988**, *110*, 2229-2237; b) P. Timmerman, M. G. A. van Mook, W. Verboom, G. J. van Hummel, S. Harkema and D. N. Reinhoudt, *Tet. Lett.* **1992**, *33*, 3377-3380.
- [4] L. Monnereau, H. El Moll, D. Sémeril, D. Matt and L. Toupet, *Eur. J. Inorg. Chem.* **2014**, 1364-1372.
- [5] *Spectral Database for Organic Compounds SDBS*. See URL: http://sdb.sdb.aist.go.jp/sdb/cgi-bin/direct_frame_disp.cgi?sdbno=2406.

- [6] Y. Nito, K. Nakada, K. Kobayashi and M. Yamanaka, *Asian Journal of Organic Chemistry* **2014**, *3*, 762-765.
- [7] D. Matt, M. Huhn, M. Bonnet, I. Tkatchenko, U. Englert and W. Kläui, *Inorg.Chem.* **1995**, *34*, 1288-1291.
- [8] T. Sokoliess, A. Opolka, U. Menyes, U. Roth and T. Jira, *Die Pharmazie* **2002**, *57*, 589-590.
- [9] W. Keim, F. H. Kowaldt, R. Goddard and C. Krüger, *Angew. Chem. Int. Ed.* **1978**, *17*, 466-467.
- [10] L. Monnereau, H. El Moll, D. Sémeril, D. Matt and L. Toupet, *Eur. J. Inorg. Chem.* **2014**, 364-1372.
- [11] H. El Moll, D. Sémeril, D. Matt and L. Toupet, *Eur. J. Org. Chem.* **2010**, 1158-1168.
- [12] A. Salzer, T. L. Court and H. Werner, *J. Organomet. Chem.* **1973**, *54*, 325-330.
- [13] M. A. Bennet, T.-N. Huang, T. W. Matheson and A. K. Smith, *Inorganic Synthesis, vol. 21*, ed. J. P. Fackler, Jr., John Wiley & Sons, New York, 1982, p. 75.
- [14] A. C. Cope and E. C. Friedrich, *J. Am. Chem. Soc.* **1968**, *90*, 909-913.
- [15] A. Altomare, M. C. Burla, M. Camalli, G. Cascarano, C. Giacovazzo, A. Guagliardi, A. G. G. Moliterni, G. Polidori and R. Spagna, *J. Appl. Crystallogr.* **1998**, *31*, 74-77.
- [16] G. M. Sheldrick, *SHELXL-97, Program for the Refinement of Crystal Structures, Univ. of Göttingen, Germany, 1997.*

Chapter III

Cavitand scission by transition metal centres – Cleaved cavitand chirality and its consequences

Abstract: Two molecules of the phosphine cavitand 5-diphenylphosphanyl-4(24),6(10),12(16),18(22)-tetramethylenedioxy-2,8,14,20-tetra-pentylresorcin[4]arene (**1**) each underwent cleavage of an O–CH₂O bond when treated with one equivalent of [Ni(η^5 -C₅H₅)(1,5-cyclooctadiene)]BF₄, thereby resulting in a bis-(phosphino-phenolato) complex (**2**) without a cyclopentadienyl ligand. The partially cleaved (*P,O*) ligands in **2** are chiral and a single-crystal X-ray structure determination of **2** has shown that the complex molecule has close to twofold rotational symmetry with both ligand units in the same absolute configuration. As expected, the primary coordination sphere has a *cis*-NiO₂P₂ geometry. In contrast, C–O bond breaking occurred only once per metal centre when **1** was treated with [RuBr₂(*p*-cymene)]₂. This led to a crystallographically characterised complex [RuBr(*P,O*)(*p*-cymene)] (**4**) along with a minor amount of a species (**5**) that is assumed to be a stereoisomer. Upon crystallisation of **4**, two distinct types of crystals were isolated from the same solution; some of these were the racemic compound, while the others were the racemic conglomerate.



Introduction

Resorcinarene-derived cavitands that have all pairs of neighbouring resorcinol units linked through methylene bridges (Figure 1) are frequently employed as rigid building blocks for the construction of functionalised, bowl-shaped molecules suitable for applications in host-guest and coordination chemistry.^[1] Cavities of this type are generally regarded as structurally very robust. However, in a recent study we have found that phosphino-cavitand **1** (Figure 1) reacted with ruthenium and palladium complexes with a readily available coordination site to form phosphino-phenolato chelate complexes in which the macrocyclic core had undergone breaking of one of the two C–OCH₂ bonds adjacent to the P-substituted resorcinol unit.^[2] The observed C–O bond cleavage was attributed to the transient formation of a “neutral” phosphine-ether chelate, which increases the strain within the eight membered ring containing the coordinated OCH₂ fragment and, therefore, facilitates nucleophilic attack of endogenous nucleophiles, in our case water, at the corresponding methylenic carbon atom. Theoretical calculations showed that C–O bond breaking may occur either before or after the attack of the nucleophile. It is worth mentioning such a structural modification has not been observed in any of the many reported studies of P^{III}-substituted resorcinarene ligands.^[1j,3]

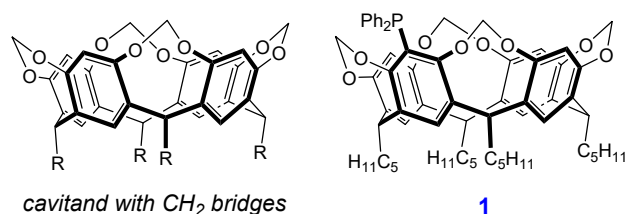
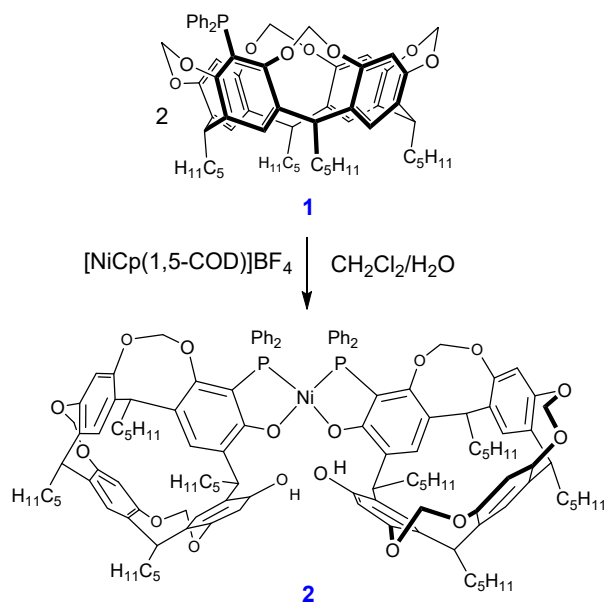


Figure 1. General structure of methylene-bridged cavitands and the formula of cavitand-phosphine **1**

As an extension of these studies, we herein describe two further examples of complexation-induced bond breaking within **1**. One of the reported reactions shows that a single metal centre may result in cracking of two independent molecules of the phosphine cavitand, possibly in a two-step sequence. In another example, involving an electronically enriched ruthenium(II) centre, C–O bond scission occurred only once. A significant aspect of the C–O bond scission is that it renders the cavitand unit chiral.

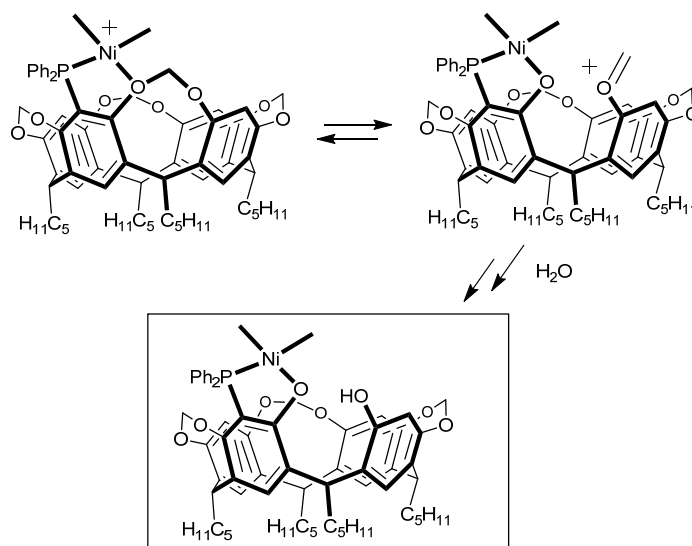
Results and Discussion

The reaction of $[\text{Ni}(\eta^5\text{-C}_5\text{H}_5)(1,5\text{-cyclooctadiene})]\text{BF}_4$ with two equiv. of phosphine cavitand **1** in wet dichloromethane afforded the bis(phosphino-phenolato) complex **2** (abbreviated $\text{Ni}(\text{P},\text{O})_2$ in the following) in 76% yield (Scheme 1) after 7 days. The mass spectrum of **2** reveals an intense peak at $m/z = 2034.91$ with the expected profile for the corresponding $[\text{M} + \text{H}^+]$ ion. Consistent with the proposed formula, the ^1H NMR spectrum of **2** shows three distinct AB systems for the three methylenic OCH_2O protons and a hydroxyl signal that integrates to 1 H (9.48 ppm) and is otherwise indicative of a complete lack of molecular symmetry. The ^{31}P NMR signal appears at $\delta = 31.1$ ppm. The *cis*-configuration of the NiO_2P_2 coordination sphere, which was revealed by a single-crystal X-ray diffraction study (*vide infra*), could not be deduced from the NMR data (although they did show that the complex must be a diamagnetic, square-planar species), principally because the signal of the aromatic PCCO carbon atom could not be assigned. The reaction shown in Scheme 1 constitutes the first example of a process in which the immediate product of a scission reaction retains sufficient activity to induce scission in a second molecule of resorcinarene.



Scheme 1. Synthesis of complex **2**

As shown in our previous study, the most plausible mechanism for the formation of **2** involves an initial displacement of 1,5-cyclooctadiene by chelation of **1** through P and ether-O donors and the subsequent cleavage of the NiO–CH₂O bond followed by the addition of H₂O to the resulting oxocarbenium fragment (Scheme 2). The *P,O* chelate that presumably forms initially must have the ability to coordinate a second molecule of **1** and induce C–O scission in that ligand also. It is not known at which stage the loss of the cyclopentadienyl unit occurs, but the facile displacement of such a ligand from a half-sandwich complex under acidic conditions was recently shown by Chetcuti *et al.*^[4] Note that the reaction leading to **2** required 7 days for completion.



Scheme 2. Possible intermediates containing a cracked cavitand fragment in the route to **2**

The exact nature of **2** was established by an X-ray diffraction study (Table 1; Figure 2), although this was of low precision due to the poor quality of the crystals obtained. Two inequivalent molecules are present in the asymmetric unit but their differences are slight and largely associated with the partly disordered pentyl chains. As observed for the vast majority of the bis(enolato-phosphine) nickel(II) complexes reported to date, the two phosphorus atoms of **2** occupy *cis*-positions.^[5] The nickel atom sits in a planar coordination environment, although one significantly distorted from square, as expected from the presence of both O and P donor atoms and of two five-membered chelate rings which cannot accommodate P–Ni–O angles of 90° (see Table 2). Interestingly, the two cavitand bowls are located on opposite sides of the metal plane, which means that the molecule essentially has *C*₂ symmetry and both

units are of the same handedness. The space group ($P2_1/c$) is such that both enantiomers of each of the inequivalent complex molecules are present in the lattice. Although crystal-packing effects must have some influence in determining the form of the complex in the solid state, the adoption of a racemic form and not a *meso* form may be due to the minimisation of repulsions between the two bulky ligands when they lie on opposite sides of the NiO_2P_2 plane.

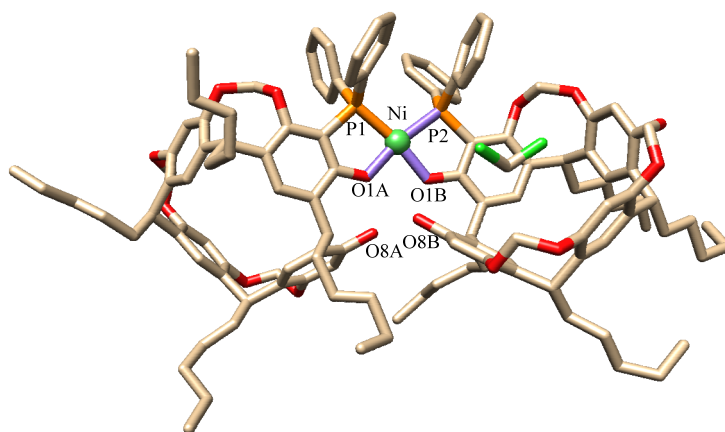


Figure 2. Solid state structure of **2**• CH_2Cl_2 . Only one of the two closely similar molecules present in the unit cell is shown. The solvent molecule and H-atoms are not shown

Table 1. Crystal Data and Structure Refinement Details

	2.CH₂Cl₂	4A	4B
chemical formula	C ₂₅₄ H ₂₉₂ Cl ₄ Ni ₂ O ₃₂ P ₄	C ₇₄ H ₈₆ BrO ₉ PRu	C ₇₅ H ₉₀ BrCl ₄ O ₈ PRu
<i>M</i> (g mol ⁻¹)	4239.96	1331.37	1473.21
cryst syst	triclinic	monoclinic	orthorhombic
space group	<i>P</i> -1	<i>P</i> 2 ₁ / <i>c</i>	<i>P</i> 2 ₁ 2 ₁ 2 ₁
<i>a</i> (Å)	16.9044(4)	10.5189(3)	12.8374(1)
<i>b</i> (Å)	19.3933(3)	36.6703(8)	20.7662(1)
<i>c</i> (Å)	35.6237(7)	17.3637(5)	25.8143(1)
<i>α</i> (deg)	93.519(1)	90	90
<i>β</i> (deg)	90.718(2)	92.117(3)	90
<i>γ</i> (deg)	100.772(2)	90	90
<i>V</i> (Å ³)	11447.7(4)	6693.1(3)	6868.42(7)
<i>Z</i>	2	4	4
<i>D</i> _{calcd} (g cm ⁻³)	1.230	1.321	1.425
<i>μ</i> (Cu Kα) (mm ⁻¹)	1.446	3.265	4.632
<i>F</i> (000)	4512	2784	3064
reflns colld	114554	95761	104342
indep reflns	33883	12844	13186
obsd reflns [<i>I</i> > 2σ(<i>I</i>)]	24017	7478	13062
<i>R</i> _{int}	0.18	0.15	0.042
params refined	2643	767	823
<i>R</i> ₁	0.1447	0.1092	0.0403
<i>wR</i> ₂	0.4064	0.3611	0.1188
<i>S</i>	0.992	1.101	1.123
Δρ (e Å ⁻³)	< 1.74	< 2.12	< 0.80

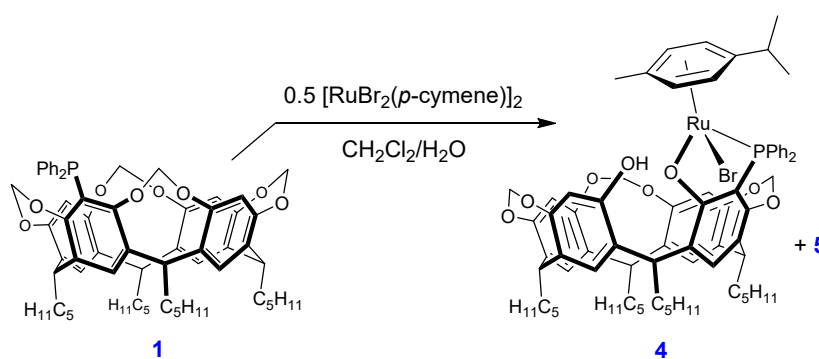
Table 2. Selected bond lengths (Å) and angles (°) for [Ni(P,O)₂] (**2**)

Bond lengths (Å)			
<i>Molecule 1</i>			
Ni(1)-O(1A)	1.869(6)	Ni(1)-O(1B)	1.872(6)
Ni(1)-P(1)	2.195(3)	Ni(1)-P(2)	2.180(2)
O(1A)-O(8A)	2.69(1)	O(1B)-O(8B)	2.68(1)
<i>Molecule 2</i>			
Ni(2)-O(1C)	1.878(5)	Ni(2)-O(1D)	1.876(6)
Ni(2)-P(3)		Ni(2)-P(4)	2.185(2)
O(1C)-O(8C)	2.182(3)	O(1D)-O(8D)	2.73(1)
	2.73(1)		
Bond angles (°)			
<i>Molecule 1</i>			
P(1)-Ni(1)-P(2)	105.1(1)	P(1)-Ni(1)-O(1B)	167.7(2)
O(1A)-Ni(1)-O(1B)	82.4(2)	P(2)-Ni(1)-O(1A)	168.9(2)
P(1)-Ni(1)-(O1A)	86.0(2)	P(2)-Ni(1)-(O1B)	86.4(2)
<i>Molecule 2</i>			
P(3)-Ni(2)-P(4)	102.8(1)	P(3)-Ni(2)-O(1D)	170.0(2)
O(1C)-Ni(2)-O(1D)	83.7(2)	P(4)-Ni(2)-O(1C)	170.3(2)
P(3)-Ni(2)-(O1C)	86.8(2)	P(4)-Ni(2)-(O1D)	86.6(2)

Klabunde *et al.* have shown that bis(phosphino-enolato) Ni(II) complexes are suitable for the initiation of olefin polymerisation reactions.^[6] Therefore, we decided to assess complex **2** as an ethylene oligomerisation catalyst. After activation of **2** with AlMe₃ in toluene (AlMe₃:Ni = 50), ethylene (20 bar, 90°C) was converted into a mixture of C₄-C₈ α-olefins.

The observed product distribution (C4: 93%, C6: 6%; C8: 1%) contrasts markedly with those of other precursors of Shell higher olefin process (SHOP) catalysts, which usually result in longer oligomers.^[7] The activity of the catalytic system was rather moderate, at seven times lower than that of the Keim's catalyst, $[\text{NiPh}(\text{Ph}_2\text{PCHC}(\text{O})\text{Ph})\text{PPh}_3]$.^[8] The formation of very short oligomers probably arises from O...H interactions between the coordinated oxygen atom and the resorcinolic OH group, which makes the oxygen atom a weaker donor. Similar effects have already been reported for other phosphino-enolato complexes.^[7, 9]

We have previously shown that the treatment of **1** with the neutral complex $[\text{RuCl}_2(p\text{-cymene})]_2$, leads quantitatively to a single form of the chelate complex $[\text{RuCl}(p\text{-cymene})(P,O)]$ (**3**).^[2] By extending this work to an investigation of the reaction of **1** with the bromido complex $[\text{RuBr}_2(p\text{-cymene})]_2$ under conditions similar to those applied for the preparation of **3**, we have now found that two isomeric products result and can be easily distinguished by their ^{31}P NMR chemical shifts. Chromatographic separation gave the bromido complex **4**, the crystal-structure determination (see below) showed it to be the analogue of **3**, in 38% yield, and a minor (15 % yield) product (**5**, 15 % yield, Scheme 3) with very similar spectroscopic properties and composition.



Scheme 3. Synthesis of **4** and **5**

Upon crystallisation of **4** (as obtained after chromatographic separation), two different forms of the crystals (Table 1) could be separated mechanically; some of these crystals were a racemic compound (A-type crystals; achiral space group $P2_1/c$; Figure 3, top) and others (B-type crystals; chiral space group $P2_12_12_1$; Figure 3, bottom) being components of a racemic conglomerate.^[10] The structure solution for the latter was superior but in both cases a

significant feature to be noted in both cases is that the complex present contains not only a chiral *P,O* ligand but also a chiral (asymmetric) Ru centre that adopts a typical piano-stool structure in which the Ru-arene vector is nearly parallel to the cavitand axis and the Ru-Br bond directed towards the exterior of the cavity. Thus, diastereomeric forms of the complex are to be expected and, on this basis, we conclude that complex **5** is the isomer where the Ru centre is inverted relative to that seen in **4** so that the Ru-Br vector is directed towards the cavitand axis. Unfortunately, it was not possible to obtain crystals of **5** suitable for a structure determination to confirm this conclusion. The structural data for both of the crystal forms of **4** are given in Tables 3 and 4. These results define a rather rare system in which the solubility difference between « racemic compound » and « racemic conglomerate » crystal forms of a chiral molecule is so slight that cocrystallisation is possible,^[11] furthermore, this occurs through the formation of different solvates.

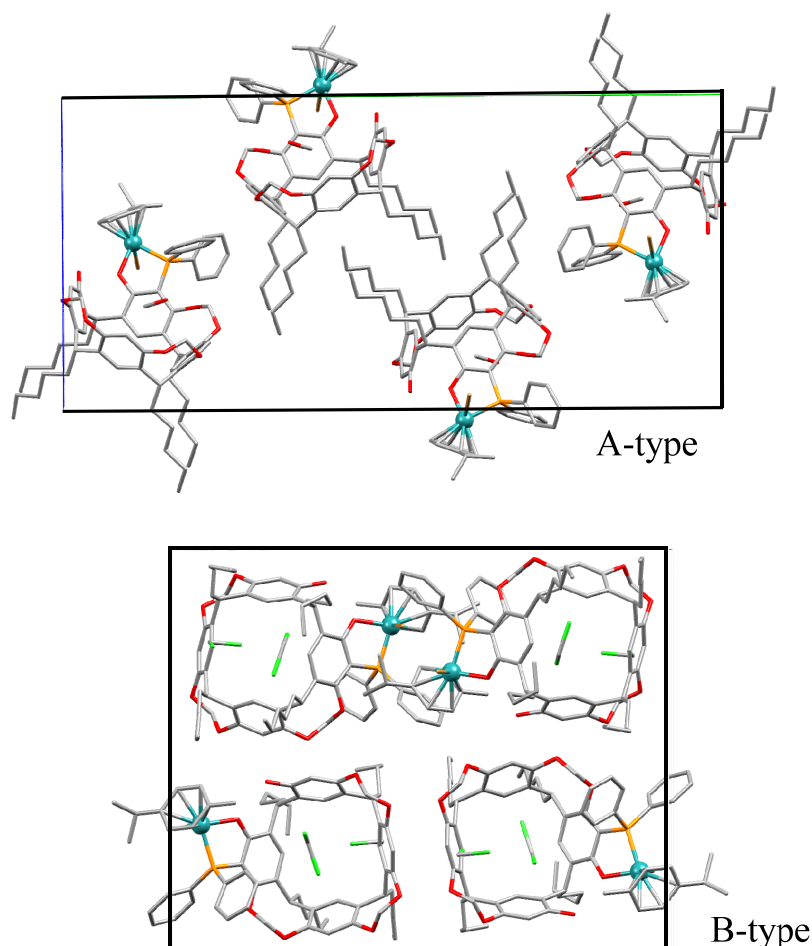


Figure 3. Unit cells in A- and B-type crystals of **4** containing respectively a racemate and a single enantiomer

Table 3. Selected bond lengths (Å) and angles (°) for **4** (A-type crystals, racemic compound)

lengths (Å)			
Ru-P	2.315(2)	Ru-O(8)	2.064(5)
Ru-Br	2.544(1)	O(8)-O(7)	2.64(1)
angles (°)			
P-Ru-O(8)	80.8(2)	O(8)-Ru-Br	83.9(2)
P-Ru-Br	85.59(6)	Ru-P-C(1)	101.0(3)

Table 4. Selected bond lengths (Å) and angles (°) for **4** (B-type crystals, single enantiomer)

lengths (Å)			
Ru-P	2.321(1)	Ru-O(8)	2.086(4)
Ru-Br	2.539(1)	O(8)-O(7)	2.61(1)
angles (°)			
P-Ru-O(8)	80.7(1)	O(8)-Ru-Br	80.7(1)
P-Ru-Br	89.08(3)	Ru-P-C(1)	100.8(2)

Conclusion

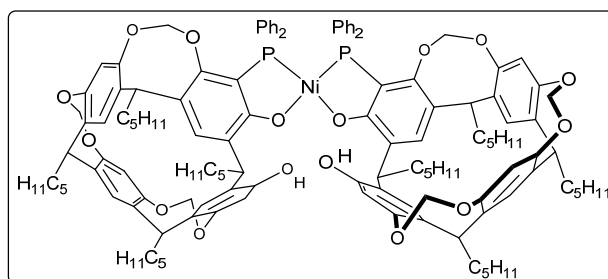
We have shown for the first time that a single Ni(II) centre is can induce consecutive C-O bond scission reactions in separate cavitand molecules. This is in contrast to the one-step reactions induced by octahedral Ru(II) complexes and a crystal-structure determination on the square-planar Ni(II) product, $[\text{Ni}(P,O)_2]$, in which the two ligand units can adopt a rather remote disposition, may be indicative of the relative facility with which an intermediate $\text{Ni}(P,O)$ species could accept a second cavitand ligand. A significant feature of the cavitand cleavage reaction is that it results in the conversion of the molecule from an achiral to a chiral form. At least in the solid state, binding of two phosphino-phenolate cleavage products to

Ni(II) centre occurs through preferential formation of the racemic form rather than the *meso* form. Although previous work on octahedral Ru(II) complexes of the present type with a chiral centre led to the isolation of a single diastereomer of the product, the substitution of a bromido ligand for a chlorido ligand has in the present work shown that two diastereomers, differing in their configuration about the Ru centre, can be formed. Intriguingly, crystallisation of the major isomer of the bromido complex has shown that crystals of both a racemic compound and a racemic conglomerate form under the same conditions, although as different solvates.

Experimental

General Methods: All manipulations involving phosphorus derivatives were performed in Schlenk-type flasks under dry nitrogen. Commercial dichloromethane (undried) was used as solvent in all reactions. CDCl₃ was passed down a 5 cm thick alumina column and stored under nitrogen over molecular sieves (4 Å). Routine ¹H, ¹³C{¹H} and ³¹P{¹H} NMR spectra were recorded with an FT Bruker AV-300 spectrometer. ¹H chemical shifts are referenced to residual protiated solvents ($\delta = 7.26$ ppm for CDCl₃), ¹³C chemical shifts are reported relative to deuteriated solvents ($\delta = 77.16$ ppm for CDCl₃) and the ³¹P NMR spectroscopic data are given relative to external H₃PO₄. Chemical shifts and coupling constants are reported in ppm and Hz, respectively. Elemental analyses were performed by the Service de Microanalyse, Institut de Chimie, Université de Strasbourg. 5-Diphenylphosphanyl-4(24),6(10),12(16),18(22)-tetramethylenedioxy-2,8,14,20-tetrapentyl resorcin[4]arene (**1**),^[1h] [Ni(η^5 -C₅H₅)(1,5-cyclooctadiene)]BF₄,^[12] and [RuBr₂(*p*-cymene)]₂^[13] were prepared according to literature procedures.

Synthesis of nickel complex **2**

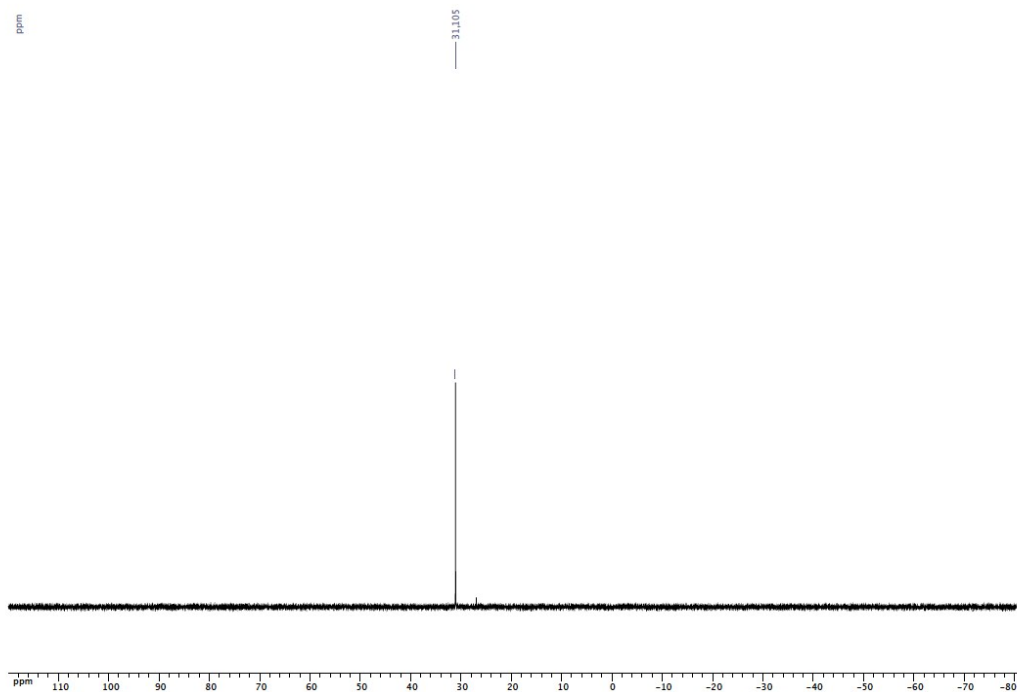


A solution of $[\text{Ni}(\eta^5\text{-C}_5\text{H}_5)(1,5\text{-cyclooctadiene})]\text{BF}_4$ (0.012 g, 0.035 mmol) in CH_2Cl_2 (50 mL) was added to a solution of cavitand-phosphine **1** (0.075 g, 0.070 mmol) in CH_2Cl_2 (20 mL). The reaction mixture was stirred at 30°C for 7 days. The solution was concentrated to ca. 2 mL and *n*-hexane (20 mL) was added. The resulting yellow precipitate was separated by filtration and purified by column chromatography (CH_2Cl_2 /petroleum ether, 1:1 v/v) to afford complex **2** as an orange solid, which was dried in vacuo. Yield 0.060 g, 76 %. ^1H NMR (400 MHz, CDCl_3): δ = 9.48 (s, 2H, OH), 7.70 (q, 4H, arom. CH, PPh_2 , $^3J = 7.5$ Hz), 7.30 (t, 2H, arom. CH, PPh_2 , $^3J = 7.0$ Hz), 7.25 (t, 2H, arom. CH, PPh_2 , $^3J = 7.5$ Hz), 7.11 (s, 2H, arom. CH, resorcinarene), 7.08 (s, 2H, arom. CH, resorcinarene), 7.07 (s, 2H, arom. CH, resorcinarene), 7.01 (t, 4H, arom. CH, PPh_2 , $^3J = 7.7$ Hz), 6.99 (s, 2H, arom. CH, resorcinarene), 6.95 (t, 4H, arom. CH, PPh_2 , $^3J = 7.5$ Hz), 6.93-6.91 (m, 4H, arom. CH, PPh_2), 6.43 (s, 2H, arom. CH, resorcinarene), 6.34 (s, 2H, arom. CH, resorcinarene), 6.16 (s, 2H, arom. CH, resorcinarene), 5.73 and 4.51 (AB spin system, 4H, OCH_2O , $^2J = 7.5$ Hz), 5.59 and 4.36 (AB spin system, 4H, OCH_2O , $^2J = 7.0$ Hz), 4.86 (t, 2H, CHCH_2 , $^3J = 7.5$ Hz), 4.72 and 3.18 (AB spin system, 4H, OCH_2O , $^3J = 7.5$ Hz), 4.67 (t, 2H, CHCH_2 , $^3J = 8.0$ Hz), 4.61 (t, 2H, CHCH_2 , $^3J = 8.0$ Hz), 4.38 (t, 2H, CHCH_2 , $^3J = 7.5$ Hz), 2.35-2.02 (m, 16H, CHCH_2), 1.43-1.25 (m, 48H, $\text{CH}_2\text{CH}_2\text{CH}_2\text{CH}_3$), 0.93 (t, 6H, CH_2CH_3 , $^3J = 7.0$ Hz), 0.91 (t, 6H, CH_2CH_3 , $^3J = 7.0$ Hz), 0.88 (t, 12H, CH_2CH_3 , $^3J = 7.0$ Hz); $^{13}\text{C}\{^1\text{H}\}$ NMR (125 MHz, CDCl_3): δ = 169.12-108.92 (arom. C.), 99.80 (s, OCH_2O), 99.47 (s, OCH_2O), 99.32 (s, OCH_2O), 36.45 (s, CHCH_2), 36.21 (s, CHCH_2), 35.62 (s, CHCH_2), 34.06 (s, CHCH_2), 32.34 (s, $\text{CH}_2\text{CH}_2\text{CH}_3$), 32.23 (s, $\text{CH}_2\text{CH}_2\text{CH}_3$), 32.11 (s, $\text{CH}_2\text{CH}_2\text{CH}_3$), 31.79 (s, $\text{CH}_2\text{CH}_2\text{CH}_3$), 30.22 (s, CHCH_2), 30.19 (s, CHCH_2), 29.92 (s, CHCH_2), 29.86 (s, CHCH_2), 27.84 (s, CHCH_2CH_2), 27.65 (s, CHCH_2CH_2), 27.50 (s, CHCH_2CH_2), 23.07 (s, CH_2CH_3), 23.01 (s, CH_2CH_3), 22.95 (s, CH_2CH_3), 22.79 (s, CH_2CH_3), 14.42 (s, CH_2CH_3), 14.32 (s, CH_2CH_3), 14.24 (s, CH_2CH_3);

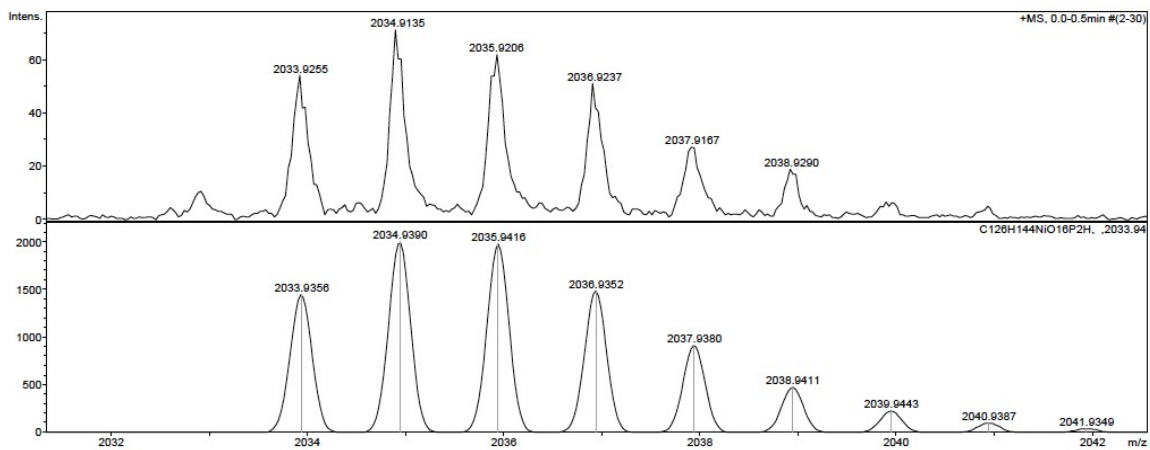
$^{31}\text{P}\{\text{H}\}$ NMR (162 MHz, CDCl_3): $\delta = 31.1$ (s, PPh_2); MS (ESI-TOF): $m/z = 2034.91$ [$\text{M} + \text{H}^+$] expected isotopic profile; elemental analysis calcd (%) for $\text{C}_{126}\text{H}_{144}\text{O}_{16}\text{P}_2\text{Ni}$ (2035.12): C 74.36, H 7.13; found (%): C 74.19, H 7.21.

Single, orange-red crystals of $\mathbf{2}\cdot\text{CH}_2\text{Cl}_2$ suitable for X-ray diffraction were obtained by slow diffusion of hexane into a CH_2Cl_2 solution of $\mathbf{2}$ at room temperature. Diffraction data for $\mathbf{2}\cdot\text{CH}_2\text{Cl}_2$, were collected on an Oxford Diffraction SuperNova EOS2 diffractometer using graphite-monochromated $\text{Cu-K}\alpha$ radiation ($\lambda = 1.54184 \text{ \AA}$). The structure was solved using SIR-97,^[14] which revealed the non-hydrogen atoms of the molecules. After anisotropic refinement, most of the hydrogen atoms were found by Fourier difference. The structure was then refined with SHELXL97^[15] using the full-matrix least-squares technique {use of F^2 ; x, y, z, β_{ij} for C, O, Br, Cl, P and Ni or Ru atoms, x, y, z in the riding mode for H atoms; for $\mathbf{2}\cdot\text{CH}_2\text{Cl}_2$: calcd. $w = 1/[\sigma^2(F_o^2) + (0.1804P)^2 + 163.4841P]$ in which $P = (F_o^2 + 2 F_c^2)/3$. Crystal and refinement data are given in Table 1 and selected bond lengths and angles in Tables 2.

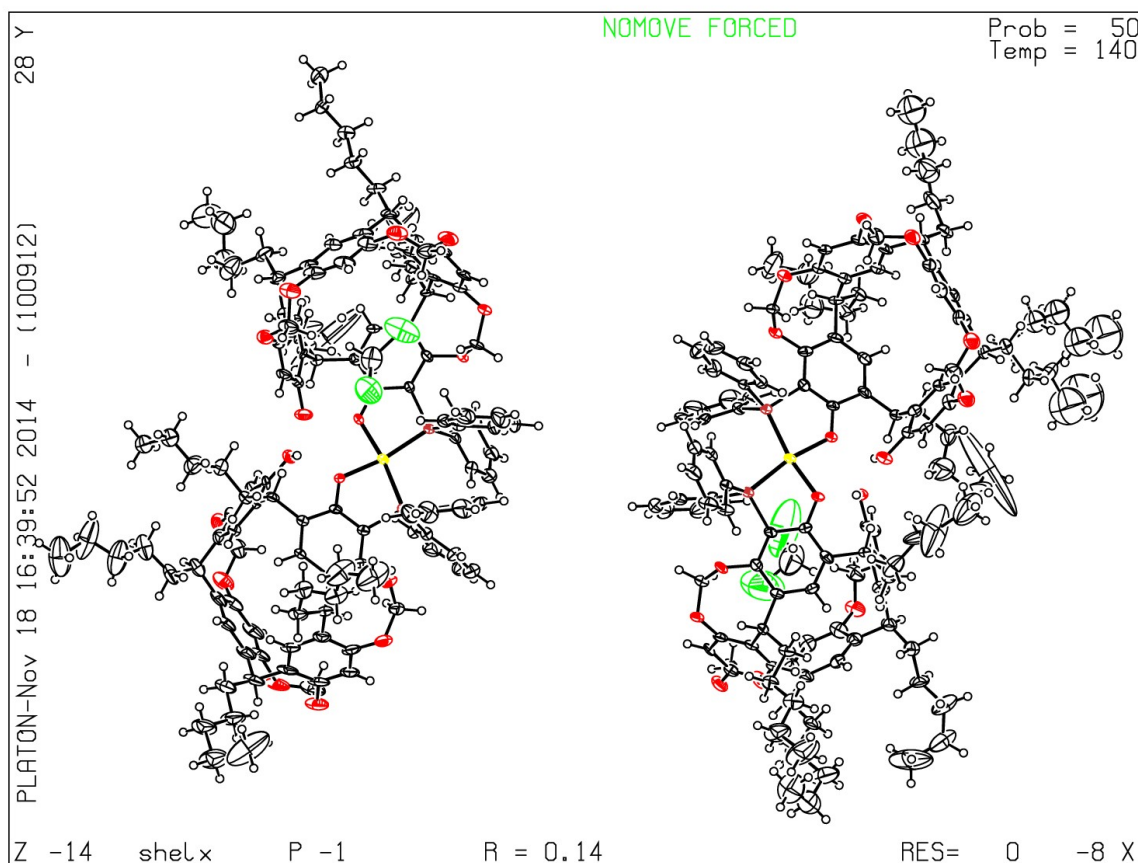
The unit cell contains two inequivalent complex molecules, and two molecules of CH_2Cl_2 , one of which lies inside a cavity. Weak diffraction by the crystal, particularly at high values, and extensive disorder of the pentyl groups are the principal causes of Checkcif alerts level A, B, and C. Although somewhat unsatisfactory, the structure solution defines the essential aspects of the chirality of the molecule. CCDC-1035085 contains the supplementary crystallographic data for $\mathbf{2}$ which can be obtained free of charge from The Cambridge Crystallographic Data Centre via www.ccdc.cam.ac.uk/data_request/cif.



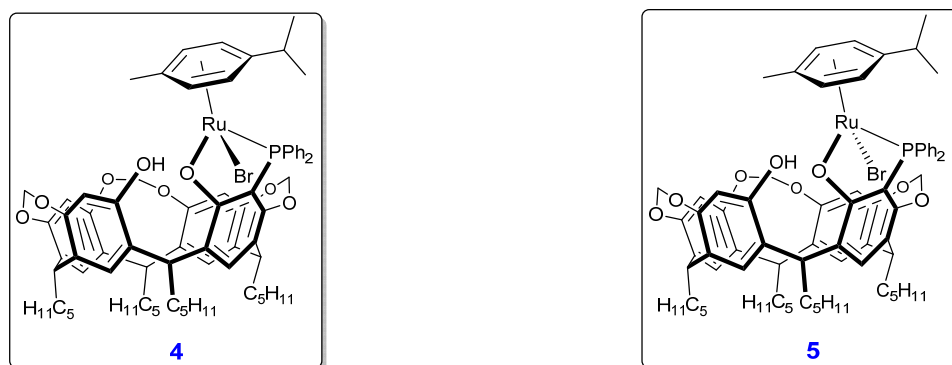
$^{31}\text{P}\{^1\text{H}\}$ NMR spectrum of **2** (CDCl_3)



Mass spectrum (ESI-TOF) of **2** (exp. spectrum (top); calculated spectrum (bottom) for $\text{C}_{126}\text{H}_{144}\text{NiO}_{16}\text{P}_2 + \text{H}$)

X-ray structure (Platon) of **2**

Synthesis of ruthenium(II) complexes **4** and **5**

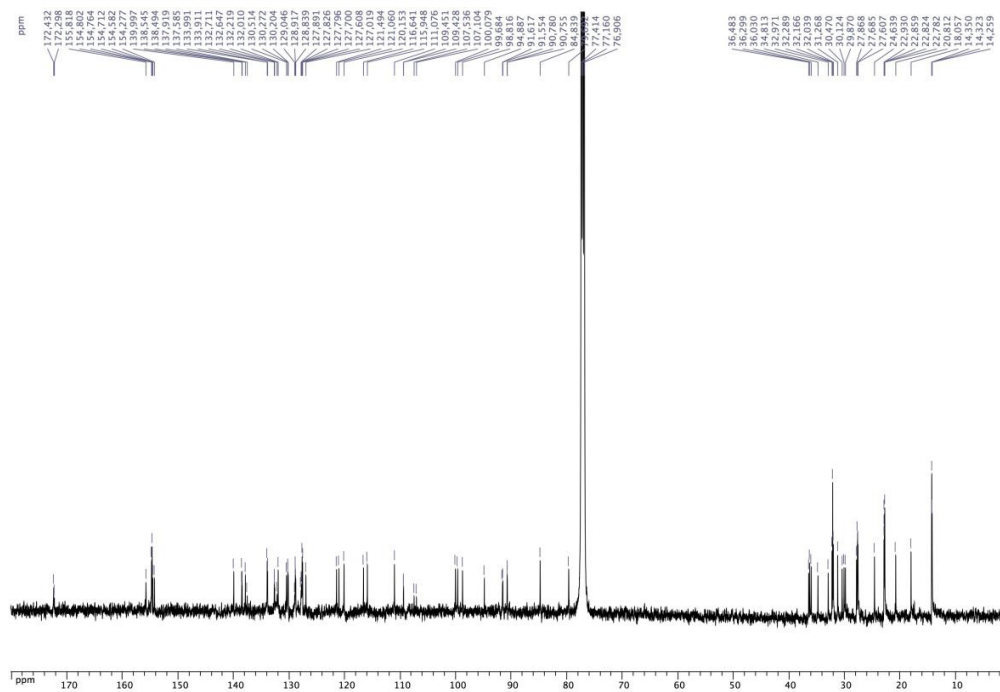


A solution of $[\text{RuBr}_2(p\text{-cymene})]_2$ (0.020 g, 0.025 mmol) in wet CH_2Cl_2 (5 mL) was added to a stirred solution of cavitand-phosphine **1** (0.050 g, 0.05 mmol) in CH_2Cl_2 (5 mL). The mixture was stirred for 16 h at room temperature. The solution was concentrated to ca. 2 mL, after which *n*-hexane (20 mL) was added to yield an orange precipitate, which was separated

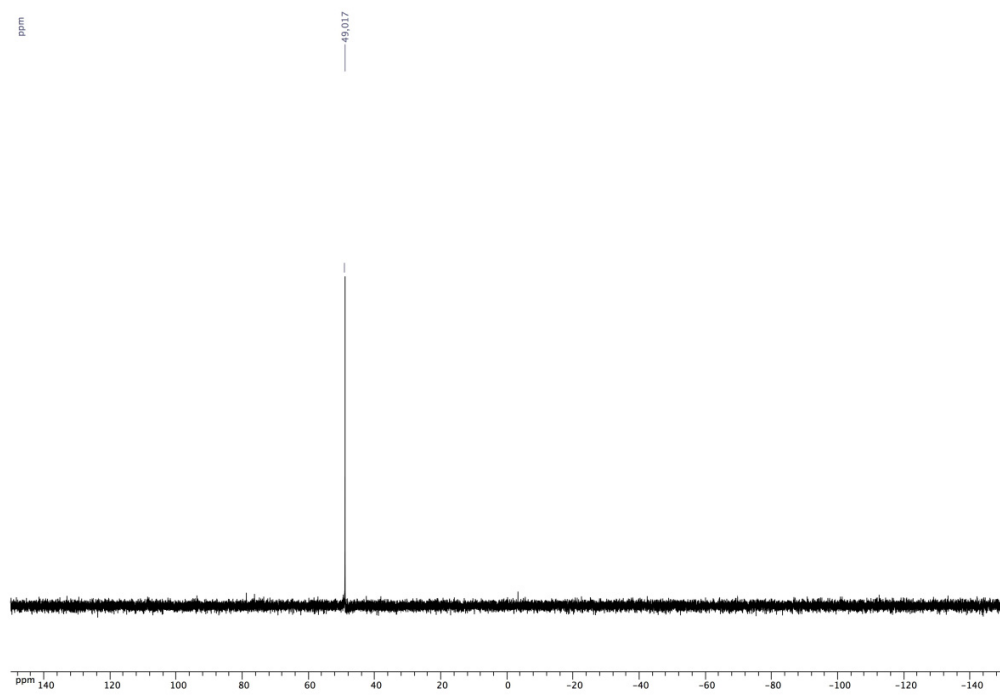
by filtration. Purification by column chromatography (CH₂Cl₂/Et₂O, 95:5 v/v) afforded complex **4** as an orange solid, which was dried in vacuo ($R_f = 0.83$; yield 0.025 g, 38 %). Chromatographic separation gave another, minor complex (**5**) (brown solid; $R_f = 0.33$; yield 0.010 g, 15%), identified by its spectroscopic and analytical parameters only (see data below).

Data for complex 4 (major): ¹H NMR (400 MHz, CDCl₃): $\delta = 10.14$ (s, 1H, OH), 7.67-7.63 (m, 2H, arom. CH, PPh₂), 7.56-7.52 (m, 2H, arom. CH, PPh₂), 7.46-7.42 (m, 6H, arom. CH, PPh₂), 7.18 (s, 1H, arom. CH, resorcinarene), 7.13 (s, 1H, arom. CH, resorcinarene), 7.05 (s, 1H, arom. CH, resorcinarene), 6.98 (s, 1H, arom. CH, resorcinarene), 6.50 (s, 1H, arom. CH, resorcinarene), 6.37 (s, 1H, arom. CH, resorcinarene), 6.19 (s, 1H, arom. CH, resorcinarene), 5.88 and 5.60 (AA' of an AA' BB' spin system, 2H, arom. CH, *p*-cymene, ³*J* = 6.0 Hz), 5.81 and 4.52 (AB spin system, 2H, OCH₂O, ²*J* = 7.2 Hz), 5.67 and 4.45 (AB spin system, 2H, OCH₂O, ²*J* = 7.2 Hz), 5.36 and 4.76 (BB' of an AA'BB' spin system, 2H, arom. CH, *p*-cymene, ³*J* = 6.0 Hz), 4.74 (t, 1H, CHCH₂, ³*J* = 8.4 Hz), 4.68 (t, 1H, CHCH₂, ³*J* = 8.0 Hz), 4.56 (t, 1H, CHCH₂, ³*J* = 8.0 Hz), 4.46 (t, 1H, CHCH₂, ³*J* = 8.2 Hz), 4.25 and 3.19 (AB spin system, 2H, OCH₂O, ²*J* = 7.4 Hz), 3.05 (hept, 1H, CH(CH₃)₂, ³*J* = 6.8 Hz), 2.31-2.08 (m, 8H, CHCH₂), 1.95 (s, 3H, CH₃ of *p*-cymene), 1.45-1.22 (m, 24H, CH₂CH₂CH₂CH₃), 1.25 (d, 3H, CH(CH₃)₂, ³*J* = 6.8 Hz), 1.13 (d, 3H, CH(CH₃)₂, ³*J* = 6.8 Hz), 0.93 (t, 3H, CH₂CH₃, ³*J* = 7.2 Hz), 0.91 (t, 3H, CH₂CH₃, ³*J* = 7.1 Hz), 0.90 (t, 3H, CH₂CH₃, ³*J* = 7.3 Hz), 0.86 (t, 3H, CH₂CH₃, ³*J* = 6.5 Hz); ¹³C{¹H} NMR (125 MHz, CDCl₃): $\delta = 172.43$ -107.10 (arom. C's), 100.08 (s, OCH₂O), 99.68 (s, OCH₂O), 98.82 (s, OCH₂O), 94.89 (s, arom. Cquat, *p*-cymene), 91.58 (d, arom. CH, *p*-cymene, ¹*J*_{PC} = 7.8 Hz), 90.77 (d, arom. CH, *p*-cymene, ¹*J*_{PC} = 3.1 Hz), 84.84 (s, arom. CH, *p*-cymene), 79.69 (s, arom. CH, *p*-cymene), 36.48 (s, CHCH₂), 36.30 (s, CHCH₂), 36.03 (s, CHCH₂), 34.81 (s, CHCH₂), 32.97 (s, CH₂CH₂CH₃), 32.29 (s, CH₂CH₂CH₃), 32.17 (s, CH₂CH₂CH₃), 32.04 (s, CH₂CH₂CH₃), 31.27 (s, CH(CH₃)₂), 30.47 (s, CHCH₂), 30.12 (s, CHCH₂), 29.87 (s, CHCH₂), 27.87 (s, CHCH₂CH₂), 27.68 (s, CHCH₂CH₂), 27.61 (s, CHCH₂CH₂), 24.64 (s, CH(CH₃)₂), 22.93 (s, CH₂CH₃), 22.86 (s, CH₂CH₃), 22.82 (s, CH₂CH₃), 22.78 (s, CH₂CH₃), 20.81 (s, CH(CH₃)₂), 18.06 (s, CH₃ of *p*-cymene), 14.35 (s, CH₂CH₃), 14.32 (s, CH₂CH₃), 14.26 (s, CH₂CH₃); ³¹P{¹H} NMR (162 MHz, CDCl₃): $\delta = 49.0$ (s, PPh₂); MS (ESI-TOF): *m/z* = 1304.43 [M⁺] expected isotopic profile; elemental analysis calcd (%) for C₇₃H₈₆BrO₈PRu (1303.40): C 67.27, H 6.65; found (%): C 67.12, H 6.55.

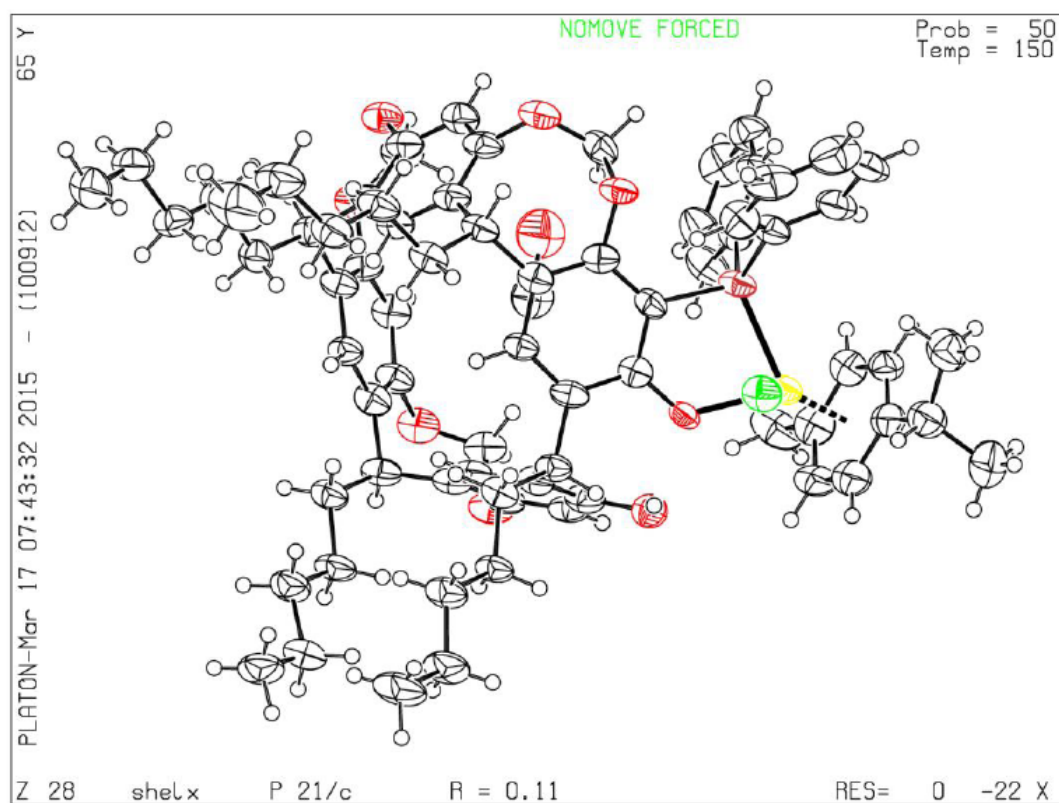
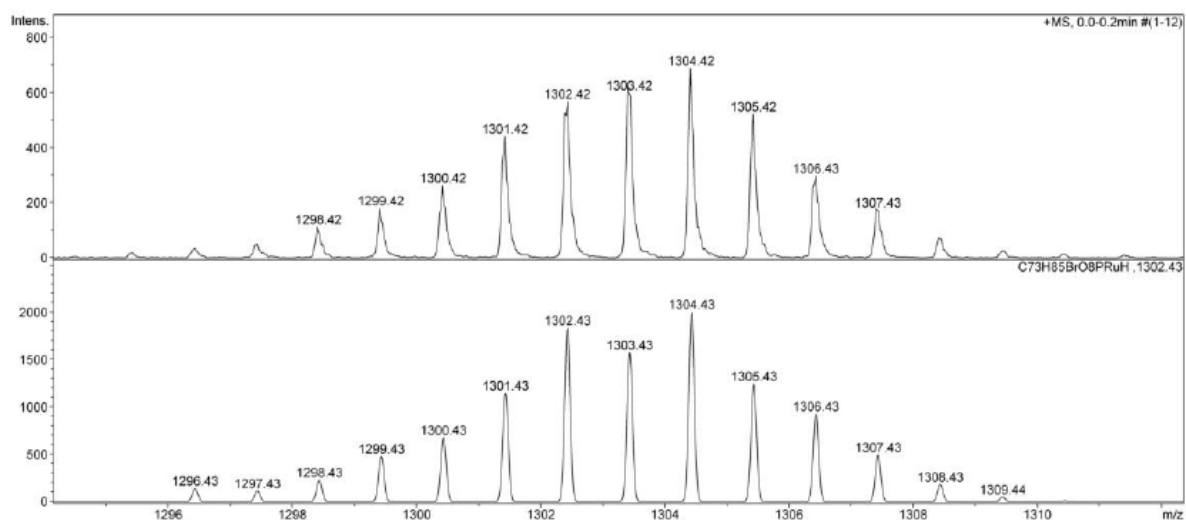
Single crystals, mechanically separated, of **4**.CH₃OH (**4A**) and **4**.2CH₂Cl₂ (**4B**) were obtained by slow diffusion of CH₃OH into a CH₂Cl₂ solution of chromatographically purified **4**.

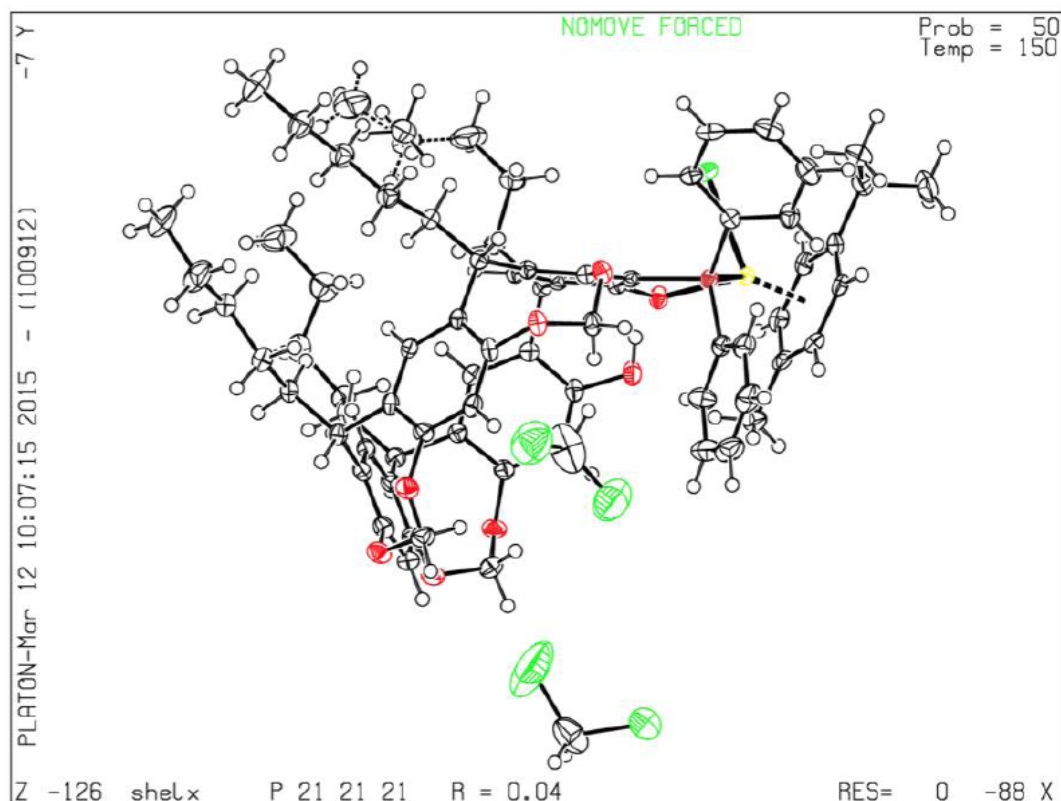


$^{13}\text{C}\{^1\text{H}\}$ NMR spectrum of **4**



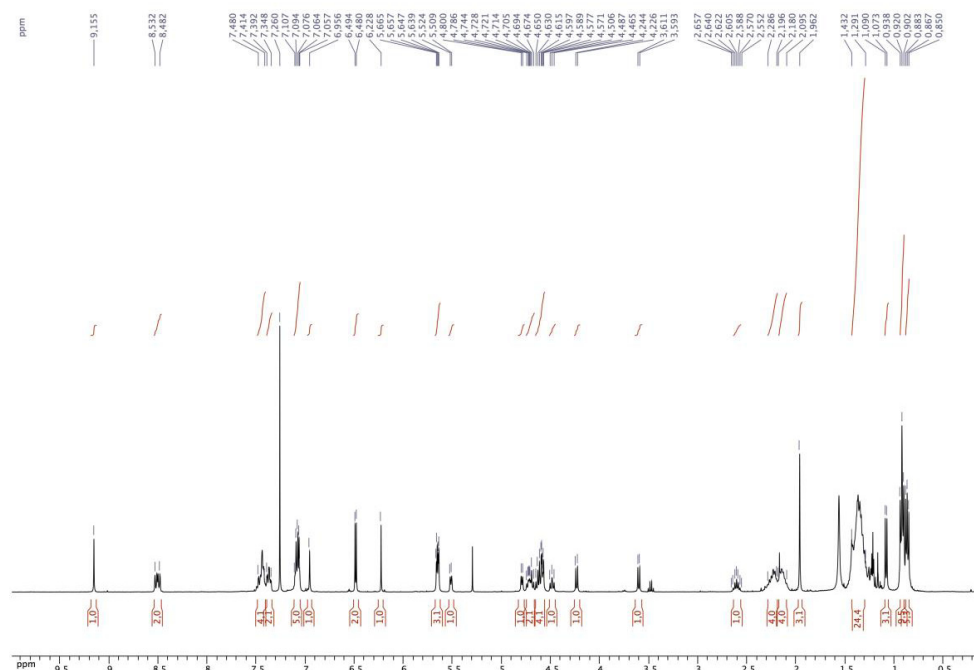
$^{31}\text{P}\{^1\text{H}\}$ NMR of **4**



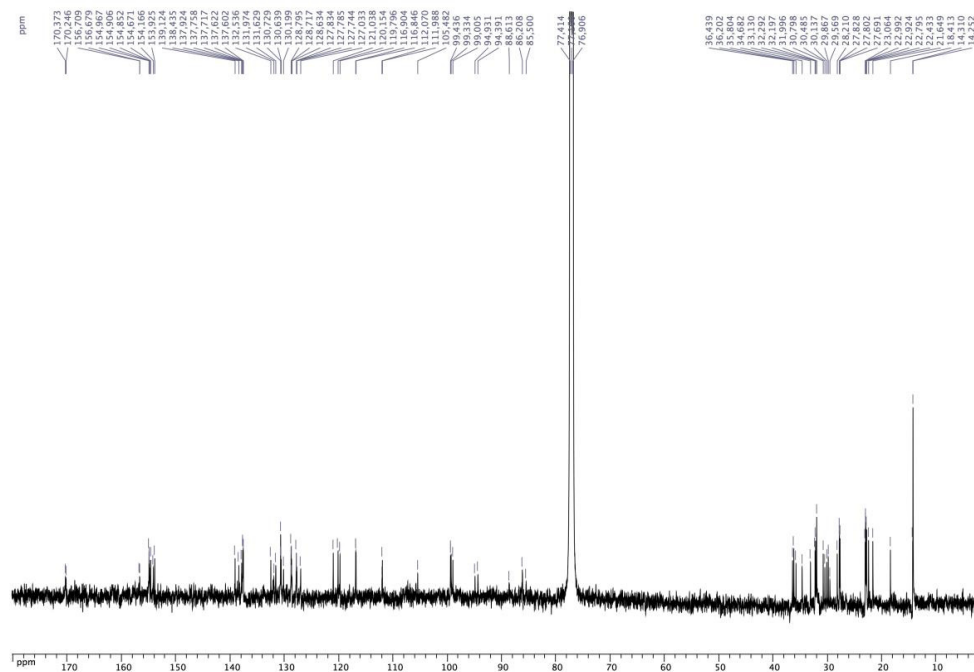
X-ray structure (Platon) of **4B**

Data for complex 5 (minor): ^1H NMR (400 MHz, CDCl_3): δ = 9.15 (s, 1H, OH), 8.53-8.48 (m, 2H, arom. CH, PPh_2), 7.48-7.41 (m, 4H, arom. CH, PPh_2), 7.39-7.35 (m, 2H, arom. CH, PPh_2), 7.11-7.06 (m, 2H, arom. CH, PPh_2), 7.09 (s, 1H, arom. CH, resorcinarene), 7.08 (s, 1H, arom. CH, resorcinarene), 7.06 (s, 1H, arom. CH, resorcinarene), 6.96 (s, 1H, arom. CH, resorcinarene), 6.49 (s, 1H, arom. CH, resorcinarene), 6.48 (s, 1H, arom. CH, resorcinarene), 6.23 (s, 1H, arom. CH, resorcinarene), 5.66 and 4.79 (AA' of an AA'BB' spin system, 2H, arom. CH, *p*-cymene, $^3J = 5.6$ Hz), 5.65 and 4.61 (AB spin system, 2H, OCH_2O , $^2J = 7.2$ Hz), 5.64 and 4.59 (AB spin system, 2H, OCH_2O , $^2J = 8.0$ Hz), 5.52 and 4.58 (BB' of an AA'BB' spin system, 2H, arom. CH, *p*-cymene, $^3J = 6.0$ Hz), 4.72 (t, 1H, CHCH_2 , $^3J = 7.4$ Hz), 4.69 (t, 1H, CHCH_2 , $^3J = 8.0$ Hz), 4.63 (t, 1H, CHCH_2 , $^3J = 8.0$ Hz), 4.49 (t, 1H, CHCH_2 , $^3J = 8.2$ Hz), 4.23 and 3.60 (AB spin system, 2H, OCH_2O , $^2J = 7.2$ Hz), 2.60 (hept, 1H, $\text{CH}(\text{CH}_3)_2$, $^3J = 6.8$ Hz), 2.29-2.20 (m, 4H, CHCH_2), 2.18-2.09 (m, 4H, CHCH_2), 1.96 (s, 3H, CH_3 of *p*-cymene), 1.43-1.29 (m, 24H, $\text{CH}_2\text{CH}_2\text{CH}_2\text{CH}_3$), 1.08 (d, 3H, $\text{CH}(\text{CH}_3)_2$, $^3J = 6.8$ Hz), 0.92 (t, 9H, CH_2CH_3 , $^3J = 7.2$ Hz), 0.88 (t, 3H, CH_2CH_3 , $^3J = 7.0$ Hz), 0.86 (d, 3H, $\text{CH}(\text{CH}_3)_2$, $^3J = 6.8$ Hz); $^{13}\text{C}\{^1\text{H}\}$ NMR (125 MHz, CDCl_3): δ = 170.37-105.48 (arom. C's), 99.44 (s, OCH_2O), 99.33 (s, OCH_2O), 99.00 (s, OCH_2O), 94.93 (s, arom. Cquat, *p*-cymene), 94.39 (s,

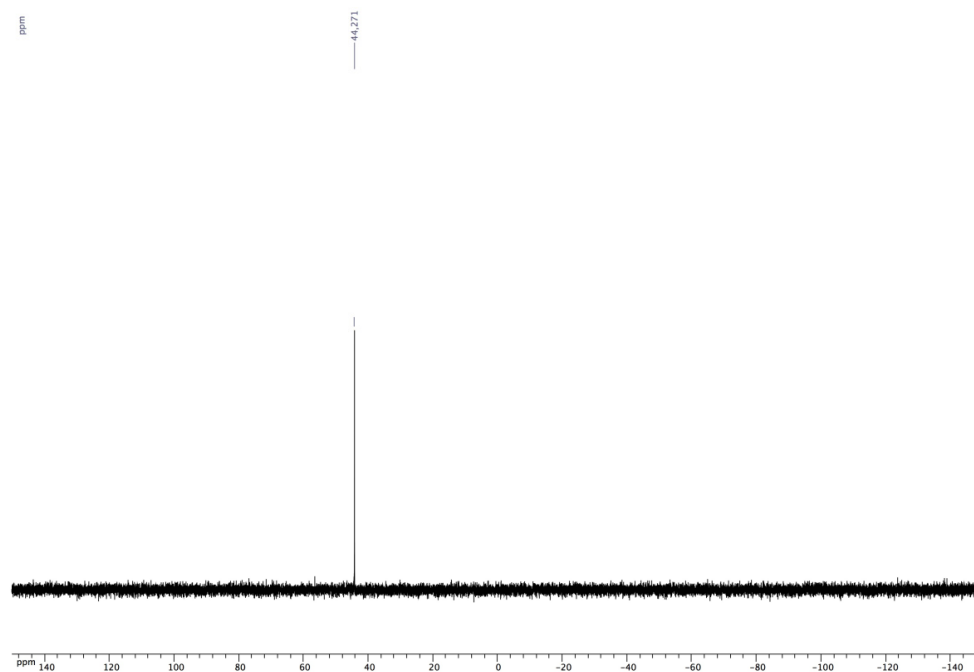
arom. CH, *p*-cymene), 88.61 (s, arom. CH, *p*-cymene), 86.21 (s, arom. CH, *p*-cymene), 85.50 (s, arom. CH, *p*-cymene), 36.44 (s, CHCH₂), 36.20 (s, CHCH₂), 35.80 (s, CHCH₂), 34.68 (s, CHCH₂), 33.13 (s, CH₂CH₂CH₃), 32.29 (s, CH₂CH₂CH₃), 32.20 (s, CH₂CH₂CH₃), 32.00 (s, CH₂CH₂CH₃), 30.80 (s, CH(CH₃)₂), 30.48 (s, CHCH₂), 30.14 (s, CHCH₂), 29.87 (s, CHCH₂), 28.21 (s, CHCH₂), 27.92 (s, CHCH₂CH₂), 27.80 (s, CHCH₂CH₂), 27.44 (s, CHCH₂CH₂), 27.69 (s, CHCH₂CH₂), 23.06 (s, CH₂CH₃), 22.99 (s, CH₂CH₃), 22.92 (s, CH₂CH₃), 22.79 (s, CH₂CH₃), 22.43 (s, CH(CH₃)₂), 21.65 (s, CH(CH₃)₂), 18.41 (s, CH₃ of *p*-cymene), 14.31 (s, CH₂CH₃), 14.25 (s, CH₂CH₃); ³¹P{¹H} NMR (162 MHz, CDCl₃): δ = 44.3 (s, PPh₂); MS (ESI-TOF): *m/z* = 1304.43 [M⁺] expected isotopic profile; elemental analysis calcd (%) for C₇₃H₈₆BrO₈PRu (1303.40): C 67.27, H 6.65; found (%): C 67.32, H 6.71.



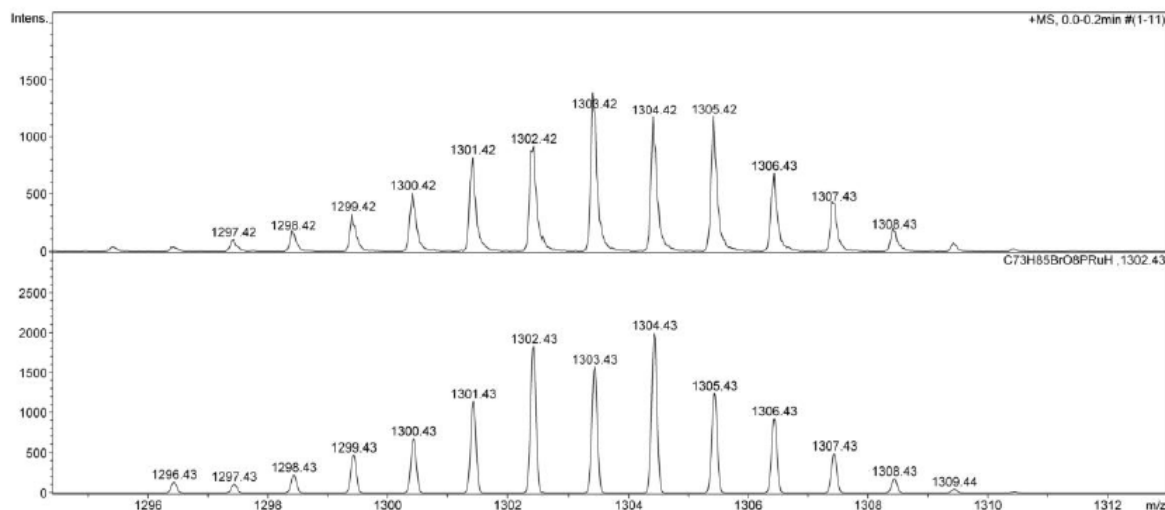
¹H NMR spectrum of **5**



$^{13}\text{C} \{^1\text{H}\}$ NMR spectrum of **5**



$^{31}\text{P} \{^1\text{H}\}$ NMR spectrum of **5**



Mass spectrum (ESI-TOF) of **5** (exp. spectrum (top)); calculated spectrum (bottom) for $C_{73}H_{85}BrO_8PRu + H$

References

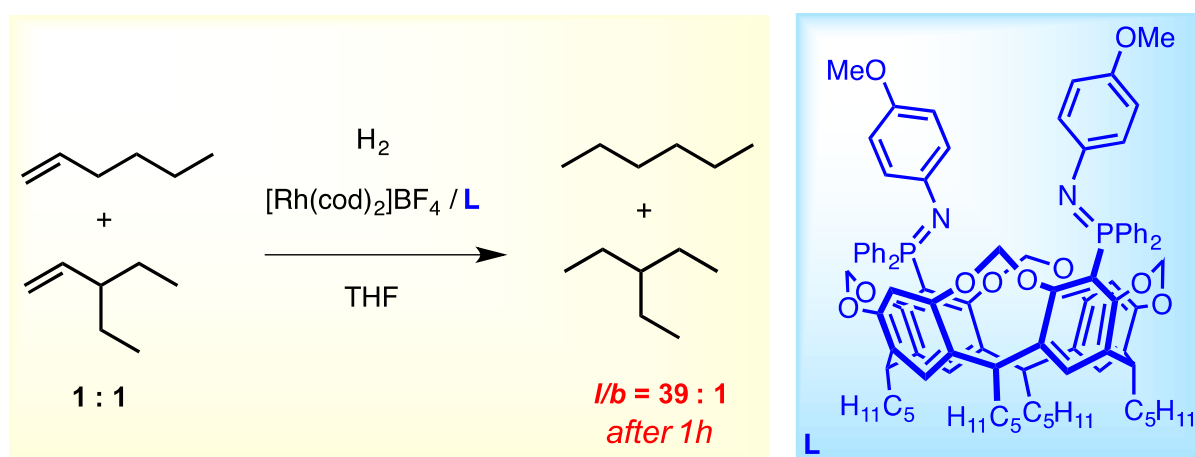
- [1] a) W. Verboom, in *Calixarenes 2001*, Z. Asfari, V. Böhmer, J. Harrowfield, J. Vicens, Eds. Kluwer, Dordrecht, 2001, pp 181-198; b) D. J. Cram, *Angew. Chem. Int. Ed.* **1988**, *27*, 1009-1020; c) F. Hof, S. L. Craig, C. Nuckolls and J. Rebek Jr., *Angew. Chem., Int. Ed.* **2002**, *41*, 1488-1508; d) G. Arnott, H. Heaney, R. Hunter and P. C. B. Page, *Eur. J. Org. Chem.* **2004**, 5126-5134; e) S. S. Zhu, H. Staats, K. Brandhorst, J. Grunenberg, F. Gruppi, E. Dalcanale, A. Luetzen, K. Rissanen and C. A. Schalley, *Angew. Chem. Int. Ed.* **2008**, *47*, 788-792; f) V. K. Jain and P. H. Kanaiya, *Russ. Chem. Rev.* **2011**, *80*, 75-102; g) R. Gramage-Doria, D. Armspach and D. Matt, *Coord. Chem. Rev.* **2013**, *257*, 776-816; h) L. Monnereau, H. El Moll, D. Semeril, D. Matt and L. Toupet, *Eur. J. Inorg. Chem.* **2014**, *2014*, 1364-1372; i) N. Montes-Garcia, J. Perez-Juste, I. Pastoriza-Santos and L. M. Liz-Marzan, *Chem. Eur. J.* **2014**, *20*, 10874-10883; j) D. Sémeril and D. Matt, *Coord. Chem. Rev.* **2014**, *279*, 58-95.
- [2] T. Chavagnan, D. Sémeril, D. Matt, J. Harrowfield and L. Toupet, *Chemistry, Eur. J.* **2015**, *21*, 6678-6681.
- [3] a) R. J. Puddephatt, *Can. J. Chem.* **2006**, *84*, 1505-1514; b) I. R. Knyazeva, A. R. Burilov, M. A. Pudovik and W. D. Habicher, *Russ. Chem. Rev.* **2013**, *82*, 150-186.
- [4] M. Henrion, A. M. Oertel, V. Ritleng and M. J. Chetcuti, *Chem. Comm.* **2013**, *49*, 6424-6426.
- [5] a) T. Jarolim and J. Podlahova, *J. Inorg. Nucl. Chem.* **1976**, *38*, 125-129; b) T. B. Rauchfuss, *Inorg. Chem.* **1977**, *16*, 2966-2968; c) P. Braunstein, T. M. G. Carneiro, D. Matt, F. Balegroune and D. Grandjean, *Organometallics* **1989**, *8*, 1737-1743; d) D. Matt, N. Sutter-Beydoun, J. P. Brunette, F. Balegroune and D. Grandjean, *Inorg. Chem.* **1993**, *32*, 3488-3492; e) J. Heinicke, M. Koesling, R. Brüll, W. Keim and H. Pritzkow, *Eur. J. Inorg. Chem.* **2000**, 299-305; f) D. G. Yakhvarov, K. R. Basvani, M. K.

- Kindermann, A. B. Dobrynin, I. A. Litvinov, O. G. Sinyashin, P. G. Jones and J. Heinicke, *Eur. J. Inorg. Chem.* **2009**, 1234-1242.
- [6] U. Klabunde, R. Mulhaupt, T. Herskovitz, A. H. Janowicz, J. Calabrese and S. D. Ittel, *J. Polym. Sci. Pol. Chem.* **1987**, *25*, 1989-2003.
- [7] P. Kuhn, D. Sémeril, C. Jeunesse, D. Matt, M. Neuburger and A. Mota, *Chem. Eur. J.* **2006**, *12*, 5210-5219.
- [8] W. Keim, F. H. Kowaldt, R. Goddard and C. Krüger, *Angew. Chem. Int. Ed.* **1978**, *17*, 466-467.
- [9] a) P. Braunstein, Y. Chauvin, S. Mercier, L. Saussine, A. Decian and J. Fischer, *Chem. Comm.* **1994**, 2203-2204; b) P. Kuhn, D. Sémeril, C. Jeunesse, D. Matt, P. Lutz and R. Welter, *Eur. J. Inorg. Chem.* **2005**, 1477-1481.
- [10] a) H. D. Flack, *Helv. Chim. Acta* **2003**, *86*, 905-921; b) H. D. Flack, *Acta Crystallogr. A* **2009**, *65*, 371-389.
- [11] S. F. Mason, *Molecular optical activity and chiral discrimination*, Cambridge University Press, Cambridge, Ch. 0, pp. 148-185.
- [12] A. Salzer, T. L. Court and H. Werner, *J. Organomet. Chem.* **1973**, *54*, 325-330.
- [13] M. G. Mendoza-Ferri, C. G. Hartinger, A. A. Nazarov, R. E. Eichinger, M. A. Jakupec, K. Severin and B. K. Keppler, *Organometallics* **2009**, *28*, 6260-6265.
- [14] A. Altomare, M. C. Burla, M. Camalli, G. Cascarano, C. Giacovazzo, A. Guagliardi, A. G. G. Moliterni, G. Polidori and R. Spagna, SIR97, an integrated package of computer programs for the solution and refinement of crystal structures using single crystal data.
- [15] G. M. Sheldrick and SHELXL-97, Program for Crystal Structure Refinement **1997**, University of Göttingen, Göttingen (Germany).

Chapter IV

Substrate-selective olefin hydrogenation with a cavitand-based bis-*N*-anisyl-iminophosphorane

Abstract: A distally-substituted resorcin[4]arene cavitand equipped with two remote *N*-anisyl-imino-phosphoranyl (AIP) units has been synthesised and assessed in competitive hydrogenation of α -olefins (rhodium catalyst). A substrate selectivity factor of 39.2 in favour of the linear olefin was observed after 1 h in the reduction of stoichiometric amounts of hex-1-ene and 3-ethyl-pent-1-ene. The catalyst was also shown suitable for the regioselective reduction of a compound with two olefinic bonds in a different steric environment. The remarkable olefin discrimination likely arises from the ability of the ligand to generate a cavity capping, *N,O*-chelator involving both AIP groups. Chelate formation positions the reactive metal sites inside the receptor moiety, the restricted size of which may retard coordination of larger α -olefins. The present study encourages further development of cavitands as shape selective catalysts.



Introduction

Substrate-selective catalysis^[1] is an elegant manner to convert selectively a specific compound from a mixture of substrates that are generally difficult to separate. If we exclude kinetic resolution of racemic mixtures, only few examples of substrate-competing experiments involving homogeneous catalysts were reported. In the latter, the competing substrates usually display quite different structures which facilitate the selection. These distinguish themselves, for example, by the presence or absence of aromatic subunits, or of that of polar extra functionalities. Thus, palladium-containing dendrimers functionalised with amide groups were found suitable for substrate specific hydrogenations of polar olefins in the presence of apolar analogues, the observed selectivity arising from strong interactions between the polar substrates and the NH groups of the catalyst.^[2] Similarly, allylic ethers tethered to pyridyl groups reacted faster than the corresponding alkenes linked to a phenyl group in transition metal catalysed hydrogenations. The rate acceleration with the former was attributed to the formation of efficient chelate complexes involving the pyridyl N atom.^[3] In some other examples, substrate discrimination resulted from supramolecular interactions, notably π - π stacking interactions between the aromatic unit of an olefinic substrate and the inner part of a catalytic cleft (e. g. based on a diphenylglycoluril unit^[4]) or a cavity (β -cyclodextrin^[5]). An approach based on the use of a bulky counter anion revealed that the combination of Wilkinson's catalyst with the Keggin $\text{SiW}_{12}\text{O}_{40}^{4-}$ anion led to preferential hydrogenation of mono-substituted olefins *vs.* disubstituted ones.^[6]

In the present study, we describe the synthesis of the cavitand-based *bis*-(*N*-anisyl-iminophosphorane) **4** (Figure 1) and its use in α -olefin-competing hydrogenations. This study was undertaken with the anticipation that the presence of a hollow space close to the coordinating centres would be helpful in the discrimination process. It is worth mentioning that to date only one resorcinarene-derived metal complex has been employed in substrate competitive reactions (Pd-catalysed allylic alkylation).^[7] Non-metallated resorcinarenes have also been employed in substrate-selective catalysis, namely as auxiliaries able to form self-assembled cavities under catalytic conditions. The resulting capsules were shown to function as containers hosting catalytic reactions occurring either with^[8] or without^[9] an organometallic catalyst.

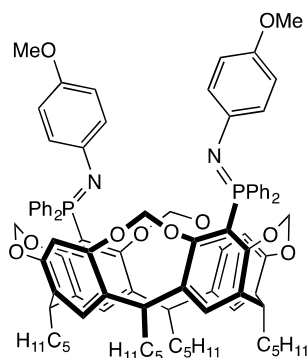
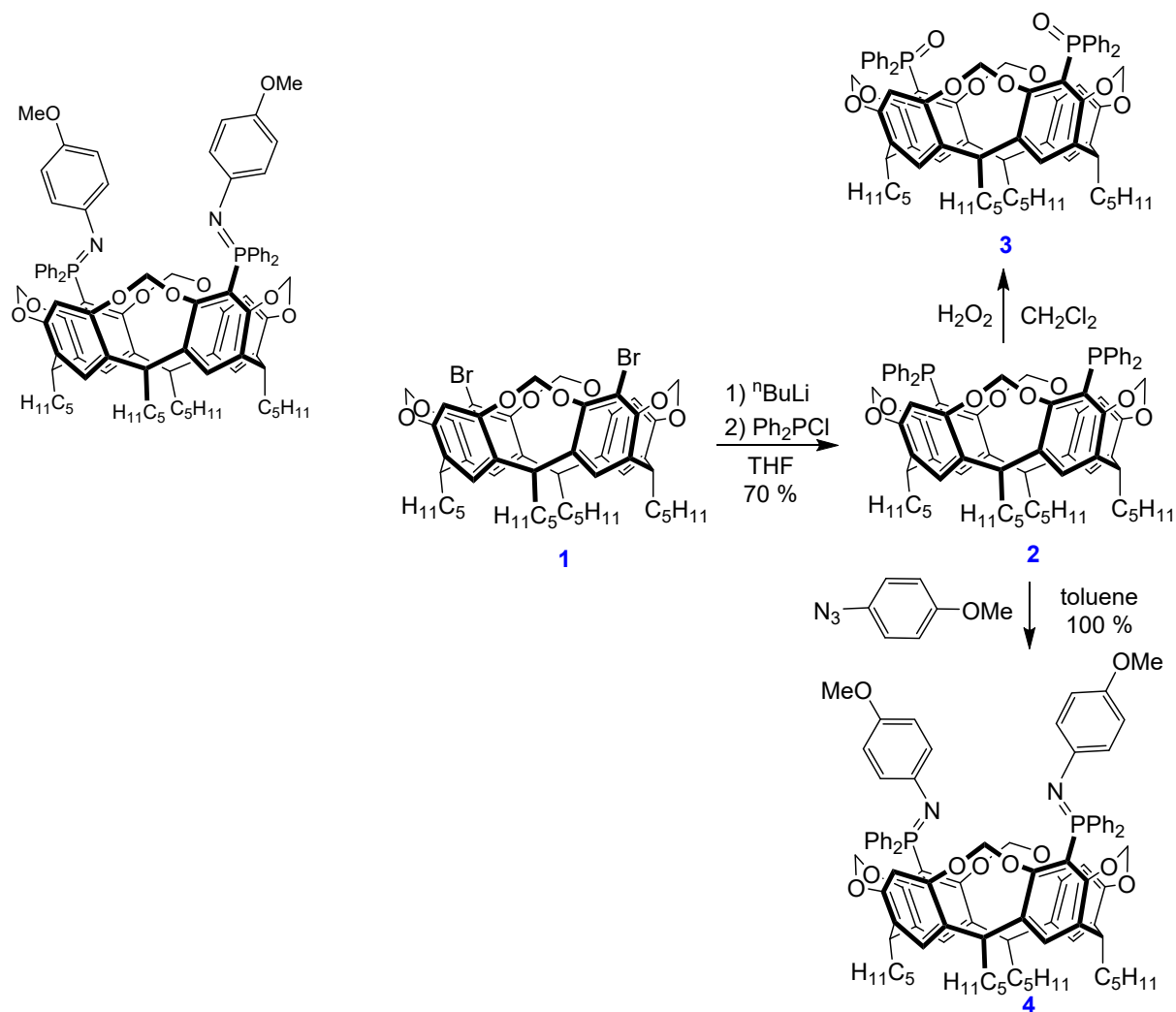


Figure 1. The resorcin[4]arene-based bis-iminophosphorane **4** used in this study

Results and Discussion

The synthesis of bis(iminophosphorane) **4** began with that of diphosphine **2**. The latter was obtained in two steps from bromo-cavitand **1** by a halogen/lithium exchange followed by reaction with ClPPh_2 (Scheme 1).^[10] The product was purified by column chromatography (yield 70%). The ^{31}P NMR spectrum of **2** shows a singlet at -16.1 ppm. The double phosphination was confirmed by an X-ray diffraction study (Figure 2). The cavitand adopts the usual bowl-shaped structure of resorcin[4]arene-derived cavitands containing OCH_2O linkers,^[10a, 11] with top rim diameters (*i.e.*, the segments linking the C-2 aromatic carbon atoms of opposite resorcinolic rings) of 7.89 and 8.14 Å. A molecule of dichloromethane is poised above the cavity entrance. In the solid the two phosphorus lone pairs of **2** are tangential to the cone delineated by the cavity core, thus contrasting somewhat with the $\text{P}=\text{O}$ vectors, skewed towards the cavitand axis, of the corresponding di(phosphine oxide) (**3**) (Scheme 1), which can be obtained by treatment of **2** with H_2O_2 and which was also structurally characterised (Figure 3).

Iminophosphorane **4** was then obtained through the Staudinger condensation^[12] of bisphosphine **2** and 4-anisyl azide (Scheme 1). The compound was characterised by elemental analysis, mass spectrometry (ESI-TOF) and NMR spectroscopy. The mass spectrum displays a strong peak at $m/z = 1427.68$ corresponding to the expected $[\text{M} + \text{H}]^+$ ion. In the ^{31}P NMR spectrum the phosphorus atoms appear as a singlet at $\delta = -6.6$ ppm. Consistent with a C_{2v} symmetrical cavitand, the ^1H NMR spectrum shows an AB pattern for the four methylenic OCH_2O groups and a unique methine signal. Compound **4** is only moderately air-stable, and therefore needs to be stored under argon. Its reaction with water led quantitatively to **3**.



Scheme 1. Synthesis of diphosphine **2**, bis(phosphine oxide) **3** and bis(iminophosphorane) **4**

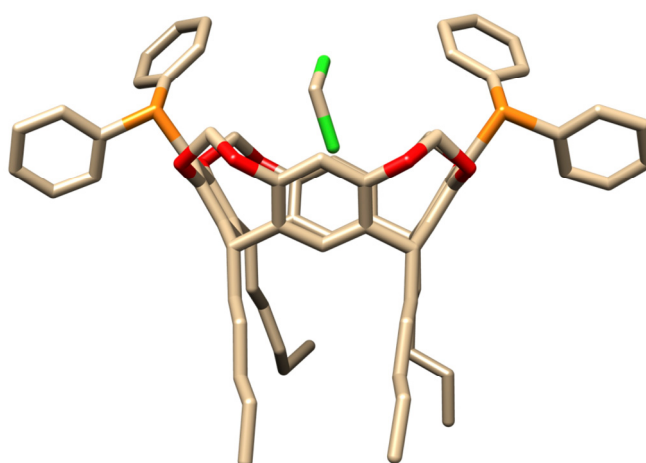


Figure 2. Molecular structure of phosphine **2**• $3\text{CH}_2\text{Cl}_2$. Only the embedded solvent molecule is shown. Top rim diameters 7.89 and 8.14 Å. Separation between the two phosphorus atoms: 10.26 Å

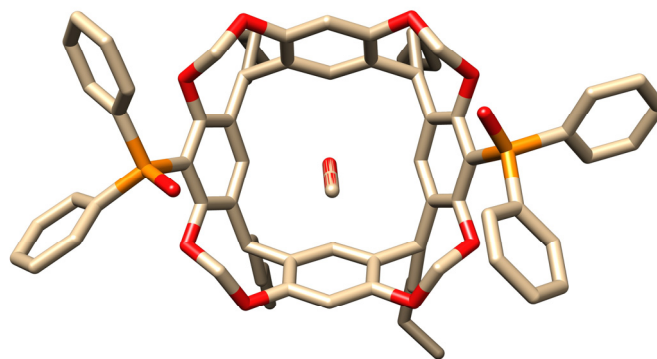
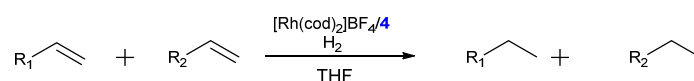


Figure 3. Molecular structure of **3**•2MeOH•H₂O. Only the embedded solvent molecule is shown. Top rim diameters 7.89 and 8.14 Å. Separation between the two phosphorus atoms: 9.98 Å


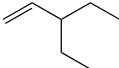

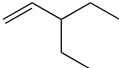

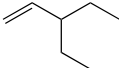

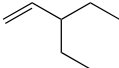




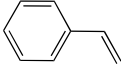
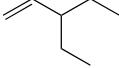
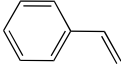
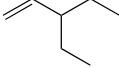
Bis(iminophosphorane) **4** was then assessed in α -olefin-competing hydrogenations (Scheme 2). The catalytically active species was generated *in situ* by mixing [Rh(cod)₂]BF₄ (1 mol %) and **4** (1 mol %).^[13] The runs were performed in THF under 5 bar H₂. Under these



Scheme 2. α -Olefin-competing hydrogenations

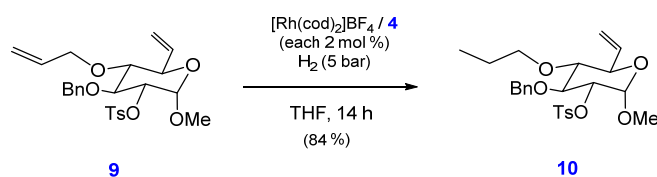
conditions, a 1:1 mixture of hex-1-ene and 3-ethyl-pent-1-ene produced hexane and 3-ethylpentane in 19.6 and 0.5 % yield, respectively, after 1 h (Table 1, entry 1), this corresponding to a product ratio of 39.2. After 8 h, the hexene conversion had reached 84.6 %, with the hexane/3-ethylpentane ratio being still as high as 4.1 (Table 1, entry 3). Carrying out the test with two linear α -olefins, namely hex-1-ene and dec-1-ene, led to preferential hydrogenation of the shorter hex-1-ene, with conversions of 13.5 and 2.5 % after 1 h for the C₆ and C₁₀ olefin, respectively (hexane/decane ratio = 5.4; Table 1, entry 4). Pursuing hydrogenation of this mixture for a further 4 h maintained the preferential hydrogenation of hex-1-ene, but with the hexane/decane ratio dropping to 4.7 (hexene conversion after 5 h: 48.1 % (Table 1, entry 5). Lower substrate selectivities after 5 h reaction time were observed when styrene was hydrogenated together with 3-ethyl-pent-1-ene, the ethylbenzene/3-ethylpentane ratio being here 2.4 for a styrene conversion of 36.2 % (Table 1, entry 7).

Table 1. Competitive hydrogenation of α -olefins catalysed by the $[\text{Rh}(\text{cod})_2]\text{BF}_4/\mathbf{4}$ system.

Entry	$\text{R}^1\text{CH}=\text{CH}_2$	$\text{R}^2\text{CH}=\text{CH}_2$	Time (h)	Hydrogenated products (%) $\text{R}^1\text{CH}_2\text{CH}_3/\text{R}^2\text{CH}_2\text{CH}_3$
1			1	19.6 / 0.5 = 39.2
2			5	62.6 / 8.4 = 7.4
3			8	84.6 / 20.4 = 4.1
4			1	13.5 / 2.5 = 5.4
5			5	48.1 / 10.2 = 4.7
6			8	77.4 / 47.8 = 1.6
7			5	36.2 / 15.0 = 2.4
8			8	58.2 / 29.0 = 2.0

Conditions: $[\text{Rh}(\text{cod})_2]\text{BF}_4$ (1 mol %), **4** (1 mol %), olefins (1.0 mmol of each), $\text{P}(\text{H}_2) = 5$ bar, THF (5 mL), r.t. The conversions were determined by GC.

Is it possible for the Rh/**4** system also to discriminate between distinct C=C double bonds belonging to the same compound? To answer this question, the glucosidic substrate **9**, which features a vinyl and an allyl substituent, was hydrogenated in the presence of **4** (Scheme 3). Applying a H_2 pressure of 5 bar and using 2 mol % of $[\text{Rh}(\text{cod})_2]\text{BF}_4$, led after 14 h, to 84 % of **10**, in which only the allylic double bond had been hydrogenated. Reduction of both double bonds was observed when maintaining the hydrogenation conditions for over 24 h.

**Scheme 3.** Intramolecular α -olefin-competing hydrogenations

In order to get some insight into the possible role played by the resorcinarene subunit in the above reactions, additional hydrogenation tests were performed (Table 2) with 1:1 mixture of hex-1-ene and dec-1-ene (THF, 5 bar H_2 , $[\text{Rh}(\text{cod})_2]\text{BF}_4$). The following results were compared to that of entry 4, Table 1, an experiment carried out with a **4**/Rh ratio of 1:1 and which led to a hexane/decane ratio of 5.4 (hexene conversion: 13.5 %) after 1 h reaction time. Lowering the **4**/Rh ratio to 1:2 increased the rate of hydrogenation, no selectivity being

observed in that case, as full conversion of both olefins was observed after 1 h (Table 2, entry 2). Increasing the 4/Rh ratio to 2:1 resulted in an hex-1-ene conversion of 33.6 % after 1 h, the hexane/decane ratio amounting here to only 1.5 (Table 2, entry 3). Comparable low substrate selectivities were observed when the reaction was carried out with 2 equiv. of mono(iminophosphorane) **5** (Figure 4; Table 2, entry 4), as well as with the cavity-free ligand **6** (hexane/decane ratio = 1.3, Table 2, entry 5). Repeating the hydrogenation runs with bis(iminophosphorane) **7**, with ⁿBu groups instead of methoxy substituents, led also to poor substrate selectivity (hexane/decane ratio of 1.6, Table 2 entry 6). These observations show that substrate discrimination is only observed if: a) two iminophosphorane units are available per Rh centre; b) the N atoms are substituted with an aryl rings that bear a methoxy group; and c) the two iminophosphorane units are tethered to the same resorcinarene platform. Finally, we found that in the absence of any ligand, the hydrogenation rates were high, the substrate selectivity being then close to zero (hexane/decane ratio = 1.1 after 1 h; Table 2 entry 7). Similar observations were made when the hydrogenation experiments were performed in the presence of phosphine oxide **3** or of 4-anisylamine (**8**), these being the typical decomposition products of **4** in the presence of water (Table 2, entries 8 and 9).

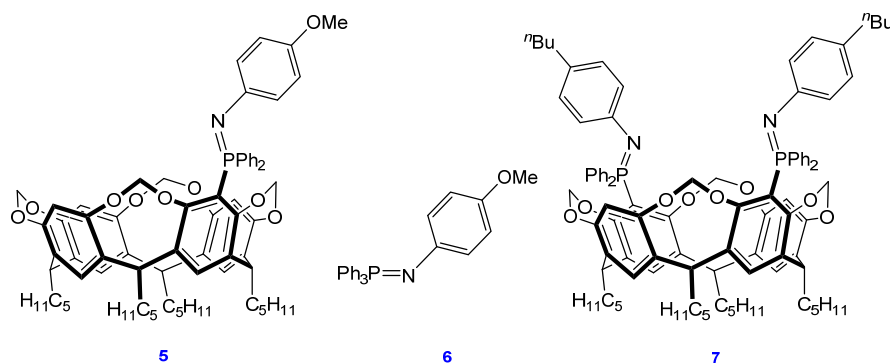

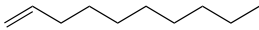


Figure 4. Iminophosphoranes **5-7** used for ranking the bis(iminophosphoranyl)-resorcin[4]arene **4**

Table 2. Competitive hydrogenation of α -olefins, influence of the ligand^[a]

Entry	R ¹ CH=CH ₂	R ² CH=CH ₂	Ligand (L/Rh)	Hydrogenated products (%) R ¹ CH ₂ CH ₃ /R ² CH ₂ CH ₃
1			4 (1/1)	13.5 / 2.5 = 5.4
2			4 (1/2)	100 / 100 = 1.0
3			4 (2/1)	33.6 / 22.0 = 1.5
4			5 (2/1)	35.3 / 19.5 = 1.8
5 ^b			6 (2/1)	26.2 / 20.3 = 1.6
6 ^c			7 (1/1)	36.4 / 22.6 = 1.6
7			/	94.8 / 83.6 = 1.1
8			3 (1/1)	94.0 / 85.2 = 1.1
9			8 (2/1)	92.7 / 87.7 = 1.1

Conditions: ^[a] [Rh(cod)₂]BF₄ (1 mol %), ligand, olefins (1.0 mmol of each), P(H₂) = 5 bar, THF (5 mL), r.t., 1 h. The conversions were determined by GC; ^[b] [Rh(cod)₂]BF₄ (0.1 mol %), **7** (0.2 mol %), olefins (each 10.0 mmol), 0.1 h; ^[c] [Rh(cod)₂]BF₄ (0.1 mol %), **7** (0.1 mol %), olefins (each 10.0 mmol), 0.25 h.

Overall, the above results unambiguously indicate that both iminophosphorane moieties of **4** are involved in the catalytic process. Owing to the large N...N separation, this cannot occur via catalytic intermediates containing a *N,N*-chelated rhodium centre. Instead, it is possible to envisage that one of the two nitrogen atoms forms with the methoxy group of the other anisyl-iminophosphorane moiety a chelating *N,O* unit that spans the wider rim of the cavitand, so as to locate the rhodium centre at the cavity entrance and orientate two free coordination sites towards the cavity interior (Figure 5). The observed substrate selectivity should then result from a shape selective process controlled by the cavity size. Note that a 2D DOSY (Diffusion-Ordered Spectroscopy) experiment carried out on a stoichiometric mixture of ligand **4** and [Rh(cod)₂]BF₄ revealed formation of a complex with a diffusion coefficient of 460 $\mu\text{m}^2 \text{s}^{-1}$ in THF. This value is close to that obtained for **4**, so that formation of an oligomer can be ruled out.

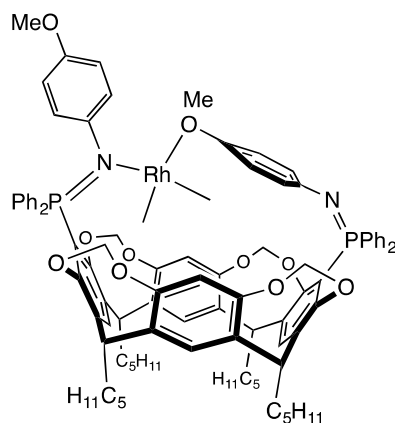


Figure 5. Proposed *N,O*-chelate rhodium intermediate

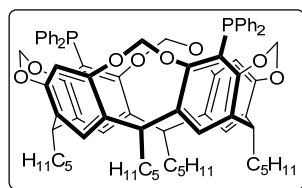
Conclusion

In summary, we have described the synthesis of a resorcinarene cavitand substituted by two remote *N*-anisyl-iminophosphoranyl units. Mixing this compound with 1 equiv. of $[\text{Rh}(\text{cod})_2]\text{BF}_4$ resulted in a hydrogenation catalyst suitable for shape and size selective transformation of binary mixtures of α -olefins. High substrate discrimination was notably observed in the reduction of a 1:1 mixture of hex-1-ene and 3-ethyl-pent-1-ene, this reaction leading to a substrate selectivity factor of 39.2 in favour of the linear olefin after 1 h reaction time. The observed substrate specificity likely arises from the formation of a *N,O*-chelate complex, which fixes the metal at the cavity entrance and forces incoming olefins to enter a restricted space ensuring the discrimination process. The catalyst further turned out to regioselectively reduce a compound having two olefinic bonds in a different steric environment. The present study illustrates the potential of cavity-shaped subunits in catalysis.

Experimental Section

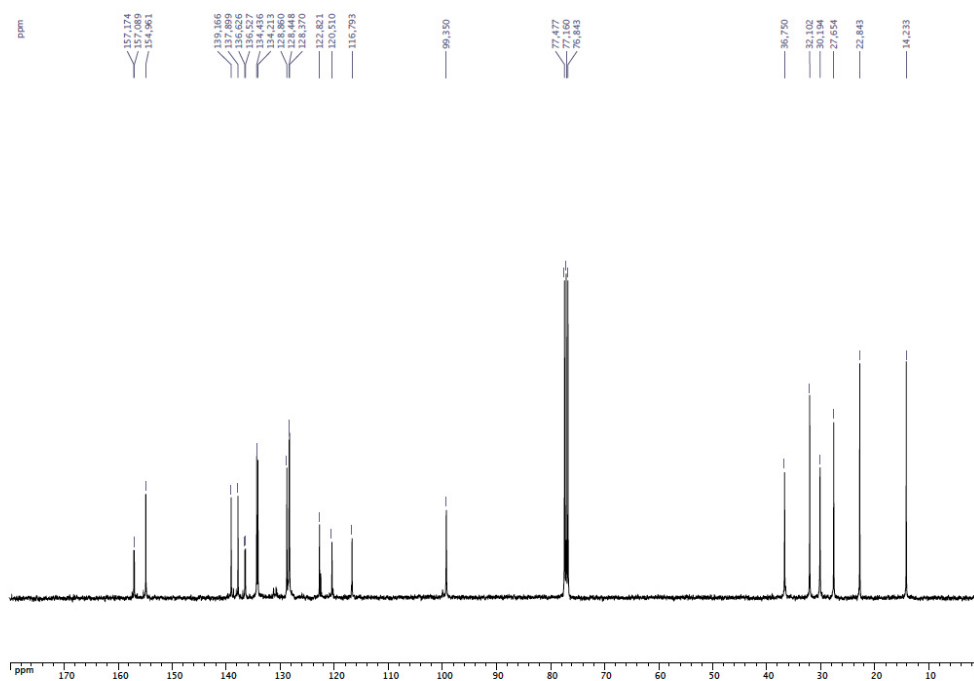
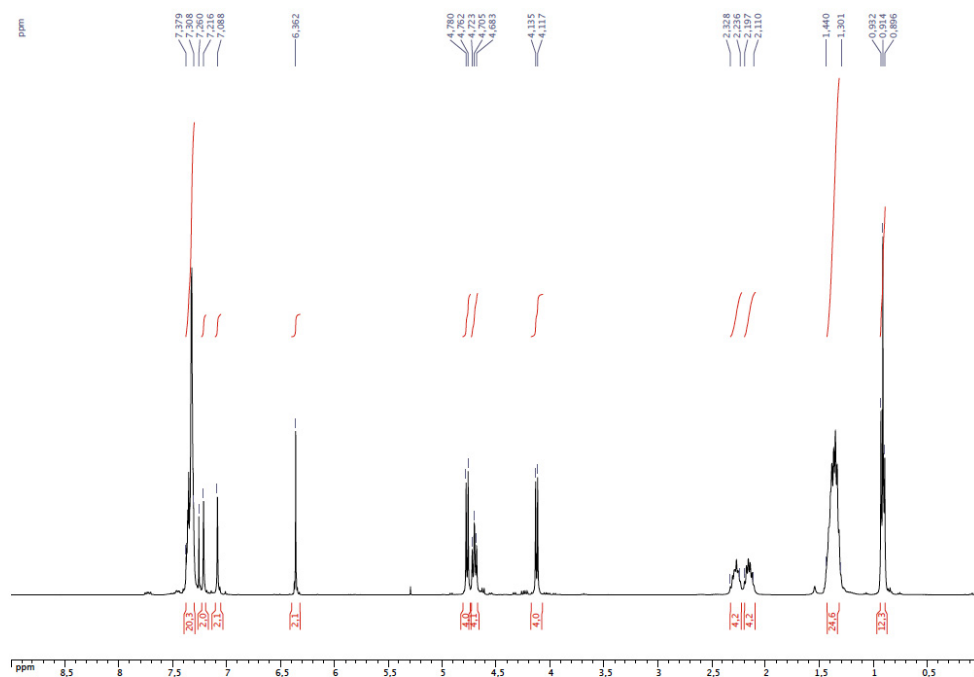
General Procedure: All manipulations involving phosphorus derivatives were performed in Schlenk-type flasks under dry argon. Solvents were dried by conventional methods and distilled immediately prior to use. CDCl_3 was passed down a 5 cm thick alumina column and stored under nitrogen over molecular sieves (4 Å). Routine ^1H , $^{13}\text{C}\{^1\text{H}\}$ and $^{31}\text{P}\{^1\text{H}\}$ spectra were recorded with Bruker FT instruments (AC 400). ^1H spectra were referenced to residual protiated solvents ($\delta = 7.16$ ppm for C_6D_6 and 7.26 ppm for CDCl_3), ^{13}C chemical shifts are reported relative to deuteriated solvents ($\delta = 128.00$ ppm for C_6D_6 and 77.16 ppm for CDCl_3),

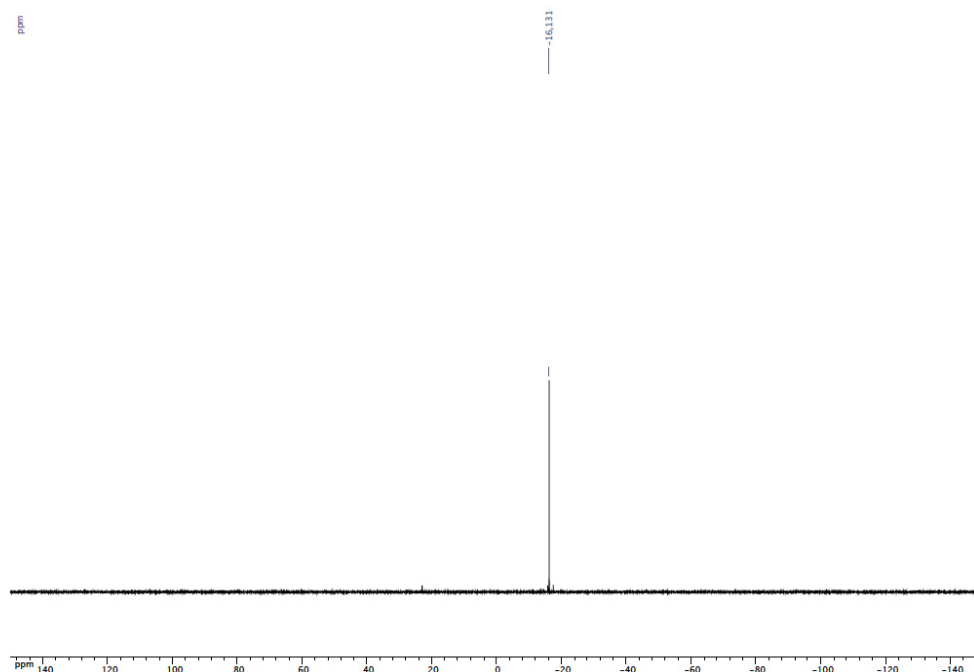
whereas the ^{31}P NMR spectroscopic data are given relative to external H_3PO_4 . Chemical shifts and coupling constants are reported in ppm and in Hz, respectively. Infrared spectra were recorded with a Bruker FT-IR Alpha-P spectrometer. Elemental analyses were performed by the Service de Microanalyse, Institut de Chimie, Université de Strasbourg. The catalytic solutions were analysed with a Varian 3900 gas chromatograph fitted with a WCOT fused silica column (25 m x 0.25 mm, 0.25 μm film thickness). 5,17-Dibromo-4(24),6(10),12(16),18(22)-tetramethylenedioxy-2,8,14,20-tetrapentylresorcin[4]arene (**1**)^[11b] and 5-(diphenylphosphanyl)-4(24),6(10),12(16),18(22)-tetramethylenedioxy-2,8,14,20-tetrapentyl resorcin[4]arene^[10a] were prepared by literature procedures. The synthesis of diolefin **9** is described in the supporting information. 4-Methoxyphenyl and 4-butylphenyl azides were synthesized by using TfN_3 according to a procedure developed by Liu and Tor.^[14] *Although we have not experienced any difficulty in handling TfN_3 , care should be taken owing to the potentially explosive nature of some azides. The reagent should be kept in solution and used immediately after its synthesis.*



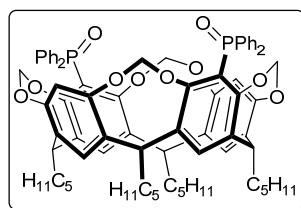
5,17-Bis(diphenylphosphanyl)-4(24),6(10),12(16),18(22)-tetramethylenedioxy-2,8,14,20-tetrapentylresorcin[4]arene (2**):** *n*-Butyllithium (1.6 m in hexane, 0.68 mL, 1.08 mmol) was slowly added to a solution of dibromo-cavitand **1** (0.500 g, 0.51 mmol) in THF (50 mL) at -78°C . After 0.5 h, the resulting dianion was quenched with chlorodiphenylphosphine (0.24 mL, 1.10 mmol) and the mixture stirred at 40°C for 16 h. The solvent was evaporated under reduced pressure and the crude product purified by column chromatography (Et_2O /petroleum ether, 20:80 v/v), yield 0.424 g, 70 %. ^1H NMR (400 MHz, CDCl_3): δ = 7.38-7.31 (m, 20H, arom. CH, PPh_2), 7.22 (s, 2H, arom. CH, resorcinarene), 7.09 (s, 2H, arom. CH, resorcinarene), 6.36 (s, 2H, arom. CH, resorcinarene), 4.77 and 4.13 (AB spin system, 8H, OCH_2O , $^2J = 7.2$ Hz), 4.70 (t, 4H, CHCH_2 , $^3J = 8.0$ Hz), 2.33-2.24 (m, 4H, CHCH_2), 2.20-2.11 (m, 4H, CHCH_2), 1.44-1.30 (m, 24H $\text{CH}_2\text{CH}_2\text{CH}_2\text{CH}_3$) 0.91 (t, 12H, CH_2CH_3 , $^3J = 7.2$ Hz); $^{13}\text{C}\{^1\text{H}\}$ NMR (100 MHz, CDCl_3): δ = 157.13-116.79 (arom. C's), 99.35 (s, OCH_2O), 36.75 (s, CHCH_2), 32.10 (s, $\text{CH}_2\text{CH}_2\text{CH}_3$), 30.19 (s, CHCH_2), 27.65 (s, CHCH_2CH_2), 22.84 (s, CH_2CH_3), 14.23 (s, CH_2CH_3); $^{31}\text{P}\{^1\text{H}\}$ NMR (162 MHz, CDCl_3): δ = -16.1 (s, PPh_2) pm;

elemental analysis calcd (%) for C₇H₈O₈P₂ (1185.41): C 77.00, H 6.97; found (%): C 76.91, H 7.05.



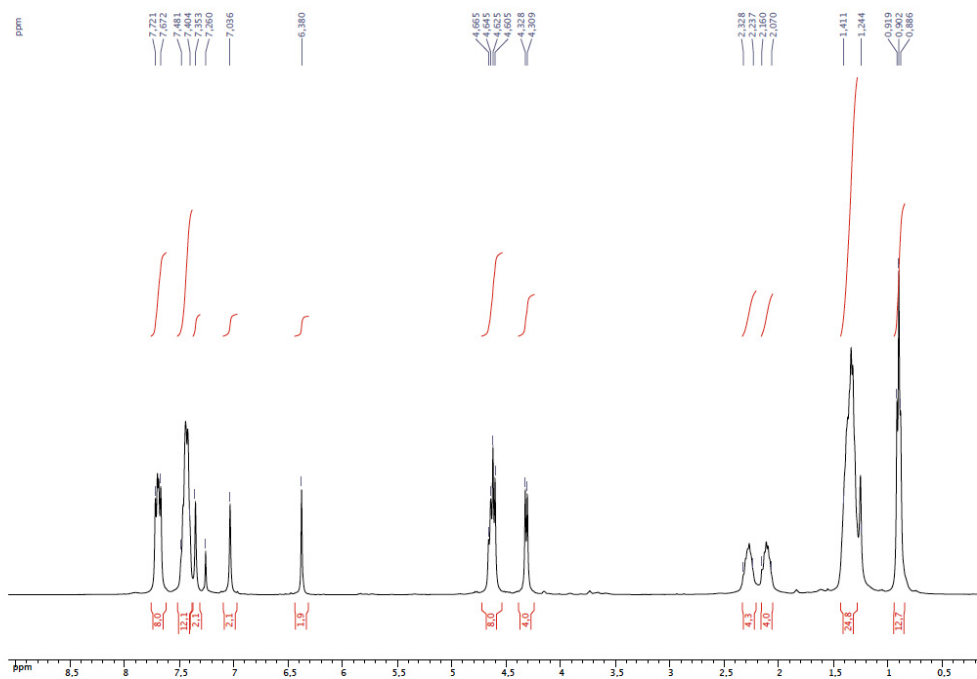


$^{31}\text{P}\{^1\text{H}\}$ NMR spectrum of **2** (CDCl_3)

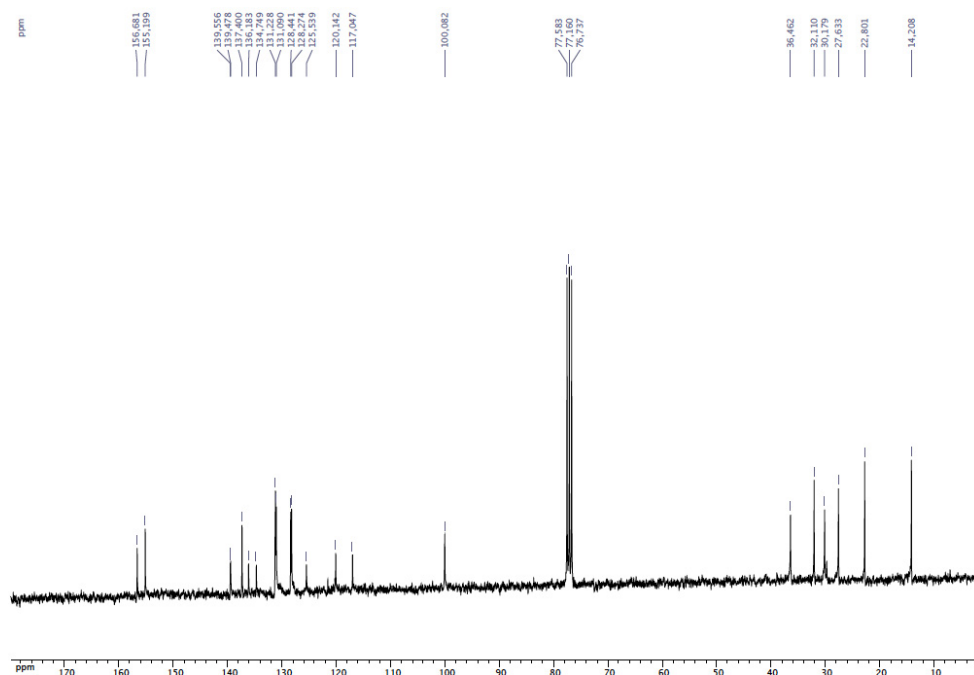


5,17-Bis(diphenylphosphinoyl)-4(24),6(10),12(16),18(22)-tetramethylenedioxy-2,8,14,20-tetrapentylresorcin[4]arene (3): To a solution of **2** (0.060 g, 0.05 mmol) in CH_2Cl_2 (10 mL) was added H_2O_2 (30% in water, 0.5 ml, 0.62 mmol). The resulting solution was stirred at room temperature for 2 h. A mixture of CH_2Cl_2 (10 mL) and water (20 mL) was then added. The two phases were separated and the water phase was washed twice with CH_2Cl_2 (2 x 10 mL). The organic solutions were all combined and dried over Na_2SO_4 . After filtration, the solution was evaporated to dryness to afford the bis-phosphine oxide as a white solid, yield 0.061 g (99 %). ^1H NMR (400 MHz, CDCl_3): δ = 7.72-7.67 (m, 8H, arom. CH, PPh_2), 7.48-7.40 (m, 12H, arom. CH, PPh_2), 7.35 (s, 2H, arom. CH, resorcinarene), 7.04 (s, 2H, arom. CH, resorcinarene), 6.38 (s, 2H, arom. CH, resorcinarene), 4.64 (t, 4H, CHCH_2 , $^3J = 8.0$ Hz), 4.61 and 4.32 (AB spin system, 8H, OCH_2O , $^2J = 7.6$ Hz), 2.33-2.24 (m, 4H, CHCH_2), 2.16-2.07 (m, 4H, CHCH_2), 1.41-1.24 (m, 24H $\text{CH}_2\text{CH}_2\text{CH}_2\text{CH}_3$) 0.90 (t, 12H, CH_2CH_3 , $^3J = 6.6$ Hz); $^{13}\text{C}\{^1\text{H}\}$ NMR (100 MHz, CDCl_3): δ = 156.68-117.05 (arom. C's), 100.08 (s, OCH_2O),

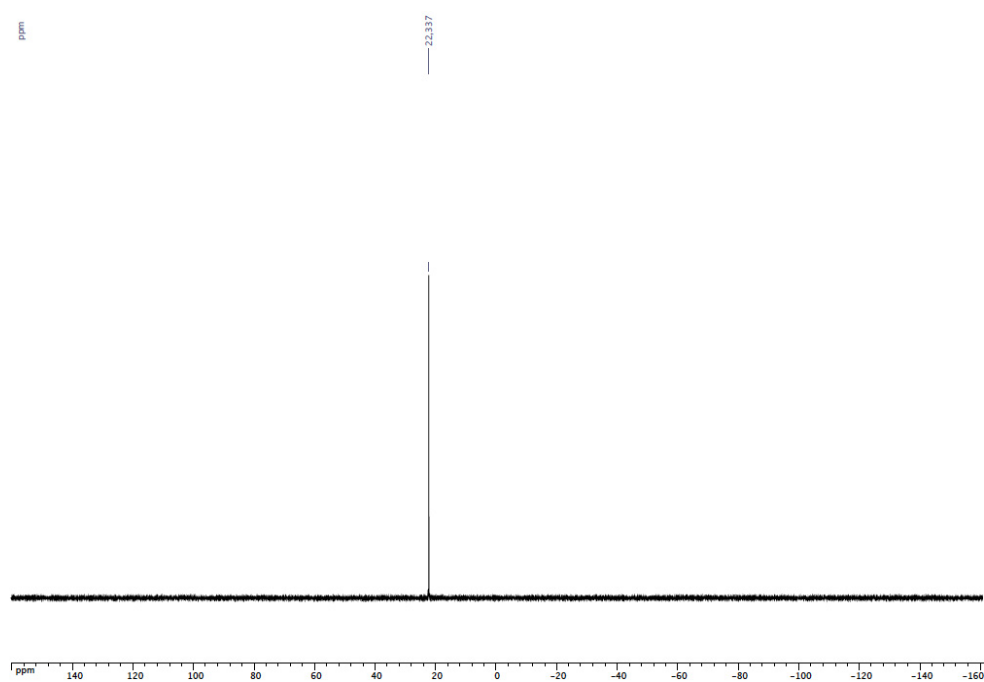
36.46 (s, CHCH₂), 32.11 (s, CH₂CH₂CH₃), 30.18 (s, CHCH₂), 27.63 (s, CHCH₂CH₂), 22.80 (s, CH₂CH₃), 14.21 (s, CH₂CH₃); ³¹P{¹H} NMR (162 MHz, CDCl₃): δ = 22.3 (s, P(O)Ph₂) ppm; elemental analysis calcd (%) for C₇₆H₈₂O₁₀P₂ (M_r = 1217.41): C 74.98, H 6.79; found (%): C 75.09, H 6.87.



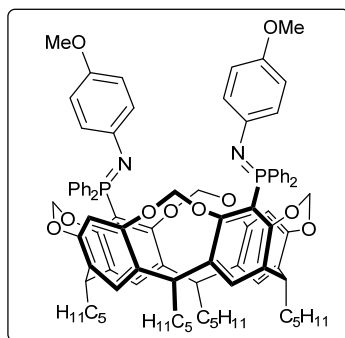
¹H NMR spectrum of **3** (CDCl₃)



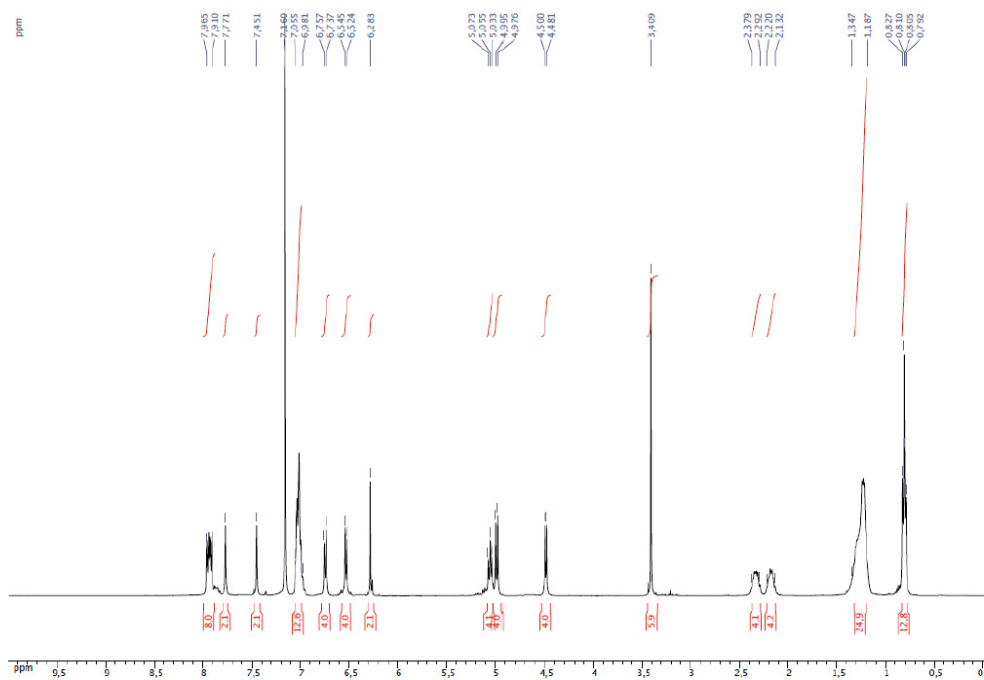
$^{13}\text{C}\{^1\text{H}\}$ NMR spectrum of **3** (CDCl_3)



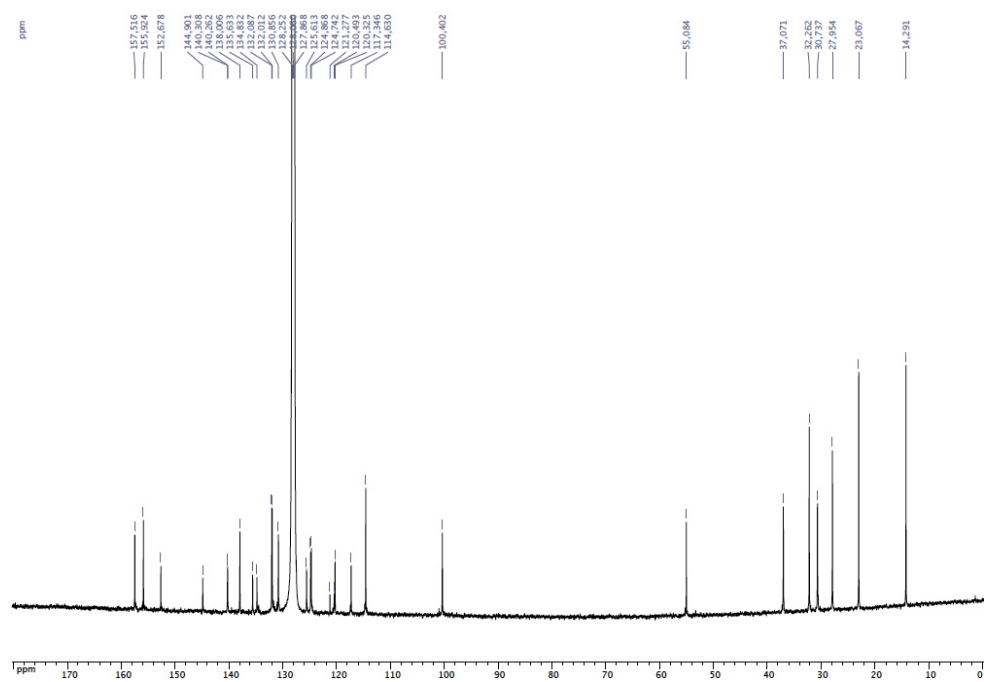
$^{31}\text{P}\{^1\text{H}\}$ NMR spectrum of **3** (CDCl_3)



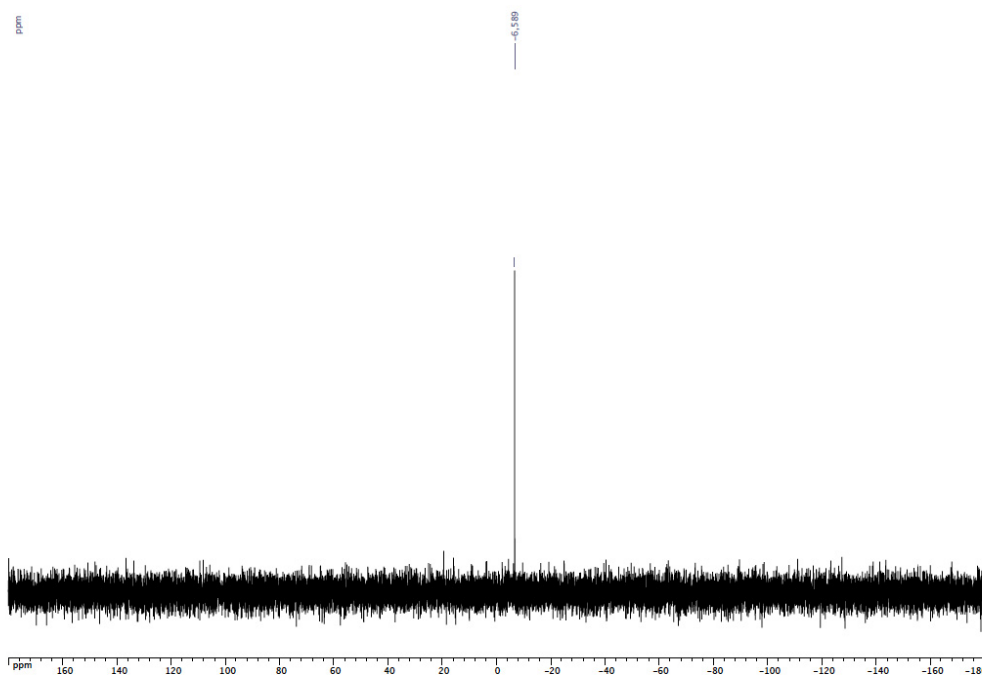
5,17-Bis(4-methoxyphenyliminodiphenylphosphoranyl)-4(24),6(10),12(16),18(22)-tetramethylenedioxy-2,8,14,20-tetrapentylresorcin[4]arene (4): A solution of 4-methoxyphenyl azide (0.134 g, 0.90 mmol) in toluene (10 mL) was added to a solution of diphosphine **2** (0.533 g, 0.45 mmol) in toluene (10 mL). After the solution had been stirred at 60 °C for 16 h, the reaction mixture was evaporated to dryness under vacuum to afford the bis(iminophosphorane) in quantitative yield (0.642 g). ^1H NMR (400 MHz, C_6D_6): δ = 7.96-7.91 (m, 8H, arom. CH, PPh_2), 7.77 (s, 2H, arom. CH, resorcinarene), 7.45 (s, 2H, arom. CH, resorcinarene), 7.05-6.98 (m, 12H, arom. CH, PPh_2), 6.75 (d, 4H, arom. CH, $\text{C}_6\text{H}_4\text{OCH}_3$, $^3J = 8.2$ Hz), 6.53 (d, 4H, arom. CH, $\text{C}_6\text{H}_4\text{OCH}_3$, $^3J = 8.2$ Hz), 6.28 (s, 2H, arom. CH, resorcinarene), 5.05 (t, 4H, CHCH_2 , $^3J = 8.0$ Hz), 4.98 and 4.49 (AB spin system, 8H, OCH_2O , $^2J = 7.6$ Hz), 3.40 (s, 6H, OCH_3), 2.37-2.29 (m, 4H, CHCH_2), 2.20-2.13 (m, 4H, CHCH_2), 1.34-1.19 (m, 24H, $\text{CH}_2\text{CH}_2\text{CH}_2\text{CH}_3$), 0.81 (t, 12H, CH_2CH_3 , $^3J = 7.0$ Hz); ^{13}C NMR (125 MHz, C_6D_6): δ = 157.52-114.63 (arom. $\text{C}'\text{s}$), 100.40 (s, OCH_2O), 55.08 (s, OCH_3), 37.07 (s, CHCH_2), 32.26 (s, $\text{CH}_2\text{CH}_2\text{CH}_3$), 30.74 (s, CHCH_2), 27.95 (s, CHCH_2CH_2), 23.07 (s, CH_2CH_3), 14.29 (s, CH_2CH_3); ^{31}P NMR (162 MHz, C_6D_6): δ = -6.6 (s, PPh_2) ppm; IR: ν = 1439 cm^{-1} ($\text{P}=\text{N}$); MS (ESI-TOF): m/z = 1427.68 [$\text{M} + \text{H}$] expected isotopic profile; elemental analysis calcd (%) for $\text{C}_{90}\text{H}_{96}\text{N}_2\text{O}_{10}\text{P}_2$ ($M_r = 1427.68$): C 75.71, H 6.78, N 1.96; found (%): C 75.58, H 6.59, N 2.07.



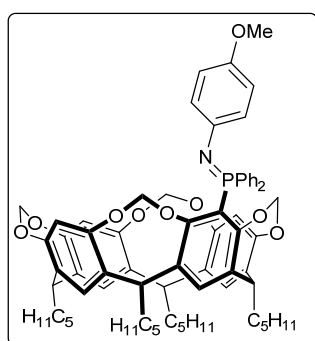
^1H NMR spectrum of **4** (C_6D_6)



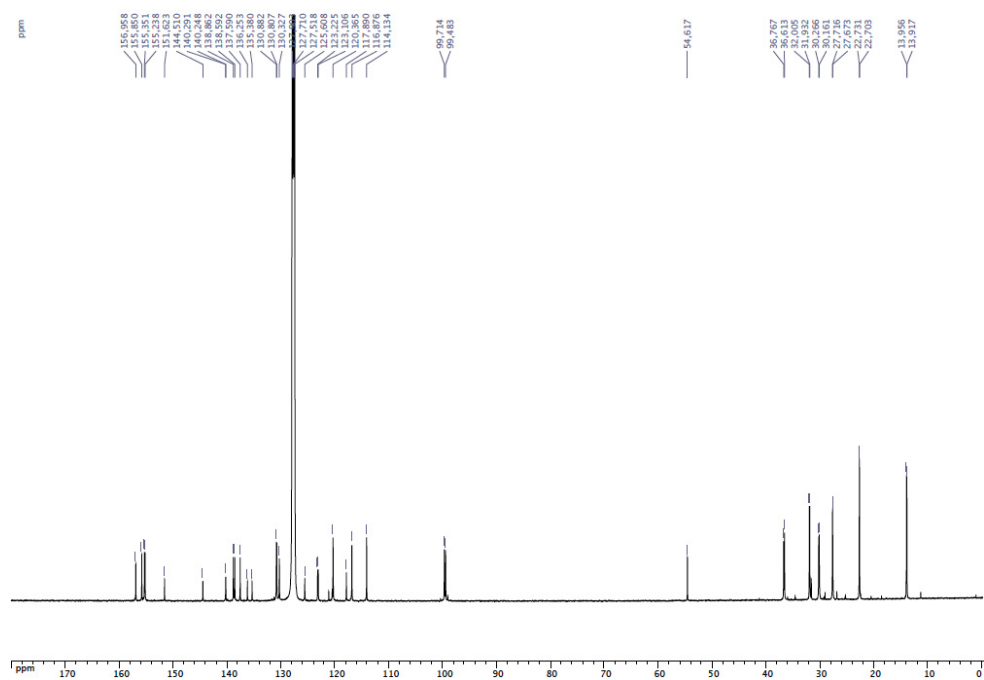
$^{13}\text{C}\{^1\text{H}\}$ NMR spectrum of **4** (C_6D_6)



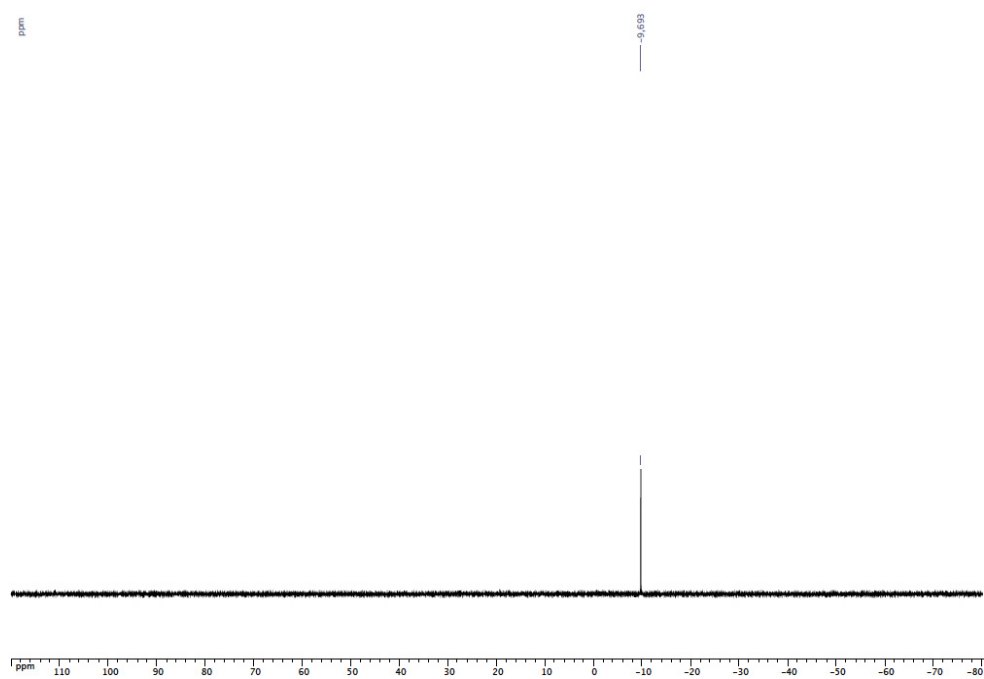
$^{31}\text{P}\{^1\text{H}\}$ NMR spectrum of **4** (C_6D_6)



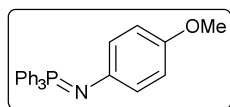
5-(4-methoxyphenyliminodiphenylphosphoranyl)-4(24),6(10),12(16),18(22)-tetramethylenedioxy-2,8,14,20-tetrapentylresorcin[4]arene (5): A solution of 4-methoxyphenyl azide (0.067 g, 0.45 mmol) in toluene (10 mL) was added to a solution of 5-(diphenylphosphanyl)-4(24),6(10),12(16),18(22)-tetramethylenedioxy-2,8,14,20-tetrapentylresorcin[4]arene (0.450 g, 0.45 mmol) in toluene (10 mL). After the solution had been stirred at 60 °C for 16 h, the reaction mixture was concentrated to dryness under vacuum to afford the iminophosphorane in quantitative yield (0.505 g). ^1H NMR (400 MHz, C_6D_6): δ = 8.01-7.97 (m, 4H, arom. CH, PPh_2), 7.79 (s, 1H, arom. CH, resorcinarene), 7.53 (s, 1H, arom. CH, resorcinarene), 7.46 (s, 2H, arom. CH, resorcinarene), 7.03-6.95 (m, 6H, arom. CH, PPh_2), 6.91 (s, 1H, arom. CH, resorcinarene), 6.27 (s, 2H, arom. CH, resorcinarene), 6.18 (d, 2H, arom. CH, $\text{C}_6\text{H}_4\text{OCH}_3$, 3J



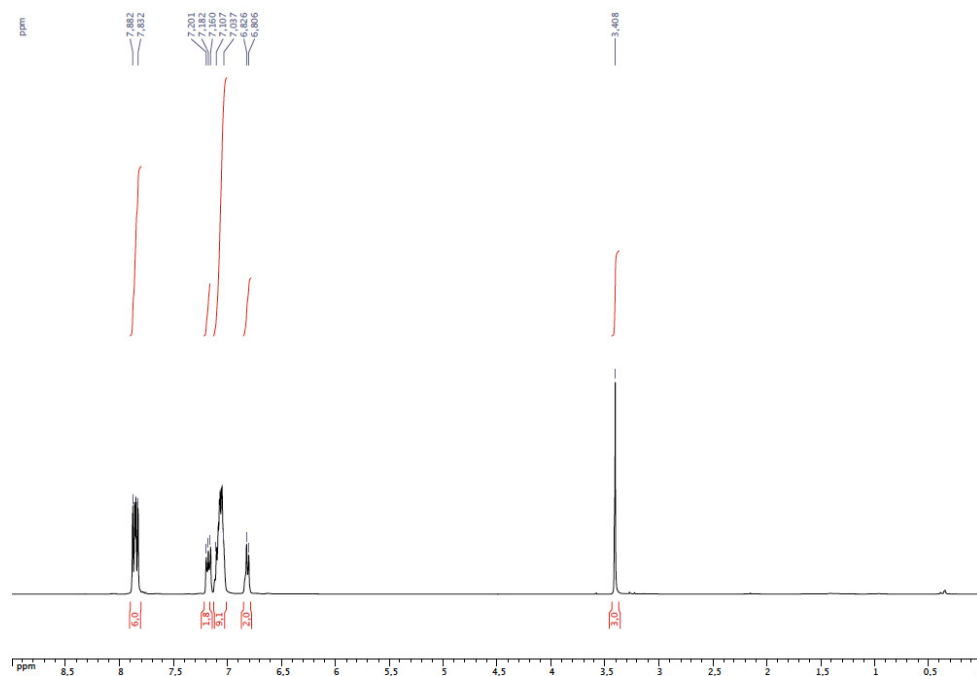
$^{13}\text{C}\{^1\text{H}\}$ NMR spectrum of **5** (C_6D_6)



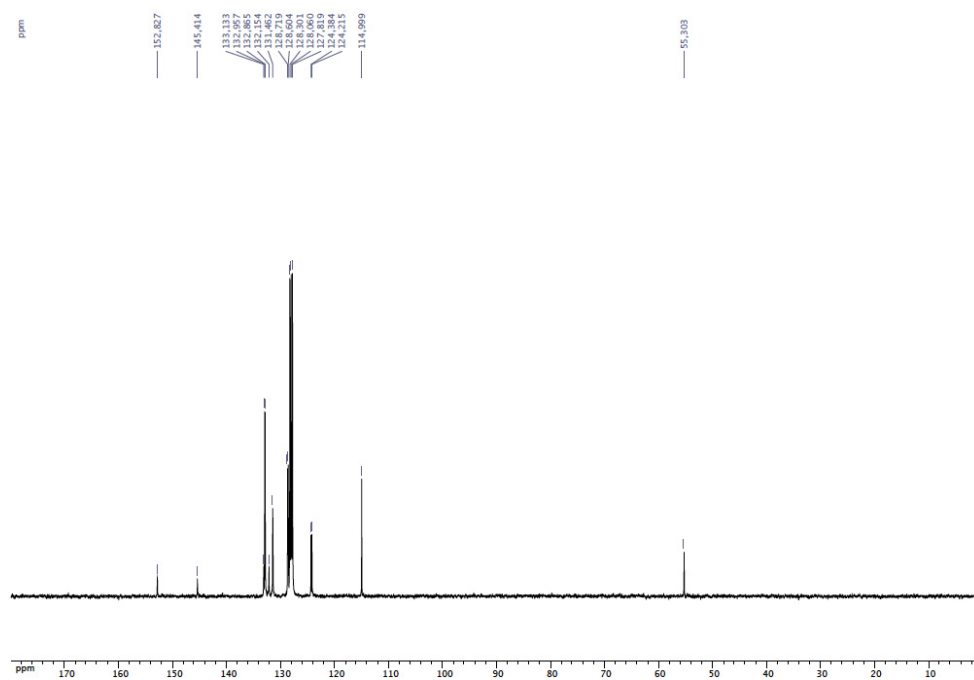
$^{31}\text{P}\{^1\text{H}\}$ NMR spectrum of **5** (C_6D_6)



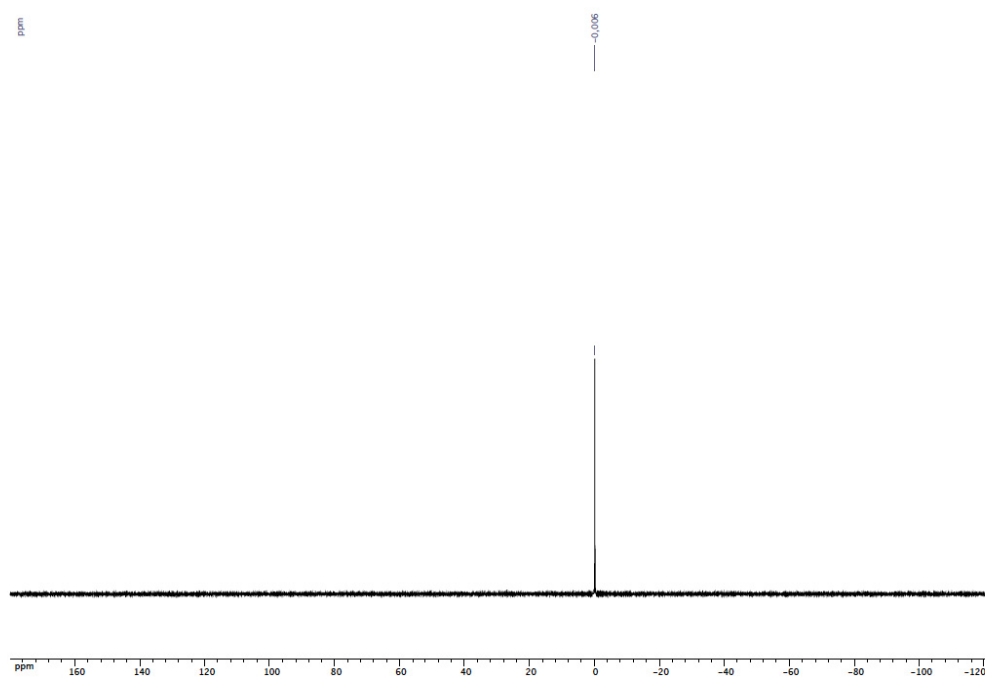
4-Methoxyphenyliminotriphenylphosphorane (6): To a solution of triphenylphosphine (0.262 g, 1.00 mmol) in toluene (10 mL) was added a solution of 4-methoxyphenyl azide (0.149 g, 1.00 mmol in toluene (10 mL)). After stirring the solution for 16 h at 60°C, the reaction mixture was evaporated to dryness under vacuum to afford quantitatively **6** (0.383 g). ^1H NMR (1400 MHz, C_6D_6): δ = 7.88-7.83 (6H, arom. CH, PPh_3), 7.19 (d, 2H, arom. CH, $\text{CH}_3\text{OC}_6\text{H}_4$, $^3J = 7.8$ Hz), 7.11-7.04 (9H, arom. CH, PPh_3), 6.81 (d, 2H, arom. CH, $\text{CH}_3\text{OC}_6\text{H}_4$, $^3J = 7.8$ Hz), 3.41 (s, 3H, CH_3O); $^{13}\text{C}\{^1\text{H}\}$ NMR (100 MHz, C_6D_6): δ = 152.82 (s, arom. Cquat.- OCH_3), 145.41 (s, arom. Cquat.-N), 132.91 (d, arom. CH, *ortho* to P, $^2J_{\text{C,P}} = 9.2$ Hz), 132.64 (d, arom. Cquat.-P, $^1J_{\text{C,P}} = 97.9$ Hz), 131.46 (s, arom. CH, $\text{C}_6\text{H}_4\text{OCH}_3$), 128.66 (d, arom. CH, *meta* to P, $^3J_{\text{C,P}} = 11.5$ Hz), 124.30 (d, arom. CH, *para* to P, $^4J_{\text{C,P}} = 16.9$ Hz), 115.00 (s, arom. CH, $\text{C}_6\text{H}_4\text{OCH}_3$), 55.30 (s, CH_3O); $^{31}\text{P}\{^1\text{H}\}$ NMR (162 MHz, C_6D_6): δ = 0.0 (s, PPh_3) ppm; IR: $\nu = 1436$ cm^{-1} (P=N); elemental analysis calcd (%) for $\text{C}_{25}\text{H}_{22}\text{OPN}$ (Mr = 383.42): C 78.31, H 5.78, N 3.65; found: (%) C 78.42, H 5.64, N 3.74%.



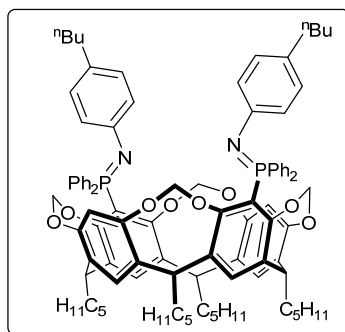
^1H NMR spectrum of **6** (C_6D_6)



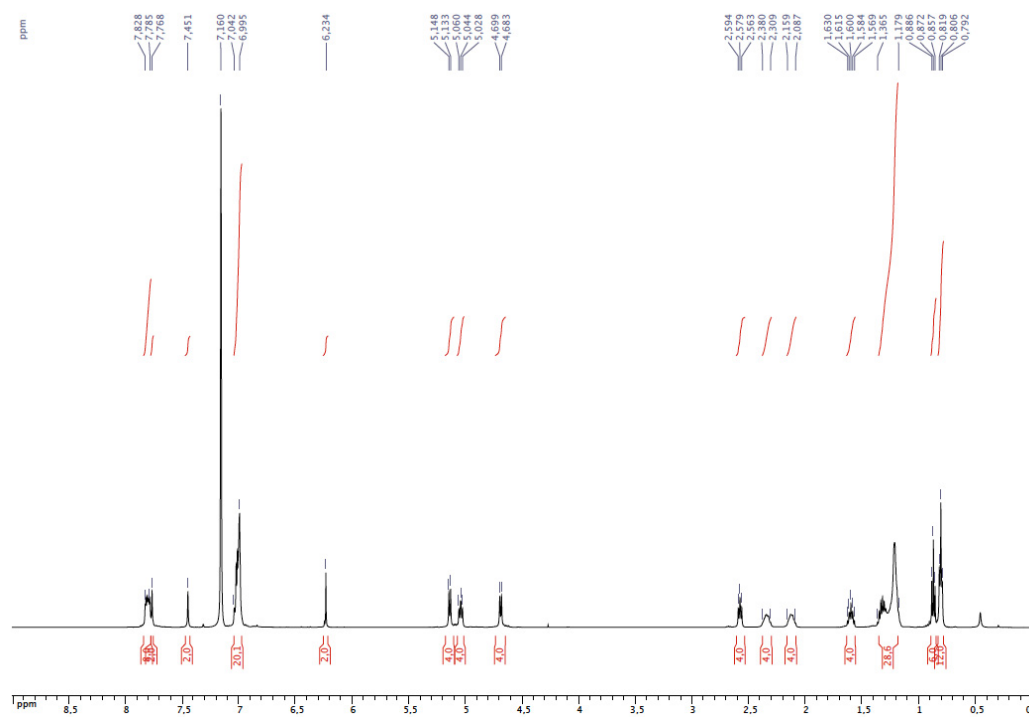
$^{13}\text{C}\{^1\text{H}\}$ NMR spectrum of **6** (C_6D_6)



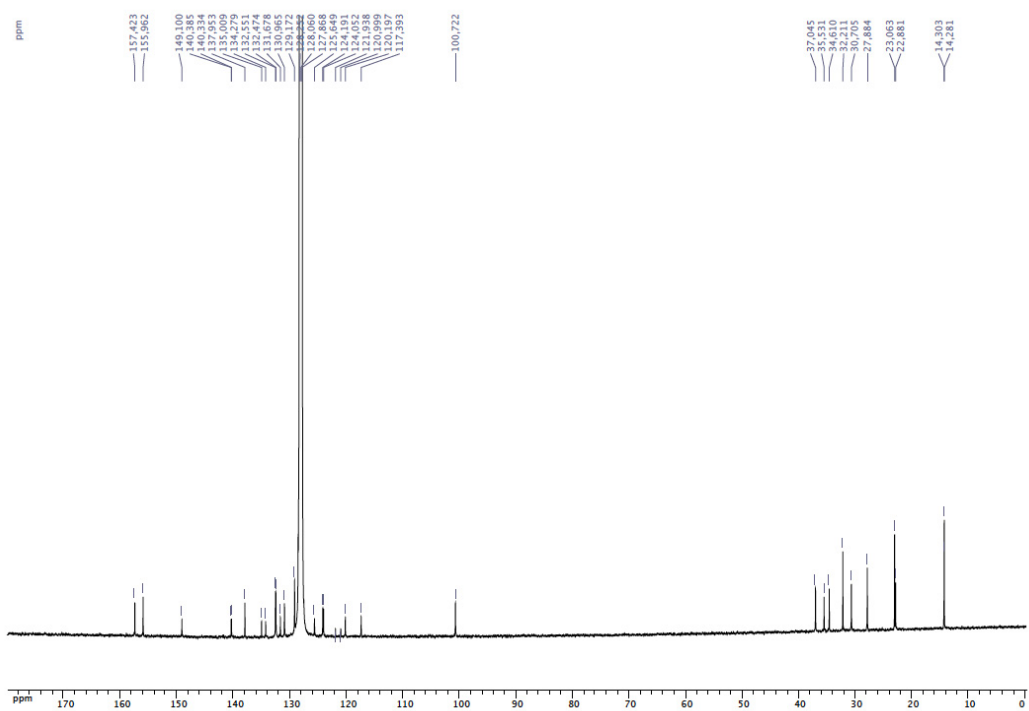
$^{31}\text{P}\{^1\text{H}\}$ NMR spectrum of **6** (C_6D_6)



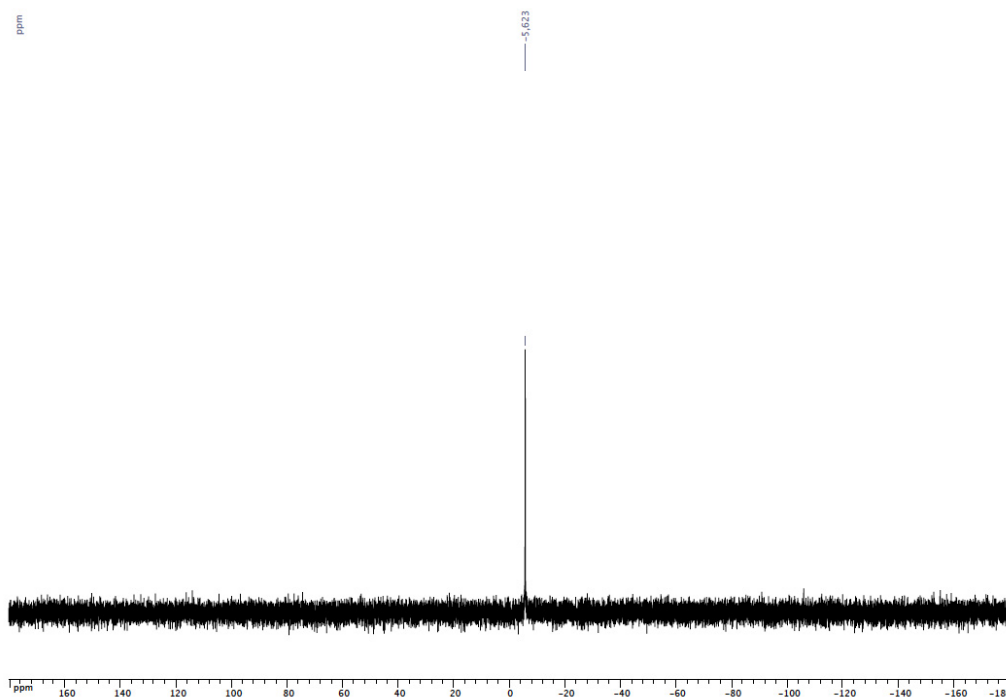
5,17-Bis(4-butylphenyliminodiphenylphosphoranyl)-4(24),6(10),12(16),18(22)-tetraethylenedioxy-2,8,14,20-tetrapentylresorcin[4]arene (7): A solution of 4-butylphenyl azide (0.157 g, 0.90 mmol) in toluene (10 mL) was added to a solution of diphosphine **2** (0.533 g, 0.45 mmol) in toluene (10 mL). After the solution had been stirred at 60 °C for 16 h, the reaction mixture was concentrated to dryness under vacuum to afford the iminophosphorane in quantitative yield (0.666 g). ^1H NMR (400 MHz, C_6D_6): δ = 7.83-7.78 (m, 8H, arom. CH, PPh_2), 7.77 (s, 2H, arom. CH, resorcinarene), 7.45 (s, 2H, arom. CH, resorcinarene), 7.04-6.99 (m, 20H, arom. CH, PPh_2 and $\text{C}_6\text{H}_4^n\text{Bu}$), 6.23 (s, 2H, arom. CH, resorcinarene), 5.14 and 4.69 (AB spin system, 8H, OCH_2O , $^2J = 7.5$ Hz), 5.04 (t, 4H, CHCH_2 , $^3J = 8.0$ Hz), 2.78 (t, 4H, $\text{C}_6\text{H}_4\text{CH}_2$, $^3J = 8.0$ Hz), 2.38-2.31 (m, 4H, CHCH_2), 2.16-2.09 (m, 4H, CHCH_2), 1.60 (quint, 4H, $\text{C}_6\text{H}_4\text{CH}_2\text{CH}_2$, $^3J = 7.7$ Hz), 1.32 (hex, 4H, CH_2CH_3 , ^nBu , $^3J = 7.7$ Hz), 1.33-1.18 (m, 24H, $\text{CH}_2\text{CH}_2\text{CH}_2\text{CH}_3$, resorcinarene), 0.87 (t, 6H, CH_2CH_3 , ^nBu , $^3J = 7.2$ Hz), 0.81 (t, 12H, CH_2CH_3 , resorcinarene, $^3J = 6.7$ Hz); ^{13}C NMR (125 MHz, C_6D_6): δ = 157.42-117.39 (arom. C's), 100.72 (s, OCH_2O), 37.04 (s, CHCH_2), 35.53 (s, $\text{C}_6\text{H}_4\text{CH}_2$), 34.61 (s, $\text{C}_6\text{H}_4\text{CH}_2\text{CH}_2$), 32.21 (s, $\text{CH}_2\text{CH}_2\text{CH}_3$, resorcinarene), 30.70 (s, CHCH_2), 27.88 (s, CHCH_2CH_2), 23.06 (s, CH_2CH_3 , resorcinarene), 22.88 (s, CH_2CH_3 , ^nBu), 14.30 (s, CH_2CH_3 , ^nBu), 13.92 (s, CH_2CH_3 , resorcinarene); ^{31}P NMR (162 MHz, C_6D_6): δ = -5.6 (s, PPh_2) ppm; IR: $\nu = 1329$ cm^{-1} ($\text{P}=\text{N}$); MS (ESI-TOF): $m/z = 1480.76$ [$\text{M} + \text{H}$] expected isotopic profile; elemental analysis calcd (%) for $\text{C}_{96}\text{H}_{108}\text{N}_2\text{O}_8\text{P}_2$ ($M_r = 1479.84$): C 77.92, H 7.36, N 1.89; found (%): C 77.98, H 7.38, N 1.87.



¹H NMR spectrum of **7** (C₆D₆)

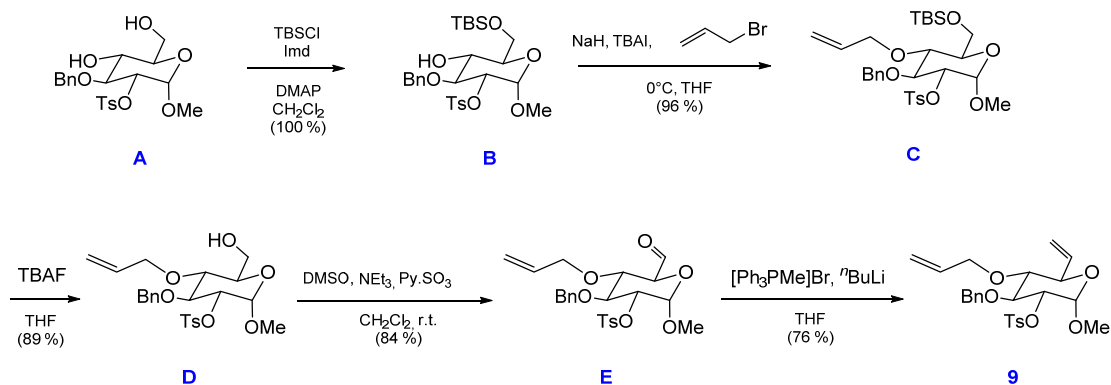


¹³C {¹H} NMR spectrum of **7** (C₆D₆)



$^{31}\text{P}\{^1\text{H}\}$ NMR spectrum of **7** (C_6D_6)

Synthesis of compound **9**



Compound **A** was prepared according to a literature procedure (C. Bauder, *Org. Biomol. Chem.*, **2008**, *6*, 2952-2960).

Synthesis of intermediate B: To a solution of diol **A** (0.868 g, 1.97 mmol) in CH_2Cl_2 (20 mL) were added successively dimethylaminopyridine (DMAP, 0.032 mg, 0.13 equiv.) and imidazole (0.952 g, 6.4 equiv.). The mixture was stirred briefly in order to obtain a clear solution to which was added dropwise a solution of *tert*-butyldimethylsilyl chloride (TBSCl, 0.952 g, 3.1 equiv.) in CH_2Cl_2 (10 mL). Stirring was continued at room temperature for 2 h

before addition of water (10 mL). The organic layer was washed with water (2 x 5 mL), then with brine (8 mL). After drying with MgSO₄, the organic layer was filtered and concentrated under reduced pressure. The crude oil was purified by chromatography on silica gel column (AcOEt/cyclohexane: 1/1, v/v) to yield **B** as a viscous colourless oil, yield 1.100 g (quantitative). ¹H NMR (500 MHz, CDCl₃): δ = 7.79 (AA' of an AA'BB' system, 2H, arom. CH, Ts, ³J = 8.2 Hz), 7.30 (m, 3H, arom. CH, Bn), 7.22 (m, 4H, arom. CH, Bn and Ts), 4.79 (d, 1H, CHOMe, ³J = 3.6 Hz), 4.64 and 4.57 (AB spin system, 2H, CH₂Ph, ²J = 11.0 Hz), 4.36 (dd, 1H, CHOTs, ³J = 9.7 Hz, ³J = 3.6 Hz), 3.79 (m, 3H, CHOBn and TBSOCH₂), 3.56 (m, 2H, CHOH and TBSOCH₂CH), 3.33 (s, 3H, OMe), 2.58 (br s, 1H, OH), 2.39 (s, 3H, CH₃C₆H₄), 0.88 (s, 9H, (CH₃)₃CSi), -0.06 (s, 3H, CH₃Si), -0.06 (s, 3H, CH₃Si); ¹³C NMR (125 MHz, CDCl₃): δ = 145.08 (s, arom. Cq), 138.19 (s, arom. Cq), 133.68 (s, arom. Cq), 129.92 (s, arom. CH), 128.58 (s, arom. CH), 128.09 (s, arom. CH), 128.06 (s, arom. CH), 127.98 (s, arom. CH), 97.65 (s, CHOMe), 79.60 (s, CHOTs), 79.06 (s, CHOBn), 75.38 (s, CH₂Ph), 72.07 (s, CHOH or TBSOCH₂CH), 70.53 (s, CHOH or TBSOCH₂CH), 63.65 (s, TBSOCH₂), 55.48 (s, CH₃O), 26.03 (s, (CH₃)₃CSi), 21.82 (s, CH₃C₆H₄), 18.49 (s, (CH₃)₃CSi), -5.27 (s, CH₃Si), -5.31 (s, CH₃Si) ppm; elemental analysis calcd (%) for C₂₇H₄₀O₈SSi (552.75): C 58.67, H 7.29; found (%): C 58.29, H 7.48; [α]_D²⁰ = + 37.1 (c = 1.93, CH₂Cl₂).

Synthesis of intermediate C: A solution of alcohol **B** (1.120 g, 2.02 mmol) in dry THF (15 mL) was added dropwise to a chilled (0 °C) suspension of NaH (60 wt.% in mineral oil, 0.197 g, 2.4 equiv.) in dry THF (15 mL). After 20 min, solid *tert*-butylammonium iodide (TBAI, 0.030 g, 0.4 equiv.) and crude allylbromide (0.355 mL, 2 equiv.) were successively added. Stirring was continued at 0 °C for 2 h and the excess of allyl bromide was quenched by slow addition of MeOH (0.5 mL) and water (10 mL). The mixture was diluted with AcOEt (35 mL) and the organic phase was washed with water (2 x 10 mL), brine (10 mL), dried over MgSO₄, filtered and concentrated under reduced pressure. The residue was purified by chromatography on silica gel column (AcOEt/cyclohexane 1/1, v/v) to afford **C** as a viscous slight yellow oil, yield 1.150 g (96 %). ¹H NMR (500 MHz, CDCl₃): δ = 7.79 (AA' of an AA'BB' system, 2H, arom. CH, Ts, ³J = 8.2 Hz), 7.29 (m, 3H, arom. CH, Bn), 7.17 (m, 4H, arom. CH, Bn and Ts), 5.82 (m, 1H, CH=CH₂), 5.17 (dd, 1H, CH₂=CH, ³J = 17.2 Hz, ²J = 1.7 Hz), 5.10 (dd, CH₂=CH, ³J = 10.4 Hz, ²J = 1.7 Hz), 4.79 (d, 1H, CHOMe, ³J = 3.7 Hz), 4.62 (s, 2H, CH₂Ph), 4.36 (dd, 1H, CHOTs, ³J = 9.7 Hz, ³J = 3.7 Hz), 4.23 (ddt, 1H, CH₂CH=CH₂, ³J = 12.3 Hz, ⁴J = 5.7 Hz, ⁴J = 1.4 Hz), 4.07 (ddt, 1H, CH₂CH=CH₂, ³J = 12.3 Hz, ⁴J = 5.6 Hz, ⁴J = 1.5 Hz), 3.90 (m, 1H, CHOBn), 3.78 (m, 2H, TBSOCH₂), 3.40 (dt, 1H,

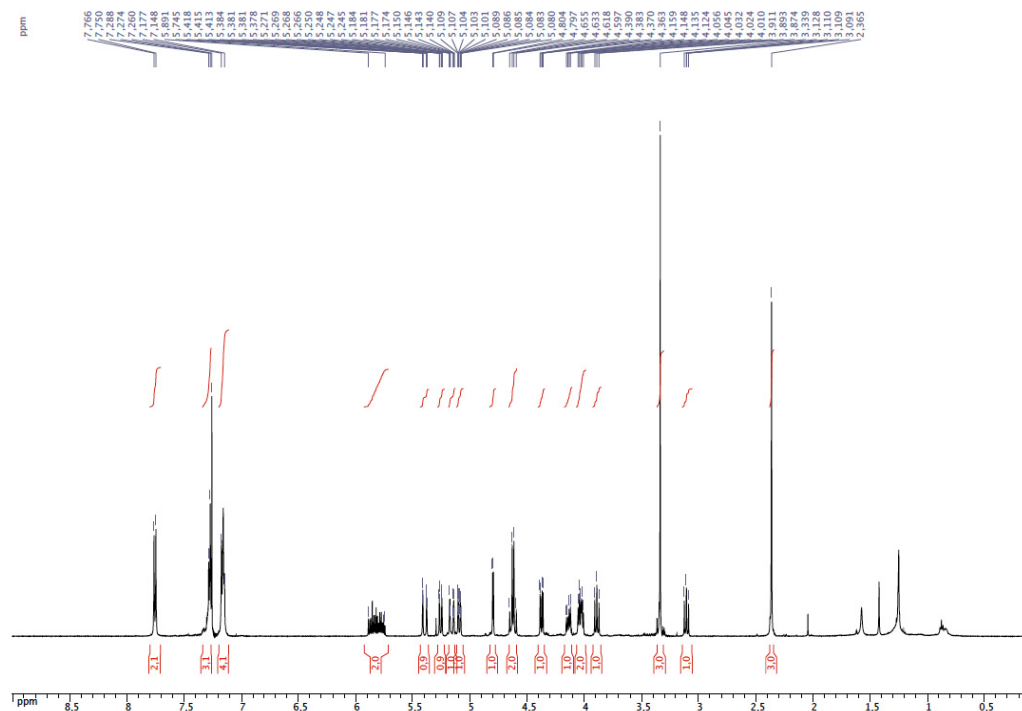
TBSOCH₂CH, ³J = 10.0 Hz, ³J = 2.9 Hz), 3.40 (dd, 1H, CHOCH₂CH=CH₂, ³J = 9.9 Hz, ³J = 8.9 Hz), 3.31 (s, 3H, OMe), 2.37 (s, 3H, CH₃C₆H₄), 0.88 (s, 9H, (CH₃)₃CSi), 0.05 (s, 6H, CH₃Si); ¹³C NMR (125 MHz, CDCl₃): δ = 144.91 (s, arom. Cq), 138.19 (s, arom. Cq), 134.75 (s, CH=CH₂), 133.86 (s, arom. Cq), 129.89 (s, arom. CH), 128.33 (s, arom. CH), 127.96 (s, arom. CH), 128.06 (s, arom. CH), 127.68 (s, arom. CH), 116.96 (s, CH=CH₂), 97.45 (s, CHOMe), 79.94 (s, CHOTs), 79.50 (s, CHOBn), 77.58 (s, CHOCH₂CH=CH₂), 75.60 (s, CH₂Ph), 73.98 (s, OCH₂CH=CH₂), 71.46 (s, TBSOCH₂CH), 61.91 (s, TBSOCH₂), 55.30 (s, CH₃O), 26.04 (s, (CH₃)₃CSi), 21.81 (s, CH₃C₆H₄), 18.47 (s, (CH₃)₃CSi), -5.05 (s, CH₃Si), -5.28 (s, CH₃Si) ppm; [α]_D²⁰ = + 62.2 (c = 1.05, CH₂Cl₂).

Synthesis of intermediate D: A solution of *tert*-butylammonium fluoride (TBAF, 1 M in THF, 2.4 mL, 1.2 equiv.) was added to a chilled (0 °C) solution of **C** (1.154 g, 1.94 mmol) in THF (20 mL). Stirring was continued at ambient temperature for 2 h (monitored by tlc) and then the reaction was quenched with water (10 mL) and diluted with AcOEt (25 mL). The organic layer was washed with water (2 x 10 mL), brine (10 mL), dried over MgSO₄, filtered and concentrated under reduced pressure. The residue was purified by chromatography on silica gel column (AcOEt/cyclohexane: 1/1, v/v) to afford a colourless viscous oil, which slowly crystallized to give alcohol **D** as a white solid, yield 0.830 g (89 %). ¹H NMR (500 MHz, CDCl₃): δ = 7.75 and 7.16 (AA'BB' system, 4H, arom. CH, Ts, ³J = 8.5 Hz), 7.27 (m, 3H, arom. CH, Bn), 7.14 (m, 2H, arom. CH, Bn), 5.82 (m, 1H, CH=CH₂), 5.18 (dd, 1H, CH₂=CH, ³J = 17.2 Hz, ²J = 1.5 Hz), 5.11 (dd, CH₂=CH, ³J = 10.5 Hz, ²J = 1.5 Hz), 4.82 (d, 1H, CHOMe, ³J = 3.6 Hz), 4.62 (s, 2H, CH₂Ph), 4.34 (dd, 1H, CHOTs, ³J = 9.8 Hz, ³J = 3.6 Hz), 4.22 (ddt, 1H, CH₂CH=CH₂, ³J = 12.3 Hz, ⁴J = 5.6 Hz, ⁴J = 1.4 Hz), 4.07 (ddt, 1H, CH₂CH=CH₂, ³J = 12.3 Hz, ⁴J = 5.9 Hz, ⁴J = 1.4 Hz), 3.91 (dd, 1H, CHOBn, ³J = 9.7 Hz, ³J = 9.1 Hz), 3.77 (AB part of an ABX spin system, CH₂OH, 2H, ²J = 12.0 Hz, ³J = 3.7 Hz, ³J = 3.0 Hz), 3.62 (X part of an ABX spin system, ddd, 1H, CHCH₂OH, ³J = 10.0 Hz, ³J = 3.8 Hz, ³J = 2.7 Hz), 3.41 (dd, 1H, CHOCH₂CH=CH₂, ³J = 10.0 Hz, ³J = 8.9 Hz), 3.35 (s, 3H, OMe), 2.36 (s, 3H, CH₃C₆H₄); ¹³C NMR (125 MHz, CDCl₃): δ = 145.01 (s, arom. Cq), 138.12 (s, arom. Cq), 134.45 (s, CH=CH₂), 133.55 (s, arom. Cq), 129.89 (s, arom. CH), 128.30 (s, arom. CH), 127.97 (s, arom. CH), 127.72 (s, arom. CH), 127.63 (s, arom. CH), 117.47 (s, CH=CH₂), 97.73 (s, CHOMe), 79.67 (s, CHOTs), 79.19 (s, CHOBn), 77.47 (s, CHOCH₂CH=CH₂), 75.43 (s, CH₂Ph), 74.10 (s, OCH₂CH=CH₂), 70.74 (s, HOCH₂CH), 61.56 (s, HOCH₂), 55.62 (s, CH₃O), 21.80 (s, CH₃C₆H₄) ppm; elemental analysis calcd (%) for C₂₄H₃₀O₈S (478.56): C 60.23, H 6.32; found (%): C 60.13, H 6.39; [α]_D²⁰ = + 77.7 (c = 1.03, CH₂Cl₂).

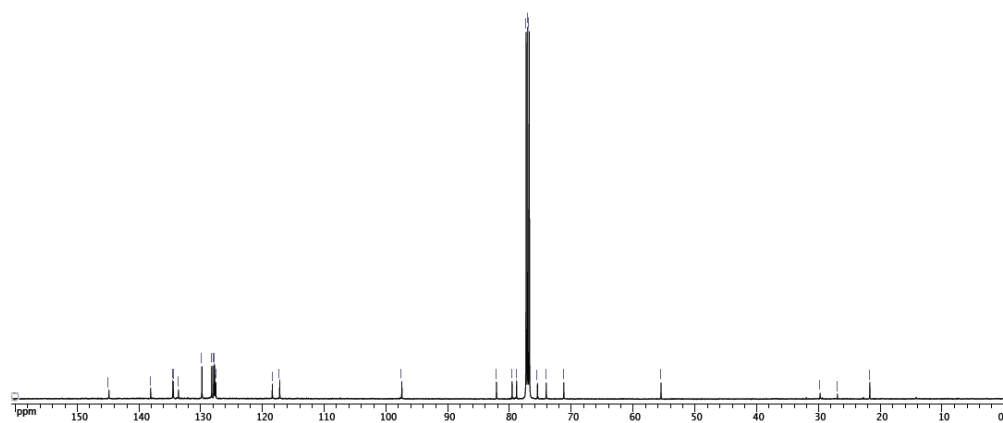
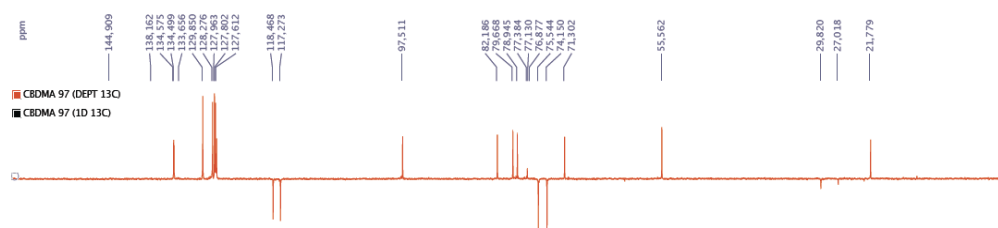
Synthesis of intermediate E: Dimethylsulfoxide (0.25 mL, 10.5 equiv.), diisopropylethyl amine (DiPEA, 0.30 mL, 5.1 equiv.) and Py.SO₃ (0.266 g, 5 equiv.) were added successively to a solution of **D** (0.161 g, 0.336 mmol) in CH₂Cl₂ (3 mL). The reaction was stirred for 2 h (monitored by tlc) at room temperature, then quenched with water (5 mL) and diluted with CH₂Cl₂ (5 mL). The aqueous layer was extracted with CH₂Cl₂ (5 mL) and the combined organic layers (CH₂Cl₂) were evaporated. The residue was diluted with Et₂O (15 mL) and washed with water (10 x 5 mL), brine (5 mL), dried over MgSO₄, filtered and concentrated under reduced pressure. The resulting crude product was purified by silica gel chromatographic column (AcOEt/cyclohexane: 1/1, v/v) to afford aldehyde **E** as a colourless viscous oil, yield 0.134 g (84 %). ¹H NMR (500 MHz, CDCl₃): δ = 4.86 (d, 1H, CHO, ³J = 0.5 Hz), 7.75 (AA' of an AA'BB' system, 2H, arom. CH, Ts, ³J = 8.0 Hz), 7.30 (m, 3H, arom. CH, Bn), 7.17 (m, 4H, arom. CH, Bn and Ts), 5.77 (m, 1H, CH=CH₂), 5.18 (dd, 1H, CH₂=CH, ³J = 17.2 Hz, ²J = 1.7 Hz), 5.14 (dd, CH₂=CH, ³J = 10.4 Hz, ²J = 1.7 Hz), 4.86 (d, 1H, CHOMe, ³J = 3.6 Hz), 4.67 and 4.63 (AB spin system, 2H, CH₂Ph, ²J = 10.5 Hz), 4.33 (dd, 1H, CHOTs, ³J = 9.8 Hz, ³J = 3.6 Hz), 4.21 (m, 1H, CH₂CH=CH₂), 4.13 (d, 1H, CHCHO, ³J = 10.4 Hz), 4.06 (m, 1H, CH₂CH=CH₂), 3.99 (dd, 1H, CHOBn, ³J = 9.8 Hz, ³J = 8.6 Hz), 3.36 (s, 3H, OMe), 3.11 (dd, 1H, CHOCH₂CH=CH₂, ³J = 10.5 Hz, ³J = 8.6 Hz), 2.38 (s, 3H, CH₃C₆H₄); ¹³C NMR (125 MHz, CDCl₃): δ = 196.98 (s, CHO), 145.23 (s, arom. Cq), 137.74 (s, arom. Cq), 133.83 (s, CH=CH₂), 133.34 (s, arom. Cq), 130.00 (s, arom. CH), 128.39 (s, arom. CH), 128.01 (s, arom. CH), 127.86 (s, arom. CH), 118.18 (s, CH=CH₂), 97.84 (s, CHOMe), 79.15 (s, CHOBn), 78.82 (s, CHOTs), 77.80 (s, CHOCH₂CH=CH₂), 75.73 (s, CH₂Ph), 74.18 (s, OCH₂CH=CH₂), 74.08 (s, OCHCH), 56.26 (s, CH₃O), 21.81 (s, CH₃C₆H₄) ppm. Note that, due to the unstable nature of aldehyde **E**, elemental analysis could not be performed.

Synthesis of compound 9: A solution of *n*-BuLi (1.43 M in cyclohexane, 1.25 mL, 2.1 equiv.) was added to a suspension of dry methyltriphenylphosphonium bromide (0.626 g, 2.07 equiv) in THF (20 mL) at -75°C. The mixture was stirred for 25 min at the same temperature and for 20 min at ambient temperature to afford a lemon coloured solution. Then aldehyde **E** (0.402 g, 8.44 mmol) in THF (10 mL) was added at -65 °C and stirring was prolonged for 3.5 h leaving the temperature to rise to room temperature. The reaction was quenched with a saturated aqueous NH₄Cl solution (2 mL), water (10 mL) and aq. HCl 10% solution (1 mL) until pH 6. After dilution with AcOEt (40 mL), the organic layer was washed with water (2 x 10 mL), brine (10 mL), dried over MgSO₄, filtered and concentrated under reduced pressure.

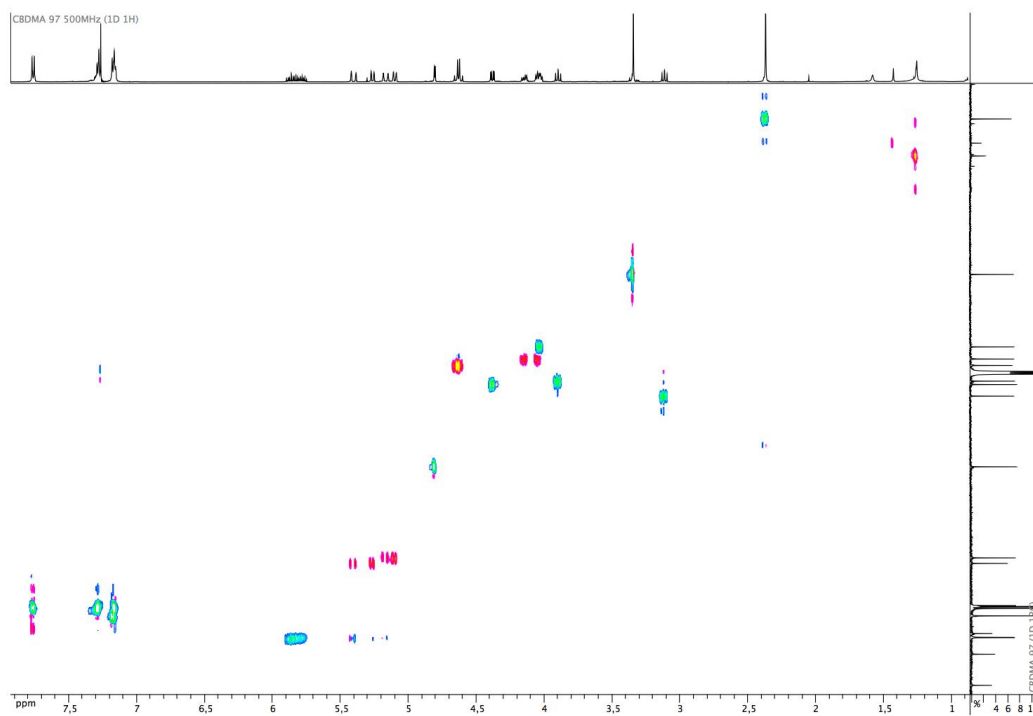
The crude was purified by chromatography on silica gel column (AcOEt/cyclohexane: 3/7, v/v) to give compound **9** as a colourless viscous oil, yield 0.289 g (72 %). ^1H NMR (500 MHz, CDCl_3): $\delta = 7.75$ (AA' of an AA'BB' system, 2H, arom. CH, Ts, $^3J = 8.2$ Hz), 7.28 (m, 3H, arom. CH, Bn), 7.17 (m, 4H, arom. CH, Bn and Ts), 5.86 (m, 1H, $\text{CH}=\text{CH}_2$), 5.79 (m, 1H, $\text{CH}_2\text{CH}=\text{CH}_2$), 5.40 (dd, 1H, $\text{CH}_2=\text{CH}$, $^3J = 17.2$ Hz, $^2J = 1.4$ Hz), 5.26 (dd, $\text{CH}_2=\text{CH}$, $^3J = 10.5$ Hz, $^2J = 1.4$ Hz), 5.16 (dd, 1H, $\text{CH}_2=\text{CHCH}_2$, $^3J = 17.2$ Hz, $^2J = 1.7$ Hz), 5.10 (dd, $\text{CH}_2=\text{CHCH}_2$, $^3J = 10.4$ Hz, $^2J = 1.7$ Hz), 4.80 (d, 1H, CHOMe , $^3J = 3.7$ Hz), 4.64 and 4.61 (AB spin system, 2H, CH_2Ph , $^2J = 11.0$ Hz), 4.38 (dd, 1H, CHOTs , $^3J = 9.8$ Hz, $^3J = 3.7$ Hz), 4.14 (m, 1H, $\text{CH}_2\text{CH}=\text{CH}_2$), 4.04 (m, 1H, $\text{CH}_2\text{CH}=\text{CH}_2$), 4.13 (m, 1H, $\text{CHCH}=\text{CH}_2$), 3.89 (t, 1H, CHOBN , $^3J = 9.3$ Hz), 3.34 (s, 3H, OMe), 3.11 (dd, 1H, $\text{CHOCH}_2\text{CH}=\text{CH}_2$, $^3J = 9.8$ Hz, $^3J = 9.1$ Hz), 2.36 (s, 3H, $\text{CH}_3\text{C}_6\text{H}_4$); ^{13}C NMR (125 MHz, CDCl_3): $\delta = 144.91$ (s, arom. Cq), 138.16 (s, arom. Cq), 134.57 (s, $\text{CH}=\text{CH}_2$), 134.50 (s, $\text{CH}=\text{CH}_2$), 133.66 (s, arom. Cq), 129.85 (s, arom. CH), 128.28 (s, arom. CH), 127.96 (s, arom. CH), 127.96 (s, arom. CH), 127.61 (s, arom. CH), 118.47 (s, $\text{CH}=\text{CH}_2$), 117.27 (s, $\text{CH}_2\text{CH}=\text{CH}_2$), 97.51 (s, CHOMe), 82.19 (s, $\text{CHOCH}_2\text{CH}=\text{CH}_2$), 79.67 (s, CHOTs), 78.94 (s, CHOBN), 75.54 (s, CH_2Ph), 74.15 (s, $\text{OCH}_2\text{CH}=\text{CH}_2$), 71.30 (s, $\text{CHCH}=\text{CH}_2$), 55.56 (s, CH_3O), 21.78 (s, $\text{CH}_3\text{C}_6\text{H}_4$) ppm; elemental analysis calcd (%) for $\text{C}_{25}\text{H}_{30}\text{O}_7\text{S}$ (474.57): C 63.27, H 6.37; found (%): C 63.57, H 6.68; $[\alpha]_{\text{D}}^{20} = +58.8$ ($c = 1.05$, CH_2Cl_2).



^1H NMR spectrum of **9** (CDCl_3)

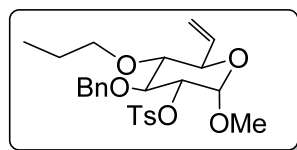


$^{13}\text{C}\{^1\text{H}\}$ NMR spectrum of **9** (CDCl_3)

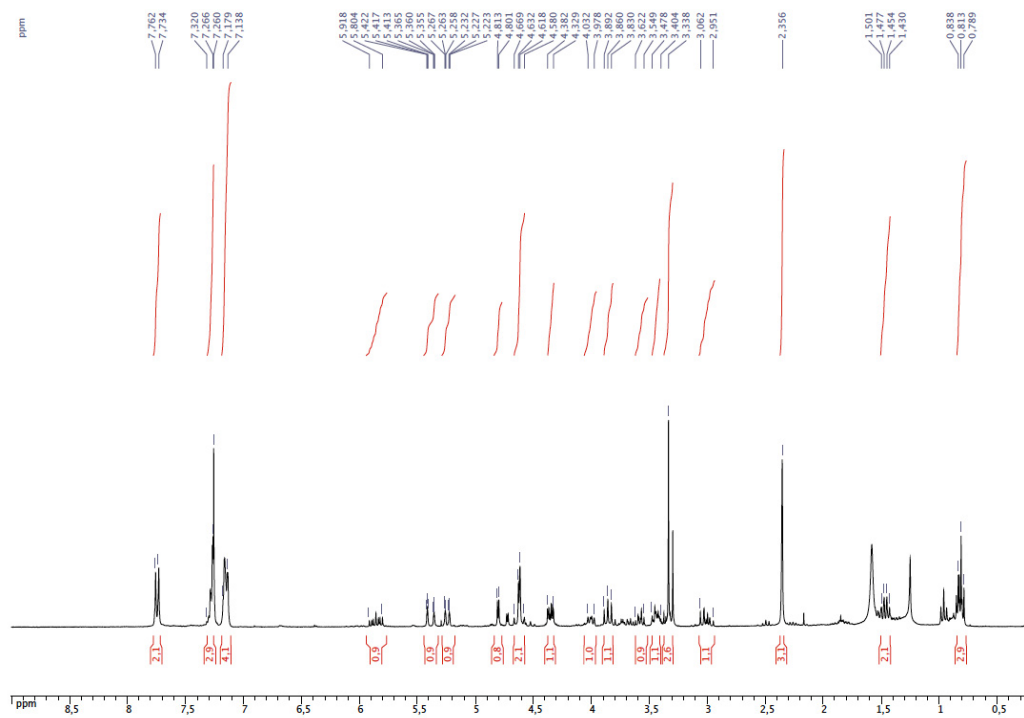


$^1\text{H}/^1\text{H}$ COSY spectrum of **9** (CDCl_3)

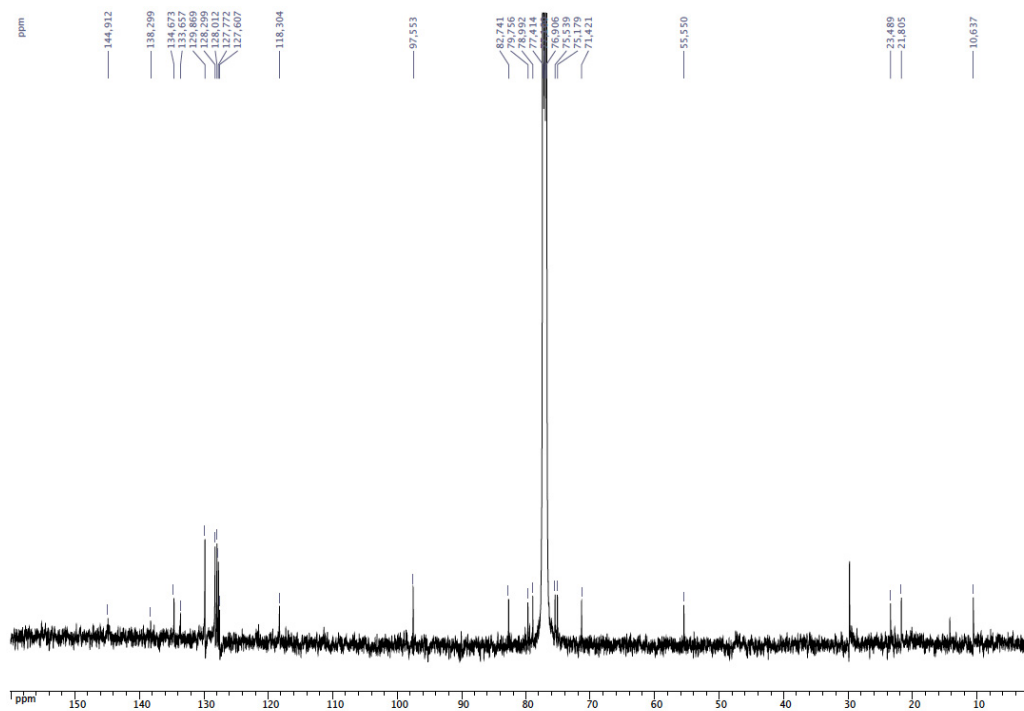
Synthesis and characterising data of **10**



The hydrogenation experiments were carried out in a glass lined 100 mL stainless steel autoclave containing a magnetic stirring bar. The autoclave was charged successively under nitrogen with $[\text{Rh}(\text{cod})_2]\text{BF}_4$ (0.001 g, 2 mol %) dissolved in THF (0.4 mL) and bis(iminophosphoranyl)resorcin[4]arene **4** (0.004 g, 2 mol %) dissolved in THF (0.2 mL). The reaction mixture was stirred at r.t. for 0.5 h before addition of diolefin **9** (0.060 g, 0.13 mmol) dissolved in THF (0.6 mL). The autoclave was flushed twice with hydrogen, then pressurised at 5 bar. After 14 h, the autoclave was depressurized and the resulting solution was evaporated under reduced pressure. The crude product was analysed by ^1H NMR (conversion = 84 %). The crude product was further purified by chromatography on silica gel column ($\text{CH}_2\text{Cl}_2/\text{petroleum ether}$: 1/1, v/v) to give compound **10** as a colourless oil, yield 0.046 g (77 %). ^1H NMR (300 MHz, CDCl_3): δ = 7.74 (AA' of an AA'BB' system, 2H, arom. CH, Ts, 3J = 8.4 Hz), 7.29 (m, 3H, arom. CH, Bn), 7.16 (m, 4H, arom. CH, Bn and Ts), 5.86 (m, 1H, $\text{CH}=\text{CH}_2$), 5.38 (ddd, 1H, $\text{CH}_2=\text{CH}$, 3J = 17.1 Hz, 2J = 1.3 Hz, 4J = 1.3 Hz), 5.24 (ddd, $\text{CH}_2=\text{CH}$, 3J = 10.8 Hz, 2J = 1.3 Hz, 4J = 1.3 Hz), 4.80 (d, 1H, CHOMe , 3J = 3.6 Hz), 4.65 and 4.60 (AB spin system, 2H, CH_2Ph , 2J = 11.3 Hz), 4.35 (m, 1H, CHOTs), 4.01 (m, 1H, $\text{CHCH}=\text{CH}_2$), 3.86 (t, 1H, CHOBn , 3J = 9.3 Hz), 3.58 (m, 1H, OCH_2), 3.44 (m, 1H, OCH_2), 3.34 (s, 3H, OMe), 3.01 (m, 1H, CHOCH), 2.36 (s, 3H, $\text{CH}_3\text{C}_6\text{H}_4$), 1.46 (hex, 2H, CH_2CH_3 , 3J = 7.2 Hz), 0.81 (t, 3H, CH_2CH_3 , 3J = 7.2 Hz); ^{13}C NMR (125 MHz, CDCl_3): δ = 144.91 (s, arom. Cq), 138.30 (s, arom. Cq), 134.67 (s, $\text{CH}=\text{CH}_2$), 133.66 (s, arom. Cq), 129.87 (s, arom. CH), 128.30 (s, arom. CH), 128.01 (s, arom. CH), 127.77 (s, arom. CH), 127.61 (s, arom. CH), 118.30 (s, $\text{CH}=\text{CH}_2$), 97.55 (s, CHOMe), 82.74 (s, $\text{CHOCH}_2\text{CH}_2$), 79.76 (s, CHOTs), 78.99 (s, CHOBn), 75.54 (s, OCH_2CH_2), 75.18 (s, CH_2Ph), 71.42 (s, $\text{CHCH}=\text{CH}_2$), 55.55 (s, CH_3O), 23.49 (s, CH_2CH_3), 21.80 (s, $\text{CH}_3\text{C}_6\text{H}_4$), 10.64 (s, CH_2CH_3) ppm; elemental analysis calcd (%) for $\text{C}_{25}\text{H}_{32}\text{O}_7\text{S}$ (476.58): C 63.00, H 6.77; found (%): C 63.65 H 6.98.

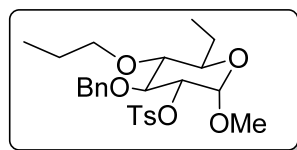


^1H NMR spectrum of **10** (CDCl_3)

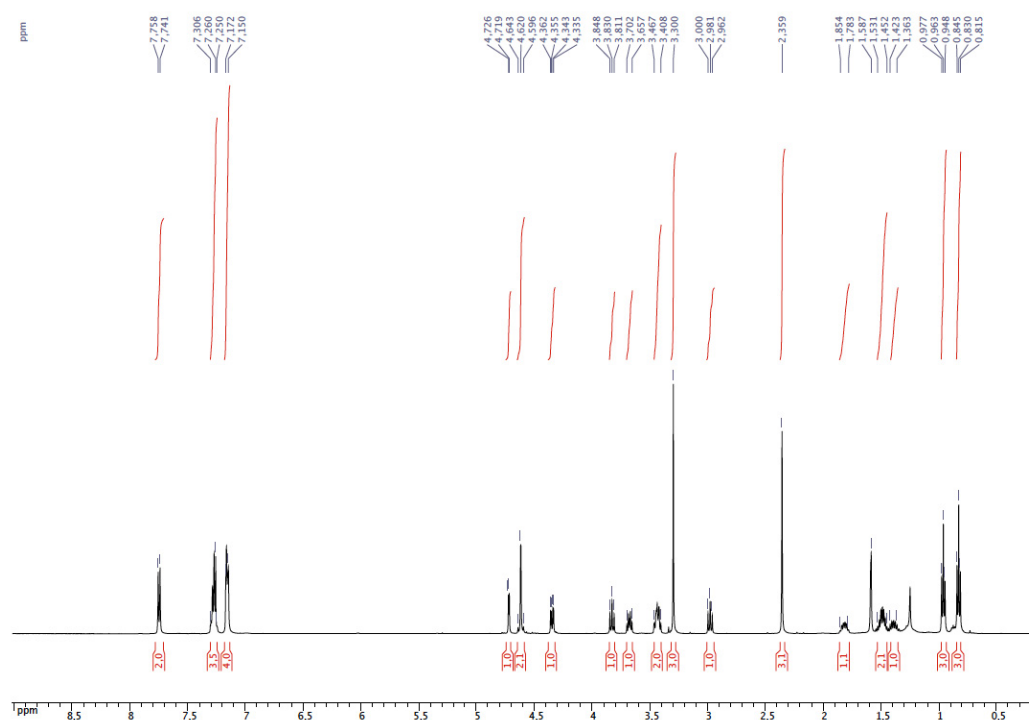


$^{13}\text{C}\{^1\text{H}\}$ NMR spectrum of **10** (CDCl_3)

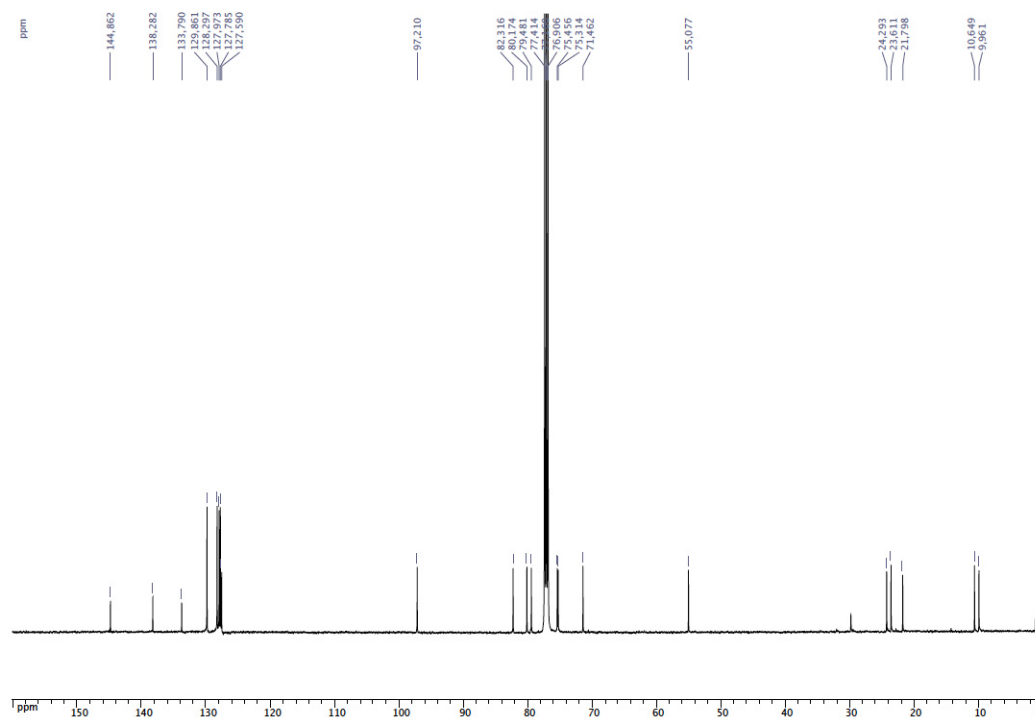
Characterising data of fully hydrogenated product



^1H NMR (500 MHz, CDCl_3): $\delta = 7.75$ (AA' of an AA'BB' system, 2H, arom. CH, Ts, $^3J = 8.5$ Hz), 7.28 (m, 3H, arom. CH, Bn), 7.16 (m, 4H, arom. CH, Bn and Ts), 4.72 (d, 1H, CHOMe , $^3J = 3.5$ Hz), 4.63 and 4.61 (AB spin system, 2H, CH_2Ph , $^2J = 11.5$ Hz), 4.35 (dd, 1H, CHOTs , $^3J = 9.5$ Hz, $^3J = 3.5$ Hz), 3.83 (t, 1H, CHOBn , $^3J = 9.2$ Hz), 3.69 (m, 1H, OCH_2), 3.43 (m, 2H, OCH_2 and CHCH_2CH_3), 3.30 (s, 3H, OMe), 2.98 (t, 1H, CHOCH , $^3J = 9.5$ Hz), 2.36 (s, 3H, $\text{CH}_3\text{C}_6\text{H}_4$), 1.82 (m, 1H, CHCH_2CH_3), 1.49 (m, 2H, $\text{CH}_2\text{CH}_2\text{CH}_3$), 1.39 (m, 1H, CHCH_2CH_3), 0.96 (t, 3H, CHCH_2CH_3 , $^3J = 7.2$ Hz), 0.83 (t, 3H, $\text{CH}_2\text{CH}_2\text{CH}_3$, $^3J = 7.5$ Hz); ^{13}C NMR (125 MHz, CDCl_3): $\delta = 144.86$ (s, arom. Cq), 138.28 (s, arom. Cq), 133.79 (s, arom. Cq), 129.86 (s, arom. CH), 128.30 (s, arom. CH), 127.97 (s, arom. CH), 127.78 (s, arom. CH), 127.59 (s, arom. CH), 97.21 (s, CHOMe), 82.32 (s, $\text{CHOCH}_2\text{CH}_2$), 80.17 (s, CHOTs), 79.48 (s, CHOBn), 75.46 (s, OCH_2CH_2), 75.31 (s, CH_2Ph), 71.46 (s, CHCH_2CH_3), 55.08 (s, CH_3O), 24.29 (s, CHCH_2H_3), 23.61 (s, $\text{CH}_2\text{CH}_2\text{CH}_3$), 21.80 (s, $\text{CH}_3\text{C}_6\text{H}_4$), 10.65 (s, $\text{CH}_2\text{CH}_2\text{CH}_3$), 9.96 (s, CHCH_2CH_3) ppm; elemental analysis calcd (%) for $\text{C}_{25}\text{H}_{34}\text{O}_7\text{S}$ (478.60): C 62.74, H 7.16; found (%): C 62.86 H 7.30.



^1H NMR spectrum of fully hydrogenated product (CDCl_3)



$^{13}\text{C}\{^1\text{H}\}$ NMR spectrum of fully hydrogenated product (CDCl_3)

General procedure for the catalytic hydrogenation of α -olefins

The hydrogenation experiments were carried out in a glass lined 100 mL stainless steel autoclave containing a magnetic stirring bar. In a typical run, the autoclave was charged successively under nitrogen with $[\text{Rh}(\text{cod})_2]\text{BF}_4$ (0.004 g, 1 mol %) and a solution of diiminophosphorane **4** (0.014 g, 1 mol %) in THF (5 mL). After stirring for 30 min, the two olefins (1.0 mmol of each) were added. Once closed, the autoclave was flushed twice with hydrogen, then pressurised to 5 bar. At the end of the catalytic run, the autoclave was depressurized and the resulting solution was passed through a Millipore filter and analysed by GC.

X-Ray crystallography

Colourless single crystals of **2** suitable for X-ray diffraction were obtained by slow diffusion of hexane into a CH_2Cl_2 solution of **2** at room temperature. The sample (0.354 x 0.272 x 0.186 mm) was mounted on an Oxford Diffraction Xcalibur Saphir 3 diffractometer with graphite-monochromatised Mo- K_α radiation. Formula of the crystals: $\text{C}_{76}\text{H}_{82}\text{O}_8\text{P}_2 \cdot 3\text{CH}_2\text{Cl}_2$, $M_r = 1440.21$, triclinic, space group $P-1$, $a = 14.1288(4)$, $b = 16.0216(5)$, $c = 17.7587(5)$ Å, $\alpha = 111.573(3)$, $\beta = 100.811(2)$, $\gamma = 90.472(2)^\circ$, $V = 3658.87(19)$ Å³, $Z = 2$, $D_x = 1.307$ mg.m⁻³, $\lambda(\text{Mo-}K_\alpha) = 0.71073$ Å, $\mu = 0.334$ mm⁻¹, $F(000) = 1516$, $T = 120(2)$ K. Data collection ($2\theta_{\text{max}}$

= 27.0°, ω scan frames via 0.7° ω rotation and 30 s per frame, range *hkl*: *h* -18 to 10, *k* -19 to 20, *l* -21 to 22) gave 28353 reflections. The data revealed 15712 independent reflections of which 10432 were observed with $I > 2.0 \sigma(I)$. The structure was solved by using SIR-97,^[15] which revealed the non-hydrogen atoms of the molecule. After anisotropic refinement, all the hydrogen atoms were found by Fourier difference. The whole structure was refined with SHELXL97^[16] by using the full-matrix least squares technique {use of F^2 ; *x*, *y*, *z*, β_{ij} for C, Cl, O and P atoms, *x*, *y*, *z* in the riding mode for H atoms; 856 variables and 10432 observations with $I > 2.0 \sigma(I)$; calcd. $w = 1/[\sigma^2(F_o^2) + (0.0995P)^2]$ in which $P = (F_o^2 + 2 F_c^2)/3$ with the resulting $R = 0.0531$, $R_w = 0.1482$ and $S_w = 0.961$, $\Delta\rho < 0.983 \text{ e}\text{\AA}^{-3}$ }.

Colourless single crystals of **3** suitable for X-ray diffraction were obtained by slow diffusion of non anhydrous methanol into a CH₂Cl₂ solution of **3** at room temperature. The sample (0.242 x 0.182 x 0.128 mm) was mounted on an Oxford Diffraction Xcalibur Saphir 3 diffractometer with graphite-monochromatised Mo-*K*_α radiation. Formula of the crystals: C₇₆H₈₂O₁₀P₂·2CH₃OH·H₂O, *Mr* = 1299.51, monoclinic, space group *P21/c*, *a* = 23.5303(4), *b* = 16.7471(2), *c* = 19.4323(3) Å, $\beta = 114.371(2)^\circ$, *V* = 6975.23(18) Å³, *Z* = 4, *D_x* = 1.236 mg.m⁻³, $\lambda(\text{Mo-}K_\alpha) = 0.71073 \text{ \AA}$, $\mu = 0.126 \text{ mm}^{-1}$, *F*(000) = 2772, *T* = 150(2) K. Data collection ($2\theta_{\text{max}} = 27.0^\circ$, ω scan frames via 0.7° ω rotation and 30 s per frame, range *hkl*: *h* -29 to 30, *k* -21 to 21, *l* -24 to 24) gave 52330 reflections. The data revealed 15160 independent reflections of which 9117 were observed with $I > 2.0 \sigma(I)$. The structure was solved by using SIR-97,^[15] which revealed the non-hydrogen atoms of the molecule. After anisotropic refinement, all the hydrogen atoms were found by Fourier difference. The whole structure was refined with SHELXL97^[16] by using the full-matrix least squares technique {use of F^2 ; *x*, *y*, *z*, β_{ij} for C, O and P atoms, *x*, *y*, *z* in the riding mode for H atoms; 817 variables and 9117 observations with $I > 2.0 \sigma(I)$; calcd. $w = 1/[\sigma^2(F_o^2) + (0.1177P)^2]$ in which $P = (F_o^2 + 2 F_c^2)/3$ with the resulting $R = 0.0570$, $R_w = 0.1553$ and $S_w = 0.859$, $\Delta\rho < 1.532 \text{ e}\text{\AA}^3$ }.

CCDC-931124 (for **2**) and CCDC-964375 (for **3**) contain the supplementary crystallographic data which can be obtained free of charge from The Cambridge Crystallographic Data Centre via www.ccdc.cam.ac.uk/data_request/cif.

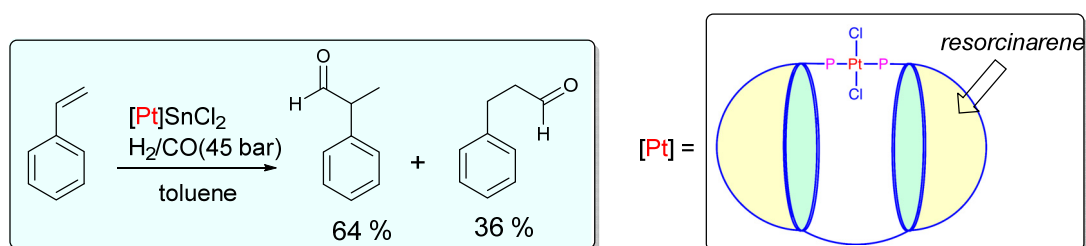
References

- [1] a) C. Torque, B. Sueur, J. Cabou, H. Bricout, F. Hapiot and E. Monflier, *Tetrahedron* **2005**, *61*, 4811-4817; b) E. Lindbäck, S. Dawaigher and K. Wärnmark, *Chem. Eur. J.* **2014**, *20*, 13432-13481.
- [2] a) M. Ooe, M. Murata, T. Mizugaki, K. Ebitani and K. Kaneda, *Nano Lett.* **2002**, *2*, 999-1002; b) T. Mizugaki, M. Murata, S. Fukubayashi, T. Mitsudome, K. Jitsukawa and K. Kaneda, *Chem. Commun.* **2008**, 241-243.
- [3] A. D. Westwell and J. M. J. Williams, *Tetrahedron* **1997**, *53*, 13063-13078.
- [4] H. K. A. C. Coolen, J. A. M. Meeuwis, P. W. N. M. van Leeuwen and R. J. M. Nolte, *J. Am. Chem. Soc.* **1995**, *117*, 11906-11913.
- [5] M. T. Reetz and S. R. Waldvogel, *Angew. Chem. Int. Ed. Engl.* **1997**, *36*, 865-867.
- [6] K. Urabe, Y. Tanaka and Y. Izumi, *Chem. Lett.* **1985**, 1595-1596.
- [7] C. Gibson and J. J. Rebek, *Org. Lett.* **2002**, *4*, 1887-1890.
- [8] A. Cavarzan, J. N. H. Reek, F. Trentin, A. Scarso and G. Strukul, *Catal. Sci. Technol.* **2013**, *3*, 2898-2901.
- [9] a) L. Catti and K. Tiefenbacher, *Chem. Commun.* **2015**, *51*, 892-894; b) S. Giust, G. La Sorella, L. Sporni, G. Strukul and A. Scarso, *Chem. Commun.* **2015**, *51*, 1658-1661; c) G. La Sorella, L. Sporni, G. Strukul and A. Scarso, *ChemCatChem* **2015**, *7*, 291-296; d) Q. Zhang and K. Tiefenbacher, *J. Am. Chem. Soc.* **2013**, *135*, 16213-16219.
- [10] a) L. Monnereau, H. El Moll, D. Sémeril, D. Matt and L. Toupet, *Eur. J. Inorg. Chem.* **2014**, 1364-1372; b) T. Chavagnan, D. Sémeril, D. Matt, J. Harrowfield and L. Toupet, *Chem. Eur. J.* **2015**, *21*, 6678-6681.
- [11] a) H. El Moll, D. Sémeril, D. Matt, M.-T. Youinou and L. Toupet, *Org. Biomol. Chem.* **2009**, *7*, 495-501; b) H. El Moll, D. Sémeril, D. Matt and L. Toupet, *Eur. J. Org. Chem.* **2010**, 1158-1168; c) N. Şahin, D. Sémeril, E. Brenner, D. Matt, I. Özdemir, C. Kaya and L. Toupet, *ChemCatChem* **2013**, *5*, 1116-1125.
- [12] H. Staudinger and J. Meyer, *Hel. Chim. Acta* **1919**, *2*, 635-646.
- [13] L. Eberhardt, D. Armspach, D. Matt, B. Oswald and L. Toupet, *Org. Biomol. Chem.* **2007**, *5*, 3340-3346.
- [14] Q. Liu and Y. Tor, *Org. Lett.* **2003**, *5*, 2571-2572.
- [15] A. Altomare, M. C. Burla, M. Camalli, G. Cascarano, C. Giacovazzo, A. Guagliardi, A. G. G. Moliterni, G. Polidori and R. Spagna, *J. Appl. Crystallogr.* **1998**, *31*, 74-77.
- [16] G. M. Sheldrick, SHELXL-97, Program for the Refinement of Crystal Structures, Univ. of Göttingen, Germany, 1997.

Chapter V

Cavitand chemistry: towards metallo-capsular catalysts

Abstract: Two long diphosphines the core of which consists of two covalently linked resorcinarene-cavitands have been synthesised. Their ability to bind transition metal ions in a chelating fashion with concomitant formation of capsular complexes was shown in their reaction with metal complexes having two available binding sites. The solid state structure of one of the complexes, a capsule with a partially embedded “*trans*-PtCl₂” unit, was determined by single X-ray diffraction analysis. This complex, once treated with SnCl₂, developed good activity in the hydroformylation of styrene. Its activity and selectivity towards the branched aldehyde were both significantly superior to those observed for the reference bis-phosphine complex *trans*-PtCl₂L₂, in which L is a monophosphine/monocavitand ligand. The observed performance is likely to reflect the formation of an intermediate with a somewhat distorted trigonal bipyramidal structure that facilitates the insertion step, as well as strong interactions involving the inner cavity wall and the metal first coordination sphere, these favouring formation of the shorter aldehyde.



Keywords: cavitands • resorcinarenes • metallo-capsule • hydroformylation • platinum

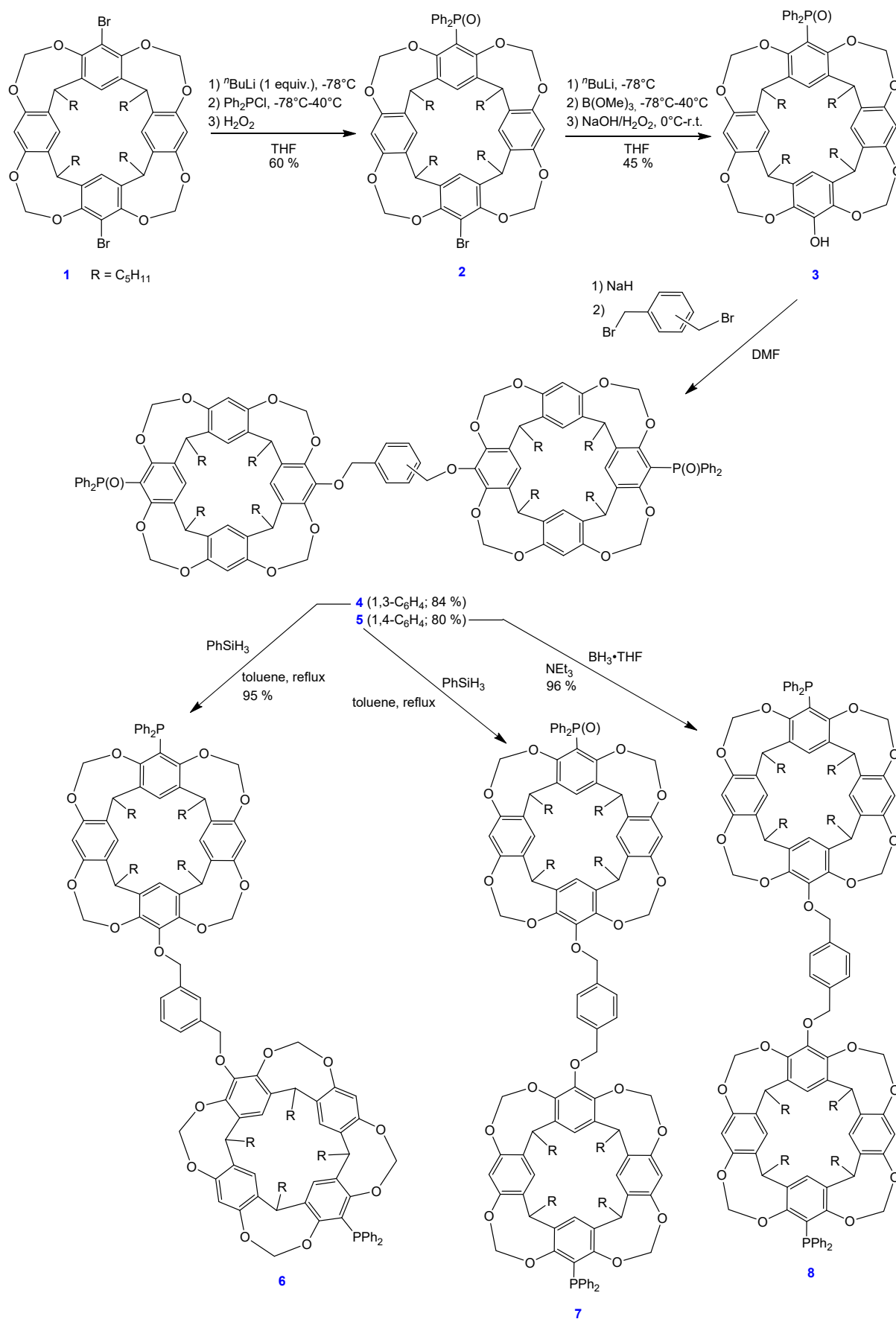
Introduction

Resorcinarene-derived cavitands are bowl-shaped molecules with restricted core flexibility.^[1] In recent years they have led to a variety of applications relevant to host-guest chemistry,^[2] separation science,^[3] coordination chemistry^[4] and catalysis.^[5] Generic compounds of this family are particularly well suited to the construction of extended molecular baskets^[6] carcerands,^[7] carceplexes,^[7c, 8] self-assembled capsules^[9] and tubes,^[10] most of these edifices being able to host small molecules or ions. Because of their rigidity, they further constitute valuable platforms for the buildup of molecules decorated with a set of circularly arranged, convergent ligands, which may result in highly selective complexants.^[11]

The present study describes the synthesis of the first P(III) ligands (**6** and **8**) based on a semi-rigid skeleton comprising two covalently linked resorcinarene moieties. Their syntheses were undertaken with the expectation that upon chelation – whenever possible – the two cavity fragments would be brought close together so as to create a container. To date, ligands containing two connected resorcinarene units are scarce, and none of these was used for forming metallo-capsules.^[12]

Results and Discussion

Diphosphines **6** and **8** were both obtained in four steps starting from dibromo-cavitand **1** (Scheme 1). Treatment of **1** with 1 equiv. of *n*BuLi followed by phosphination with Ph₂PCl and subsequent oxidation with H₂O₂ gave phosphine oxide **2** in 60 % yield. Conversion of **2** to the hydroxylated derivative **3** was achieved via formation of a boronate, which was submitted to oxidative carbon-boron bond cleavage with H₂O₂. The structure of **3** was determined by an X-ray diffraction study (Figure 1). The compound crystallised as a self-assembled dimeric capsule resulting from hydrogen bonds between the phosphoryl and the hydroxyl groups of two independent molecules. Both cavitands adopt the usual bowl-shaped structure of resorcin[4]arene-derived cavitands with OCH₂O linkers,^[5b, 5d, 13] with top rim diameters (*i.e.*, the segments linking the C-2 aromatic carbon atoms of opposite resorcinolic rings) of 7.97 and 8.02 Å. Each cavitand moiety hosts a molecule of methanol (Figure 1).



Scheme 1. Stepwise synthesis of the cavitand-phosphines **6**, **7**, and **8**

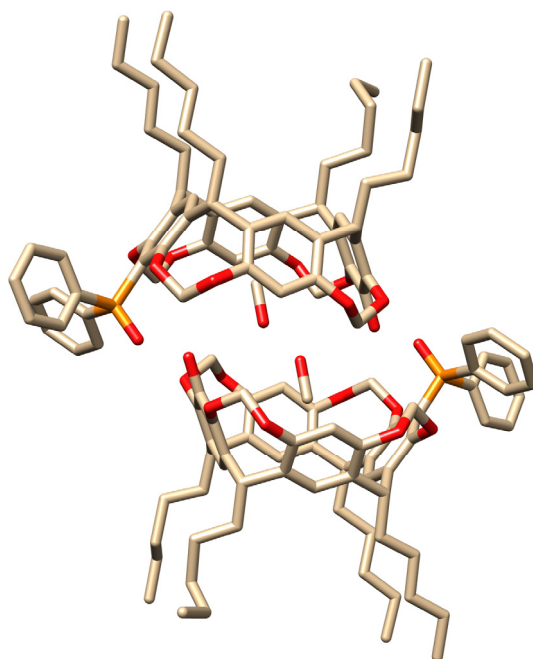


Figure 1. Supramolecular capsule generated during the crystallisation of phosphine oxide **3**. A molecule of methanol is embedded in each resorcinarene moiety of the dimer. Important distance (Å): OH...O=P 2.58

Alkylation of **3** with 1,3- or 1,4-di(bromomethyl)-benzene (0.5 equiv.) gave **4** (84 % yield) and **5** (80 % yield), respectively. The solid state structure of the diphosphorylated compound **5** was established by a single crystal X-ray diffraction study (Figure 2). Reduction of **4** to diphosphine **6** was achieved quantitatively by refluxing for 48 h a toluene solution of the bis-(phosphine oxide) in the presence of phenylsilane. Applying similar reductive conditions to **5** did not lead to the expected diphosphine **8** (as checked by ^{31}P NMR), but instead gave the mixed phosphine-phosphine oxide **7** (39 % yield after purification by column chromatography) (see experimental section). Nevertheless, **8** formed quantitatively when the reduction of **5** was performed with $\text{BH}_3\cdot\text{THF}$ in refluxing NEt_3 (24 h).

The NMR spectra (^1H , ^{13}C , ^{31}P) of **6** and **8** are consistent with C_s symmetrical structures. In the corresponding ^{31}P NMR spectra, the phosphino groups appear as singlets, at -16.0 (**6**) and -16.1 (**8**) ppm, respectively.

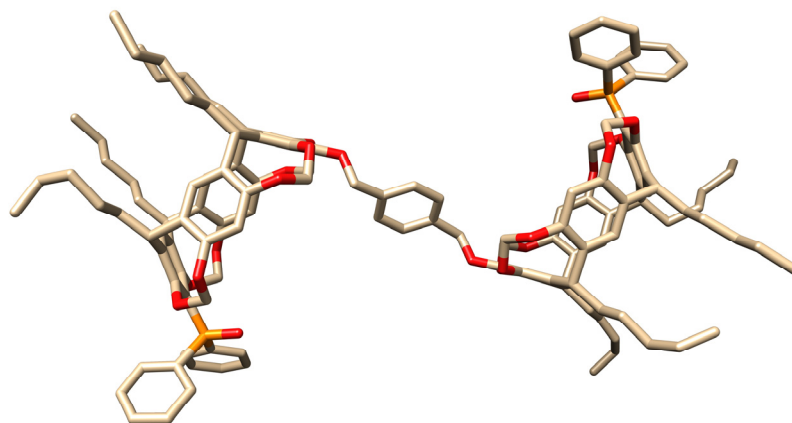
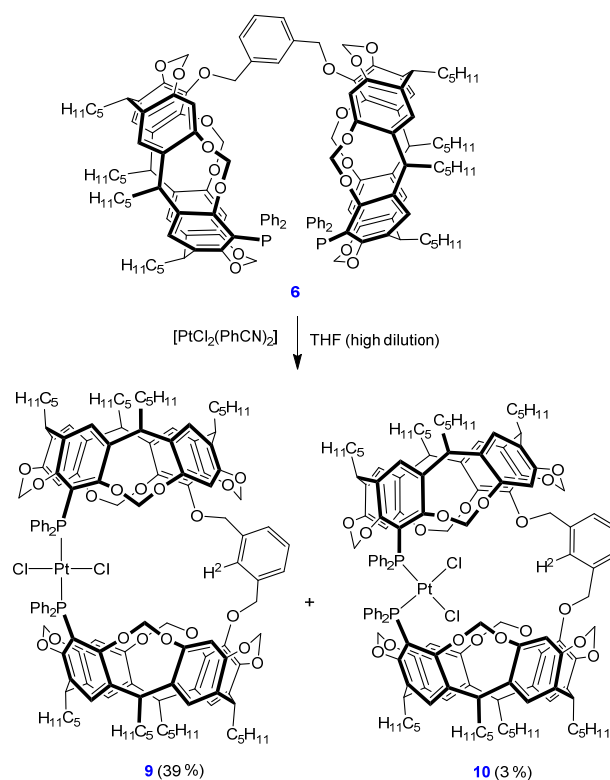


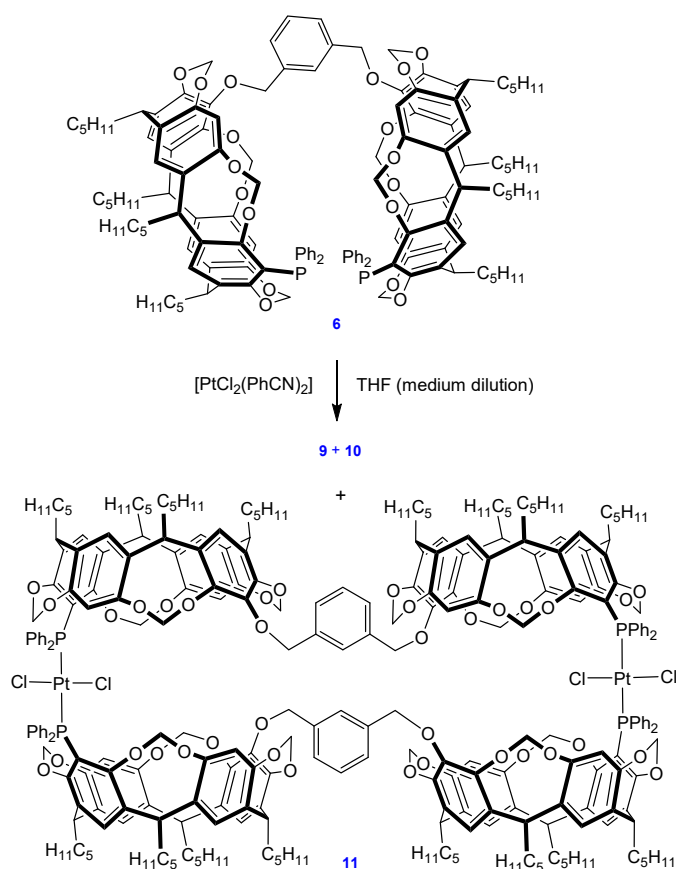
Figure 2. Molecular structure of the diphosphorylated double cavitand **5**. The solvent molecules (CH_2Cl_2 , MeOH) have been omitted for clarity. P...P separation: 19.8 Å

In order to assess the ability of **6** to behave as a chelating ligand, its reaction with $[\text{PtCl}_2(\text{PhCN})_2]$ was investigated under high dilution conditions ($5 \cdot 10^{-5}$ M) (Scheme 2). The ^{31}P NMR spectrum of the crude reaction mixture revealed the formation of two platinum complexes, **9** and **10** (present in a 9:1 ratio), which were separated by column chromatography indicative of the formation of PtCl_2P_2 units with the metal atom coordinated



Scheme 2. Reaction of **6** with $[\text{PtCl}_2(\text{PhCN})_2]$ under high dilution conditions

to *trans*- and *cis*-disposed P atoms, respectively (*trans*-**9**: $J(\text{PPt}) = 2702$ Hz; *cis*-**10**: $J(\text{PPt}) = 3171$ Hz).^[14] The formation of a chelate complex could be demonstrated formally only for complex **9**, this being inferred from its ESI-TOF mass spectrum, which displays a strong peak at m/z 2422.94 corresponding to the $[\text{M} + \text{Na}]$ cation (see experimental section). Interestingly, the NMR signal of the aromatic H-2 atom of the central phenylene link of **9** ($\delta_{\text{H-2}} = 8.10$ ppm) is strongly upfield-shifted with respect to its analogue in free **6** ($\delta_{\text{H-2}} = 7.55$ ppm). This arises from its proximity to the two *o*-positioned OCH_2 oxygen atoms which are both brought nearby the H-2 atom upon complex formation. As the same feature was observed for **10** ($\delta_{\text{H-2}} = 8.05$ ppm), we tentatively assign a chelated structure also for this complex. We further observed that by repeating the reaction under lower dilution conditions ($1.4 \cdot 10^{-3}$ M), beside **9**, the bimetallic complex $[(\text{trans-PtCl}_2)_2(\mu\text{-}P,P\text{-}\mathbf{6})_2]$ (**11**) also formed (Scheme 3). Complex **11** was characterised by ^1H -, ^{13}C -, and ^{31}P -NMR, MS and elemental analysis (see experimental part). Consistent with a rather unstrained metallo-macrocylic structure, the signal of the two H-2 atoms of **11** ($\delta_{\text{H-2}} = 7.52$ ppm) appears close to that of free **6**.



Scheme 3. Reaction of **6** with $[\text{PtCl}_2(\text{PhCN})_2]$ under medium dilution conditions

The proof for the capsular nature of complex **9** came from a single crystal X-ray diffraction study (Figure 3). The metallo-capsule crystallised with a molecule of chloroform nested inside the cavity (Note that in the solid the inner CHCl_3 molecule is disordered over three positions). The general shape of **9** is that of an open seashell, thus resulting in a container having two portals with different sizes (opening heights ca. 3 Å and 6 Å, respectively). The platinum atom is in a planar square coordination environment with Pt-P (2.3435(10) and 2.3199(10) Å) and Pt-Cl (2.3144(9) and 2.2997(9) Å) bond lengths typical for *trans*-[PtCl₂(phosphine)₂] complexes based on triarylphosphines.^[15] One of the chlorido ligands is located inside the capsule interior, while the other is pushed towards its exterior. Interestingly, both phosphorus atoms lie somewhat above the plane defined by the aromatic ring to which they are grafted (distances to the planes: 0.54 Å and 0.29 Å, respectively), this reflecting important strain within the macrocyclic structure.

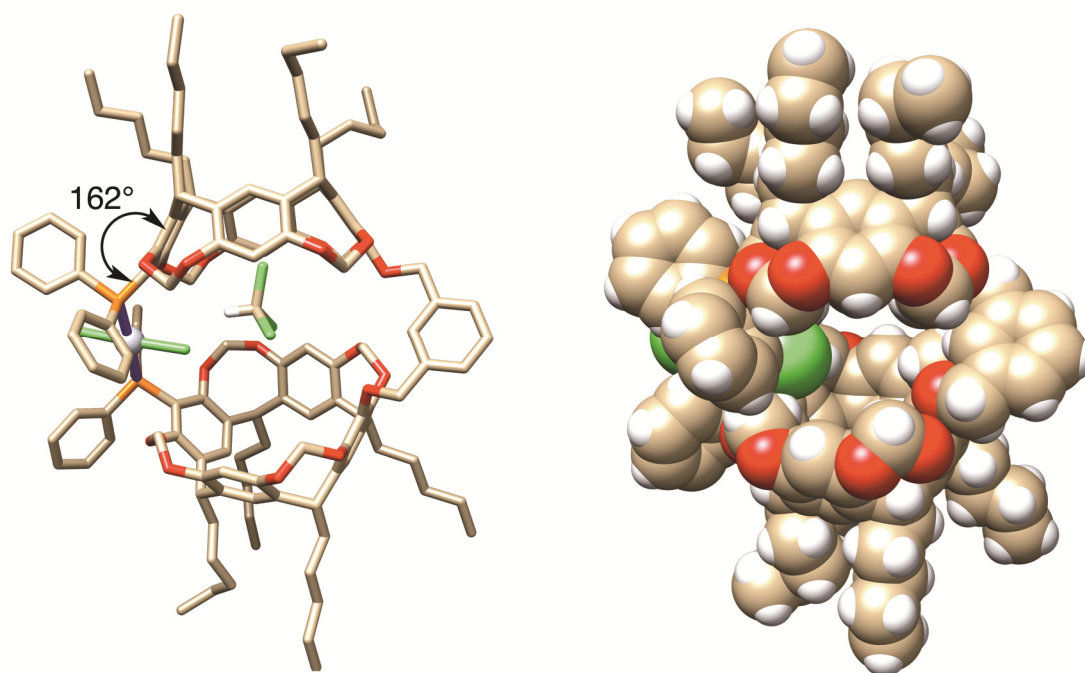
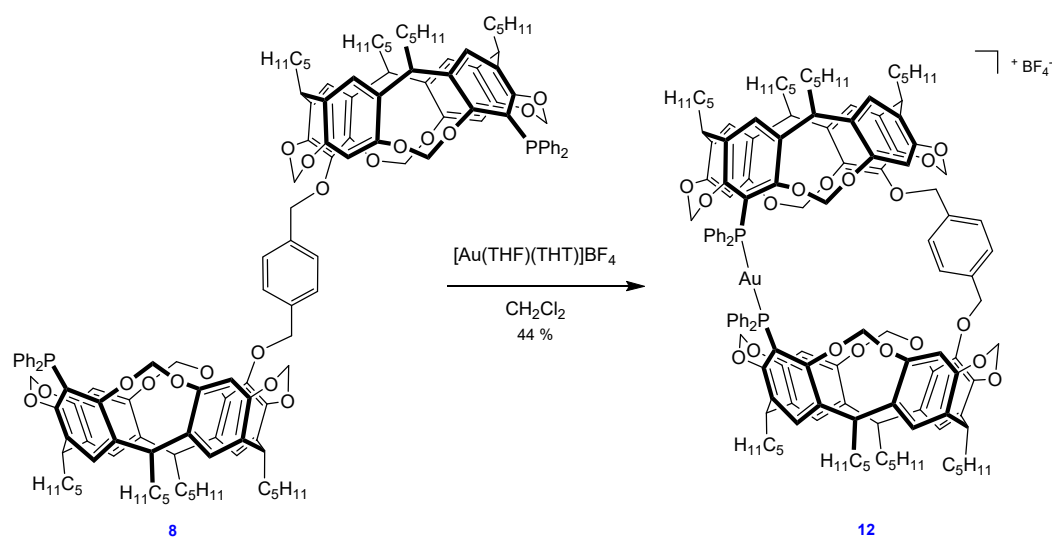
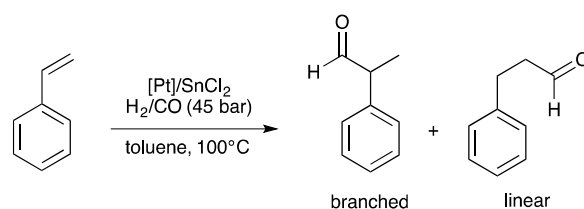


Figure 3. Left: molecular structure of *trans*-[PtCl₂(**6**)] (**9**) with a molecule of CHCl_3 embedded in the capsule. The right view shows a CPK model in which the inner cavity solvent is not represented. The solvent molecules located outside the cavity are not shown. Both views show the wider mouth of the shell

The ability of diphosphine **8** to behave, like **6**, as a chelator was demonstrated by its reaction with $[\text{Au}(\text{THF})(\text{THT})]\text{BF}_4$, which is an ideal precursor for forming linear P-M-P arrangements (Scheme 4). The ^{31}P NMR spectrum of the crude reaction mixture revealed the presence of a compound characterised by singlet at $\delta = 30.1$ ppm, together with trace amounts of di(phosphine oxide) **5**. After purification on column chromatography, the complex $[\text{Au}(\mathbf{8})]\text{BF}_4$ (**12**) was obtained in 44 % yield. Chelate formation was inferred from the corresponding mass spectrum, which showed a unique peak at m/z 2332.01, with the isotopic profile as expected for the corresponding $[\text{M} - \text{BF}_4]$ cation. The ^1H NMR spectrum of **12** displayed slightly broad signals (although being well resolved), these reflecting rapid conformational changes within the $-\text{CH}_2\text{C}_6\text{H}_4\text{CH}_2-$ linking unit. Cooling the solution down to -80°C did, however, not allow to freeze out these dynamics (see experimental section).



Scheme 4. Formation of $[\text{Au}(\mathbf{8})]\text{BF}_4$ (**12**)



Scheme 5. Platinum-catalysed hydroformylation of styrene

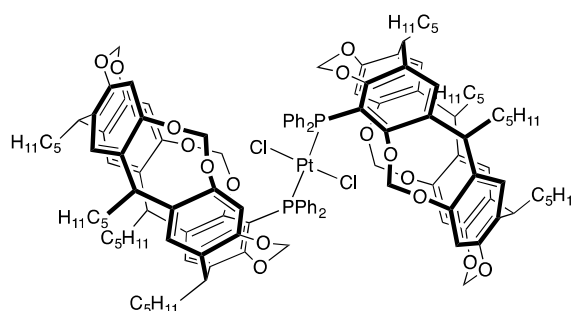
The catalytic chemistry of platinum complexes with large, chelating diphosphines has been well documented. Thus, for example, Kollár *et al.* have shown that platinum *Xantphos* complexes (*Xantphos* is a ligand with a natural bite angle quite larger than 90°) efficiently catalyse the hydroformylation of styrene (Scheme 5), thereby leading to high proportions of linear aldehyde (87 %).^[18]

Styrene hydroformylation tests with **9** were carried out in the presence of SnCl₂ as activator (2 equiv. per Pt) and by applying standard "oxo-conditions" (P(CO/H₂) = 45 bar; T = 100°C; reaction time 24 h). Under these conditions, metallo-capsule **9** produced aldehydes with a conversion of 55 % and a regioselectivity towards the branched product of 64 % (Table 1, entry 1). For comparison, when performing this run with the less sterically constrained bis-(phosphino-monocavitand) complex **13** (Figure 4), a conversion of only 15 % and a branched/linear ratio of 54:46 were found (Table 1, entry 2). Even lower branched aldehyde selectivity was observed with *trans*-[PtCl₂(PPh₃)₂] (Table 1, entry 3). Note that only trace amounts of hydrogenated by-products were observed with the above resorcinarene-phosphine complexes. Clearly, these findings unambiguously show that encapsulation of the catalytic centre inside **6** had a beneficial role on both activity and regioselectivity. Consistent with the generally accepted Pt-catalysed olefin hydroformylation mechanism, a trigonal bipyramidal [PtH(SnCl₃)P₂(olefin)] complex forms at the beginning of the catalytic cycle, which then undergoes insertion of the olefin into Pt–H bond.^[16] Due to the highly strained metallo-macrocyclic structure of **9**, it is likely that the [PtH(SnCl₃)P₂(styrene)] intermediate formed in the catalytic cycle adopts a distorted trigonal bipyramidal structure, so as to bring the hydrido ligand close to the adjacent olefin, thereby facilitating the corresponding insertion step. Furthermore, molecular models show that the shape of the branched acyl unit in formation is better suited to the size of the cavity than the linear one (the branched acyl fragment being able to escape sideways). This may explain the observed branched selectivity.

Table 1. Platinum-catalysed hydroformylation of styrene.

Entry	Platinum complex	Conversion (%)	Aldehydes distribution	
			Linear (%)	Branched (%)
1	9	55	36	64
2	13	15	46	54
3	<i>trans</i> -[PtCl ₂ (PPh ₃) ₂]	40	53	47

General conditions: [Pt] (1 mol %), SnCl₂ (2 mol %), styrene (1 mmol), P(CO/H₂) = 45 bar, T = 100°C, toluene (5 mL), 24 h. The conversions were determined by ¹H NMR.

**Figure 4.** Platinum complex **13** used for ranking the capsular complex **9**

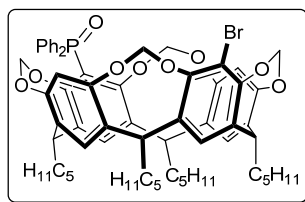
Conclusion

We have described the stepwise synthesis of two long diphosphines the core of which comprises two resorcin[4]arene moieties linked respectively through a $-\text{OCH}_2-(o\text{-C}_6\text{H}_4)-\text{CH}_2\text{O}-$ and a $-\text{OCH}_2-(p\text{-C}_6\text{H}_4)-\text{CH}_2\text{O}-$ spacer moiety. The two diphosphines have their phosphorus atoms separated respectively by 34 and 35 bonds. Under high dilution conditions, diphosphine **6** forms readily with transition metal centres having two free binding sites, *trans* and/or *cis* chelate complexes with concomitant formation of a capsular compound in which the metal is fully or partially embedded in the cavity. X-ray analysis of *trans*-[PtCl₂**6**] revealed that the corresponding capsule possesses a rather large portal, seemingly sufficient for enabling the entry of small substrates. Activation of *trans*-[PtCl₂**6**] with SnCl₂ resulted in a good styrene hydroformylation catalyst, with an activity and a selectivity towards the

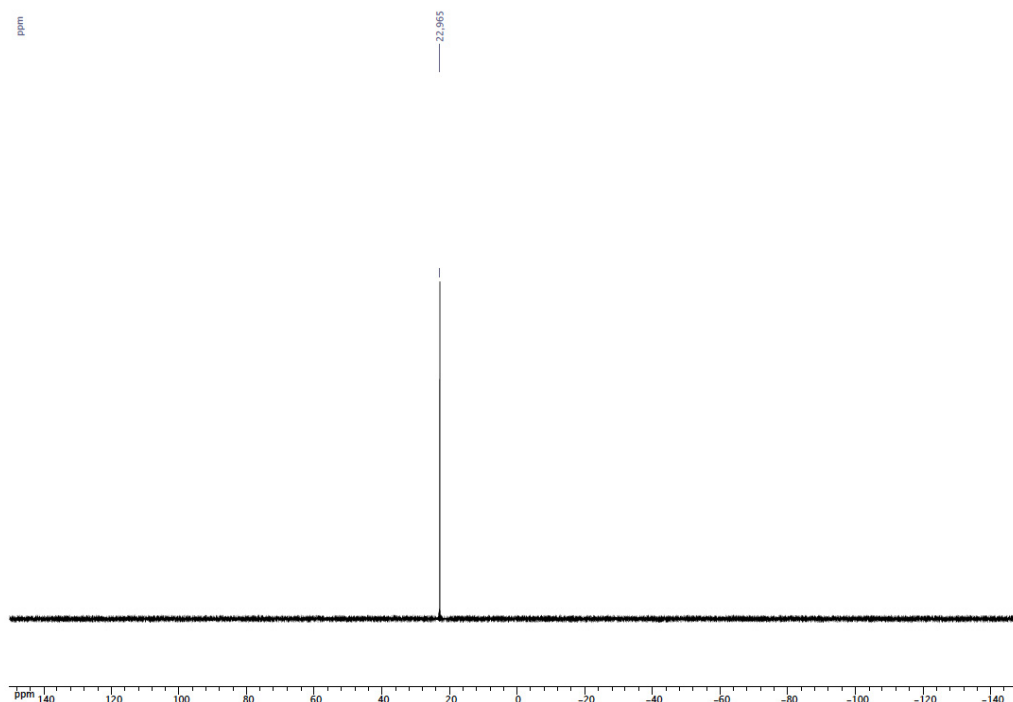
branched aldehyde significantly superior to those of *trans*-[PtCl₂(PPh₃)₂] as well as those of an analogue devoid of any capsular unit. The origin of this performance is likely to reflect strong steric interactions within penta-coordinated intermediates involving the capsule wall and the coordinated substrate. Further studies are aimed at exploiting the potential of resorcinarene-based metallo-capsules in carbon-carbon bond forming reactions.

Experimental Section

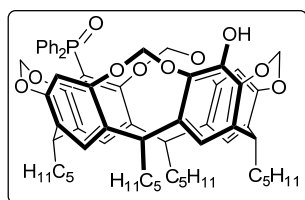
General Procedure: All manipulations involving phosphorus derivatives were performed in Schlenk-type flasks under dry argon. Solvents were dried by conventional methods and distilled immediately prior to use. CDCl₃ was passed down a 5 cm thick alumina column and stored under nitrogen over molecular sieves (4 Å). Routine ¹H, ¹³C{¹H} and ³¹P{¹H} spectra were recorded with Bruker FT instruments (AC 300, 400 and 500 spectrometers). ¹H spectra were referenced to residual protiated solvents ($\delta = 7.26$ ppm), ¹³C chemical shifts are reported relative to deuteriated solvents ($\delta = 77.16$ ppm), whereas the ³¹P NMR spectroscopic data are given relative to external H₃PO₄. Chemical shifts and coupling constants are reported in ppm and in Hz, respectively. The catalytic solutions were analysed by using a Varian 3900 GC equipped with a WCOT fused silica column (25 m x 0.25 mm). Elemental analyses were performed by the Service de Microanalyse, Institut de Chimie, Université de Strasbourg. The 5,17-dibromo-4(24),6(10),12(16),18(22)-tetramethylenedioxy-2,8,14,20-tetrapentylresorcin [4]arene (**1**)^[5a] and 5-diphenylphosphanyl-4(24),6(10),12(16),18(22)-tetramethylenedioxy-2,8,14,20-tetrapentylresorcin-[4]arene^[17] were prepared by literature procedures.



5-(Diphenylphosphanoyl)-17-bromo-4(24),6(10),12(16),18(22)-tetramethylenedioxy-2,8,14,20-tetrapentylresorcin[4]arene (2): *n*-Butyllithium (1.6 M in hexane, 1.41 mL, 2.26 mmol) was rapidly added to a solution of 1,3-dibromoresorcinarene **1** (2.000 g, 2.05 mmol) in THF (150 mL) at -78°C . After 0.5 h, the generated carbanion was quenched with chlorodiphenylphosphine (0.41 mL, 2.26 mmol). The resulting mixture was allowed to reach r.t. and then heated at 40°C for 16 h. The solution was cooled down to 0°C and was quenched with H_2O_2 (30 % in water, 5 mL). After 1 h at r.t., a solution of $\text{Na}_2\text{S}_2\text{O}_5$ (10 % in water, 30 mL) was slowly added. The mixture then was extracted into EtOAc (50 mL). The aqueous phase was further extracted with EtOAc (3 x 30 mL), the combined organic phases were washed with NaHCO_3 (10 % in water, 20 mL), water (20 mL), brine (20 mL) and dried over MgSO_4 . The solvent was then evaporated under reduced pressure and the crude product purified by column chromatography ($\text{CH}_2\text{Cl}_2/\text{Et}_2\text{O}$, 9:1 v/v; $R_f = 0.3$: $\text{CH}_2\text{Cl}_2/\text{Et}_2\text{O}$, 9:1 v/v), yield 1.350 g (60 %). ^1H NMR (400 MHz, CDCl_3): $\delta = 7.72$ - 7.68 (m, 4H, arom. CH, PPh_2), 7.48 - 7.40 (m, 6H, arom. CH, PPh_2), 7.37 (s, 1H, arom. CH, resorcinarene), 7.06 (s, 1H, arom. CH, resorcinarene), 7.05 (s, 2H, arom. CH, resorcinarene), 6.45 (s, 2H, arom. CH, resorcinarene), 5.83 and 4.54 (AB spin system, 4H, OCH_2O , $^2J = 7.5$ Hz), 4.77 (t, 2H, CHCH_2 , $^3J = 8.0$ Hz), 4.64 (t, 2H, CHCH_2 , $^3J = 8.0$ Hz), 4.59 and 4.25 (AB spin system, 4H, OCH_2O , $^2J = 7.5$ Hz), 2.33 - 2.25 (m, 2H, CHCH_2CH_2), 2.22 - 2.12 (m, 6H, CHCH_2CH_2), 1.43 - 1.30 (m, 24H $\text{CH}_2\text{CH}_2\text{CH}_2\text{CH}_3$), 0.91 (t, 6H, CH_2CH_3 , $^3J = 7.5$ Hz), 0.90 (t, 6H, CH_2CH_3 , $^3J = 7.0$ Hz); $^{13}\text{C}\{^1\text{H}\}$ NMR (100 MHz, CDCl_3): $\delta = 156.47$ - 113.47 (arom. C's), 99.85 (s, OCH_2O), 99.92 (s, OCH_2O), 37.05 (s, CHCH_2), 36.46 (s, CHCH_2), 32.09 (s, $\text{CH}_2\text{CH}_2\text{CH}_3$), 32.05 (s, $\text{CH}_2\text{CH}_2\text{CH}_3$), 30.03 (s, CHCH_2), 29.99 (s, CHCH_2), 27.60 (s, CHCH_2CH_2), 22.77 (s, CH_2CH_3), 14.21 (s, CH_2CH_3), 14.19 (s, CH_2CH_3); $^{31}\text{P}\{^1\text{H}\}$ NMR (162 MHz, CDCl_3): $\delta = 23.0$ (s, $\text{P}(\text{O})\text{Ph}_2$) ppm; MS (ESI-TOF): $m/z = 1097.42$ [$\text{M} + \text{H}$] expected isotopic profile; elemental analysis calcd (%) for $\text{C}_{64}\text{H}_{72}\text{O}_9\text{P}$ ($M_r = 1033.23$): C 75.64, H 7.14; found (%): C 75.35, H 7.08.

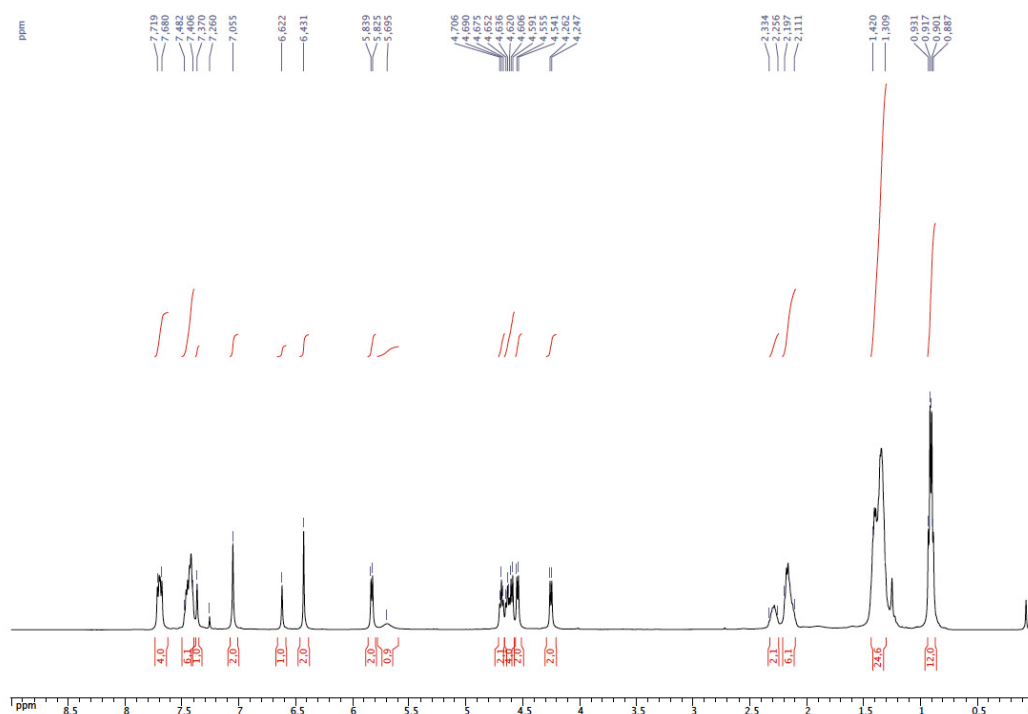


$^{31}\text{P}\{^1\text{H}\}$ NMR spectrum of **2** (CDCl_3)

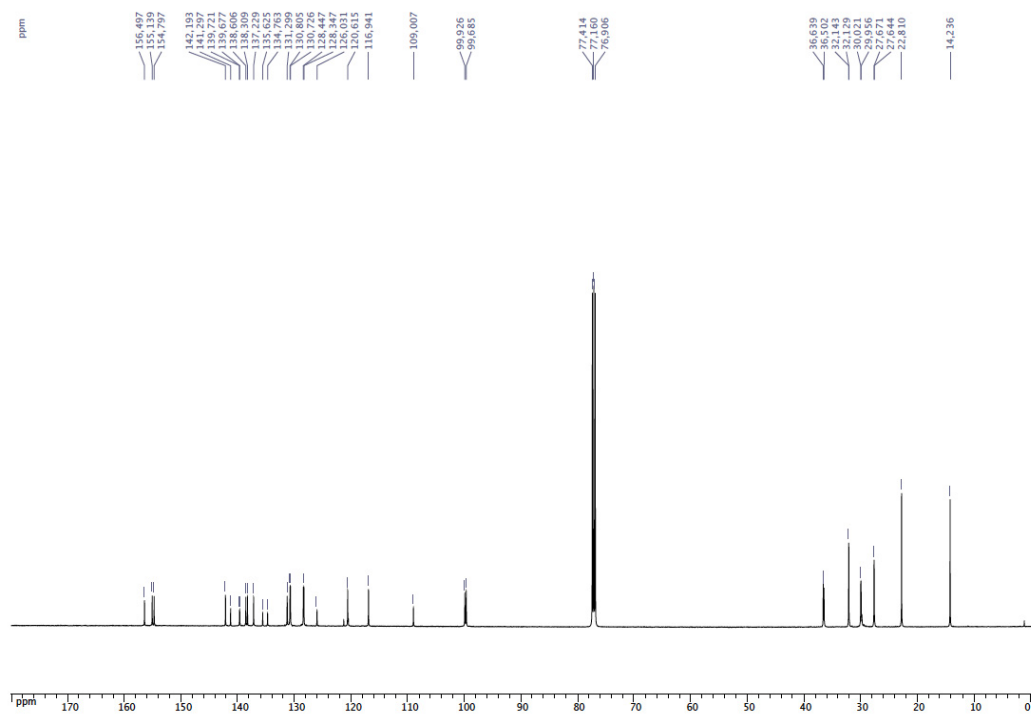
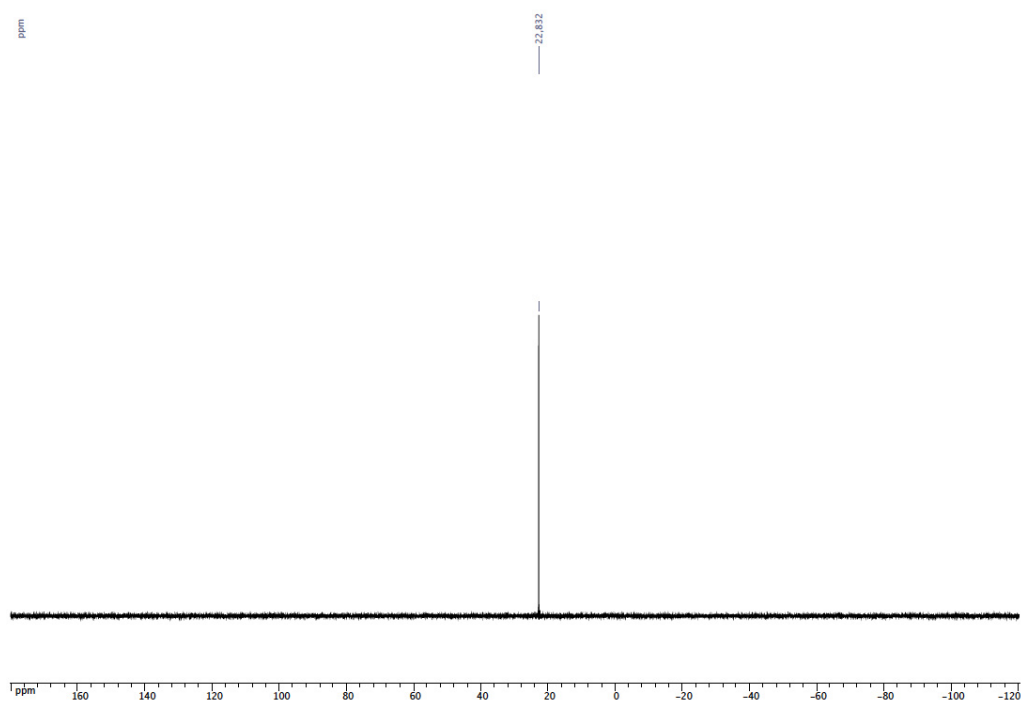


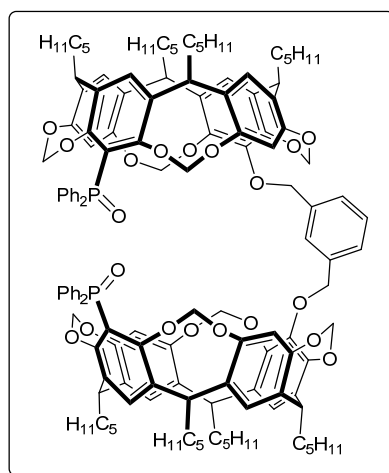
5-(Diphenylphosphanyl)-17-hydroxy-4(24),6(10),12(16),18(22)-tetramethylenedioxy-2,8,14,20-tetrapentylresorcin[4]arene (3): *n*-Butyllithium (1.6 M in hexane, 1 mL, 1.61 mmol) was rapidly added to a solution of **2** (1.600 g, 1.46 mmol) in THF (50 mL) at -78°C . After 0.5 h, the generated carbanion was quenched with trimethyl borate (0.81 mL, 7.30 mmol). The resulting mixture was stirred at r.t. for 18 h. The solution was cooled down to 0°C and was quenched with H_2O_2 (30 % in water, 5 mL) and NaOH (3 M, 5 mL) then stirred at r.t. for 16 h. After cautious addition of $\text{Na}_2\text{S}_2\text{O}_5$ (10 % in water, 30 mL) the mixture was extracted into EtOAc (50 mL). The aqueous phase was further extracted with EtOAc (3 x 30 mL), the combined organic phases were washed with NaHCO_3 (10 % in water, 20 mL), water (20 mL), brine (mL) and dried over MgSO_4 . The solvent was then evaporated under reduced

pressure and the crude product purified by column chromatography (CH₂Cl₂/Et₂O, 5:5 v/v; *R_f* = 0.28: CH₂Cl₂/Et₂O, 5:5 v/v), yield 0.680 g (45 %). ¹H NMR (400 MHz, CDCl₃): δ = 7.72-7.68 (m, 4H, arom. CH, PPh₂), 7.48-7.41 (m, 6H, arom. CH, PPh₂), 7.37 (s, 1H, arom. CH, resorcinarene), 7.05 (s, 2H, arom. CH, resorcinarene), 6.62 (s, 1H, arom. CH, resorcinarene), 6.43 (s, 2H, arom. CH, resorcinarene), 5.83 and 4.55 (AB spin system, 4H, OCH₂O, ²*J* = 7.0 Hz), 4.69 (t, 2H, CHCH₂, ³*J* = 7.7 Hz), 4.64 (t, 2H, CHCH₂, ³*J* = 8.0 Hz), 4.60 and 4.25 (AB spin system, 4H, OCH₂O, ²*J* = 7.5 Hz), 2.33-2.26 (m, 2H, CHCH₂CH₂), 2.20-2.11 (m, 6H, CHCH₂CH₂), 1.42-1.31 (m, 24H CH₂CH₂CH₂CH₃), 0.92 (t, 6H, CH₂CH₃, ³*J* = 7.0 Hz), 0.90 (t, 6H, CH₂CH₃, ³*J* = 7.0 Hz); ¹³C{¹H} NMR (100 MHz, CDCl₃): δ = 156.50-109.01 (arom. C's), 99.93 (s, OCH₂O), 99.68 (s, OCH₂O), 36.64 (s, CHCH₂), 36.50 (s, CHCH₂), 32.14 (s, CH₂CH₂CH₃), 32.13 (s, CH₂CH₂CH₃), 30.02 (s, CHCH₂), 29.96 (s, CHCH₂), 27.67 (s, CHCH₂CH₂), 27.64 (s, CHCH₂CH₂), 22.81 (s, CH₂CH₃), 14.24 (s, CH₂CH₃); ³¹P{¹H} NMR (162 MHz, CDCl₃): δ = 22.8 (s, P(O)Ph₂) ppm; MS (ESI-TOF): *m/z* = 1055.48 [M + Na] expected isotopic profile; elemental analysis calcd (%) for C₆₄H₇₃O₁₀P (*M_r* = 1033.23): C 74.40, H 7.12; found (%): C 74.45, H 7.19.

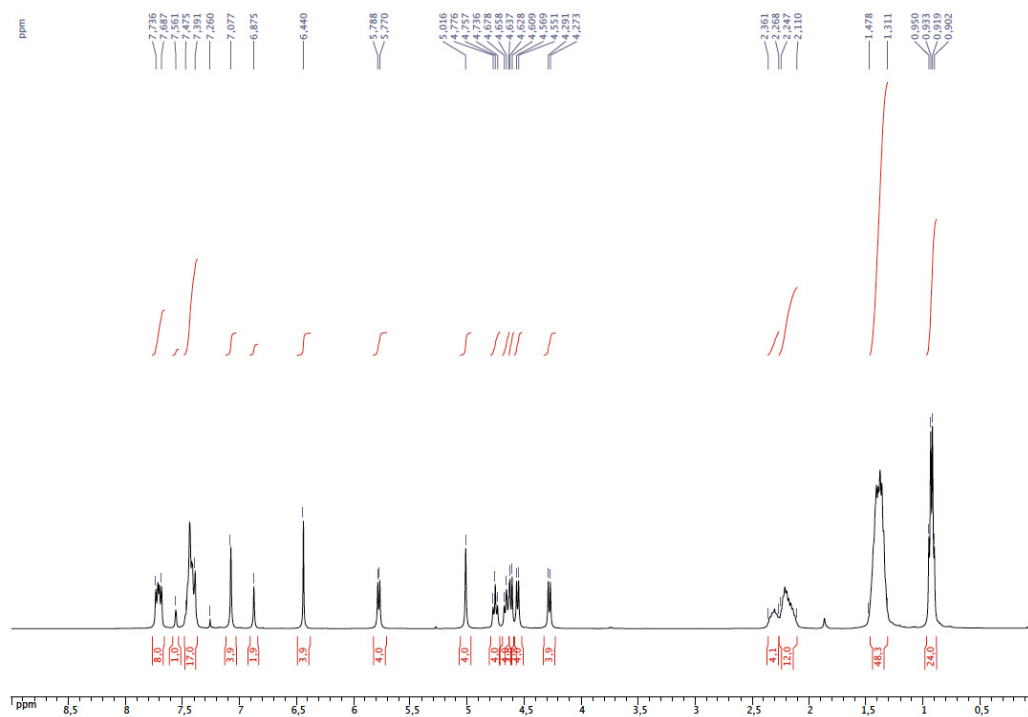


¹H NMR spectrum of **3** (CDCl₃)

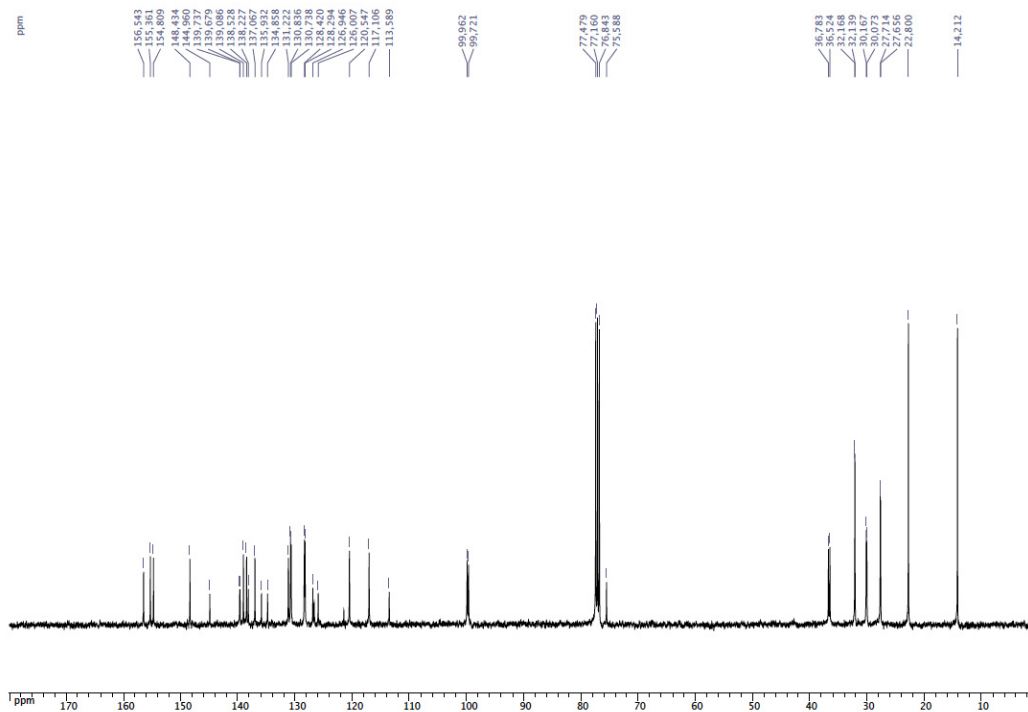
 $^{13}\text{C}\{^1\text{H}\}$ NMR spectrum of **3** (CDCl_3) $^{31}\text{P}\{^1\text{H}\}$ NMR spectrum of **3** (CDCl_3)



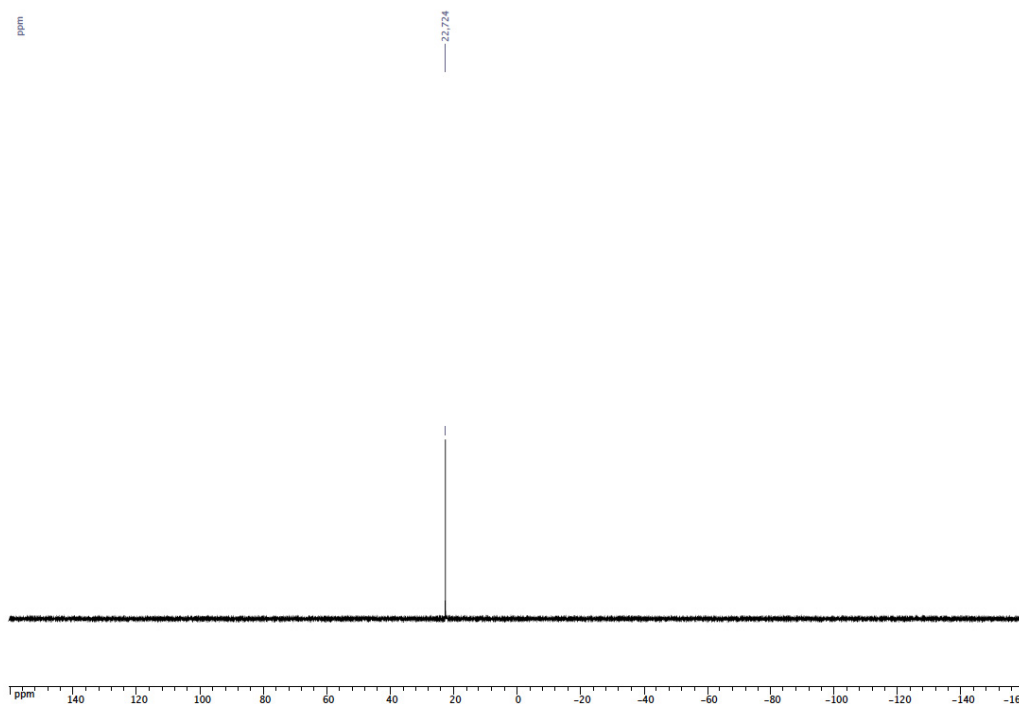
1,3-Bis-[5-(diphenylphosphano)-4(24),6(10),12(16),18(22)-tetramethylenedioxy-2,8,14,20-tetrapentylresorcin[4]aren-17-oxymethyl]benzene (4): NaH (60 % oil dispersion, 0.079 g, 1.98 mmol) was added to a solution of **3** (1.950 g, 1.89 mmol) in DMF (60 ml). After 0.5 h, 1,3-bis(bromomethyl)benzene (0.250 g, 0.94 mmol) was added and the reaction mixture stirred for 18 h at r.t. The reaction mixture was poured into HCl (3 M, 65 mL), extracted with CH₂Cl₂ (3 x 30 mL) and the organic layer was dried over MgSO₄. The solvent was then evaporated under reduced pressure and the crude product purified by column chromatography (CH₂Cl₂/Et₂O, 7:3 v/v; *R_f* = 0.3: CH₂Cl₂/Et₂O, 7:3 v/v), yield 1.712 g (84 %). ¹H NMR (400 MHz, CDCl₃): δ = 7.74-7.69 (m, 8H, arom. CH, PPh₂), 7.56 (s, 1H, arom. CH, CH₂C₆H₄CH₂), 7.47-7.39 (m, 15H, arom. CH, PPh₂ and CH₂C₆H₄CH₂), 7.39 (s, 2H, arom. CH, resorcinarene), 7.08 (s, 4H, arom. CH, resorcinarene), 6.87 (s, 2H, arom. CH, resorcinarene), 6.44 (s, 4H, arom. CH, resorcinarene), 5.78 and 4.62 (AB spin system, 8H, OCH₂O, ²*J* = 7.2 Hz), 5.02 (s, 4H, CH₂C₆H₄CH₂), 4.76 (t, 4H, CHCH₂, ³*J* = 8.0 Hz), 4.66 (t, 4H, CHCH₂, ³*J* = 8.2 Hz), 4.62 and 4.28 (AB spin system, 8H, OCH₂O, ²*J* = 7.2 Hz), 2.36-2.27 (m, 4H, CHCH₂CH₂), 2.25-2.11 (m, 12H, CHCH₂CH₂), 1.48-1.31 (m, 48H CH₂CH₂CH₂CH₃), 0.93 (t, 12H, CH₂CH₃, ³*J* = 6.8 Hz), 0.92 (t, 12H, CH₂CH₃, ³*J* = 6.8 Hz); ¹³C{¹H} NMR (100 MHz, CDCl₃): δ = 156.54-113.59 (arom. C's), 99.96 (s, OCH₂O), 99.72 (s, OCH₂O), 75.59 (s, CH₂C₆H₄CH₂), 36.78 (s, CHCH₂), 36.52 (s, CHCH₂), 32.17 (s, CH₂CH₂CH₃), 32.14 (s, CH₂CH₂CH₃), 30.17 (s, CHCH₂), 30.07 (s, CHCH₂), 27.71 (s, CHCH₂CH₂), 27.66 (s, CHCH₂CH₂), 22.80 (s, CH₂CH₃), 14.21 (s, CH₂CH₃); ³¹P{¹H} NMR (162 MHz, CDCl₃): δ = 22.7 (s, P(O)Ph₂) ppm; MS (ESI-TOF): *m/z* = 2191.03 [M + Na] expected isotopic profile; elemental analysis calcd (%) for C₁₃₆H₁₅₂O₂₀P₂ (*M_r* = 2168.59): C 75.32, H 7.06; found (%): C 75.44, H 7.12.



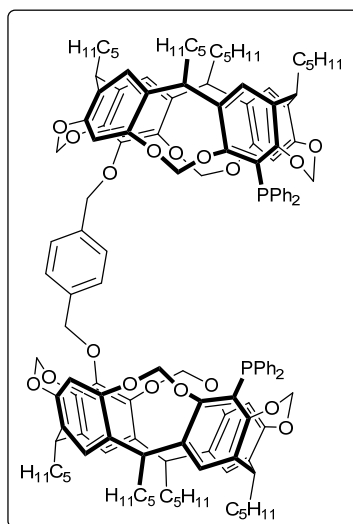
^1H NMR spectrum of **4** (CDCl_3)



$^{13}\text{C}\{^1\text{H}\}$ NMR spectrum of **4** (CDCl_3)

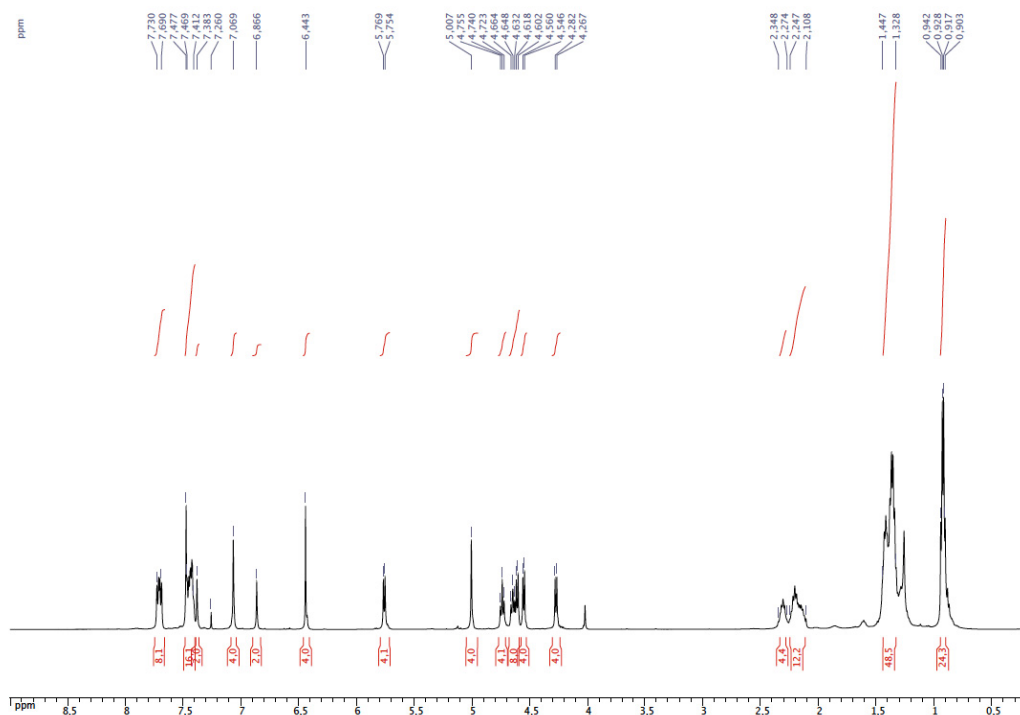


$^{31}\text{P}\{^1\text{H}\}$ NMR spectrum of **4** (CDCl_3)

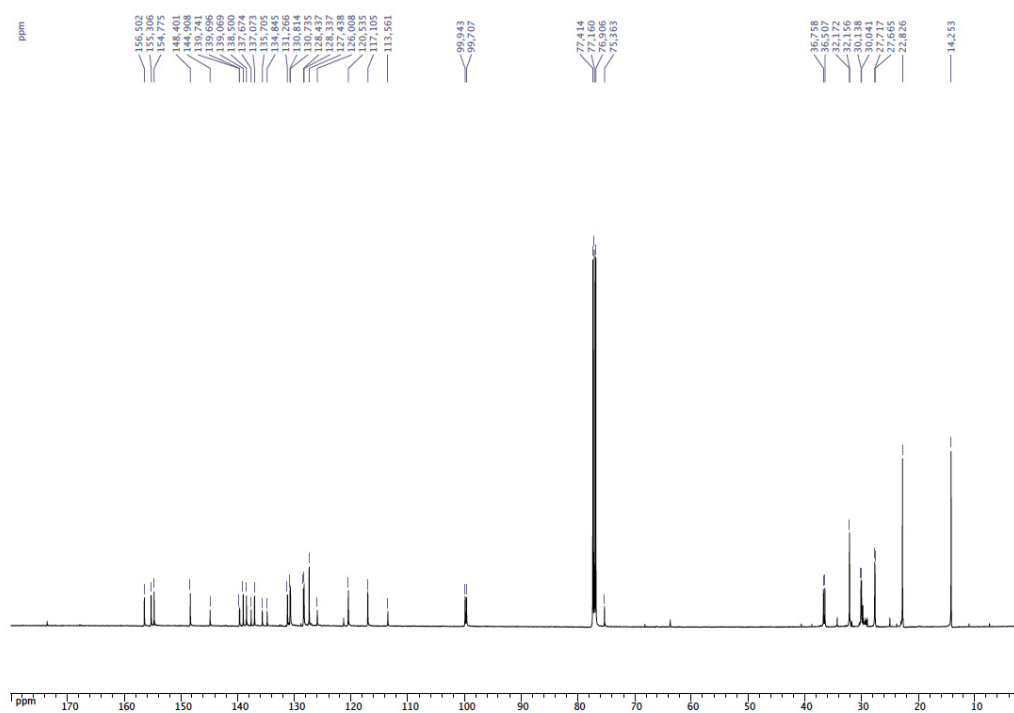


1,4-Bis-[5-(diphenylphosphanoyl)-4(24),6(10),12(16),18(22)-tetramethylenedioxy-2,8,14,20-tetrapentylresorcin[4]aren-17-oxymethyl]benzene (5): NaH (60 % oil dispersion, 0.021 g, 0.53 mmol) was added to a solution of **3** (0.520 g, 0.50 mmol) in DMF (30 ml). After 0.5 h, 1,4-bis(bromomethyl)benzene (0.063 g, 0.24 mmol) was added and the reaction mixture stirred for 18 h at r.t. The reaction mixture was poured into HCl (3 M, 10 mL), extracted with CH_2Cl_2 (50 mL) and the organic layer was dried over MgSO_4 . The solvent was then

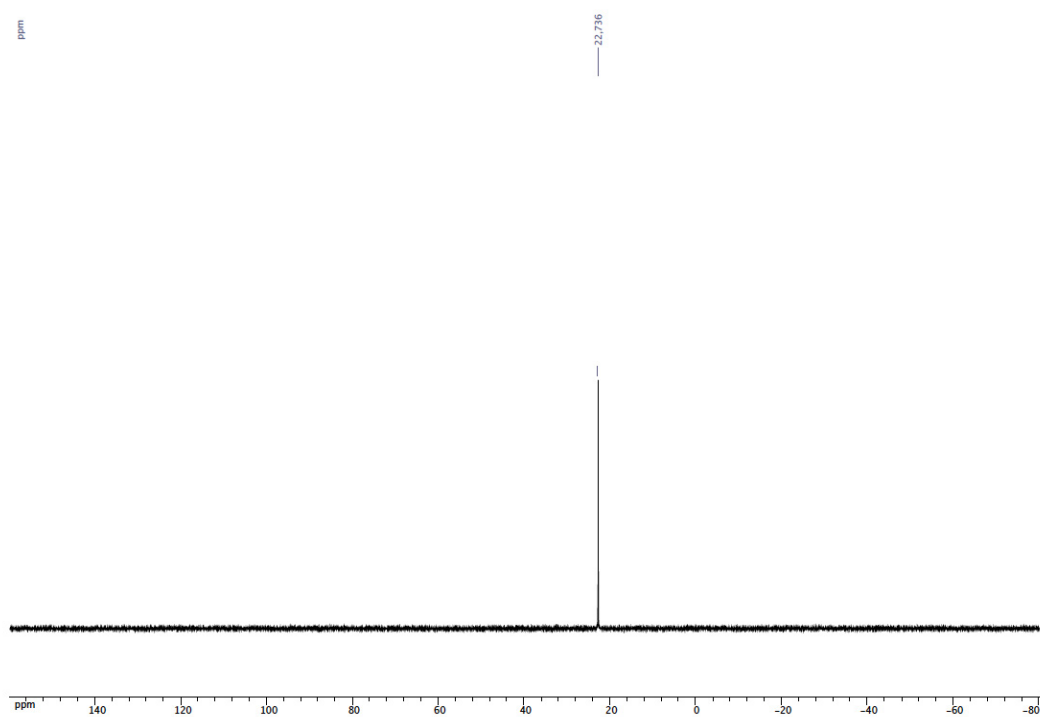
evaporated under reduced pressure and the crude product purified by column chromatography (CH₂Cl₂/Et₂O, 7:3 v/v; *R_f* = 0.28: CH₂Cl₂/Et₂O, 7:3 v/v), yield 0.410 g (80 %). ¹H NMR (400 MHz, CDCl₃): δ = 7.73-7.69 (m, 8H, arom. CH, PPh₂), 7.48 (s, 4H, arom. CH, CH₂C₆H₄CH₂), 7.47-7.41 (m, 12H, arom. CH, PPh₂), 7.38 (s, 2H, arom. CH, resorcinarene), 7.07 (s, 4H, arom. CH, resorcinarene), 6.87 (s, 2H, arom. CH, resorcinarene), 6.44 (s, 4H, arom. CH, resorcinarene), 5.76 and 4.55 (AB spin system, 8H, OCH₂O, ²*J* = 7.5 Hz), 5.01 (s, 4H, CH₂C₆H₄CH₂), 4.70 (t, 4H, CHCH₂, ³*J* = 8.0 Hz), 4.65 (t, 4H, CHCH₂, ³*J* = 8.0 Hz), 4.61 and 4.27 (AB spin system, 8H, OCH₂O, ²*J* = 7.5 Hz), 2.35-2.27 (m, 4H, CHCH₂CH₂), 2.25-2.11 (m, 12H, CHCH₂CH₂), 1.45-1.33 (m, 48H CH₂CH₂CH₂CH₃), 0.93 (t, 12H, CH₂CH₃, ³*J* = 7.0 Hz), 0.92 (t, 12H, CH₂CH₃, ³*J* = 7.0 Hz); ¹³C{¹H} NMR (100 MHz, CDCl₃): δ = 156.50-113.56 (arom. C's), 99.94 (s, OCH₂O), 99.71 (s, OCH₂O), 75.36 (s, CH₂C₆H₄CH₂), 36.76 (s, CHCH₂), 36.51 (s, CHCH₂), 32.17 (s, CH₂CH₂CH₃), 32.16 (s, CH₂CH₂CH₃), 30.14 (s, CHCH₂), 30.04 (s, CHCH₂), 27.72 (s, CHCH₂CH₂), 27.66 (s, CHCH₂CH₂), 22.83 (s, CH₂CH₃), 14.25 (s, CH₂CH₃); ³¹P{¹H} NMR (162 MHz, CDCl₃): δ = 22.7 (s, P(O)Ph₂) ppm; MS (ESI-TOF): *m/z* = 2169.04 [M + H], 2191.02 [M + Na] expected isotopic profile; elemental analysis calcd (%) for C₁₃₆H₁₅₂O₂₀P₂ (*M_r* = 2168.59): C 75.32, H 7.06; found (%): C 75.47, H 7.15.



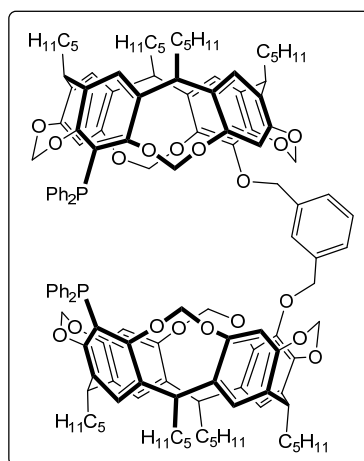
¹H NMR spectrum of **5** (CDCl₃)



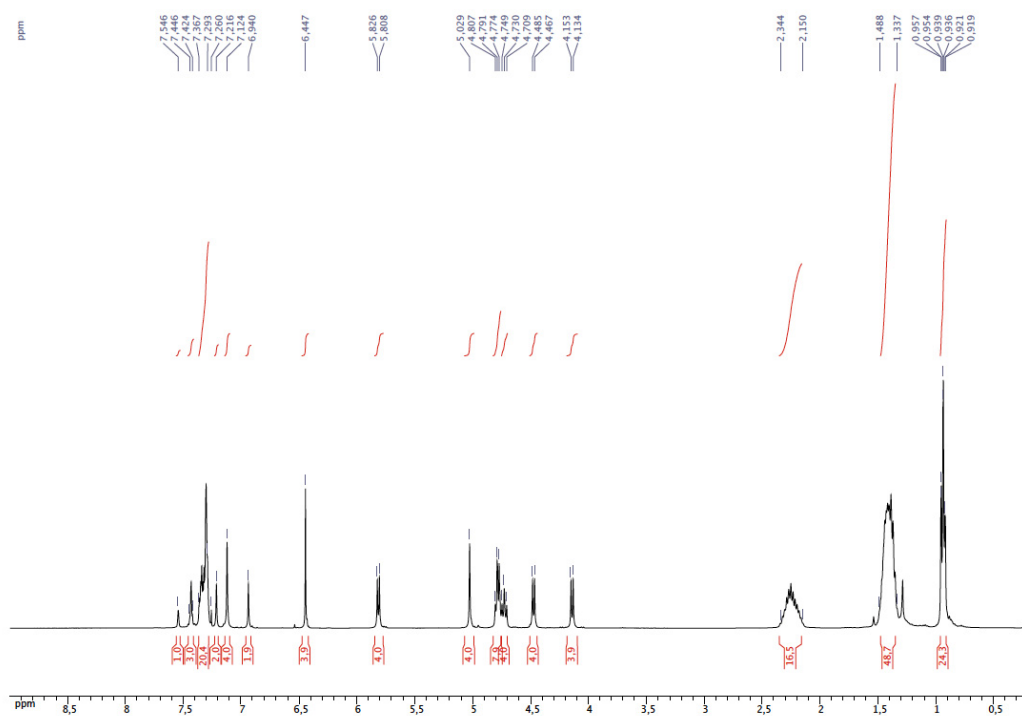
$^{13}\text{C}\{^1\text{H}\}$ NMR spectrum of **5** (CDCl_3)



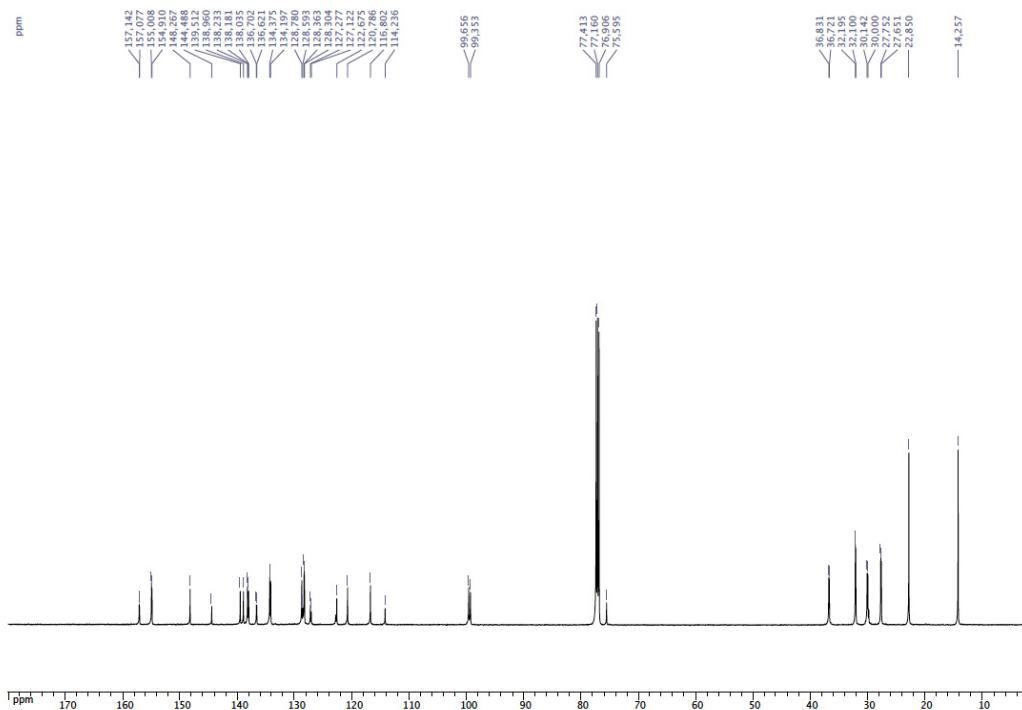
$^{31}\text{P}\{^1\text{H}\}$ NMR spectrum of **5** (CDCl_3)



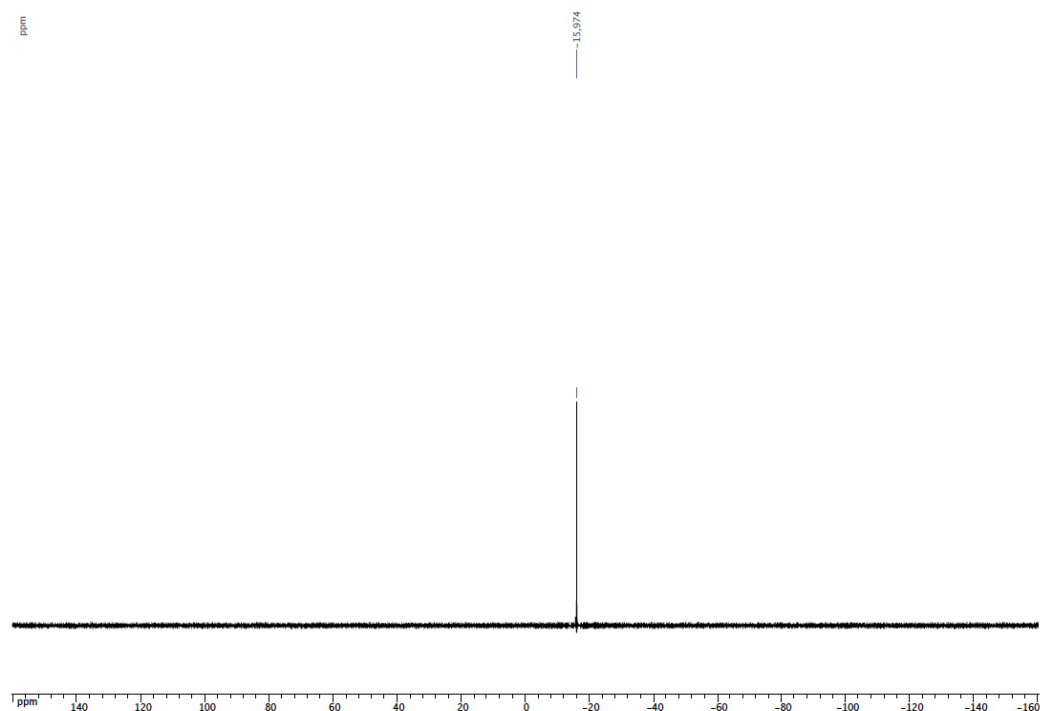
1,3-Bis-[5-(diphenylphosphanyl)-4(24),6(10),12(16),18(22)-tetramethylenedioxy-2,8,14,20-tetrapentylresorcin[4]aren-17-oxymethyl]benzene (6): Phenylsilane (0.23 mL, 1.86 mmol) was added to a solution of **4** (0.200 g, 0.093 mmol) in toluene (20 mL) at r.t. The resulting mixture was heated at 120°C for 48 h. The solvent was then evaporated under reduced pressure and the crude product was dissolved in CH₂Cl₂ (3 mL) and precipitated with methanol (50 mL). The white precipitate obtained was filtered and washed with cold methanol (3 x 10 mL) to afford **6** as a white solid, yield 0.188 g (95 %). ¹H NMR (400 MHz, CDCl₃): δ = 7.55 (s, 1H, arom. CH, CH₂C₆H₄CH₂), 7.45-7.42 (m, 3H, arom. CH, CH₂C₆H₄CH₂), 7.37-7.29 (m, 20H, arom. CH, PPh₂), 7.22 (s, 2H, arom. CH, resorcinarene), 7.10 (s, 4H, arom. CH, resorcinarene), 6.94 (s, 2H, arom. CH, resorcinarene), 6.45 (s, 4H, arom. CH, resorcinarene), 5.82 and 4.48 (AB spin system, 8H, OCH₂O, ²J = 7.2 Hz), 5.03 (s, 4H, CH₂C₆H₄CH₂), 4.79 (t, 4H, CHCH₂, ³J = 8.0 Hz), 4.78 and 4.14 (AB spin system, 8H, OCH₂O, ²J = 7.6 Hz), 4.73 (t, 4H, CHCH₂, ³J = 8.0 Hz), 2.34-2.15 (m, 16H, CHCH₂CH₂), 1.49-1.34 (m, 48H CH₂CH₂CH₂CH₃), 0.94 (t, 12H, CH₂CH₃, ³J = 7.2 Hz), 0.93 (t, 12H, CH₂CH₃, ³J = 7.1 Hz); ¹³C{¹H} NMR (100 MHz, CDCl₃): δ = 157.14-114.24 (arom. C's), 99.66 (s, OCH₂O), 99.35 (s, OCH₂O), 75.59 (s, CH₂C₆H₄CH₂), 36.83 (s, CHCH₂), 36.72 (s, CHCH₂), 32.19 (s, CH₂CH₂CH₃), 32.10 (s, CH₂CH₂CH₃), 30.14 (s, CHCH₂), 30.00 (s, CHCH₂), 27.75 (s, CHCH₂CH₂), 27.65 (s, CHCH₂CH₂), 22.85 (s, CH₂CH₃), 14.26 (s, CH₂CH₃); ³¹P{¹H} NMR (162 MHz, CDCl₃): δ = -16.0 (s, PPh₂) ppm; MS (ESI-TOF): m/z = 2137.06 [M + H] expected isotopic profile; elemental analysis calcd (%) for C₁₃₆H₁₅₂O₁₈P₂ (M_r = 2136.60): C 76.45, H 7.17; found (%): C 76.49, H 7.24.



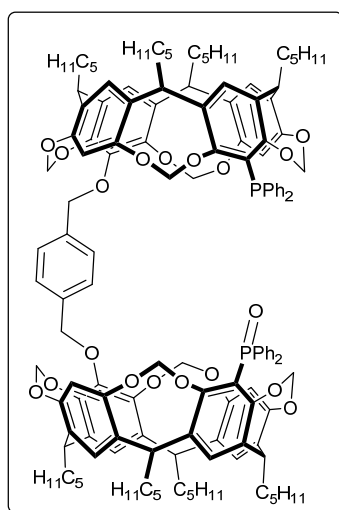
¹H NMR spectrum of **6** (CDCl₃)



¹³C{¹H} NMR spectrum of **6** (CDCl₃)

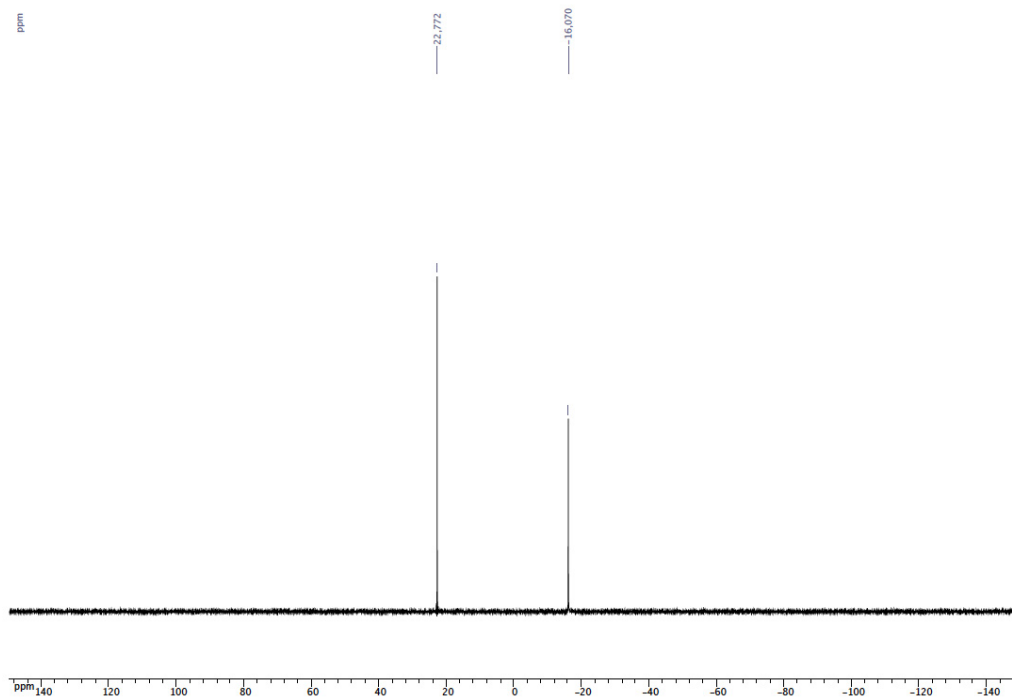


$^{31}\text{P}\{^1\text{H}\}$ NMR spectrum of **6** (CDCl_3)

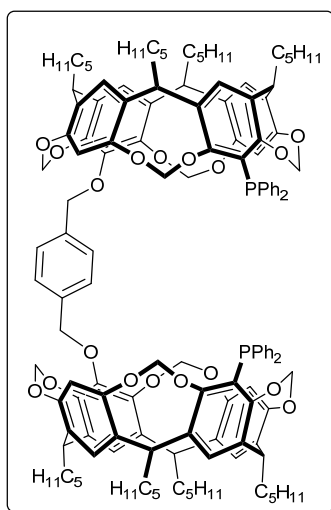


1-[5-(Diphenylphosphanyl)-4(24),6(10),12(16),18(22)-tetramethylenedioxy-2,8,14,20-tetrapentylresorcin[4]aren-17-oxymethyl]-4-[5-(diphenylphosphanyl)-4(24),6(10),12(16),18(22)-tetramethylenedioxy-2,8,14,20-tetrapentylresorcin[4]aren-17-oxymethyl]benzene (7**):** Phenylsilane (0.36 mL, 2.95 mmol) was added to a solution of **5** (0.800 g, 0.376 mmol) in toluene (20 mL) at r.t. The resulting mixture was heated at 120°C for 48 h. The solvent was

then evaporated under reduced pressure and the crude product purified by column chromatography ($\text{CH}_2\text{Cl}_2/\text{Et}_2\text{O}$, 9:1 v/v; $R_f = 0.3$: $\text{CH}_2\text{Cl}_2/\text{Et}_2\text{O}$, 9:1 v/v), yield 0.310 g (39 %). ^1H NMR (400 MHz, CDCl_3): $\delta = 7.74$ - 7.70 (m, 4H, arom. CH, PPh_2), 7.50 - 7.42 (m, 10H, arom. CH, PPh_2), 7.39 (s, 1H, arom. CH, resorcinarene), 7.35 - 7.29 (m, 10H, arom. CH, PPh_2 and $\text{CH}_2\text{C}_6\text{H}_4\text{CH}_2$), 7.20 (s, 1H, arom. CH, resorcinarene), 7.11 (s, 2H, arom. CH, resorcinarene), 7.08 (s, 2H, arom. CH, resorcinarene), 6.92 (s, 1H, arom. CH, resorcinarene), 6.88 (s, 1H, arom. CH, resorcinarene), 6.45 (s, 2H, arom. CH, resorcinarene), 6.44 (s, 2H, arom. CH, resorcinarene), 5.80 and 4.45 (AB spin system, 4H, OCH_2O , $^2J = 7.0$ Hz), 5.77 and 4.56 (AB spin system, 4H, OCH_2O , $^2J = 7.2$ Hz), 5.02 (s, 4H, $\text{CH}_2\text{C}_6\text{H}_4\text{CH}_2$), 5.01 (s, 4H, $\text{CH}_2\text{C}_6\text{H}_4\text{CH}_2$), 4.76 (t, 4H, CHCH_2 , $^3J = 7.2$ Hz), 4.76 and 4.13 (AB spin system, 4H, OCH_2O , $^2J = 7.5$ Hz), 4.71 (t, 2H, CHCH_2 , $^3J = 7.7$ Hz), 4.66 (t, 2H, CHCH_2 , $^3J = 8.0$ Hz), 4.56 and 4.28 (AB spin system, 4H, OCH_2O , $^2J = 7.5$ Hz), 2.34 - 2.14 (m, 16H, CHCH_2CH_2), 1.46 - 1.34 (m, 48H $\text{CH}_2\text{CH}_2\text{CH}_2\text{CH}_3$), 0.94 (t, 12H, CH_2CH_3 , $^3J = 7.0$ Hz), 0.93 (t, 6H, CH_2CH_3 , $^3J = 7.2$ Hz), 0.92 (t, 6H, CH_2CH_3 , $^3J = 7.0$ Hz); $^{13}\text{C}\{^1\text{H}\}$ NMR (100 MHz, CDCl_3): $\delta = 157.17$ - 113.61 (arom. C's), 99.94 (s, OCH_2O), 99.71 (s, OCH_2O), 99.64 (s, OCH_2O), 99.36 (s, OCH_2O), 75.38 (s, $\text{CH}_2\text{C}_6\text{H}_4\text{CH}_2$), 75.33 (s, $\text{CH}_2\text{C}_6\text{H}_4\text{CH}_2$), 36.81 (s, CHCH_2), 36.77 (s, CHCH_2), 36.71 (s, CHCH_2), 36.51 (s, CHCH_2), 32.17 (s, $\text{CH}_2\text{CH}_2\text{CH}_3$), 32.08 (s, $\text{CH}_2\text{CH}_2\text{CH}_3$), 30.14 (s, CHCH_2), 30.04 (s, CHCH_2), 29.99 (s, CHCH_2), 27.72 (s, CHCH_2CH_2), 27.66 (s, CHCH_2CH_2), 27.64 (s, CHCH_2CH_2), 22.83 (s, CH_2CH_3), 14.24 (s, CH_2CH_3); $^{31}\text{P}\{^1\text{H}\}$ NMR (162 MHz, CDCl_3): $\delta = 22.8$ (s, $\text{P}(\text{O})\text{Ph}_2$), -16.1 (s, PPh_2) ppm; MS (ESI-TOF): $m/z = 2153.05$ [$\text{M} + \text{H}$] expected isotopic profile; elemental analysis calcd (%) for $\text{C}_{136}\text{H}_{152}\text{O}_{19}\text{P}_2$ ($M_r = 2152.60$): C 75.88, H 7.12; found (%): C 75.92, H 7.21.

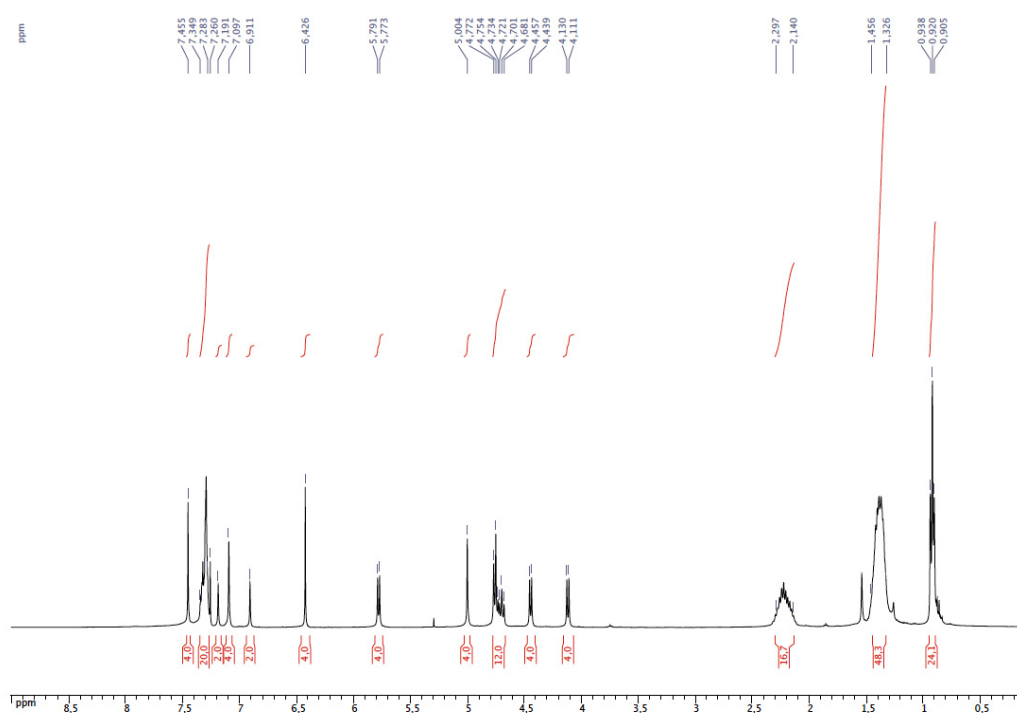


$^{31}\text{P}\{^1\text{H}\}$ NMR spectrum of **7** (CDCl_3)

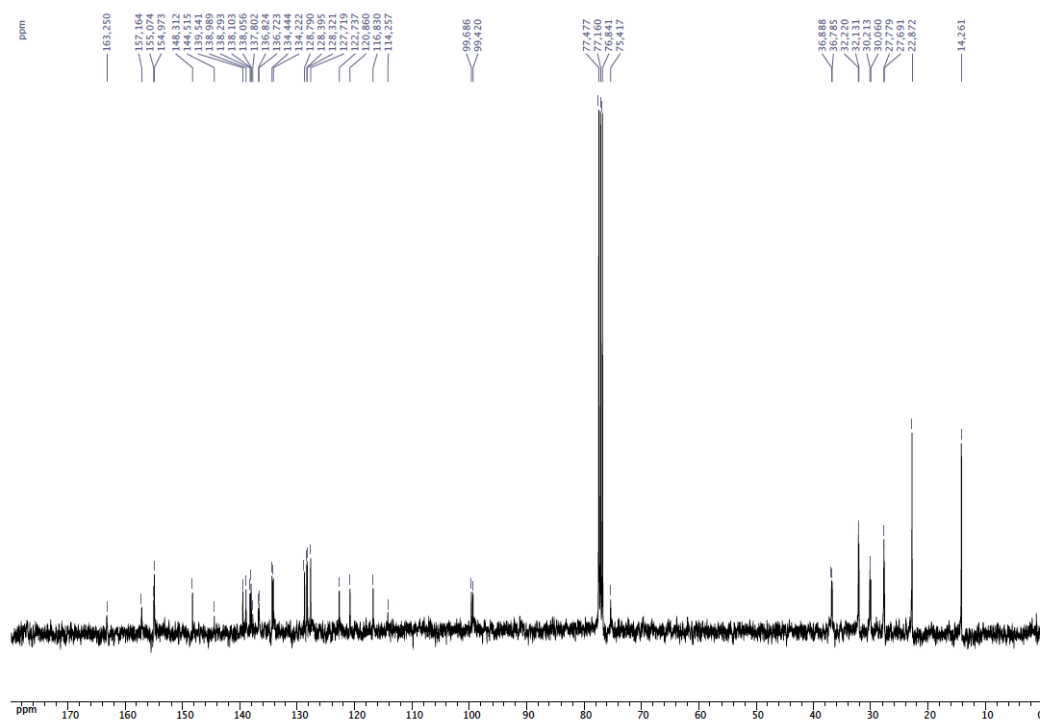


1,4-Bis-[5-(diphenylphosphanyl)-4(24),6(10),12(16),18(22)-tetramethylenedioxy-2,8,14,20-tetrapentylresorcin[4]aren-17-oxymethyl]benzene (8): $\text{BH}_3 \cdot \text{THF}$ (1.0 M in THF, 5 mL, 5 mmol) was added to a solution of **5** (0.500 g, 0.231 mmol) in Et_3N (10 mL) at 0°C . The resulting mixture was then heated under reflux for 24 h. The solvent was evaporated under reduced pressure and the crude product was dissolved in CH_2Cl_2 (3 mL) before precipitation

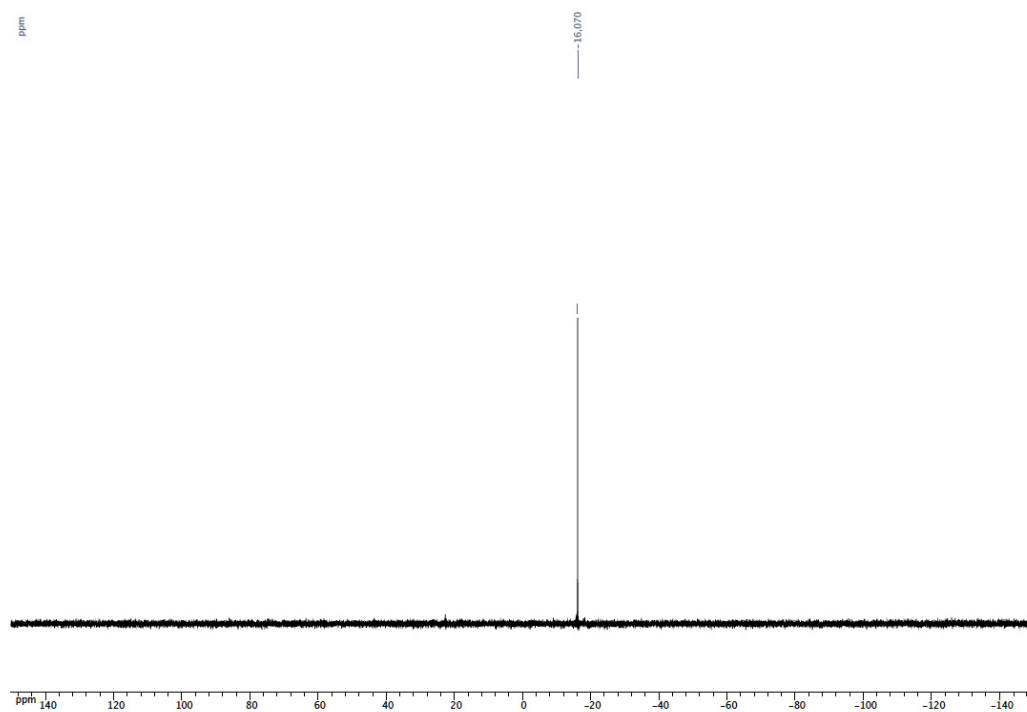
with methanol (20 mL). The white product was filtered, washed with cold methanol (3 x 10 mL) and dried under vacuum, yield 0.473 g (96 %). ^1H NMR (400 MHz, CDCl_3): $\delta = 7.46$ (s, 4H, arom. CH, $\text{CH}_2\text{C}_6\text{H}_4\text{CH}_2$), 7.35-7.28 (m, 20H, arom. CH, PPh_2), 7.19 (s, 2H, arom. CH, resorcinarene), 7.10 (s, 4H, arom. CH, resorcinarene), 6.91 (s, 2H, arom. CH, resorcinarene), 6.43 (s, 4H, arom. CH, resorcinarene), 5.78 and 4.45 (AB spin system, 8H, OCH_2O , $^2J = 7.2$ Hz), 5.00 (s, 4H, $\text{CH}_2\text{C}_6\text{H}_4\text{CH}_2$), 4.76 and 4.12 (AB spin system, 8H, OCH_2O , $^2J = 7.6$ Hz), 4.75 (t, 4H, CHCH_2 , $^3J = 7.6$ Hz), 4.70 (t, 4H, CHCH_2 , $^3J = 8.0$ Hz), 2.32-2.14 (m, 16H, CHCH_2CH_2), 1.45-1.31 (m, 48H $\text{CH}_2\text{CH}_2\text{CH}_2\text{CH}_3$), 0.94 (t, 12H, CH_2CH_3 , $^3J = 6.8$ Hz), 0.92 (t, 12H, CH_2CH_3 , $^3J = 7.2$ Hz); $^{13}\text{C}\{^1\text{H}\}$ NMR (100 MHz, CDCl_3): $\delta = 163.25$ -114.26 (arom. C's), 99.69 (s, OCH_2O), 99.42 (s, OCH_2O), 75.42 (s, $\text{CH}_2\text{C}_6\text{H}_4\text{CH}_2$), 36.89 (s, CHCH_2), 36.78 (s, CHCH_2), 32.22 (s, $\text{CH}_2\text{CH}_2\text{CH}_3$), 32.13 (s, $\text{CH}_2\text{CH}_2\text{CH}_3$), 30.21 (s, CHCH_2), 30.06 (s, CHCH_2), 27.78 (s, CHCH_2CH_2), 27.69 (s, CHCH_2CH_2), 22.87 (s, CH_2CH_3), 14.26 (s, CH_2CH_3); $^{31}\text{P}\{^1\text{H}\}$ NMR (162 MHz, CDCl_3): $\delta = -16.1$ (s, PPh_2) ppm; elemental analysis calcd (%) for $\text{C}_{136}\text{H}_{152}\text{O}_{18}\text{P}_2$ ($M_r = 2136.60$): C 76.45, H 7.17; found (%): C 76.52, H 7.26.



^1H NMR spectrum of **8** (CDCl_3)

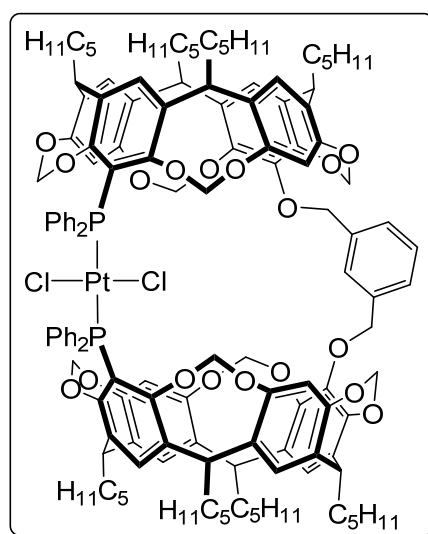


¹³C {¹H} NMR spectrum of **8** (CDCl₃)



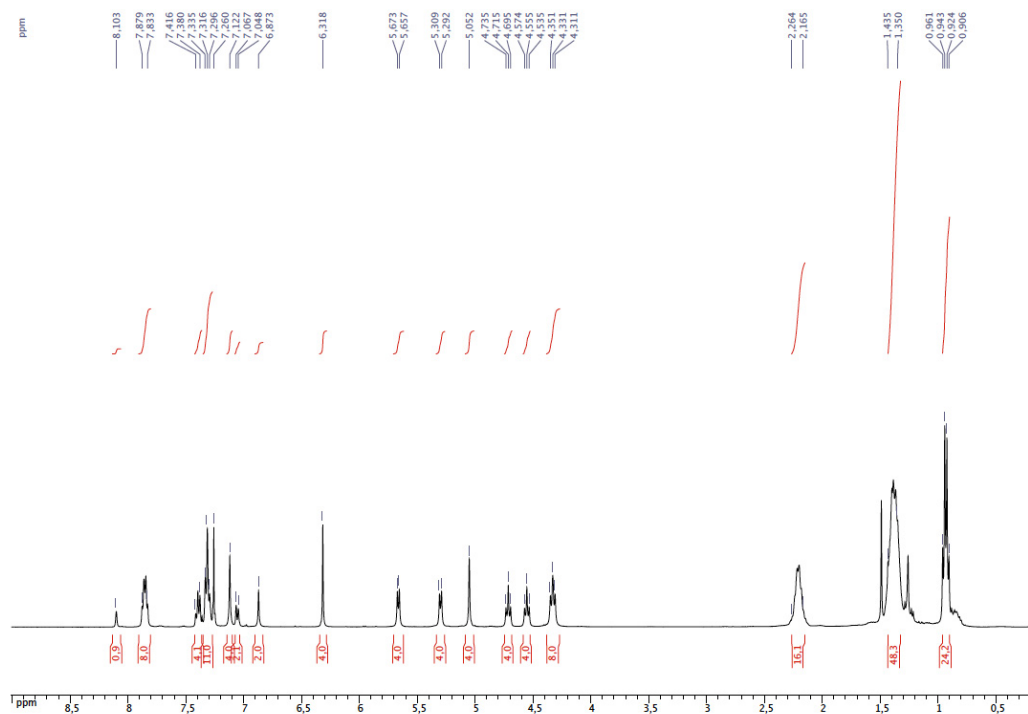
³¹P {¹H} NMR spectrum of **8** (CDCl₃)

***P,P*-Dichlorido-{1,3-bis-[5-(diphenylphosphanyl)-4(24),6(10),12(16),18(22)-tetramethylenedioxy-2,8,14,20-tetrapentylresorcin[4]aren-17-oxymethyl]benzene}-platinum(II) (9 and 10):** A solution of **6** (0.100 g, 0.05 mmol) in THF (200 mL) was added dropwise to a solution of [PtCl₂(PhCN)₂] (0.022 g, 0.05 mmol) in THF (750 mL). The resulting mixture was heated at 65°C for 36 h. The solvent was then evaporated under reduced pressure and the crude product purified by column chromatography (Petroleum ether/Et₂O, 86:14 v/v).

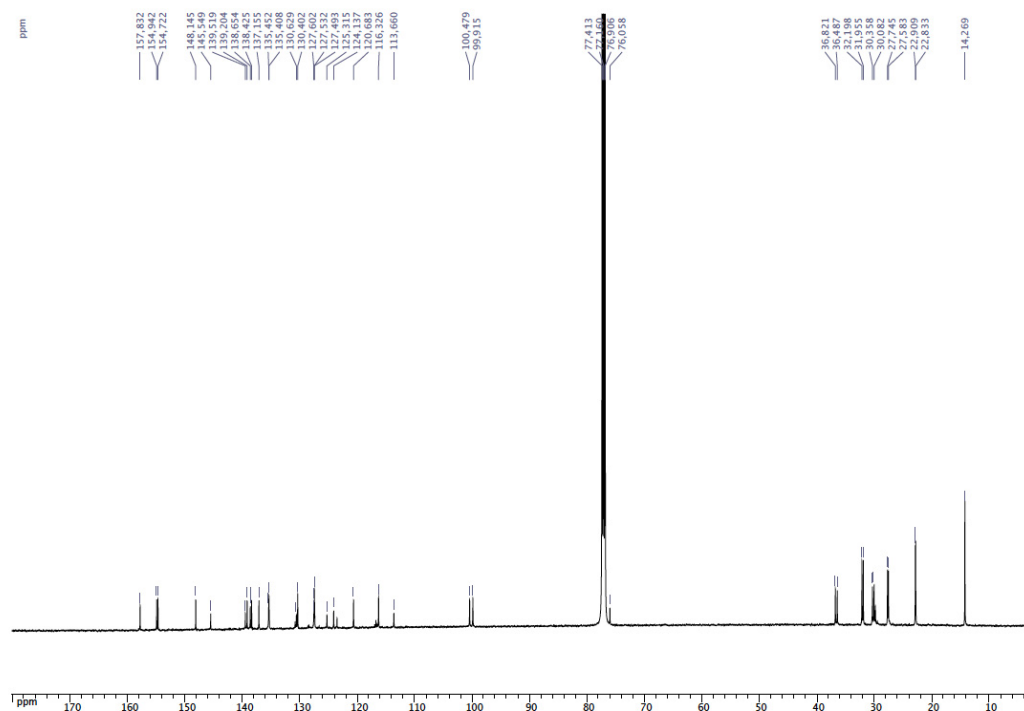


***trans*-[PtCl₂(**6**)] (9):** *R_f* = 0.51 (Petroleum ether/Et₂O, 7:3 v/v) yellow solid, yield 0.053 g (39 %). ¹H NMR (400 MHz, CDCl₃): δ = 8.10 (s, 1H, arom. CH, CH₂C₆H₄CH₂), 7.88-7.83 (m, 8H, arom. CH, PPh₂), 7.42-7.38 (m, 4H, arom. CH, PPh₂), 7.35-7.30 (m, 9H, arom. CH, PPh₂ and CH₂C₆H₄CH₂), 7.32 (s, 2H, arom. CH, resorcinarene), 7.12 (s, 4H, arom. CH, resorcinarene), 7.05 (d, 2H, arom. CH, CH₂C₆H₄CH₂, ³*J* = 7.6 Hz), 6.87 (s, 2H, arom. CH, resorcinarene), 6.32 (s, 4H, arom. CH, resorcinarene), 5.66 and 4.34 (AB spin system, 8H, OCH₂O, ²*J* = 6.4 Hz), 5.30 and 4.32 (AB spin system, 8H, OCH₂O, ²*J* = 6.8 Hz), 5.05 (s, 4H, CH₂C₆H₄CH₂), 4.71 (t, 4H, CHCH₂, ³*J* = 8.0 Hz), 4.55 (t, 4H, CHCH₂, ³*J* = 7.8 Hz), 2.26-2.16 (m, 16H, CHCH₂CH₂), 1.43-1.35 (m, 48H CH₂CH₂CH₂CH₃), 0.94 (t, 12H, CH₂CH₃, ³*J* = 7.2 Hz), 0.93 (t, 12H, CH₂CH₃, ³*J* = 7.2 Hz); ¹³C{¹H} NMR (125 MHz, CDCl₃): δ = 157.83-113.66 (arom. C's), 100.48 (s, OCH₂O), 99.91 (s, OCH₂O), 76.06 (s, CH₂C₆H₄CH₂), 36.82 (s, CHCH₂), 36.49 (s, CHCH₂), 32.20 (s, CH₂CH₂CH₃), 31.95 (s, CH₂CH₂CH₃), 30.36 (s, CHCH₂), 30.08 (s, CHCH₂), 27.74 (s, CHCH₂CH₂), 27.58 (s, CHCH₂CH₂), 22.91 (s, CH₂CH₃), 22.83 (s, CH₂CH₃), 14.27 (s, CH₂CH₃); ³¹P{¹H} NMR (162 MHz, CDCl₃): δ = 12.1 (s with Pt satellites, PPh₂, *J*_{Pt} = 2702 Hz) ppm; MS (ESI-TOF): *m/z* = 2422.94 [M + Na]

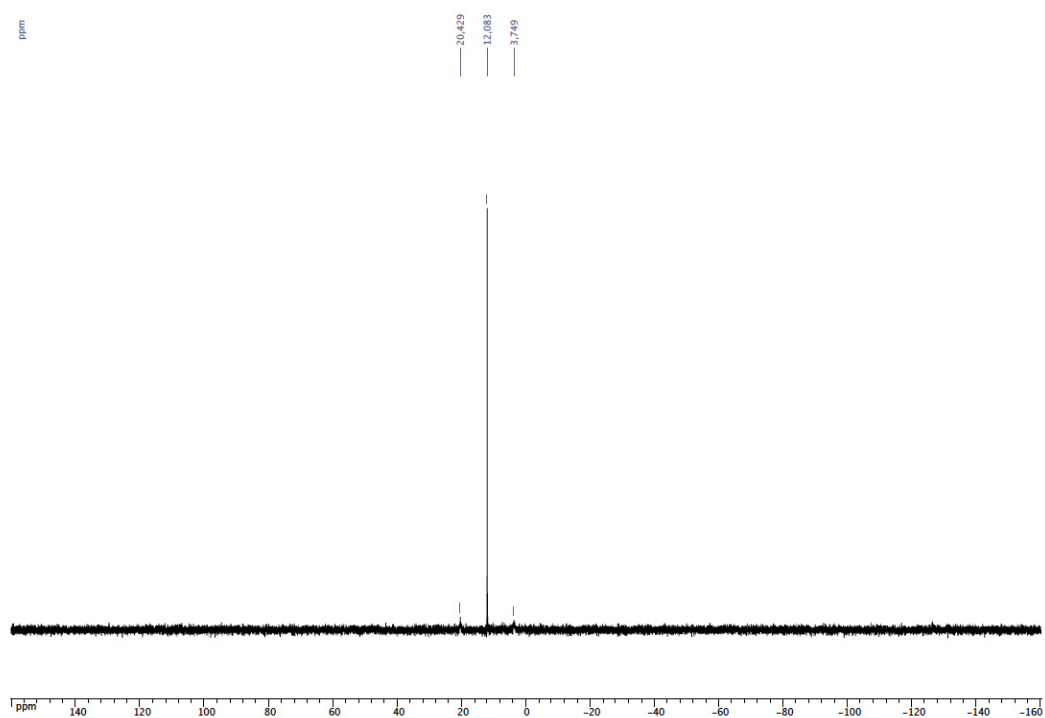
expected isotopic profile; elemental analysis calcd (%) for $C_{136}H_{152}O_{18}P_2PtCl_2$ ($M_r = 2402.59$): C 67.99, H 6.38; found (%): C 68.05, H 6.49.



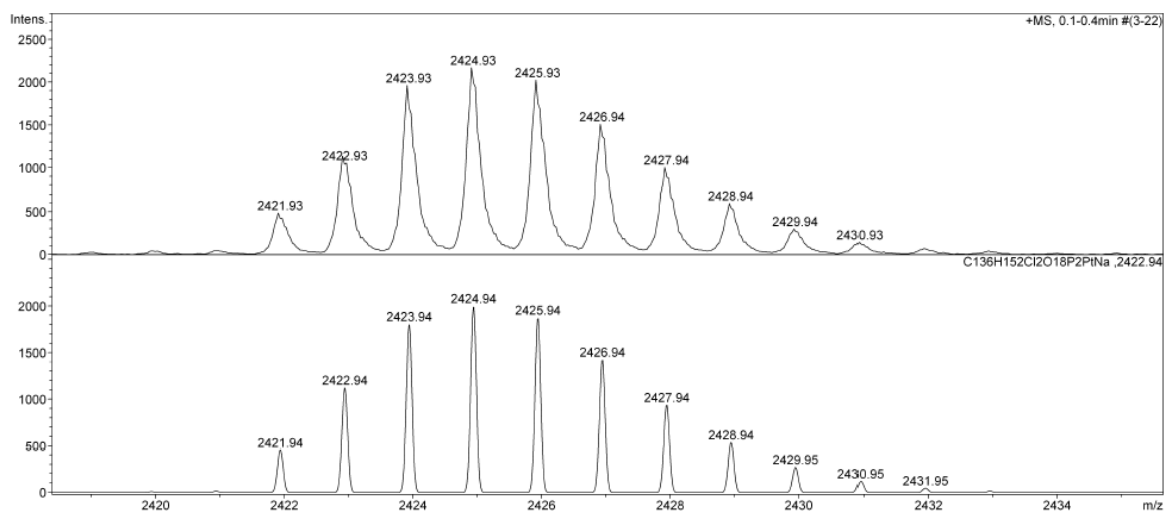
1H NMR spectrum of **9** ($CDCl_3$)



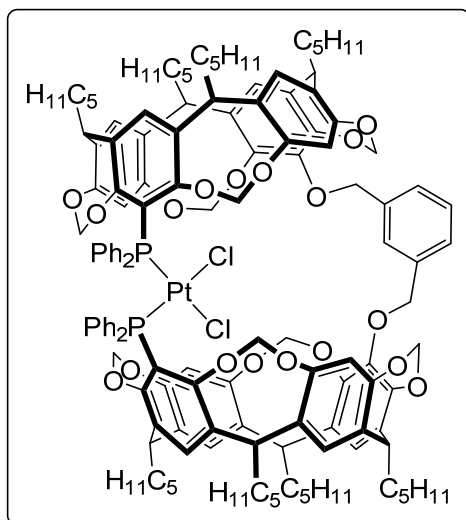
$^{13}C\{^1H\}$ NMR spectrum of **9** ($CDCl_3$)



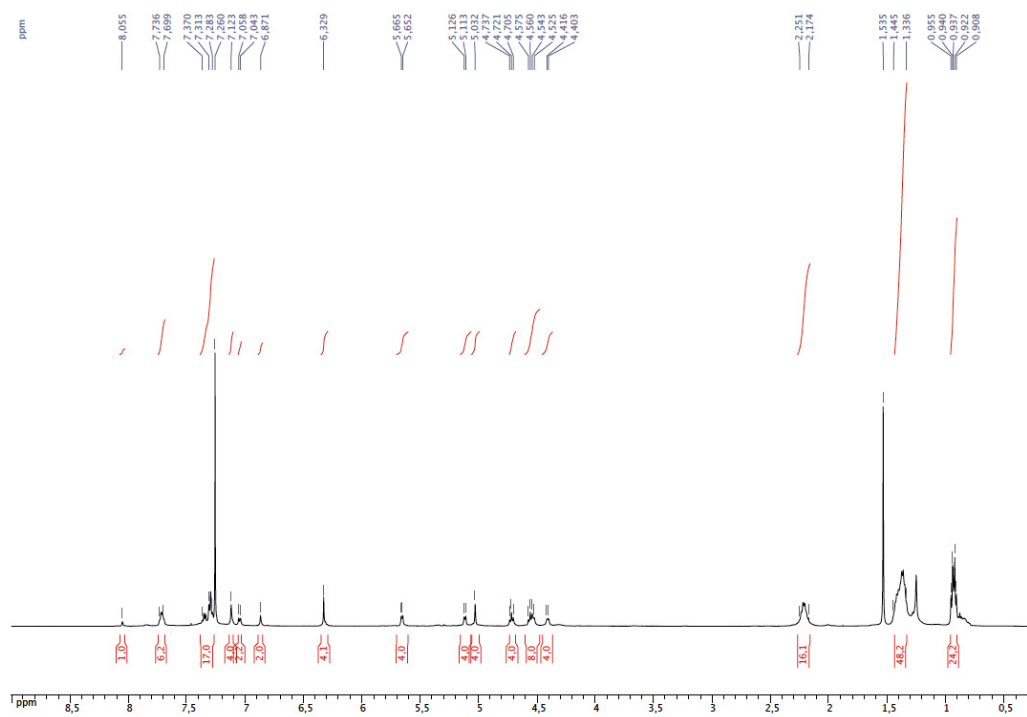
$^{31}\text{P}\{^1\text{H}\}$ NMR spectrum of **9** (CDCl_3)



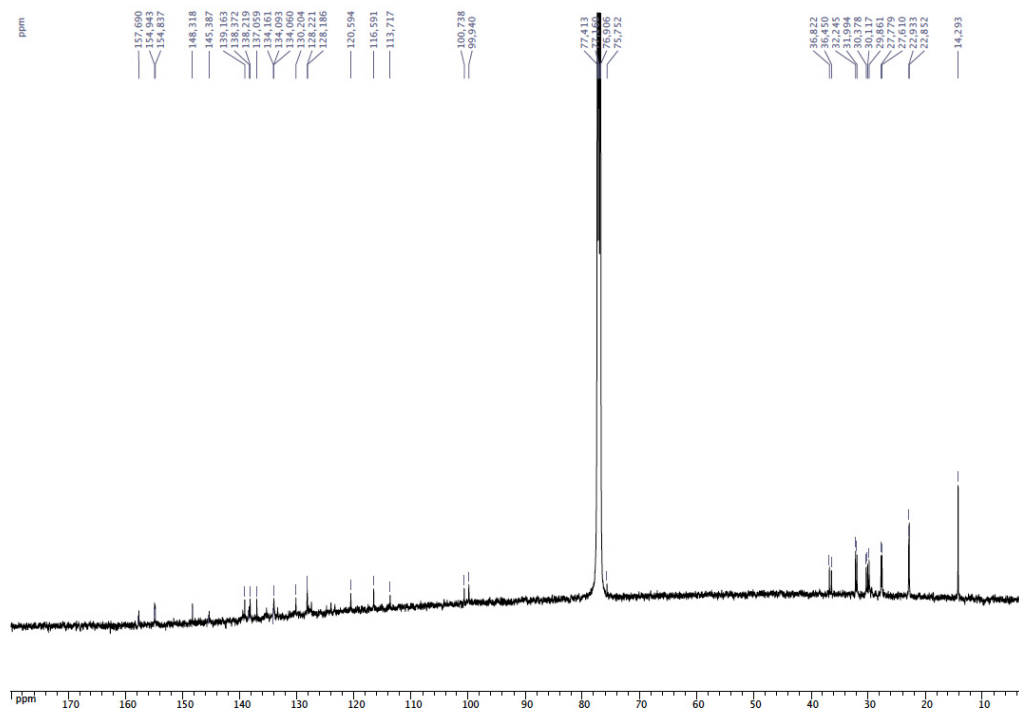
Mass spectrum (ESI-TOF) of **9** (exp. spectrum (top); calculated spectrum (bottom) for $\text{C}_{136}\text{H}_{152}\text{Cl}_2\text{O}_{18}\text{P}_2\text{Pt} + \text{Na}$)



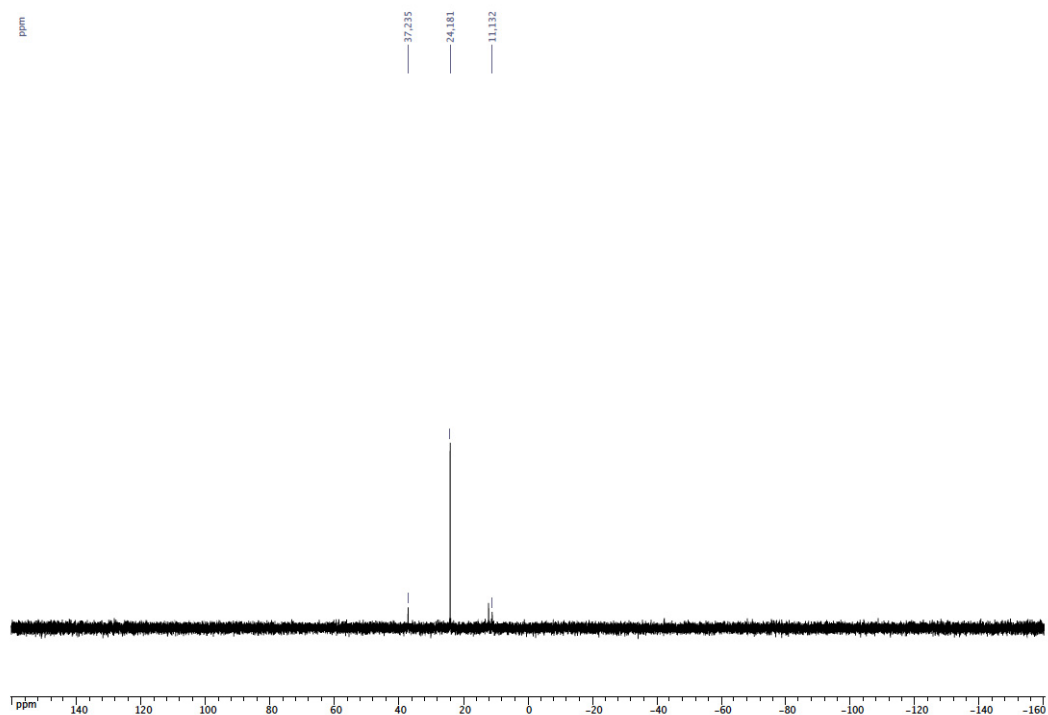
***cis*-[PtCl₂(6)] (10):** $R_f = 0.52$ (Petroleum ether/Et₂O, 7:3 v/v) white solid, yield 0.004 g (3 %). ¹H NMR (400 MHz, CDCl₃): $\delta = 8.05$ (s, 1H, arom. CH, CH₂C₆H₄CH₂), 7.74-7.70 (m, 6H, arom. CH, PPh₂), 7.37-7.28 (m, 15H, arom. CH, PPh₂ and CH₂C₆H₄CH₂), 7.31 (s, 2H, arom. CH, resorcinarene), 7.12 (s, 4H, arom. CH, resorcinarene), 7.05 (d, 2H, arom. CH, CH₂C₆H₄CH₂, ³*J* = 7.5 Hz), 6.87 (s, 2H, arom. CH, resorcinarene), 6.33 (s, 4H, arom. CH, resorcinarene), 5.66 and 4.41 (AB spin system, 8H, OCH₂O, ²*J* = 6.5 Hz), 5.12 and 4.53 (AB spin system, 8H, OCH₂O, ²*J* = 6.5 Hz), 5.03 (s, 4H, CH₂C₆H₄CH₂), 4.72 (t, 4H, CHCH₂, ³*J* = 8.0 Hz), 4.56 (t, 4H, CHCH₂, ³*J* = 7.5 Hz), 2.256-2.17 (m, 16H, CHCH₂CH₂), 1.44-1.34 (m, 48H CH₂CH₂CH₂CH₃), 0.94 (t, 12H, CH₂CH₃, ³*J* = 7.5 Hz), 0.92 (t, 12H, CH₂CH₃, ³*J* = 7.0 Hz); ¹³C{¹H} NMR (125 MHz, CDCl₃): $\delta = 157.69$ -113.72 (arom. C's), 100.74 (s, OCH₂O), 99.94 (s, OCH₂O), 75.75 (s, CH₂C₆H₄CH₂), 36.82 (s, CHCH₂), 36.45 (s, CHCH₂), 32.24 (s, CH₂CH₂CH₃), 31.99 (s, CH₂CH₂CH₃), 30.38 (s, CHCH₂), 30.12 (s, CHCH₂), 29.86 (s, CHCH₂), 27.78 (s, CHCH₂CH₂), 27.62 (s, CHCH₂CH₂), 22.93 (s, CH₂CH₃), 22.85 (s, CH₂CH₃), 14.29 (s, CH₂CH₃); ³¹P{¹H} NMR (121 MHz, CDCl₃): $\delta = 24.2$ (s with Pt satellites, PPh₂, $J_{\text{PPt}} = 3171$ Hz) ppm; elemental analysis calcd (%) for C₁₃₆H₁₅₂O₁₈P₂PtCl₂ ($M_r = 2402.59$): C 67.99, H 6.38; found (%): C 68.14, H 6.55.



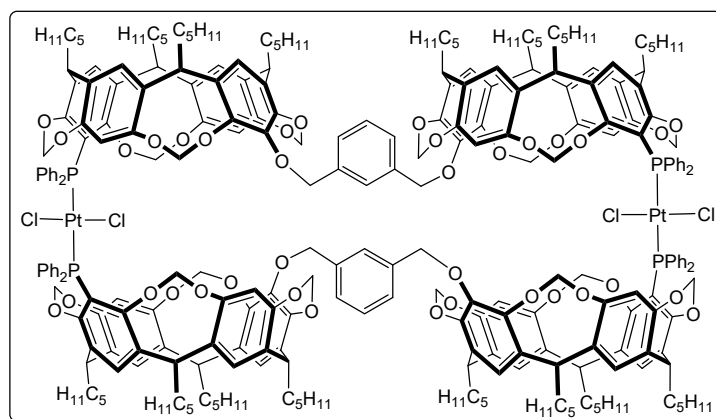
¹H NMR spectrum of **10** (CDCl₃)



¹³C{¹H} NMR spectrum of **10** (CDCl₃)

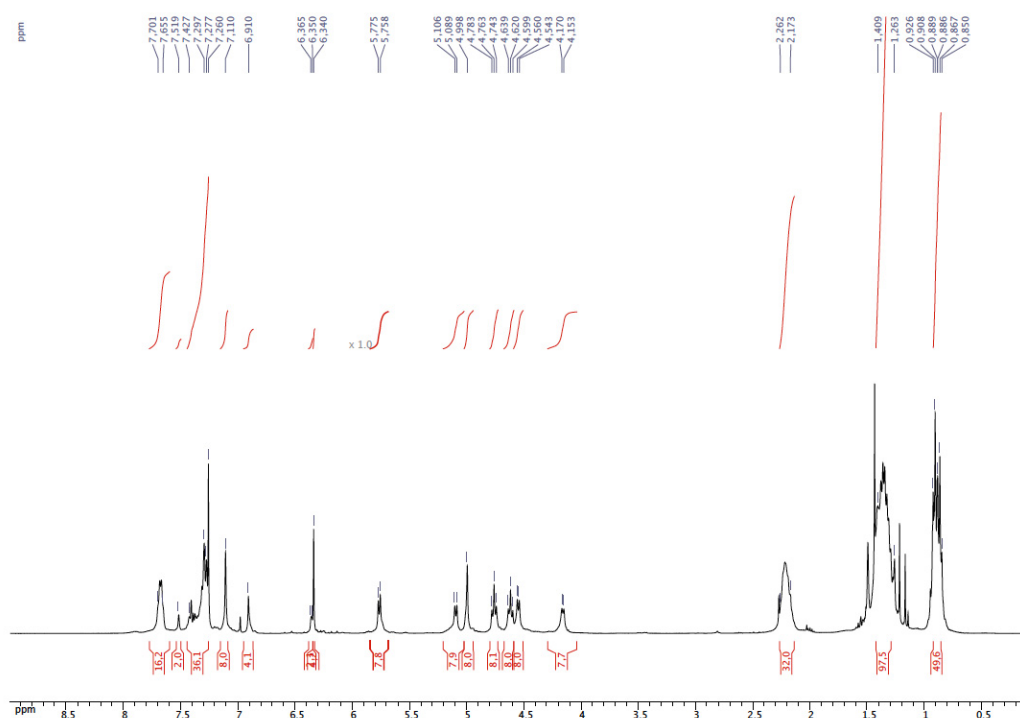


$^{31}\text{P}\{^1\text{H}\}$ NMR spectrum of **10** (CDCl_3)

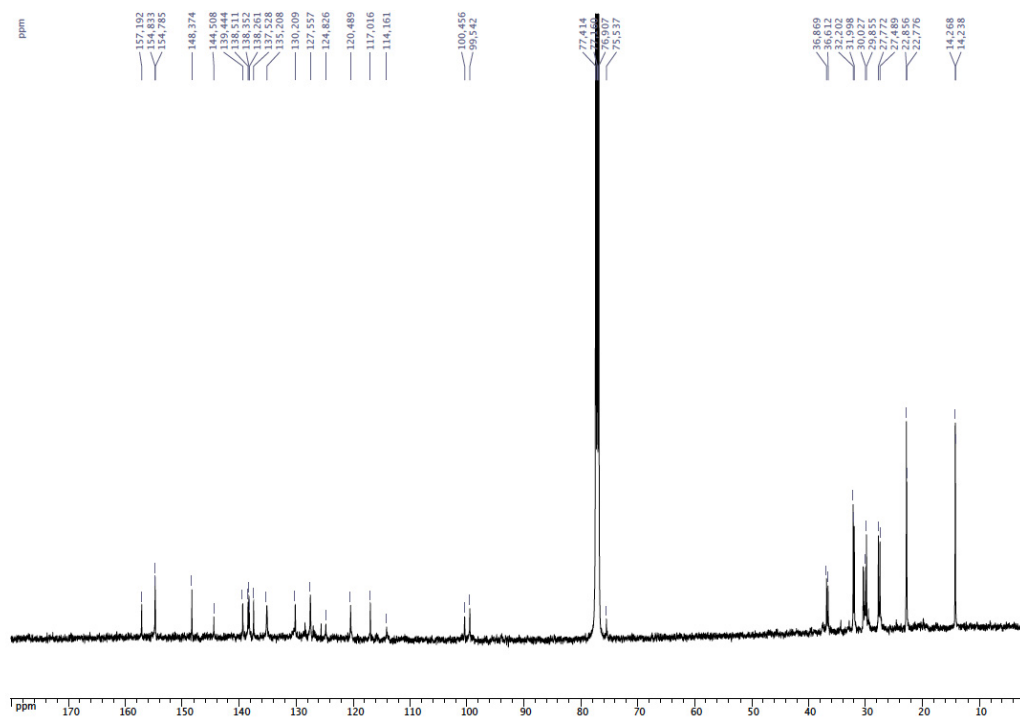


Synthesis of $[(trans\text{-PtCl}_2)_2(\mu_2\text{-}P,P\text{-6})_2]$ (11**):** A solution of **6** (0.150 g, 0.07 mmol) in THF (200 mL) was added dropwise to a solution of $[\text{PtCl}_2(\text{PhCN})_2]$ (0.033 g, 0.07 mmol) in THF (300 mL). The resulting mixture was heated at 65°C for 36 h. The solvent was then evaporated under reduced pressure and the crude product purified by column chromatography (petroleum ether/ Et_2O , 86:14 v/v) to afford *cis*- $[\text{PtCl}_2(\mathbf{6})]$ (**10**) (trace amounts), *trans*- $[\text{PtCl}_2(\mathbf{6})]$ (**9**) (0.033 g, yield 20 %) and $[(trans\text{-PtCl}_2)_2(\mu_2\text{-}P,P\text{-6})_2]$ (**11**) ($R_f = 0.28$, petroleum

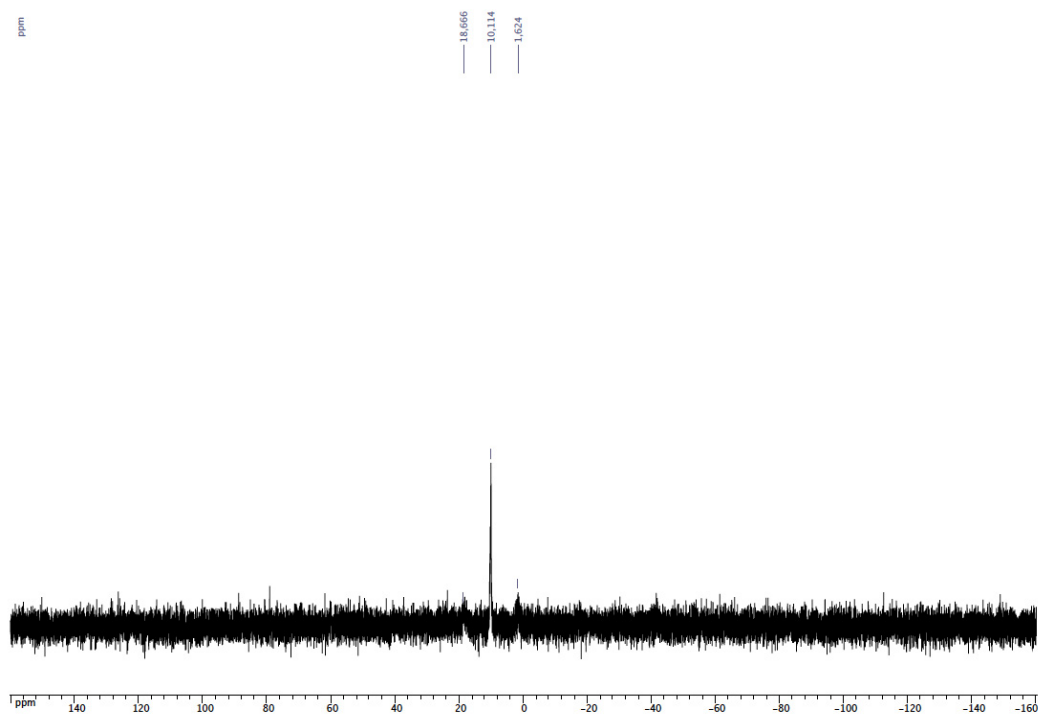
ether/Et₂O, 7:3, v/v) (0.040 g, yield 24 %). ¹H NMR (400 MHz, CDCl₃): δ = 7.70-7.65 (m, 16H, arom. CH, PPh₂), 7.52 (s, 2H, arom. CH, CH₂C₆H₄CH₂), 7.43-7.28 (m, 28H, arom. CH, PPh₂ and CH₂C₆H₄CH₂), 7.30 (s, 8H, arom. CH, resorcinarene), 7.11 (s, 8H, arom. CH, resorcinarene), 6.91 (s, 4H, arom. CH, resorcinarene), 6.36-6.35 (m, 2H, arom. CH, CH₂C₆H₄CH₂), 6.34 (s, 4H, arom. CH, resorcinarene), 5.77 and 4.55 (AB spin system, 16H, OCH₂O, ²J = 6.8 Hz), 5.09 and 4.16 (AB spin system, 16H, OCH₂O, ²J = 6.8 Hz), 5.00 (s, 8H, CH₂C₆H₄CH₂), 4.76 (t, 8H, CHCH₂, ³J = 8.0 Hz), 4.62 (t, 8H, CHCH₂, ³J = 8.0 Hz), 2.26-2.17 (m, 32H, CHCH₂CH₂), 1.41-1.26 (m, 96H CH₂CH₂CH₂CH₃), 0.91 (t, 24H, CH₂CH₃, ³J = 7.2 Hz), 0.87 (t, 24H, CH₂CH₃, ³J = 7.2 Hz); ¹³C{¹H} NMR (125 MHz, CDCl₃): δ = 157.19-114.16 (arom. C's), 100.46 (s, OCH₂O), 99.54 (s, OCH₂O), 75.54 (s, CH₂C₆H₄CH₂), 36.87 (s, CHCH₂), 36.61 (s, CHCH₂), 32.20 (s, CH₂CH₂CH₃), 32.00 (s, CH₂CH₂CH₃), 30.03 (s, CHCH₂), 29.85 (s, CHCH₂), 27.77 (s, CHCH₂CH₂), 27.49 (s, CHCH₂CH₂), 22.86 (s, CH₂CH₃), 22.78 (s, CH₂CH₃), 14.27 (s, CH₂CH₃), 14.24 (s, CH₂CH₃); ³¹P{¹H} NMR (162 MHz, CDCl₃): δ = 10.1 (s with Pt satellites, PPh₂, J_{Pt} = 2761 Hz) ppm; MS (ESI-TOF): m/z = 2438.91 [M + 2 K]²⁺ expected isotopic profile; elemental analysis calcd (%) for C₂₇₂H₃₀₄O₃₆P₄Pt₂Cl₄ (M_r = 4805.17): C 67.99, H 6.38; found (%): C 68.10, H 6.56.



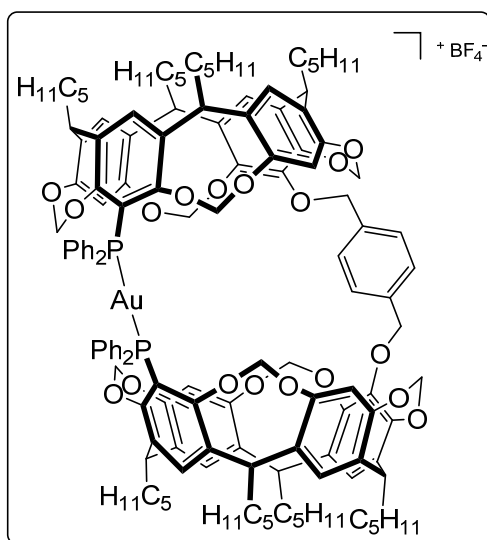
¹H NMR spectrum of **11** (CDCl₃)



$^{13}\text{C}\{^1\text{H}\}$ NMR spectrum of **11** (CDCl_3)

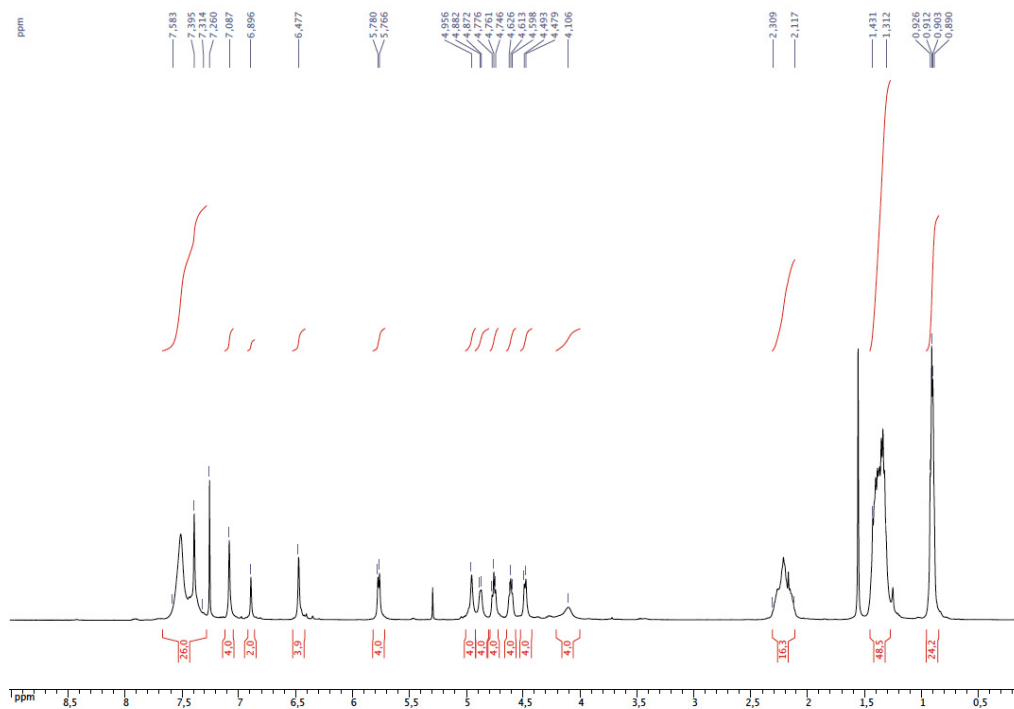


$^{31}\text{P}\{^1\text{H}\}$ NMR spectrum of **11** (CDCl_3)

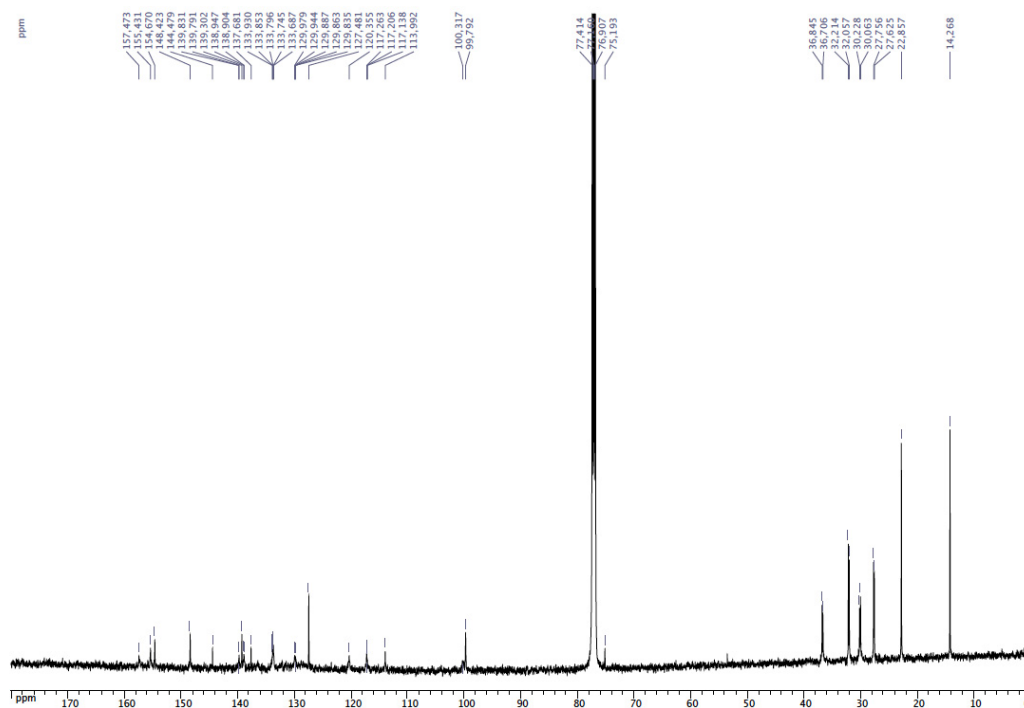


{1,4-Bis-[5-(diphenylphosphanyl)-4(24),6(10),12(16),18(22)-tetramethylenedioxy-2,8,14,20-tetrapentylresorcin[4]aren-17-oxymethyl]benzene}-gold(I) tetrafluoroborate (12): A solution of AgBF_4 (0.010 g, 0.05 mmol) in THF (10 mL) was added to a solution of $[\text{AuCl}(\text{THT})]$ (0.016, 0.05 mmol) in CH_2Cl_2 (20 mL). After stirring for 5 min, the solution was decanted to eliminate AgCl . The supernatant was filtered through Celite and added to a solution of diphosphine **8** (0.110 g, 0.05 mmol) in CH_2Cl_2 (200 mL). After 5 h, the solvent was evaporated under reduced pressure and the crude product purified by column chromatography ($\text{CH}_2\text{Cl}_2/\text{Et}_2\text{O}$, 9:1, v/v) to afford gold complex **12** as a white solid, yield 0.055 g (44 %) ($R_f = 0.27$, $\text{CH}_2\text{Cl}_2/\text{Et}_2\text{O}$, 8:2, v/v). ^1H NMR (500 MHz, CDCl_3): $\delta = 7.58\text{--}7.39$ (m, 24H, arom. CH, $\text{CH}_2\text{C}_6\text{H}_4\text{CH}_2$ and PPh_2), 7.39 (s, 2H, arom. CH, resorcinarene), 7.09 (s, 4H, arom. CH, resorcinarene), 6.90 (s, 2H, arom. CH, resorcinarene), 6.47 (s, 4H, arom. CH, resorcinarene), 5.77 and 4.48 (AB spin system, 8H, OCH_2O , $^2J = 7.0$ Hz), 4.96 (s, 4H, $\text{CH}_2\text{C}_6\text{H}_4\text{CH}_2$), 4.88 and 4.11 (AB spin system, 8H, OCH_2O , A part appears as a doublet with $^2J = 5.0$ Hz and the B part appears as a large singlet), 4.76 (t, 4H, CHCH_2 , $^3J = 7.5$ Hz), 4.61 (t, 4H, CHCH_2 , $^3J = 7.0$ Hz), 2.31–2.12 (m, 16H, CHCH_2CH_2), 1.43–1.31 (m, 48H, $\text{CH}_2\text{CH}_2\text{CH}_2\text{CH}_3$), 0.91 (t, 12H, CH_2CH_3 , $^3J = 7.0$ Hz), 0.90 (t, 12H, CH_2CH_3 , $^3J = 7.2$ Hz); $^{13}\text{C}\{^1\text{H}\}$ NMR (125 MHz, CDCl_3): $\delta = 157.47\text{--}113.99$ (arom. C's), 100.32 (s, OCH_2O), 99.79 (s, OCH_2O), 75.19 (s, $\text{CH}_2\text{C}_6\text{H}_4\text{CH}_2$), 36.84 (s, CHCH_2), 36.71 (s, CHCH_2), 32.21 (s, $\text{CH}_2\text{CH}_2\text{CH}_3$), 32.06 (s, $\text{CH}_2\text{CH}_2\text{CH}_3$), 30.23 (s, CHCH_2), 30.06 (s, CHCH_2), 27.76 (s, CHCH_2CH_2), 27.62 (s, CHCH_2CH_2), 22.86 (s, CH_2CH_3), 14.27 (s, CH_2CH_3); $^{31}\text{P}\{^1\text{H}\}$ NMR (162 MHz, CDCl_3): $\delta = 22.8$ (s, PPh_2) ppm; MS (ESI-TOF): $m/z = 2332.01$ [$\text{M} - \text{BF}_4$]

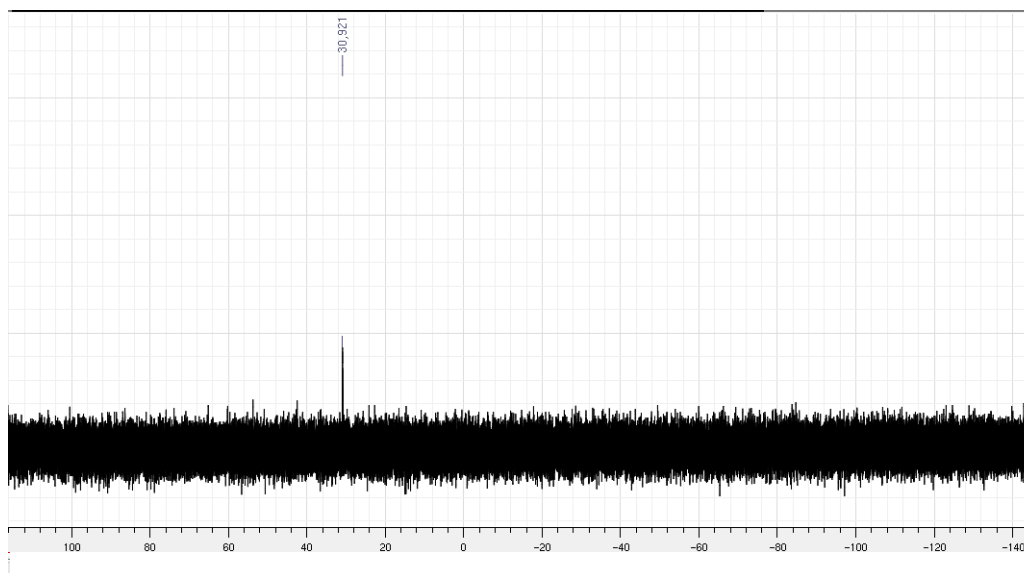
expected isotopic profile; elemental analysis calcd (%) for $C_{136}H_{152}O_{18}P_2AuBF_4$ ($M_r = 2420.37$): C 67.49, H 6.33; found (%): C 67.10, H 6.29.



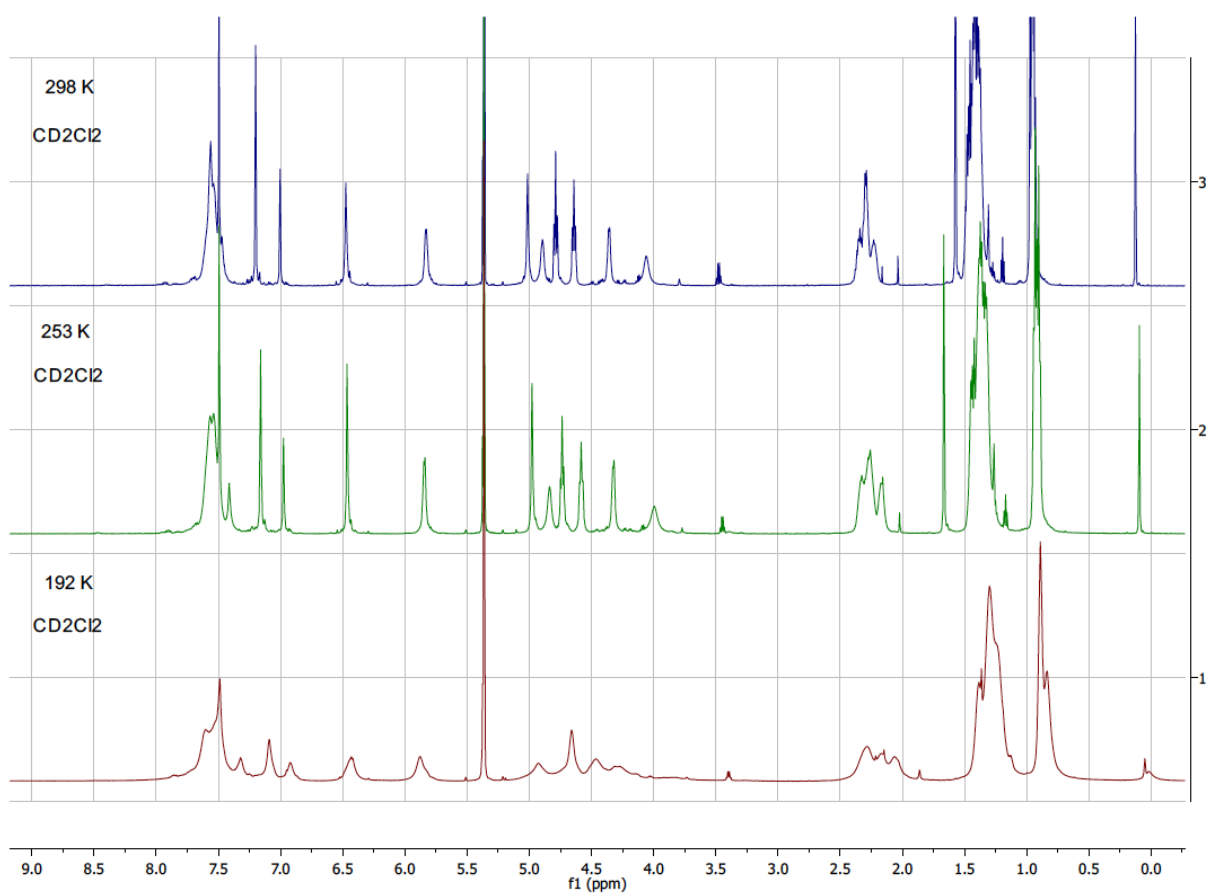
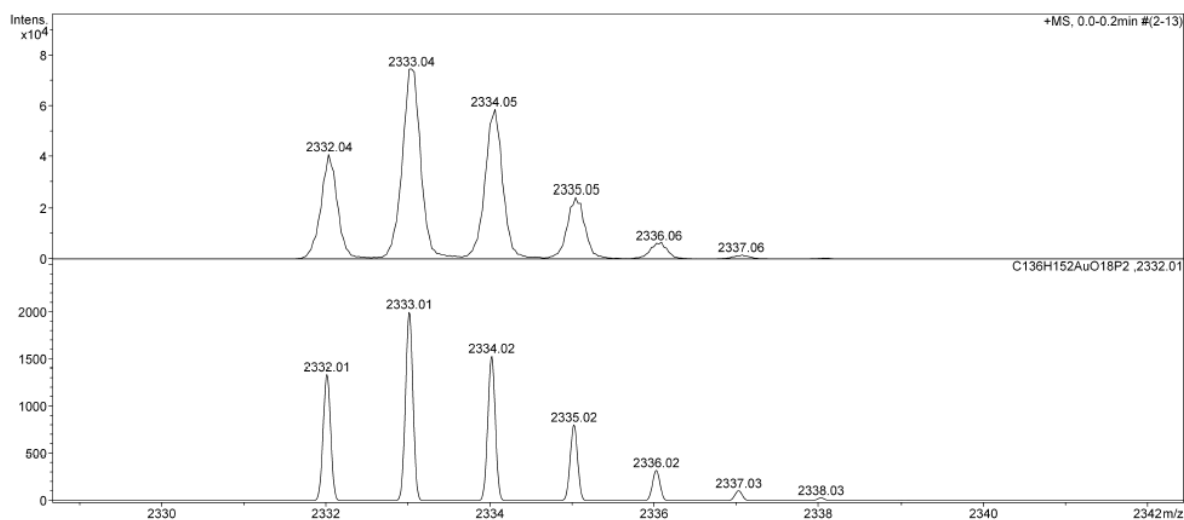
1H NMR spectrum of **12** ($CDCl_3$)

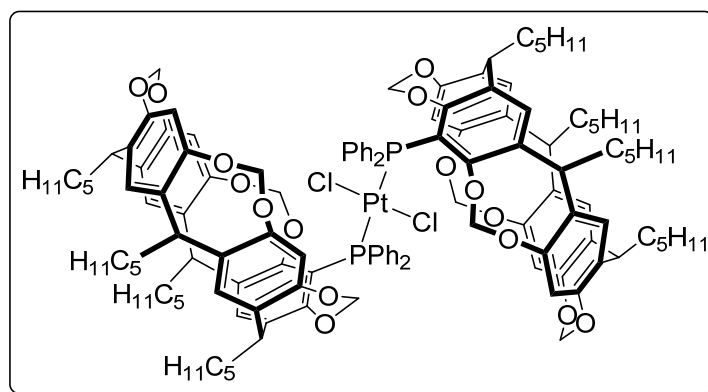


$^{13}\text{C}\{^1\text{H}\}$ NMR spectrum of **12** (CDCl_3)

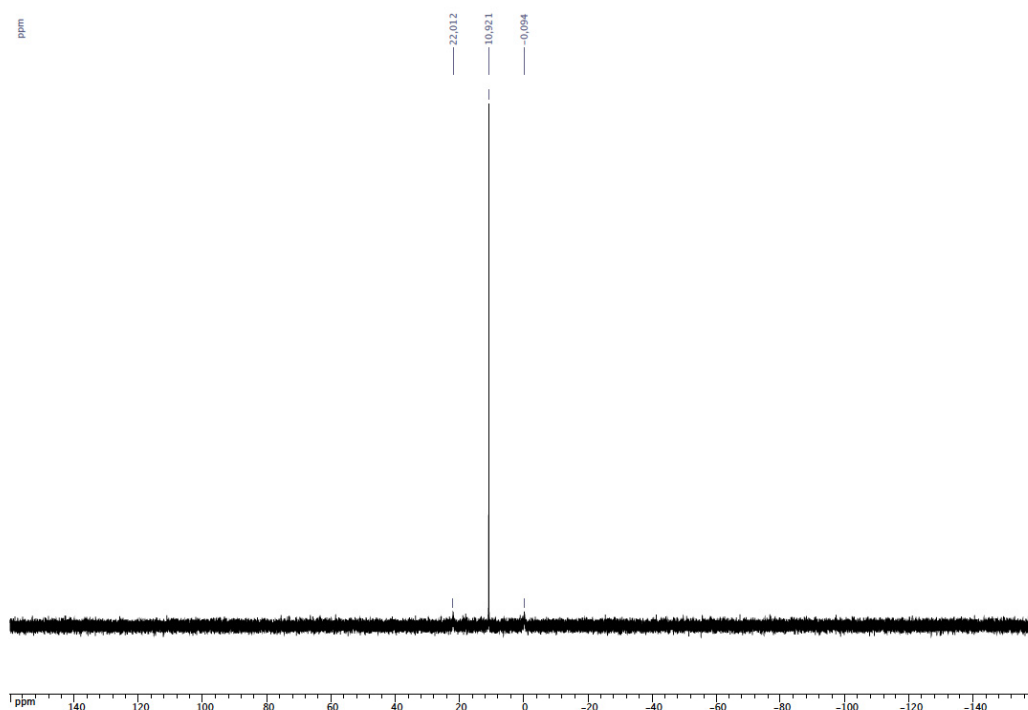


$^{31}\text{P}\{^1\text{H}\}$ NMR spectrum of **12** (CDCl_3)





***trans-P,P*-Dichloridobis[5-diphenylphosphanyl-4(24),6(10),12(16),18(22)-tetramethylene dioxy-2,8,14,20-tetrapentylresorcin[4]arene]platinum(II) (13)**: A solution of 5-diphenylphosphanyl-4(24),6(10),12(16),18(22)-tetramethylenedioxy-2,8,14,20-tetrapentylresorcin[4]arene (0.200 g, 0.2 mmol) in CH₂Cl₂ (10 mL) was added to a stirred solution of [PtCl₂(PhCN)₂] (0.047 g, 0.1 mmol) in CH₂Cl₂ (10 mL). After stirring at 40°C for 12 h, the solvent was evaporated under reduced pressure and the crude product was purified by column chromatography (Petroleum ether/Et₂O, 3:1 v/v; *R_f* = 0.1: Petroleum ether/Et₂O, 7:3 v/v) to afford **13** as a yellow solid, yield 0.181 g (80 %). ¹H NMR (300 MHz, CDCl₃): δ = 7.71-7.65 (m, 8H, arom. CH, PPh₂), 7.42-7.30 (m, 14H, arom. CH, PPh₂ and resorcinarene), 7.13 (s, 2H, arom. CH, resorcinarene), 7.12 (s, 4H, arom. CH, resorcinarene), 6.54 (s, 2H, arom. CH, resorcinarene), 6.37 (s, 4H, arom. CH, resorcinarene), 5.72 and 4.62 (AB spin system, 8H, OCH₂O, ²*J* = 7.2 Hz), 5.22 and 4.21 (AB spin system, 8H, OCH₂O, ²*J* = 7.5 Hz), 4.74 (t, 4H, CHCH₂, ³*J* = 8.1 Hz), 4.63 (t, 4H, CHCH₂, ³*J* = 7.9 Hz), 2.27-2.17 (m, 16H, CHCH₂CH₂), 1.44-1.32 (m, 48H CH₂CH₂CH₂CH₃), 0.92 (t, 12H, CH₂CH₃, ³*J* = 6.6 Hz), 0.92 (t, 12H, CH₂CH₃, ³*J* = 6.6 Hz); ¹³C{¹H} NMR (125 MHz, CDCl₃): δ = 157.21-116.79 (arom. C's), 100.59 (s, OCH₂O), 99.40 (s, OCH₂O), 36.61 (s, CHCH₂), 36.49 (s, CHCH₂), 32.18 (s, CH₂CH₂CH₃), 31.96 (s, CH₂CH₂CH₃), 30.40 (s, CHCH₂), 30.01 (s, CHCH₂), 27.72 (s, CHCH₂CH₂), 27.51 (s, CHCH₂CH₂), 22.84 (s, CH₂CH₃), 22.79 (s, CH₂CH₃), 14.26 (s, CH₂CH₃); ³¹P{¹H} NMR (121 MHz, CDCl₃): δ = 10.9 (s with Pt satellites, PPh₂, *J*_{PPt} = 2686 Hz) ppm; MS (ESI-TOF): *m/z* = 2304.87 [M + K] expected isotopic profile; elemental analysis calcd (%) for C₁₂₈H₁₄₆O₁₆P₂PtCl₂ (*M_r* = 2268.45): C 67.77, H 6.49; found (%): C 67.82, H 6.62.



$^{31}\text{P}\{^1\text{H}\}$ NMR spectrum of **13** (CDCl_3)

X-Ray crystallography data of structure of compound 5: Colourless single crystals of **5** suitable for X-ray diffraction were obtained by slow diffusion of MeOH into a CH_2Cl_2 solution of **5** at room temperature. The sample (0.264 x 0.188 x 0.115 mm) was mounted on a Oxford Diffraction Xcalibur Saphir 3 diffractometer with graphite-monochromatised Mo- K_α radiation. Formula of the crystals: $\text{C}_{136}\text{H}_{152}\text{O}_{20}\text{P}_2 \cdot 3.5\text{CH}_3\text{OH} \cdot 2\text{CH}_2\text{Cl}_2$, $M_r = 2450.61$, triclinic, space group $P-1$, $a = 15.718(1)$, $b = 20.701(2)$, $c = 23.169(2)$ Å, $\alpha = 66.591(8)$, $\beta = 72.853(6)$, $\gamma = 83.773(6)^\circ$, $V = 6610.4(1)$ Å³, $Z = 2$, $D_x = 1.231$ mg.m⁻³, $\lambda(\text{Mo-}K_\alpha) = 0.71073$ Å, $\mu = 0.182$ mm⁻¹, $F(000) = 2610$, $T = 140(2)$ K. Data collection ($2\theta_{\text{max}} = 27.5^\circ$, ω scan frames via 0.7° ω rotation and 30 s per frame, range hkl : h -20 to 20, k -26 to 26, l -29 to 29) gave 65586 reflections. The data revealed 28852 independent reflections of which 8716 were observed with $I > 2.0 \sigma(I)$. The structure was solved by using SIR-97,^[21] which revealed the non-hydrogen atoms of the molecule. After anisotropic refinement, all the hydrogen atoms were found by Fourier difference. The whole structure was refined with SHELXL-2014/6^[20] by using the full-matrix least squares technique {use of F^2 ; x , y , z , β_{ij} for C, Cl, O and P atoms, x , y , z in the riding mode for H atoms; 1556 variables and 8716 observations with $I > 2.0 \sigma(I)$; calcd. $w = 1/[\sigma^2(F_o^2) + (0.1032P)^2 + 2.7232P]$ in which $P = (F_o^2 + 2 F_c^2)/3$ with the

resulting $R = 0.1147$, $R_w = 0.4070$ and $S_w = 0.999$, $\Delta\rho < 1.004 \text{ e}\text{\AA}^{-3}$. The level A and B alerts in the checkcif file mainly come from poor diffraction at high theta and the presence of height pentyl groups, which have large thermal motions and disorders. The presence of 3.5 molecules of methanol and 2 molecules of dichloromethane led to a fast desolvation, which is complete after 30 seconds.

X-Ray crystallography data of structure of complex 9: Colourless single crystals of **9** suitable for X-ray diffraction were obtained by slow diffusion of hexane into a $\text{CHCl}_3/\text{C}_6\text{H}_6$ (9:1 v/v) solution of **9** at room temperature. The sample (0.280 x 0.250 x 0.200 mm) was mounted on a Bruker APEX-II CCD diffractometer with graphite-monochromatised Mo- K_α radiation. Formula of the crystals: $\text{C}_{136}\text{H}_{152}\text{Cl}_2\text{O}_{18}\text{P}_2\text{Pt}\cdot 3\text{CHCl}_3$, $M_r = 2760.72$, triclinic, space group $P-1$, $a = 16.5230(6)$, $b = 20.3555(8)$, $c = 21.5059(8) \text{ \AA}$, $\alpha = 67.261(1)$, $\beta = 86.837(1)$, $\gamma = 77.753(1)^\circ$, $V = 6516.3(4) \text{ \AA}^3$, $Z = 2$, $D_x = 1.407 \text{ mg}\cdot\text{m}^{-3}$, $\lambda(\text{Mo-}K_\alpha) = 0.71073 \text{ \AA}$, $\mu = 1.392 \text{ mm}^{-1}$, $F(000) = 2856$, $T = 173(2) \text{ K}$. Data collection ($2\theta_{\text{max}} = 29.44^\circ$, ω scan frames via $0.7^\circ \omega$ rotation and 30 s per frame, range hkl : h -23 to 23, k -28 to 28, l -30 to 30) gave 144477 reflections. The data revealed 37937 independent reflections of which 28508 were observed with $I > 2.0 \sigma(I)$. The structure was solved by using SHELXS-2013,^[20] which revealed the non-hydrogen atoms of the molecule. After anisotropic refinement, all the hydrogen atoms were found by Fourier difference. The whole structure was refined with SHELXL^[21] by using the full-matrix least squares technique {use of F^2 ; x, y, z, β_{ij} for C, Cl, O, P and Pt atoms, x, y, z in the riding mode for H atoms; 1563 variables and 28508 observations with $I > 2.0 \sigma(I)$; calcd. $w = 1/[\sigma^2(F_o^2) + (0.0803P)^2 + 9.9275P]$ in which $P = (F_o^2 + 2 F_c^2)/3$ with the resulting $R = 0.0567$, $R_w = 0.1517$ and $S_w = 1.028$, $\Delta\rho < 2.967 \text{ e}\text{\AA}^{-3}$.

CCDC-1492100 (**3**), 1026012 (**5**) and 1492101 (**9**) contain the supplementary crystallographic data which can be obtained free of charge from The Cambridge Crystallographic Data Centre via www.ccdc.cam.ac.uk/data_request/cif.

General procedure for the hydroformylation experiments: The hydroformylation experiments were carried out in a glass-lined 100 mL stainless steel autoclave that contained a magnetic stirring bar. In a typical run, the autoclave was charged with the platinum complex

(1 mol %) and SnCl₂.H₂O (4.5 mg, 2 mol %). The autoclave was purged twice with argon before introduction under argon of toluene (5 mL) and styrene (0.11 mL, 1 mmol). Afterwards, the autoclave was pressurised with 40 bar of syn-gas (CO/H₂, 1:1 v/v) before being heated at 100°C (at 100°C, P(CO/H₂) = 45 bar). After 24 h, the autoclave was cooled to 15°C, and depressurized in *ca.* 30 minutes. The reaction mixture was then evaporated and analysed by ¹H NMR.

References

- [1] a) J. R. Moran, S. Karbach and D. J. Cram, *J. Am. Chem. Soc.* **1982**, *104*, 5826-5828; b) V. K. Jain and P. H. Kanaiya, *Russ. Chem. Rev.* **2011**, *80*, 75-102.
- [2] a) P. Ballester and M. A. Sarmentero, *Org. Lett.* **2006**, *8*, 3477-3480; b) F. H. Zelder, R. Salvio and J. Rebek, *Chem. Commun.* **2006**, 1280-1282; c) A. B. Rozhenko, W. W. Schoeller, M. C. Letzel, B. Decker, C. Agena and J. Mattay, *Chem. Eur. J.* **2006**, *12*, 8995-9000; d) B. Dubessy, S. Harthong, C. Aronica, D. Bouchu, M. Busi, E. Dalcanale and J. P. Dutasta, *J. Org. Chem.* **2009**, *74*, 3923-3926; e) F. Tancini, R. M. Yebeutchou, L. Pirondini, R. De Zorzi, S. Geremia, O. A. Scherman and E. Dalcanale, *Chem. Eur. J.* **2010**, *16*, 14313-14321; f) E. Biavardi, C. Tudisco, F. Maffei, A. Motta, C. Massera, G. G. Condorelli and E. Dalcanale, *P. N. A. S.* **2012**, *109*, 2263-2268.
- [3] a) P. K. Thallapally, B. P. McGrail and J. L. Atwood, *Chem. Comm.* **2007**, 1521-1523; b) N. Li, R. G. Harrison and J. D. Lamb, *J. Incl. Phenom. Macro.* **2014**, *78*, 39-60.
- [4] a) R. J. Puddephatt, *Can. J. Can.* **2006**, *84*, 1505-1514; b) H. El Moll, D. Sémeril, D. Matt and L. Toupet, *Eur. J. Org. Chem.* **2010**, 1158-1168.
- [5] a) C. Gibson and J. Rebek, *Org. Lett.* **2002**, *4*, 1887-1890; b) H. El Moll, D. Sémeril, D. Matt, M.-T. Youinou and L. Toupet, *Org. Biomol. Chem.* **2009**, *7*, 495-501; c) R. J. Hooley and J. Rebek, *Chemistry & Biology* **2009**, *16*, 255-264; d) H. El Moll, D. Sémeril, D. Matt and L. Toupet, *Adv. Synth. Catal.* **2010**, *352*, 901-908; e) D. Sémeril and D. Matt, *Coord. Chem. Rev.* **2014**, *279*, 58-95; f) M. Kaloğlu, N. Şahin, D. Sémeril, E. Brenner, D. Matt, I. Özdemir, C. Kaya and L. Toupet, *Eur. J. Chem.* **2015**, 7310-7316.
- [6] D. M. Rudkevich and J. Rebek, *Eur. J. Org. Chem.* **1999**, 1991-2005.
- [7] a) B. C. Gibb, *Cavitands, in Encyclopedia of Supramolecular Chemistry*, J. L. Atwood, J. W. Steed Eds., Marcel Dekker, Inc. 2004, pp 219-222 **2004**; b) R. Warmuth and S. Makowiec, *J. Am. Chem. Soc.* **2007**, *129*, 1233-1241; c) F. Liu, R. C. Helgeson and K. N. Houk, *Acc. Chem. Res.* **2014**, *47*, 2168-2176.
- [8] A. Jasat and J. C. Sherman, *Chem. Rev.* **1999**, *99*, 931-967.
- [9] K. Kobayashi and M. Yamanaka, *Chem. Soc. Rev.* **2015**, *44*, 449-466.
- [10] H. Mansikkamäki, S. Busi, M. Nissinen, A. Ahman and K. Rissanen, *Chem. Eur. J.* **2006**, *12*, 4289-4296.
- [11] a) H. Boerrigter, T. Tomasberger, W. Verboom and D. N. Reinhoudt, *Eur. J. Org. Chem.* **1999**, 665-674; b) J. Gout, A. Višnjevac, S. Rat, O. Bistri, N. Le Poul, Y. Le Mest and O. Reinaud, *Eur. J. Inorg. Chem.* **2013**, *2013*, 5171-5180.
- [12] a) N. Şahin, D. Sémeril, E. Brenner, D. Matt, C. Kaya and L. Toupet, *Turk. J. Chem.* **2015**, *39*, 1171-1179; b) D. Shimoyama, H. Yamada, H. Ikeda, R. Sekiya and T. Haino, *Eur. J. Org. Chem.* **2016**, 3300-3303.

- [13] N. Şahin, D. Sémeril, E. Brenner, D. Matt, İ. Özdemir, C. Kaya and L. Toupet, *ChemCatChem* **2013**, *5*, 1115-1125.
- [14] P. S. Pregosin, in *Phosphorus-31 NMR Spectroscopy in Stereochemical Analysis*, (Eds.: J. G. Verkade, and L. D. Quin), VCH, Deerfield Beach, USA, 1987, pp. 465-530.
- [15] a) M. H. Johansson and S. Otto, *Acta Cryst* **2000**, e12-e15; b) L. Monnereau, D. Sémeril, D. Matt and L. Toupet, *Transition Met. Chem.* **2013**, *38*, 821-825.
- [16] T. Papp, L. Kollár and T. Kégl, *Organometallics* **2013**, *32*, 3640-3650.
- [17] L. Monnereau, H. El Moll, D. Sémeril, D. Matt and L. Toupet, *Eur. J. Inorg. Chem.* **2014**, 1364-1372.
- [18] G. Petöcz, Z. Berente, T. Kégl and L. Kollár, *J. Organomet. Chem.* **2004**, *689*, 1188-1193.
- [19] G. M. Sheldrick, *Acta Crystallogr., Sect. A* **2008**, *64*, 112-122.
- [20] G. M. Sheldrick, *Acta Cryst. C* **2015**, *71*, 3-8.
- [21] G. M. Sheldrick, *SHELXL-97, Program for Crystal Structure Refinement*, University of Göttingen, Germany, 1997.

Conclusion générale

L'objectif de cette thèse était de synthétiser des coordinats phosphorés construits sur des cavitands résorcinaréniques et d'exploiter les propriétés intrinsèques de telles cavités en catalyse. Dans cette étude, trois familles de ligands ont été considérées ayant pour caractéristique commune la présence d'un ou deux atomes de phosphore trivalents connectés au bord supérieur du macrocycle cavitaire. Les coordinats étudiés sont des phosphines et iminophosphoranes.

L'étude des propriétés complexantes de la phosphine **L** (Figure 1) a permis de mettre en évidence une réaction inhabituelle de ce cavitand (chapitres 2 et 3). En effet, la réaction de la

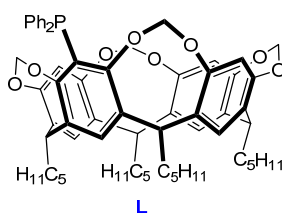


Figure 1. Phosphine **L** construite sur une plate-forme résorcine[4]arène

monophosphine **L** avec $[\text{RuCl}_2(p\text{-cymène})]_2$ ne conduit pas au complexe $[\text{RuCl}_2(p\text{-cymène})(\mathbf{1})]$ attendu, mais à la formation d'un complexe phosphino-phénolate, résultant du *clivage* d'une liaison O-CH₂ et de la perte d'une unité méthylénique (Figure 2).

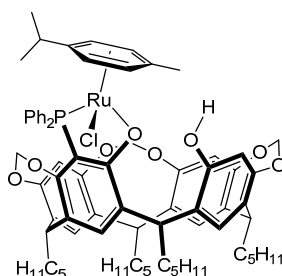


Figure 2. Complexe phosphino-phénolate de ruthénium obtenu par clivage O-CH₂

Le clivage ci-dessus est en fait un phénomène général se produisant à chaque fois que des phosphines cavitaires du type **L** sont opposés à des espèces cationiques. Aucune fracture analogue n'avait été observée auparavant, et ce, alors que de nombreuses études ont déjà été consacrées à la chimie des résorcinarènes au cours des trente dernières années. Ainsi, la réaction de deux équivalents de **L** avec $[\text{NiCp}(\text{cod})]\text{BF}_4$ conduit au complexe clivé de nickel montré en **Figure 3**. Ce complexe, associé au co-catalyseur AlMe_3 oligomérisé l'éthylène. La distribution des produits (C4: 93%, C6: 6%; C8: 1%) contraste fortement avec celle observés avec les précurseurs habituels de catalyseurs de type SHOP (c'est-à-dire de complexes de Ni(II) comportant un coordinat phosphino-énolate), qui fournissent normalement des α -oléfines plus longues (C4-C30+). La formation d'oligomères très courts observée ici résulte probablement de l'existence, dans les intermédiaires catalytiques, d'interactions O...H entre l'atome d'oxygène coordonné et le groupement OH résorcinolique, diminuant ainsi le caractère donneur de l'atome d'oxygène. Le résultat net de cette liaison est de favoriser le processus d'élimination réductrice.

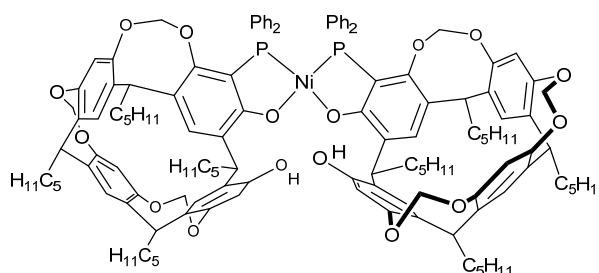


Figure 3. Complexe *phosphino-phénolate* de nickel

Le chapitre 4 décrit la synthèse de plusieurs iminophosphorane-cavitands qui ont été testés comme catalyseurs sélectifs pour l'hydrogénation compétitive d'oléfines. Pour cette seconde série de ligands, notre attention s'est portée sur des cavitands portant deux substituants *iminophosphorane* ($-\text{R}_2\text{P}=\text{NAr}$) greffées en positions distales sur le bord supérieur de la cavité (**Figure 4**). L'objectif était de former par *N,N*-chélation des métallo-résorcinarènes ayant leur centre métallique soit entièrement plongé dans la cavité, soit situé en aplomb de celle-ci.

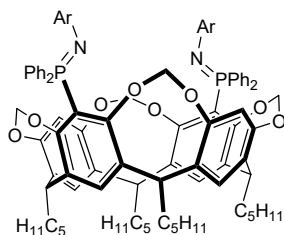


Figure 4. (Diiminophosphorane)-cavitands étudiés (Ar = *n*-Bu, *p*-anisyl)

L'un des diiminophosphoranes synthétisés, celui ayant les deux atomes d'azote substitués par un groupe *p*-anisyle, a été utilisé pour l'hydrogénation compétitive d'oléfines de tailles inégales. Ainsi, lorsqu'un mélange de 1:1 d'hex-1-ène et de 3-éthyl-pent-1-ène est hydrogéné en présence d'une quantité catalytique du di-anisyliminophosphorane et de $[\text{Rh}(\text{cod})_2]\text{BF}_4$ (1:1) (1 h, 5 bar de H_2), l'hex-1-ène – c'est-à-dire l'oléfine la moins encombrée – est hydrogéné préférentiellement, le rapport entre les quantités d'hexane et de 3-éthyl-pentane produites pouvant atteindre 98:2 en début de réaction.

Dans le prolongement du programme ci-dessus, il nous a semblé intéressant d'assembler de manière covalente des entités résorcinaréniques pour la confection de métallo-capsules. L'objectif était d'utiliser de tels complexes dans des réactions catalytiques hautement sélectives, l'espace capsulaire étant censé favoriser la formation de régioisomères dont la forme et la dimension sont adaptées à celle de la cavité (ceci conduisant ainsi à une sélectivité de forme). Dans ce but, nous avons synthétisé le bis-cavitand montré en Figure 5. La formation d'une métallo-capsule a effectivement été observée lors de la réaction entre $[\text{PtCl}_2(\text{PhCN})_2]$ et le cavitand double considéré. La métallo-capsule a fait l'objet de tests d'hydroformylation réalisés en présence du co-catalyseur SnCl_2 . En hydroformylation du styrène, la proportion d'isomère branché formé est de 64%, ce qui contraste significativement avec des phosphines classiques telles que PPh_3 (43%) ou Xantphos (13 %). La sélectivité observée est vraisemblablement liée à la formation d'espèces capsulaires dont la forme intérieure, qui contient le centre catalytique, est stériquement mieux adaptée au développement de l'isomère branché.

L'ensemble des résultats présentés constitue une nouvelle illustration du potentiel des coordinats cavitaires en catalyse homogène.

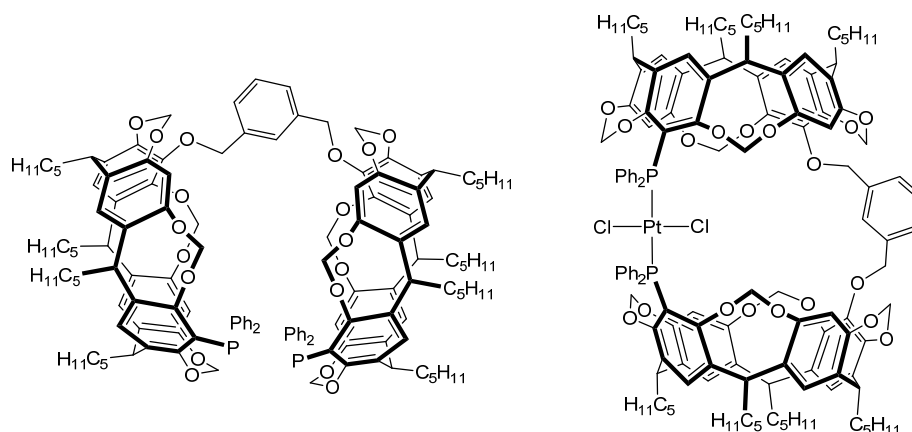


Figure 5. Bis-cavitand utilisé (gauche) pour la formation d'une métallo-capsule (droite).

Perspectives :

Les résultats obtenus durant cette thèse permettent d'envisager les études suivantes :

- exploiter la chiralité inhérente du macrocycle résorcinarénique phosphino-phénol développé aux chapitres 2 et 3 en catalyse asymétrique.
- étendre le travail sur les métallo-capsules du chapitre 5 à la synthèse de complexes adaptés à des réactions de formation de liaison carbone-carbone ou carbone-azote. On peut anticiper que les performances de ces catalyseurs, en termes de sélectivité, seront contrôlées par la forme et la taille de l'espace contenant le centre catalytique. Il serait également intéressant de rendre hydrosoluble ce type de métallo-capsule en y greffant, par exemple, des groupements *ammonium*. Les nanoréacteurs hydrosolubles ainsi générés fonctionneraient alors comme des solvants monomoléculaires immergés dans l'eau.

PHOSPHINES ET IMINOPHOSPHORANES RESORCINARENIQUES POUR LA CATALYSE. FORMATION DE COMPLEXES CAPSULAIRES

Résumé

Ce mémoire est consacré à la synthèse et à l'étude de coordinats phosphorés originaux construits sur des résorcinarènes rigidifiés. Trois types de ligands ont été élaborés : 1) des phosphines tertiaires obtenues par ancrage de groupes $-PPh_2$ sur des cycles aromatiques d'un résorcinarène générique. Celles-ci réagissent avec des espèces cationiques en formant des complexes chélate P,O résultant du clivage d'une liaison $C-O$ localisée en *ortho* du cycle phosphoré. Ce type de cassure, inédit, permet d'accéder à des catalyseurs d'oligomérisation d'éthylène pour la production de chaînes courtes; 2) des diiminophosphoranes obtenus par fonctionnalisation distale d'un résorcinarène-cavitand. Un ligand de cette famille donne lieu à des sélectivités de forme en hydrogénation (Rh) de mélanges d'oléfines; 3) des phosphino-cavitands doubles permettant d'engendrer, par chélation, des métallo-capsules. L'une d'entre elles (Pt) conduit à des sélectivités remarquables en hydroformylation du styrène.

Mots clés : catalyseurs capsulaires, résorcinarènes, cavitands, phosphines, iminophosphoranes

Abstract

This thesis describes the synthesis of three types of phosphorus-containing resorcinarene cavitand: a) compounds with diphenylphosphino groups grafted to the wider rim of a generic cavity. These phosphines undergo facile, directed $C-O$ bond breaking upon reaction with transition metal ions in the presence of exogenous or endogenous nucleophiles. A nickel complex of this type was shown suitable for the low pressure production of short α -olefins starting from ethylene; b) cavitands distally-substituted by two iminophosphoranyl groups ($-Ph_2P=NAr$). One of them ($Ar = p$ -anisyl), when combined with Rh(I), resulted in a shape-selective olefin hydrogenation catalyst; 3) double phosphino-cavitands, which upon chelation gave metallo-capsular complexes in which the metal centre is either fully or partially embedded in the resulting cavity. A platinum complex of this type resulted in the selective hydroformylation of styrene into the expected branched aldehyde.

Keywords: resorcinarenes, metallo-capsule, phosphine, iminophosphorane, catalysis